ДОКЛАДЫ
АКАДЕМИИ НАУК СССР

PROCEEDINGS OF THE ACADEMY OF SCIENCES

OF THE USSR

Physical Chemistry Section

(DOKLADY AKADEMII NAUK SSSR)

IN ENGLISH TRANSLATION

VOL. 114 NOS. 1-6

CONSULTANTS BUREAU, INC.

227 WEST 17TH STREET, NEW YORK 11, N. Y.

an agency for the interpretation of international knowledge

PROCEEDINGS OF THE ACADEMY OF SCIENCES OF THE USSR

(DOKLADY AKADEMII NAUK SSSR)

Section: PHYSICAL CHEMISTRY

Volume 114, Issues 1-6

May-June, 1957

Editorial Board:

Acad. L. A. Artsimovich, Acad. A. G. Betekhtin, Acad. S. A. Vekshinsky, Acad. A. N. Kolmogorov (Asst. to Editor in Chief), Acad. A. L. Kursanov, Acad. S. A. Lebedev, Acad. I. N. Nazarov, Acad. A. I. Nekrasov, Acad. A. I. Oparin (Editor in Chief), Acad. E. N. Pavlovsky, Acad. L. I. Sedov, Acad. N. M. Strakhov, Acad. A. N. Frumkin (Asst. to Editor in Chief)

(A Publication of the Academy of Sciences of the USSR)

IN ENGLISH TRANSLATION

Copyright, 1958

CONSULTANTS BUREAU, INC.

227 West 17th Street

New York 11, N. Y.

Printed in the United States

Annual Subscription	$160.00
Single Issue	35.00

Note: The sale of photostatic copies of any portion of this copyright translation is expressly prohibited by the copyright owners. A complete copy of any article in this issue may be purchased from the publisher for $5.00.

SIGNIFICANCE OF ABBREVIATIONS MOST FREQUENTLY ENCOUNTERED IN SOVIET PERIODICALS

FIAN	Phys. Inst. Acad. Sci. USSR.
GDI	Water Power Inst.
GITI	State Sci.-Tech. Press
GITTL	State Tech. and Theor. Lit. Press
GONTI	State United Sci.-Tech. Press
Gosenergoizdat	State Power Press
Goskhimizdat	State Chem. Press
GOST	All-Union State Standard
GTTI	State Tech. and Theor. Lit. Press
IL	Foreign Lit. Press
ISN (Izd. Sov. Nauk)	Soviet Science Press
Izd. AN SSSR	Acad. Sci. USSR Press
Izd. MGU	Moscow State Univ. Press
LEIIZhT	Leningrad Power Inst. of Railroad Engineering
LET	Leningrad Elec. Engr. School
LETI	Leningrad Electrotechnical Inst.
LETIIZhT	Leningrad Electrical Engineering Research Inst. of Railroad Engr.
Mashgiz	State Sci.-Tech. Press for Machine Construction Lit.
MEP	Ministry of Electrical Industry
MES	Ministry of Electrical Power Plants
MESEP	Ministry of Electrical Power Plants and the Electrical Industry
MGU	Moscow State Univ.
MKhTI	Moscow Inst. Chem. Tech.
MOPI	Moscow Regional Pedagogical Inst.
MSP	Ministry of Industrial Construction
NII ZVUKSZAPIOI	Scientific Research Inst. of Sound Recording
NIKFI	Sci. Inst. of Modern Motion Picture Photography
ONTI	United Sci.-Tech. Press
OTI	Division of Technical Information
OTN	Div. Tech. Sci.
Stroiizdat	Construction Press
TOE	Association of Power Engineers
TsKTI	Central Research Inst. for Boilers and Turbines
TsNIEL	Central Scientific Research Elec. Engr. Lab.
TsNIEL-MES	Central Scientific Research Elec. Engr. Lab.–Ministry of Electric Power Plants
TsVTI	Central Office of Economic Information
UF	Ural Branch
VIESKh	All-Union Inst. of Rural Elec. Power Stations
VNIIM	All-Union Scientific Research Inst. of Meteorology
VNIIZhDT	All-Union Scientific Research Inst. of Railroad Engineering
VTI	All-Union Thermotech. Inst.
VZEI	All-Union Power Correspondence Inst.

Note: Abbreviations not on this list and not explained in the translation have been transliterated, no further information about their significance being available to us. – Publisher.

INVESTIGATION OF ADSORPTION AT HIGH PRESSURES

B. N. Vasilyev, B. P. Bering, Academician M. M. Dubinin and V. V. Serpinsky

In order to elucidate a number of fundamental problems of the physical theory of adsorption it is essential to perform adsorption experiments over a wide range of temperature and pressure. In the majority of cases measurements of physical adsorption are carried out at a single temperature and over a very narrow temperature range. For this reason it is not possible to gauge from the experimental results of such investigations the accuracy with which a given theory describes the temperature dependence of adsorption. Extension of the temperature range of adsorption measurements leads inevitably to the necessity of extending the pressure range accordingly. Up to the present very few investigations of this nature have been undertaken because of the considerable difficulties arising in experiments at high pressures. The most systematic investigations of adsorption of gases at high pressures have been described in papers [1-4]. Individual cases have been reported in [5-6] and in other contributions. However, the experimental data obtained in the course of most of these investigations did not permit of an unequivocal solution of the problems, either on account of low accuracy of measurements or as a result of an unsuitable choice of the objects of study.

In an endeavor to fill in this gap partly we have undertaken a systematic investigation of physical adsorption of carbon dioxide on silica gel over a wide temperature range, namely, from $-85°$ to $40°$, thus including the critical temperature ($t_{cr} = 31°$), and at pressures ranging from 0 to 85 atm. For this purpose we constructed a special apparatus which has been described in detail [7], its characteristic feature being the absence of compressors and manometers which would normally be required when working at high pressures. Adsorption measurements were carried out by the volumetric method, the volume of the dead-space being determined with helium. All the necessary calculations were carried out using empirical data obtained in the course of investigations of the P, V, T-diagram of CO_2 in a precision meteorological work [8]. Since within the range investigated CO_2 is characterized by considerable deviations from the ideal gas, we have in all the subsequent thermodynamic calculations replaced the pressure P by the fugacity $\underline{f}$. Using the well-known thermodynamic method (see, for example, [9]) we have, therefore, calculated the fugacities of CO_2 over the range from 0 to 100 atms applying the empirical Beattie-Bridgeman equation of state [10] which is at present regarded as the most accurate one for CO_2.

The adsorbents used were two samples of silica gel received from the laboratory of A. V. Kiselev. One of these was a fine-pore gel S-340, having a specific surface of $S_{(B.E.T.)} = 573\ m^2/g$ and a limiting adsorption space of $V_a = 0.47\ cm^3/g$; the other sample was the large-pore gel E-II ($S_{B.E.T.} = 325\ m^2/g$ and $V_a = 1.61\ cm^3/g$). In the case of the S-340 adsorption isotherms were determined at 25, 0, -20, -30, -40, -50, -60, -70, -78 and $-85°$ over the relative fugacity range (f/f_s) from 0 to 1 (at temperatures below the critical point) and over a range of $\underline{f}$ from 0 to 60 atm for the temperatures of 32 and $40°$. In the case of the E-II only three isotherms were obtained, namely, at 0, -40 and $-50°$ for relative fugacities up to $f/f_s = 1$. In all cases the reproducibility of the measurements was excellent.

The adsorption isotherms obtained for the silica gel S-340 are plotted in Fig. 1 in the coordinates of log f and $\underline{a}$. As the temperature is increased from $-85°$ the curve a (log f) is displaced to the right, and at $-60°$ there appears an adsorption hysteresis loop. This loop becomes most distinct at $-50°$; it becomes narrower gradually as the temperature is increased and disappears altogether near the critical temperature, although it is practically indiscernible already at $-20°$. In accordance with the theory of capillary condensation adsorption hysteresis can occur only within the range over which existence of a liquid phase of the substance

adsorbed is possible. In our case the normal liquid phase of CO_2 can exist within the temperature range from −56.6° (m. p.) to 31° (crit. temp.). In this respect our experimental results would appear to be in agreement with the theory. However, as will be shown below, there are strong reasons to believe that at temperatures below −56.6° the adsorbed phase exists in the state of a supercooled liquid. If this is so, then the disappearance of the hysteresis loop below −60° cannot be explained by considerations based on the above theory and requires further investigation.

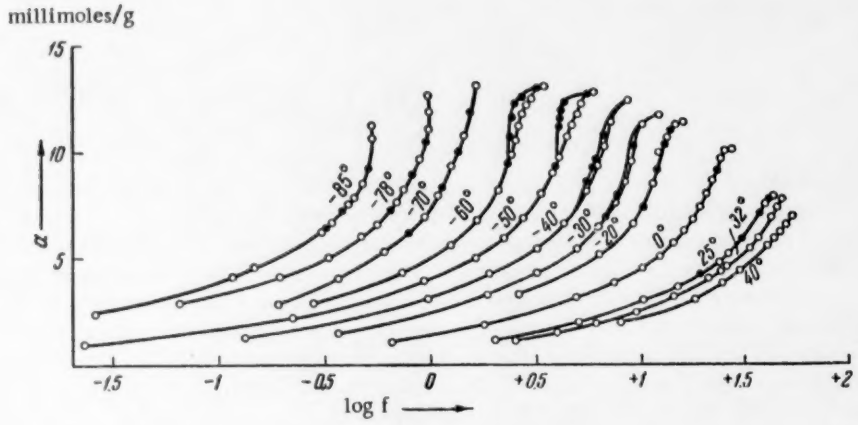

Fig. 1

From our measurements it is possible to calculate the pore volume distribution curves $dv/dr = \varphi(r)$ in terms of the pore radius r for a range of temperatures. It is clear that in the case of adsorbents with a rigid adsorbing network the curve $\varphi(r)$ should be independent of temperature. In Fig. 2 are plotted the curves $\varphi(r)$ calculated for −30° (curve 1) and −50° (curve 2) for the S-340, having taken into account corrections for the thickness of the adsorption layer [12] calculated from adsorption isotherms determined for the large-pore silica gel E-II. It will be observed that the two curves differ greatly from each other. The maximum of curve 1 is displaced along the abscissa by approximately 25% relative to the maximum of curve 2, and at the same time the latter curve indicates that the pore volumes of the silica gel are more monodisperse than would appear from curve 1. We see, therefore, that in this case the position of the maximum and the shape of the distribution curve depend on the temperature. This fact may be an indication of the inapplicability of the Kelvin formula to describe liquid menisci having a radius of curvature $r \approx 20$ A. It is not possible, of course, to determine a priori the lower limit for r below which the formula ceases to be valid; this limit can only be found by experiment. It would, however, be rash to say on the basis of this single experiment where exactly this limit lies. In order to solve this problem further investigations are necessary.

In the case of the curves in Fig. 1 the adsorption a was calculated as excess adsorption by Gibbs' method. It is well-known that at high pressures the quantity a determined by this method may differ considerably from the total amount of the substance contained in the adsorption space. Since at $f/f_s = 1$ the entire space V_a is filled with the substance, $a = a_s + V_a\delta$, where a_s is the limiting value of adsorption and δ is the density of the gas under these conditions. If V_a is taken as the true volume of the adsorption space (determined from the limiting sorption of nitrogen), it is easy to find the mean density $\rho_a = a/V_a$ of the adsorbed substance in the volume V_a.

In Fig. 3 is plotted the graph of ρ_a as a function of the density ρ of normal liquid CO_2 at the same temperatures. The values of ρ_a at −20, −30, −40, and −50° exceed the corresponding values of ρ by about 6%. However, as we approach the critical temperature the mean density ρ_a exceeds ρ by 14 % (at 25°). This abnormally excessive value of ρ_a is most readily explained by the high compressibility β near the critical temperature ($\beta = \infty$). As a result, even a weak field of adsorption forces acting beyond the boundary

of the first adsorption layer may effect a considerable increase in density within the polymolecular layers.

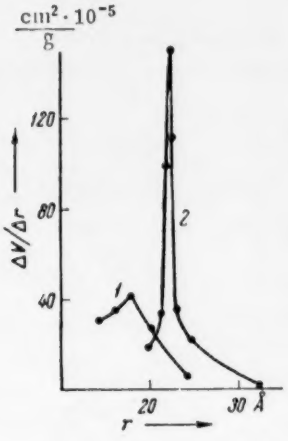

Fig. 2

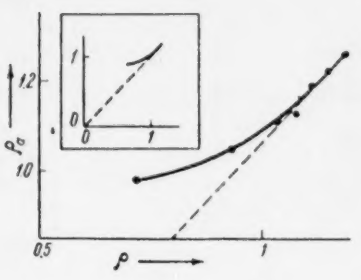

Fig. 3

Analysis of the isotherms plotted in Fig. 1 showed that the experimental data obtained can be expressed satisfactorily by the Dubinin-Zaverina equation [11] for carbons of the 2nd structural type. However, near the critical temperature the characteristic curves calculated from the Polyani theory ($\epsilon = -RT \ln h = \psi(av)$, where $h = f/f_s$ and $\underline{v}$ is the molar volume of CO_2) were found to depend somewhat on T. The curves $\psi(av)$ calculated for 0 and 25° are situated above the single characteristic curve obtained for the remaining temperatures. This position of the curves $\psi(av)$ is apparently caused by the said anomalous density ρ_a near the critical temperature (see Fig. 3). If we calculate the curves $\psi(av)$ for the total adsorbed content $\underline{a}$ and for the effective density ρ_a, we obtain a single curve for all temperatures, including 0 and 25°.

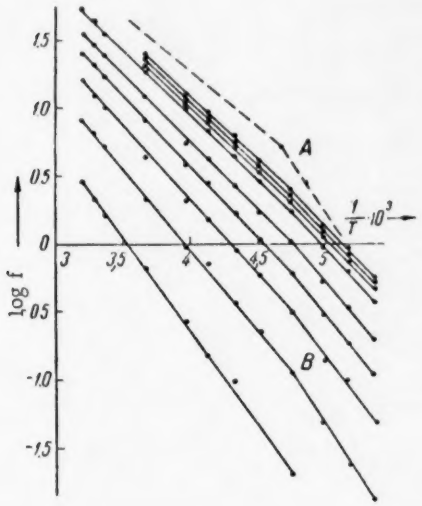

Fig. 4

In Fig. 4 are plotted the adsorption isosteres (coordinates log $\underline{f}$ and 1/T) constructed with the aid of the isotherms of Fig. 1, for values equal to 1, 2, . . . , 10 millimoles/g. Each of these isosteres consists of two linear portions which intersect within a narrow temperature range around −60°. The dotted line in the upper portion of Fig. 4 is the corresponding curve $\log f = \varphi(1/T)$ for ordinary CO_2. The point of intersection on this curve, situated at −56.6°, corresponds to the melting of solid CO_2. The difference between the slopes of the two linear portions of the curve at A — the point of transition from the solid to the liquid phase — gives approximately a measure of the heat effect of the transition, $-\Delta H^0$, which is equal to 2.0 kcal / / mole. It seems natural to regard the points of inflexion on the adsorption isosteres as an indication of the occurrence of a phase transition in the adsorbed substance as well. In fact, if a phase transition similar to crystallization were taking place throughout the mass of the adsorbed substance, the heat effect $-\Delta H$ of such a process, which would be approximately equal to the difference of the tangents of the angles of slope of the isosteres at the transition point (for example, at B), should increase with increasing adsorption and should approach

the value of $-\Delta H^0$ at point A for the ordinary condensed phase of CO_2. Contrary to this the quantity $-\Delta H$ does not increase, but decreases with increasing $\underline{a}$, as will be seen at once from Fig. 4. For $\underline{a}$ = 10 millimoles/g the inflexion on the corresponding isostere is hardly observable.

The form of the isosteres in Fig. 4 can easily be explained if it is assumed that the phase transition takes place only in the first adsorbed layer, while at temperatures below the transition point the remainder of the adsorbed substance exists as a supercooled liquid.

The phenomenon of phase transition discovered by us appears to be the two dimensional analog of crystallization and is due to a "freezing out" of consecutive degrees of freedom of the adsorbed molecules. We may mention that in Coolidge's investigation [3] no inflexion of the CO_2 adsorption isosteres was observed under similar conditions, probably because of a lower degree of accuracy of the measurements.

LITERATURE CITED

[1] J. W. McBain and G. T. Britton, J. Am. Chem. Soc. 52, 2198 (1930).

[2] H. E. Morris and O. Maass, Canad. J. Res. 9, 240 (1933).

[3] A. S. Coolidge, J. Am. Chem. Soc. 56, 554 (1934).

[4] A. Antropoff, Koll. Z. 129, 11 (1952).

[5] H. Briggs and W. Cooper, Proc. Roy. Soc. Edinburgh, 41, 119 (1921).

[6] V. T. Palvelev, Proc. Acad. Sci. USSR 62, 779 (1948).

[7] B. N. Basilyev, J. Phys. Chem. 31, 498 (1957).

[8] H. Michels and C. Michels, Proc. Roy. Soc., London, A153, 214 (1935).

[9] Lewis and Randall, Chemical Thermodynamics, London, 1936.

[10] J. A. Beattie and O. C. Bridgeman, Z. f. Phys. 62, 95 (1930).

[11] M. M. Dubinin and E. D. Zaverina, J. Phys. Chem., 23, 1129 (1949).

[12] M. M. Dubinin and E. G. Zhukovskaya, J. Phys. Chem. 30, 1840 (1956).

Institute of Physical Chemistry,
Academy of Sciences of the USSR

Received January 9, 1957.

KINETIC RELATIONSHIPS DURING IGNITION BY A HOT SURFACE IN CONDITIONS OF THE INTERNAL COMBUSTION ENGINE

A. N. Voinov

(Presented by Academician N. N. Semenov, November 13, 1956)

In a recent paper [1] the author has described results of an experimental investigation of ignition of gases by a hot surface in an apparatus operating on a single work cycle and closely simulating conditions in the internal combustion engine. Certain relationships of the ignition temperatures (T_i) to compression temperatures and pressures (T_c and P_c) have been established for a number of motor fuels.

On the basis of the thermodynamic theory of the ignition of gases by a hot surface it appears possible to calculate from the experimental relationships $T_i = f(T_c)$, at P_c = const., the corresponding values of the apparent energies of activation, while from the relationships $T_i = F(P_c)$ at T_c = const. one could determine the order of reactions taking place close to the hot surface at temperatures of 700-900°. In view of the fact that data on the mechanism of chemical reactions at such temperatures are extemely scarce the results of our investigations may be of considerable interest, the more so because they extend over a comparatively wide range of different motor fuels.

From theoretical considerations Ya. B. Zeldovich has shown [2] that the critical conditions of ignition of a gas by a hot surface are determined by the existence of zero gradient of temperature within the reacting gas close to that surface. This means that ignition will take place when the hot surface is at a temperature at which heat transfer from the reaction zone to adjacent layers of cooler gas will be fully compensated by the heat of reactions proceeding within the gas layer close to the hot surface. If it is assumed that for large values of activation energies the thickness, ξ, of the layer within which the essential part of the reaction takes place, is small as compared with the distance, l, between the hot and the cool surface, and if, consequently, the differences between the temperature gradients during and in the absence of reaction are neglected, it is possible to establish relationships connecting the ignition temperature, T_i, to the dimensions of the combustion vessel and to the temperature, T_0, of its cool walls for a known relation of the rate of reaction to the temperature and pressure, $W = F(T_i, P)$. In the case of a plane-parallel chamber of infinite dimensions, and assuming that heat loss from the hot surface takes place by conduction alone, this relationship will have the form

$$l = \sqrt{\frac{\lambda E (T_i - T_0)^2}{2F(T_i, P) R T_i^2}}, \qquad (1)$$

It is clear that the nature of the problem will not change essentially in the case of other types of heat transfer, in particular for heat transfer by turbulent pulsations; as before, critical conditions for ignition will correspond to zero gradient of temperature near the hot surface. In conditions where the hot surface is swept by a turbulent stream of the gas the essential difference in the process would lie in the temperature gradient being almost entirely confined to a comparatively narrow boundary layer, while the temperature of the remaining mass of gas would be practically unaltered, especially in the case where the dimensions of the hot surface are small.

Without entering into the question of the actual structure of the boundary layer let us introduce into our considerations the notion of a "reduced film", i. e. let us assume that there exists a certain distance, δ, between the wall at a temperature T_i and the gas at a temperature T_0 for which heat transfer by molecular motion, determined by the parameter λ (assuming a linear temperature gradient across the film) is equal to the actual amount of heat given off by the hot surface and determined by its coefficient of heat conduction α, i. e. we have the relation

$$\lambda (T_i - T_0) \delta = \alpha (T_i - T_0),$$

from which

$$\delta = \frac{\lambda}{\alpha}. \tag{2}$$

Substituting the latter relation into Formula (1) we have:

$$\alpha = \sqrt{\frac{\lambda 2F (T_i P) RT_i^2}{E (T_i - T_0)^2}}. \tag{3}$$

This expression is a much more general condition of ignition of gases by a hot surface and can be equally applied to any other conditions of heat transfer which can be defined in terms of the quantity α •. However, it must be borne in mind that the possibility of ignition does by no means depend on the mean value of the coefficient of heat conduction referred to the total surface area of the body circumflowed by the gas, but by its minimum values at localized points on that surface. This circumstance complicates considerably the theoretical treatment of the problem of ignition of a gas by a hot body moving relative to it, if one wishes to operate with relations between ignition temperature and certain parameters which have a large effect on the conditions of heat transfer, such as, for example, the dimensions of a hot spherical pellet shot into the gas, or its speed, as has been done by some investigators [3-5]. More complicated still is the problem of ignition of the working substance in an internal combustion engine by contact with some overheated parts or with incandescent areas of the carbon deposit, when the process is attended by an intensive and extremely erratic turbulent motion of the explosive mixture.

The problem becomes much more simplified if, as has been done in our experiments, the conditions of flow of the fuel mixture over the hot surface are kept constant and only its temperature and pressure are varied. The generalized relation connecting heat transfer with turbulent flow of gas has the form $Nu = CRe^n$. In the case of gas flowing round any body whatever situated in the stream, the values of C and n depend both on the Reynolds number, Re, referred to the dimensions of the body in question, as well as on the turbulence of the flow. In a gas stream with a normal turbulence (close to the walls), for values of $80 < Re < 5 \cdot 10^3$ (referred to the dimensions of the body), the index n is equal to 0.46, while for values of $5 \cdot 10^3 < Re < 5 \cdot 10^4$, n = 0.6. The latter value is also valid in the case of strong turbulence behind screens. In the case of turbulence of medium intensity as in the internal combustion engine – we can, without introducing serious errors, put n = 0.5.

At a given rate of revolution of the engine the speed at which the gaseous mixture flows past the hot surface may be taken to be constant, i. e. independent of temperature and pressure, and therefore $\alpha = C\lambda \nu^{-0.5}$. Consequently, if the reactions taking place obey Arrhenius' law, expression (3) may be written:

$$\frac{T_i}{T_i - T_c} \sqrt{\frac{\nu P_C^n e^{-E/RT_i}}{\lambda E}} = \text{const}. \tag{4}$$

• A similar problem in a more general form has been solved in [3].

By means of this relation it is possible to calculate the mean values of activation energy and orders of reaction making use of the experimental curves $T_i = f(T_c)$ at P_c = const., on the assumption that E does not change within the range of variation of T_c in question. Since it is not the absolute values of λ and ν, but only their relative variations with temperature which are of significance in this calculation, we can, without introducing any serious errors, substitute these values for the fuel mixture investigated by the corresponding values for air, referring them to the temperature of the gas streaming past the hot surface, i. e., to T_c.

TABLE 1

Apparent Activation Energies (kcal/mole) for Different Fuels During Ignition by a Hot Surface Within Different Ranges of Compression Temperature; $\alpha = 1$; $P_c = 8.25$ atm.abs. Ignition Temperatures T_i at the Limits of the Given Range of Compression Temperatures Are Indicated in Brackets

Fuel	Range of T_c, °K	
	550–650	650–725
Benzene	77 (1198 / 1180)	77 (1180 / 1164)
Iso-octane	60 (1187 / 1163)	42 (1163 / 1130)
Coal gas	73 (1159 / 1140)	73 (1140 / 1122)
Aviation petrol B-70	70 (1165 / 1140)	68 (1140 / 1117)
Tryptane	56 (1162 / 1137)	56 (1137 / 1113)
Di-isobutylene	37 (1162 / 1121)	37 (1121 / 1083)
Cumene	36 (1179 / 1134)	36 (1134 / 1098)
50% iso-octane + 50% heptane	21 (1183 / 1098)	10 (1098 / 1053)*

* In the range 650-680° K.

In Table 1 are given experimentally determined values of T_i corresponding to a series of compression temperatures T_c, for different fuels in stoichiometric ratio with air, at a constant compression pressure P_c = = 8.25 atm. abs., as well as the corresponding calculated values of the apparent activation energies E_a over the intervals of T_c investigated. The values of T_c and P_c are, in this case, largely conditional, because no account has been taken of the heating up of the fuel mixture as a result of reactions taking place before the actual ignition.

From the data in Table 1 it will be evident that the values of E_a are constant at those compression temperatures at which, under the conditions of experiment, the fuel mixture is still far removed from the state in which it ignites spontaneously. However, as pre-ignition processes begin to develop within the mixture as a result of heating by compression above the known limit, the values of E_a calculated by means of formula (4) drop sharply. This decrease of E_a may be the result of two causes: acceleration of reactions close to the hot surface by active products resulting from pre-ignition oxidation processes within the bulk of the mixture, and reduction of the rate of heat transfer resulting from a rise of temperature of the mixture in the course of these same pre-ignition oxidation processes.

Calculations show that the effect of the latter factor on the calculated values of E_a can be very considerable. Thus, in order to obtain at high compression temperatures the same value E_a = 60 kcal/mole calculated for iso-octane for the range of T_c from 550 to 650° K, it is sufficient to assume that the actual temperature of the compressed mixture is only 38° above the value used in the calculation on the assumption that any spontaneous heating processes are absent, i. e. we may put T_c = 763° K, instead of 725° K. Similarly, if we take it that the activation energy of the 50% octane mixture is constant and approximately equal to the activation energy of iso-octane, for example, if it is put equal to 50 kcal/mole, then the ignition temperature T_i = 1100° K should correspond to a compression temperature $T_c \cong 780°$ K, and not 650° K (as indicated in Table 1), i. e. 130° higher. In the case of paraffinic fuels such a spontaneous heating towards the end of the pre-ignition stage of oxidation does, in fact, take place.

In view of the above it can be assumed that the lowering of ignition temperatures observed as the fuel mixture approaches the condition of spontaneous ignition by compression is entirely due to the rise in temperature during the pre-ignition stages; on the other hand, the lowering of the apparent energies of activation at high values of T_c must be regarded as entirely ficticious.

As regards the calculated values of E_a within the range of T_c where pre-ignition processes have little effect, in the case of such fuels as benzene, iso-octane, coal gas and petrol B-70 (E_a = 70-77 kcal/mole) these values are considerably higher than those obtained in experiments on ignition by compression [6], or ignition by hot bodies [3-5], but they are very close to results obtained in heated containers at temperatures >680°C [7, 8], approaching energies at which rupture of the fundamental intramolecular bonds takes place. By contrast, in the

case of di-isobutylene and cumene the apparent activation energies obtained were considerably lower (36-37 kcal/ mole) and remained constant at all compression temperatures; there are, therefore, no reasons to assume that in this case pre-ignition processes were effective. The literature records no data on the activation energies of these hydrocarbons within the temperature range in question.

TABLE 2

Orders of Reaction for Different Fuels on Ignition by a Hot Surface; $\alpha = 1$; P_c = 4-12 atm.abs., T_c = 637-652° K

Fuel	T_i, °K	E_a, kcal/mole	n
Benzene	1185-1180	77	0.1
Iso-octane	1172-1140	60	0.6
Di-isobutylene	1150-1060	37	0.8

Making use of the experimentally determined relations $T_i = f(P_c)$ at $T_c \cong$ const. (see [1], Fig. 2) and applying formula (4) it is possible to calculate the order of reaction on ignition by a hot surface, taking corresponding values of E_a from Table 1. In both cases only those ranges of P_c and T_c are taken into consideration over which the distorting effects due to spontaneous heating before ignition are absent.

In Table 2 are shown the orders of reaction for three fuels calculated by this method; the values indicated are the mean values for the investigated range of P_c and T_c, and hence also for that of T_i. It will be seen that in the case of iso-octane and di-isobutylene the values of n are close to those indicated in the literature and obtained, for example, on ignition of fuels by injection into hot air [7]. By contrast, the order of reaction calculated for benzene is very nearly zero. This, apparently, is an indication that here heterogenous processes play the predominant role, accompanied by a high degree of saturation of the surface.

Institute of Chemical Physics
Academy of Sciences of the USSR

Received November 10, 1956

LITERATURE CITED

[1] A. N. Voinov, Proc. Acad. Sci. USSR, 113, No. 6 (1957).*

[2] Ya. B. Zeldovich, J. Expt.-Theor.Phys., 9, No. 12, 1530 (1939).

[3] L. N. Khitrin and S. A. Goldenberg, Proc. Acad. Sci. USSR, 103, No.2, 277 (1955).

[4] R. S. Silver, Phil. Mag., (7) 23, 633 (1937).

[5] S. Paterson, Phil. Mag., (7) 28, 1 (1939).

[6] H. Teichmann, Zs. Elektrochem., 47, 297 (1941).

[7] A. V. Zagulin, Trans. LIKhF, 1931, p. 92.

[8] M. Pechard, Publ. Minist. de l'aire, No. 132 (1938).

[9] A. I. Serbinov, Symp. "Internal Combustion Engines Working on the Principle of Ignition by Compression", 1951, p. 99.

* See C. B. Translation.

INVESTIGATION OF THE STRUCTURE OF HUMIC ACIDS IN BITUMINOUS COALS

V. I. Kasatochkin and N. K. Larina

(Presented by Academician P. A. Rebinder, November 24, 1956)

Investigation of the structure and properties of humic acids is of general interest because it provides a means of obtaining information about the chemical structure of the organic matter of bituminous coals.

TABLE 1

Humic acids	W^l	A^l	C^g	H^g	A^s	C/H
	in percent					
From coal D, oxid. with H_2O_2	7.55	0.31	63.81	3.62	0.35	17.6
From coal G, oxid with H_2O_2	5.72	0.25	64.42	3.50	0.28	18.4
From coal PZH, oxid with H_2O_2	8.38	0.42	64.75	3.25	0.47	19.9
From coal K, oxid. with H_2O_2	6.37	0.40	65.48	3.20	0.46	20.4
From coal G, oxid. with HNO_3	8.37	0.37	61.60	3.14	0.41	18.7

In the present investigation the humic acids were obtained by mild oxidation of Donetz bituminous coals D, G, PZh and K with hydrogen peroxide and in the case of coal G also with nitric acid, followed by dissolution in 2% sodium hydroxide (see Table 1). The samples were investigated by the following methods: determination of the optical density of the alkaline solutions, determination of the precipitation threshold with $CaCl_2$, infrared absorption spectroscopy and X-ray diffraction.

In Fig. 1 are shown the results of determinations of the optical densities of alkaline solutions of humic acids obtained from bituminous coals of progressive rank, referred to the same carbon content. The positions of the optical density curves indicate a continuous adsorption spectrum and can be interpreted in terms of the structure of humic acids which is characterized by the linking of aromatic nuclei to aliphatic side chains [1]. On this basis the continuous adsorption spectrum can be ascribed to the mobility of the π-electrons within the carbon lattice constituting a conjugated system. The optical density increases regularly with rank of coal from which the given humic acids have been obtained [5, 6], which is a direct indication of increasing ratio of carbon making up the aromatic lattice to carbon contained in the side chains of the humic acid molecules.

On oxidation of coal G with hydrogen peroxide different yields of humic acids were obtained, namely, 3.5 and 26.5%. The optical density curves for these samples were found to be identical within the limits of experimental error and it can, therefore, be concluded that the nature of the molecules of humic acids is not altered in the course of the oxidation process.

The infrared absorption spectra in the region from 2.8 to 10 μ were obtained with the infrared spectrophotometer IKS-11 with LiF and NaCl prisms. Within the region of the C – H valence vibrations there are found absorption maxima at 3.42 and 3.50 μ which correspond to methylene groups, a maximum at 3.3 μ corresponding to aromatic CH groups, and also a maximum at 3.38 μ corresponding to terminal methyl groups. The intensity

of the maximum corresponding to aromatic CH groups in the humic acids increases with coal rank [2], just as it does in the case of the original coals, which indicates a lowering of the extent of substitution of the aromatic nuclei by side chains with progressive rank of coal from which the humic acids have been obtained (Fig. 2). Absorption bands appear at 5.9 and 8.0 μ which correspond to vibrations of the C = O and C – O linkages.

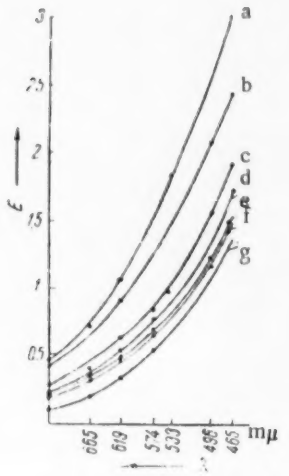

Fig. 1. Optical densities of humic acid solutions obtained from coals of progressive rank: a) from a weathered coal; b) from coal G oxidized with HNO_3; c) from coal K oxidized with H_2O_2; d) from coal PZh, oxidized with H_2O_2; e) from coal G oxidized with H_2O_2; f) from coal D oxidized with H_2O_2; g) from brown coal.

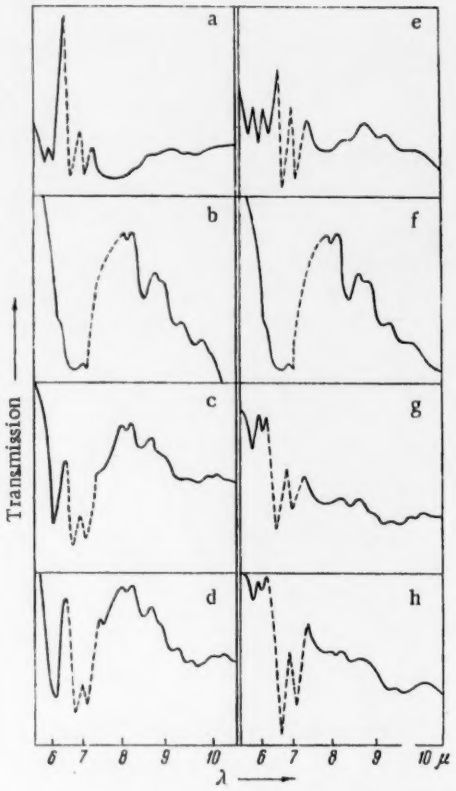

Fig. 2. Infrared absorption curves of humates and humic acids obtained from bituminous coals: a) humic acids obtained from coal PZh oxidized with H_2O_2; b) Na-humates from coal PZh; c) Ba-humates from coal PZh; d) Ca-humates from coal PZh; e) humic acids from coal G, oxidized with HNO_3; f) products of interaction of humates with HCl; g) product of deuterium exchange with humic acids from coal PZh; h) mixed Na-Ba humates obtained from coal PZh.

The absorption spectrum of the products of deuterium exchange, obtained by treating the humic acids from coal PZh with deuterium oxide, D_2O, reveals a decrease of intensity of the band at 8.0 μ. The spectra of Na, Ca and Ba humates are characterized by the disappearance of the absorption bands at 5.9 and 8.0 μ, which is due to the transition of the carboxyl group into the ionic form [3].

Comparison of the absorption spectra of the deuterated humic acids with those of the humates shows that the bands at 5.9 and 8.0 μ found in the former ought to be ascribed to the C = O and C – OH linkages in the carboxyl groups.

On treatment of the humates with hydrochloric acid the original spectra of the humic acids are again obtained. This is due to the reversibility of the exchange between the hydrogen of the carboxyl groups and the metal ions. The fact that the absorption spectra of Ba-humates, precipitated from alkaline solutions of humic acids (Fig. 2), are identical with the spectrum of Na-humates indicates that partial substitution of Na-ions by

Ba-ions has taken place with the formation of molecules of mixed Na and Ba humates containing only a small proportion of the latter, but sufficient to lower their solubility.

The infrared absorption spectra of humic acids obtained from coal G by treatment with nitric acid have an absorption maximum at 6.55 μ, which corresponds to vibrations in the NO_2 group.

Precipitation thresholds were determined by the minimum amount of $CaCl_2$ (mg.-equivs.) necessary to start precipitation of humic acids from their alkaline solutions, referred to the given percentage of carbon. It will be observed that the precipitation threshold decreases regularly with increasing percentage of carbon (Fig. 3) [7].

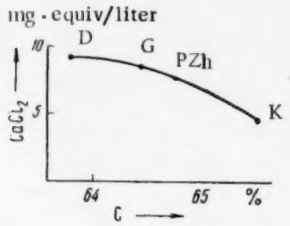

Fig. 3. Precipitation thresholds of humic acids obtained from coals different rank.

The interaction of alkaline solutions of humic acids with $CaCl_2$ may be visualized as an ion-exchange process with the formation of complexes of two or more humic acid molecules linked through their carboxyl groups by the bivalent calcium. As a result the stability of humic acid molecules in solution is lowered, thus facilitating precipitation of mixed Ca and Na humates [4] with a low percentage of calcium.

As a result of the presence of an excess of the hydrophylic nitro groups the precipitation thresholds of humic acids obtained by oxidation of coal G with HNO_3 are found to lie higher than the precipitation thresholds of humic acids obtained by oxidation of the coal with H_2O_2.

The observed lowering of the stability of humic acid solutions with progressive coal rank is connected with the increasing proportion of carbon organized in aromatic nuclei (resulting from the lowering of the extent of substitution by side-chain radicals), and is, consequently, determined by the increasing hydrophobic character of the core of the molecules.

TABLE 2

Material	Original coal		Humic acids	
	d_{002}, A	Δ^0_{002},	d_{002} A	Δ^0_{002}
Coal D	3.5	7.5	3.5	7.5
Coal G	3.5	7	3.5	7
Coal PZh	3.5	6.5	3.5	6.5
Na-humates (PZh)	-	-	6.0	6.5
Ba-humates (PZh)	-	-	-	-

X-ray diffraction diagrams of the coals, humic acids and humates were obtained with filtered Cu-radiation in cylindrical cameras having a radius of 45 mm. In Table 2 are shown the mean distance between the planes of the carbon lattices, d_{002}, and the angular half-width of the interference band (002), Δ^0_{002}, which is a measure of the ordered arrangement of the lattices [1]. The interference bands with the indices (100) have the same diffuse appearance in the case of all the samples examined. This indicates that the linear dimensions of the carbon lattices are small and do not change substantially.

Comparison of these X-ray diffraction data shows that both the dimensions of the carbon lattices as well as their ordered arrangement are the same for the humic acids and for the original coals.

On X-ray diffraction diagrams of Na-humates it is possible to observe a displacement of the (002) band towards small angles. This indicates a considerable increase of the interplanar distances between the carbon lattices – up to d_{002} = 6 A – as compared with the corresponding value for humic acids and for the original

coal PZh for which both of d_{002} = 3.5 A. In the case of Ba-humates the interference band (002) cannot be observed at all, which is an indication of complete disorder in the orientation of the carbon lattices. The increase of the interplanar distance can be accounted for by additional repulsive electrostatic forces due to peripheral carboxyl groups present in Na-humates in the ionized form. The disordered arrangement of the carbon lattices in Ba-humates is due to the formation of rigid links between the carboxyl groups through the barium. The observed changes in the interplanar distances and in the degree of orientation of the carbon lattices in Na- and Ba-humates are a direct confirmation of the absence of any bonds between these lattices in alkaline solutions of humic acids and furnish a proof of the true nature of humic acid solutions, i. e. that the humic acid molecules exist as individual carbon lattices with aliphatic side chains.

The experimental results of this investigation of the structure of humic acids obtained from bituminous coals provide a confirmation of the structure proposed earlier [1] which visualizes humic acid molecules as consisting of individual plane aromatic carbon-ring lattices to which are attached side chains with various oxygen-containing and other functional groups. On this basis the oxidation process of the coal substance may be defined as the oxidative destruction of a macromolecule giving rise to the formation of individual structural units which can pass into alkaline solutions owing to the presence of carboxyl groups formed in the oxidation process. However, a more precise definition of this structure in terms of a structural formula [8] is, in our opinion, not possible because the carbon-ring lattices constituting the core of the humic acid molecules have a certain distribution according to their dimensions — a distribution also present among the structural units of the original coals — and because the functional groups are distributed statistically among the molecules.

The importance of investigations of the structure of humic acids in relation to the problem of the chemical structure of the organic matter of bituminous coals arises from the fact that the carbon skeleton of humic acid molecules fully resembles that of the structural units of the organic matter of coal itself.

Received October 29, 1956

LITERATURE CITED

[1] V. I. Kasatochkin, Bull. Acad. Sci. USSR, Div. Tech. Sci., No.9 (1951); No. 10 (1953); Proc. Acad. Sci. USSR, 88, 759 (1952).

[2] I. K. Brown, J. Chem. Soc., 1955, 744.

[3] L. I. Bellamy, The Infra-red Spectra of Complex Molecules, London, 1954.

[4] G. L. Stadnikov, Koll. Zs., 47, 136 (1929).

[5] M. M. Kononova and N. P. Belchikova, Proc. Acad. Sci. USSR, 72, 125 (1950).

[6] T. A. Kukharenko, Proc. Acad. Sci. USSR, 89, 133 (1953).

[7] N. P. Belchikova, Trans. Soil Inst. Acad. Sci. USSR, 38, 33 (1951).

[8] W. Fuchs, Die Chemie d. Kohle, Berlin, 1931.

CONCERNING THE CHANGE OF THE ELECTROCHEMICAL ACTIVITY OF ZIRCONIUM UNDER THE ACTION OF RADIATION

I. L. Rozenfeld and E. K. Oshe

(Presented by Academician A. N. Frumkin, December 30, 1956)

By irradiating the elements Zr–Al and Zr–Fe in a flowing electrolyte (3% NaCl) with a stream of high energy (0.8 Mev) electrons at an intensity of 15 $\mu a/cm^2$ there was observed a sharp increase in the current of the couples. This current rose immediately after the beginning of irradiation and exceeded the couple current prior to irradiation by 15-20 fold. During the further course of the entire experiment (one hour) this current changed relatively little. On completion of irradiation the current sharply fell, almost reaching the initial value.

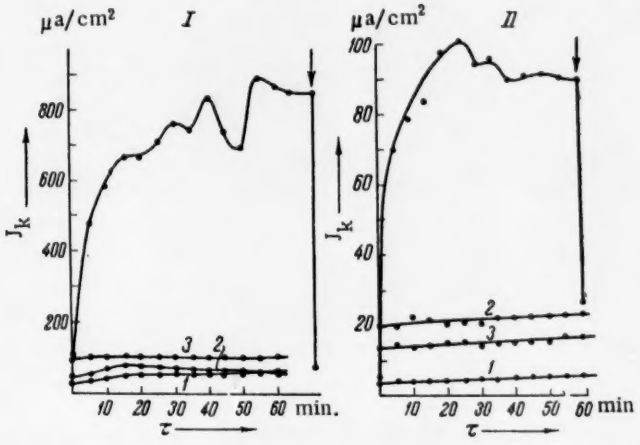

Fig. 1. The change with time of the current strength of the couples Zr–Al (I) and Zr–Fe (II) in 3% NaCl: 1) in the absence of radiation, at room temperature; 2) in the absence of radiation, at the temperature which is established during irradiation; 3) by irradiating the anode (Al or Fe, respectively); 4) by irradiating the cathode (Zr); the arrow indicates the instant at which irradiation was stopped.

Experiments in which only the anode or the cathode was subjected to irradiation showed that the effect in question is observed only through irradiating the cathode (Zr). This effect is not produced on irradiation of the anode (Al or Fe). The results of these experiments are represented by the Curves 3 and 4 in Fig. 1. For comparison there are also presented curves showing the time dependence of the current strength of the elements,

in the absence of radiation, at room temperature (Fig. 1, Curve 1) and at that temperature which is produced at the metal-electrolyte boundary surface as a result of the absorption of the energy of radiation (Fig. 1, Curve 2).

Electrodes which had served as anodes in experiments involving irradiation were subjected to much more extensive disintegration than was the case in experiments under these same conditions but in the absence of radiation. In Figure 2 are presented photographs of the surface of aluminum electrodes which had served as anodes in combination with zirconium electrodes under irradiation and in the absence of the latter (the duration of the experiments was 1 hour under identical conditions).

It is impossible to explain the observed effect as the result of the action of any of those factors which have so far been advanced as the principle accelerators of the electrode processes under irradiation. The influence of temperature was studied in control experiments. It proved to be insignificant (Fig. 1, Curve 2). Long-lived products of radioactive disintegration also could not be classed among the principle stimulators since their stationary concentration could not have exceeded 0.001 N. This is also shown by the sharp decrease in the current strength on completion of irradiation. Anodic polarization because of electrons which were absorbed by the electrodes did not exceed 7-8 μ a/cm^2 whereas in the experiment the current of the element under irradiation rose to 800 μ a/cm^2 (the pair Zr–Al).

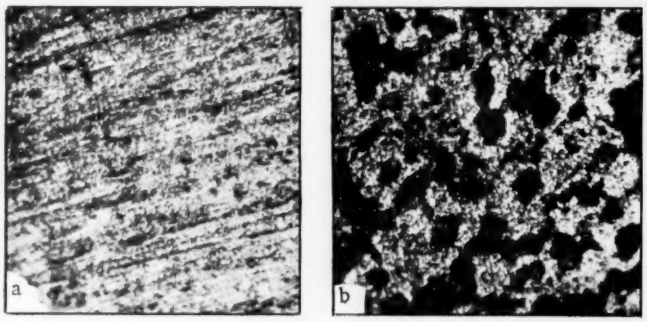

Fig. 2. View of the surface of aluminum electrodes which had served in couples with zirconium in 3% NaCl: a) in the absence of radiation at room temperature, b) under irradiation of the zirconium cathode.

It seems to us to be possible to explain the change of the electrochemical activity of the zirconium electrode under irradiation in terms of those alterations in the physical properties of the oxide film on the zirconium cathode which can be brought about by radiation. The majority of oxide films are typical semiconductors. The latter, as is known, possess the characteristic property of being extremely sensitive in their electrical properties to all sorts of external influences. Thus, irradiation produces, in most cases, a sharp increase of the electrical conductivity of semiconductors. This comes about through the transfer of electrons out of the filled zone, or from additive levels, into the conducting zone, at the expense of the radiational energy which is absorbed in the semiconductor. If in our experiment the oxide film on the cathode (ZrO_2) is considered as a semiconductor, then under the action of radiation the electrical resistance of this film decreases because of "radiational conductivity."* If account is taken of the fact that the current strength of an element is determined by the rate of the cathodic reaction of oxygen reduction and if it is admitted that this latter is

* That conductivity which is brought about by the action of either electromagnetic or corpuscular radiation we designate as radiational conductivity in analogy with photoconductivity, which results from the action of light.

limited by the high resistance of the semiconducting film upon the cathode, then irradiation, leading to the appearance of radiational conductivity in the film, must accelerate this cathode reaction and lead to a sharp increase in the current strength of the element.

At the same time, if we accept the proposed mechanism, it is impossible to expect that irradiation of the anode could lead to an observable increase of the current strength of the element; this is confirmed by experiment.

Radiational conductivity in a semi-conductor arises directly after initiation of irradiation and disappears on completion of the latter. This assures a rapid growth of the current strength at the beginning of irradiation and a sharp decrease on its completion.

The relationship between the current strength of a couple and the intensity of radiation was studied theoretically and experimentally. If it is supposed that the basic source of free electrons is the filled zone, then proceeding from the elementary conceptions of the photoconductivity of semiconductors, the change in the concentration of the free electrons in the conducting zone can be expressed in the following form:

$$\frac{dn}{dt} = \alpha I - kn^2, \tag{1}$$

where α is the quantum yield, I is the intensity of radiation, k is the coefficient of recombination, and n is the concentration of electrons in the conducting zone. Under stationary conditions (1) takes the form:

$$\alpha I = kn^2. \tag{2}$$

The left part of this equation represents the number of electrons which are liberated under radiation of intensity I; the right part is the number of electrons which are returning into the filled zone.

The strength of the current flowing through the irradiated semiconductor located between the electrodes is expressed in the following form:

$$i = 2\,neu\frac{\Delta V}{d}S, \tag{3}$$

where ΔV is the difference of potential between the electrodes, S is the area of the electrodes, d is the thickness of the semiconductor, n is the concentration of the current carriers of given sign, u is the mobility of the latter and e is the charge of the carriers. Taking (2) and (3) into account, we obtain:

$$i = \frac{2\Delta VSeu}{d}\sqrt{\frac{\alpha}{k}I}. \tag{4}$$

If it is considered that the increase of the current strength of a couple under irradiation is determined principally by the radiational conductivity in the semiconducting oxide film, then, designating the constant quantities which enter into (4) by A, we obtain the following relationship between the current strength of the couple and the intensity of radiation

$$J_k = J_k^0 + A\sqrt{I},$$

where J_k^0 is the current strength of the couple in the absence of radiation and I is the intensity of radiation.

In Fig. 3 there are shown curves giving the relation between the current strength of the Zr–Al couple and the intensity of radiation, these having been obtained by calculation • (Curve 1) and experimentally (Curve 2).

• The magnitude of the constant k is found from experimental data on the relation between J_k and I at a single value of the quantity I.

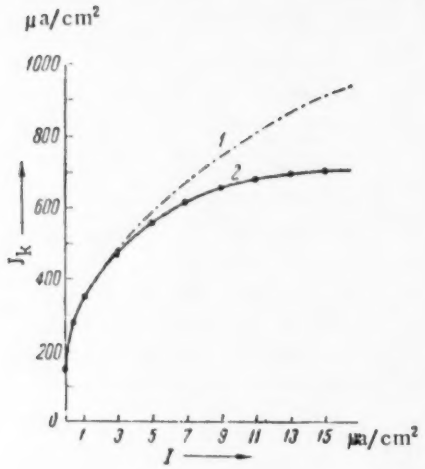

Fig. 3. The relation between the current strength of the couple Zr−Al in 3% NaCl and the intensity of the electron radiation: 1) calculated curve; 2) experimental curve.

The Institute of Physical Chemistry of the Academy of Sciences of the USSR

It follows from these graphs that at relatively low intensity of radiation there is a satisfactory agreement between the theoretical and experimental curves. The departure of the experimental curve from the calculated at higher intensities is obviously due to the presence of anodic polarization, which was not taken into account in the calculations.

In conclusion, it should be noted that the question as to the influence of short-lived disintegration products remains open. Further investigation must show whether it is possible to completely ascribe the increase in the electrochemical activity of the zirconium cathode under irradiation to the enhanced conductivity of the semiconductive film or whether it is necessary to also take into account the depolarizing action of short-lived radicals.

Received December 14, 1956.

THE PROPERTIES OF PLASTIC MASSES FILLED WITH GRAPHITE AND THE EFFECT OF HIGH FILLING*

B. L. Tsetlin, L. P. Yanova, G. K. Sibirskaya and
Academician P. A. Rebinder

As is known, the properties of the various materials based on high molecular compounds can be essentially improved by the introduction of active fillers. The action of such active fillers is brought about by the influence of the surface of their particles on the development of structure in the filled organic medium. It has been shown in a series of investigations [1-5] that in those cases where a space structure can develop in this medium (a coagulation net), the particles of the active filler serve as centers of development for such structure, giving rise to an increase of its durability (strengthening). This also determines the strengthening action of active fillers in such systems as rubbers treated with bitumen, etc.

We have investigated the influence of graphite as an active filler in a series of systems, more precisely in the systems graphite-bakelite resin and graphite-polyvinyl chloride. Systems of this kind have great practical significance in connection with the problem of obtaining stable thermally conducting materials for the preparation of chemical heat-exchange apparatus. The earlier known plastic materials with graphite fillers (of the types "grafolit" and "faolit T"), containing 50-60 weight percent of filler, do not possess adequate mechanical strength and their thermal conductivity does not exceed $3\text{-}5 \times 10^{-3}$ cal/cm·sec·deg [6].

In investigating the character of the change of the properties of materials filled with graphite over a wide interval of compositions, we have started from the supposition that on approaching the limiting resin capacity, when practically all of the resin goes into the form of a fully structured film on the surface of the filler particles and produces a sturdy coagulation net of these particles which interact through the thin residual layers of the filled medium, there must be observed a sharp increase in the strength of the material as well as its other characteristics.

For their subsequent investigation, samples of given composition were obtained in the following way. A calculated quantity of powdered graphite** was mixed with the corresponding quantity of resin solution: in the case of the phenolformaldehyde resin, ethyl alcohol served as the solvent (there was taken bakelite lac No. 21); in the case of polyvinyl chloride, dichloroethane. The resulting paste was dried to complete removal of the solvent. The necessary samples were prepared from the powders produced in this way by pressing them in closed press-forms with electrical heating and under conditions which were uniform for each system.

There were investigated the mechanical strength, the thermal stability and the thermal conductivity, i.e., those properties which are the most important ones from the point of view of the practical problem at hand. In

---

* This work was carried out in the Institute of Physical Chemistry of the Academy of Sciences of the USSR in 1949 and 1950; its results were outlined in Institute Reports Nos. 191 (June, 1950) and 454 (July, 1951).

** In the experiments which are described here there was employed a graphite from the Botogolski region which is used as a raw material in the preparation of lead pencils.

the case of the graphite-bakelite systems the mechanical strength was evaluated from experiment on monoaxial compression of samples 10 · 10 · 3 mm at 20 and 120°; in the case of systems with polyvinyl chloride the strength was evaluated from experiments on the penetration of a cylinder of small diameter (2 mm). As an arbitrary measure of the strength there was taken in this case the pressure under which there occurred either shearing, for the highly filled, brittle samples, or observable plastic flow, for the relatively low filled plastic

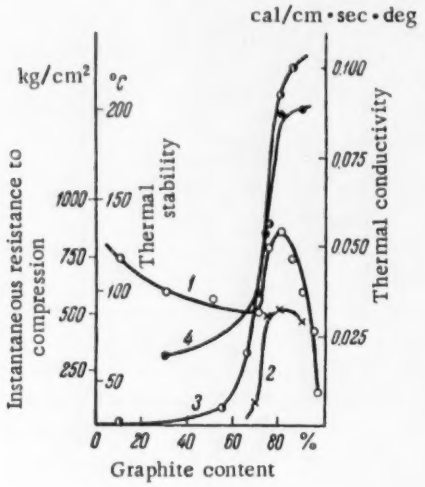

Fig. 1. The influence of composition on the properties of samples from the graphite-bakelite system: 1 and 2) mechanical strength at 20° (1) and at 120° (2), 3) thermal conductivity, 4) thermal stability.

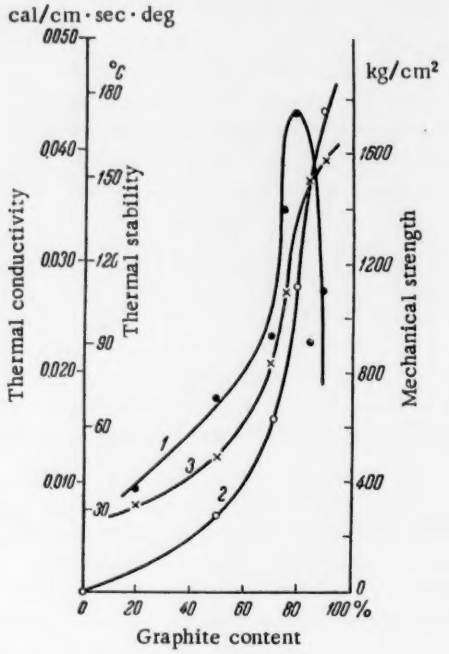

Fig. 2. The influence of composition on the properties of samples from the graphite-polyvinyl chloride system: 1) mechanical strength at 20°, 2) thermal conductivity, 3) thermal stability.

samples. Evaluation of the relative thermal stability was carried out from the thermo-mechanical curves [7] by determining that temperature at which the deformation of the sample reached a certain arbitrary magnitude under a fixed load which was continually acting in the course of the experiment; the thermo-mechanical curves were obtained with the aid of the apparatus of [8] under a constant heating rate of 50° per hour; this deformation regime meets the conditions for penetration of cylinders of small diameter: in the case of graphite-bakelite compositions the diameter of the cylinder was equal to 0.9 mm with a load of 7 kg; in the case of graphite-polyvinyl chloride compositions the diameter amounted to 5 mm with a load of 5 kg. The thermal conductivity of most samples was investigated by the comparative method of Christiansen; the thermal conductivity of highly filled graphite-bakelite samples were measured by an absolute method* ; for samples of intermediate composition data obtained by the two methods were in satisfactory agreement.

The results of investigation are presented in Figs. 1 and 2 in the form of curves showing the relationship between the properties of the experimental samples and their content of the filler. Consideration of these results shows that all of the investigated properties actually undergo a sharp rise on passage from samples with

---

* These determinations were performed in the Institute of General and Inorganic Chemistry of the Academy of Sciences of the USSR in the laboratory of N. N. Sirot, to whom the authors express their thanks.

relatively low filling (containing less than 70 weight percent, i.e., less than, say, 60 volume percent) over to highly filled samples. Thus, the thermal conductivity, which shows a steady increase over the entire interval of composition, experiences a sharp rise on passage to samples which contain 75-80 weight percent of filler, reaching a value of about 0.1 cal/cm·sec·deg, at a content of 80-85 weight percent of graphite, this corresponding approximately to the thermal conductivity of lead.

Special interest attaches to the new relation which is expressed in the peculiar course of the mechanical strength curve, although there is a certain difference here between the two investigated systems. For graphite-bakelite samples the strength of the material falls on the introduction of graphite up to 50-60 weight percent, but on going over to specimens containing 75-80 weight percent of graphite there is noted a considerable strengthening of the material, which is especially great in experiments carried out at elevated temperature; further increase in the content of the filler (up to 90-95 weight percent) once more leads to a rapid diminution of the strength. In the graphite-polyvinyl chloride system, with an increase in the content of the filler the strength of the material increases throughout the entire composition range, although even here the transition to highly filled specimens is marked out by an abrupt strengthening, and, after passage through a maximum in the region of approximately 80 weight percent content of graphite, the strength, as in the first case, rapidly falls. The thermal stability shows the same trend in both cases; after relatively slowly increasing in the region of low filled samples, its magnitude undergoes a sharp elevation with transition to highly filled specimens.

Thus, the experimental data shows that a narrow range of compositions, which is obviously close to the maximum resin capacity (i.e., for the studied systems, at graphite contents around 80 weight percent or 70 volume percent), is characterized by an optimum of the most important properties of the material. This phenomenon has been designated by us as the "effect of high filling." The sharp increase in the thermal conductivity on transition to highly filled specimens is obviously brought about by the disappearance in the narrow region of limiting resin capacity of the thick layers of organic binder which separate the particles of the highly thermally conductive filler. The maximum on the mechanical strength curves is determined by the fact that in the optimum region of highly filled compositions all of the resin which is present in the composition is maximally structured by the surface action of the grains of graphite.* The decrease in the strength of specimens in the graphite-bakelite system which is brought about by the introduction of relatively small quantities of graphite results, in all likelihood, from the appearance of inhomogeneities in the material and, at the same time, from the presence of additional dangerous positions of overstrain and of "nuclei" of disintegration. The formation of structure in the resin under the influence of the filler still does not play a pronounced role, since the layers of resin which separate the particles of the filler have a considerable thickness and a coagulation structure has not yet formed from the particles of filler; in addition the strength of the bakelite resin is so great at ordinary temperatures that a small number of regions tending to produce structure in it would not reflect on the strength of the material as a whole. The steady increase of strength over the regions of low filled graphite-polyvinyl chloride samples indicate that a more uniform system is obtained here wherein the effect of structure formation immediately acquires a great role which, even by itself, has great significance in the case of polymeric resins of linear structure; it is possible that a certain role is also played by the traces of solvent which are difficultly separated through drying.

From the point of view of the ideas which have been developed here there is also to be understood the course of the curves of thermal stability, the study of which shows that the strengthening effect is brought out more strongly at higher temperatures.

Of course, it should be kept in view that the characteristics of the highly filled system must in a great measure be determined not only by the absorptive-structural forming action of the filler, but also by the "volume" properties of the starting components– the resin and the graphite. In particular, the nature and the dispersion of the graphite can be reflected in the character of the effect of high filling. It is possible that in this effect a definite role is played by the friction between those particles of the filler which are in contact with one another.

---

* From the relaxational character of the process of rupture of polymeric materials it follows that structural formation in them under the action of active fillers will not be reflected in strength in relation to rapidly applied loads (shock); for this reason highly filled compositions possess relatively low stability to shock.

The investigations which have been carried out in our laboratory on systems based on polystyrol and polyethylene filled with graphite confirm the fact that the effect of high filling has general significance for such systems.

Technological investigations performed on the background of this work have led to the preparation of materials highly filled with graphite, or graphitic plastics, which are already in use in the chemical industry as thermal conducting plastic masses.

LITERATURE CITED

[1] P. A. Rebinder and V. B. Margaritov, J. Rubber Industry 12, 991 (1935); V. B. Margaritov, The Physico-Chemical Technology of Latex and Rubber, Moscow-Leningrad, 1941.

[2] P. A. Rebinder, G. A. Ab, and S. Ya. Veiler, Proc. Acad. Sci. USSR 31, 5, 444 (1941).

[3] Z. V. Volkova and N. M. Sobinyakova, Colloid J. 3, 6, 553 (1937).

[4] Ya. B. Aron and P. A. Rebinder, Proc. Acad. Sci. USSR 52, 3, 235 (1946).

[5] P. Rebinder, Disc. Farad. Soc. 18, 151 (1954); L. A. Abduragimova, P. A. Rebinder, and N. N. Serb-Serbina, Colloid J. 17, 3, 184 (1955).*

[6] I. F. Kanavetz and A. I. Lebedev, Organic Chem. Industry 3, 170 (1939).

[7] V. A. Kargin and T. I. Sogolova, J. Phys. Chem. 23, 5, 530 (1949).

[8] B. L. Tsetlin, V. I. Gavrilov, N. A. Velinkovskaya and V. V. Kochkin, Factory Lab., 3, 352 (1956).

The Institute of Physical Chemistry
of the Academy of Sciences of the USSR

Received December 17, 1956.

* Original Russian pagination. See C. B. Translation.

DETERMINATION OF THE OXIDATION-REDUCTION POTENTIALS OF p-HYDROXYPHENYLGLYCINE

Ya. M. Veprik and G. P. Faerman

(Presented by Academician A. N. Tereninyi, September 20, 1956)

There is still no universally accepted explanation of the mechanism and rules of the process of photographic development. One explanation, the so-called "electrochemical" theory of development, in contrast to other theories, is not only qualitative, but, in principle, it also admits of quantitative confirmation [1]. For such confirmation, it is necessary to know the electrochemical potentials of the silver particles of a developable photographic image and the oxidation-reduction potentials of the developing agents at different pH values and in the presence of the other components of the developer.

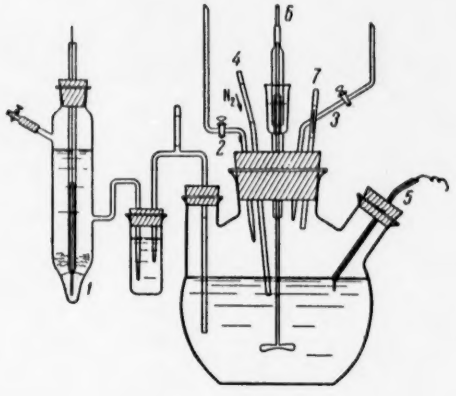

Fig. 1. Reaction vessel: 1) saturated calomel electrode; 2) buret; 3) microburet; 4) inlet for purified nitrogen; 5) platinum electrode; 6) stirrer with liquid seal; 7) gas vent.

Measurement of the oxidation-reduction potentials of the developing agents is very difficult owing to the ease of oxidation of these substances and the instability of the oxidation products. As a result, it is impossible to use the "method of mixtures" [2, 3], and methods based on titration with oxidizing agents [4] are applicable only under conditions such that the titration is carried out in an atmosphere of inert gas containing the least amount of oxygen. Therefore, the amount of data available in the literature on the oxidation-reduction potentials of developing agents at various pH values is very limited. More complete data are available for p-aminophenol, methyl-p-aminophenol (metol), and hydroquinone [5-9]. Data are available for several substances over limited pH ranges [8].

We set as our goal the experimental determination of the oxidation-reduction potentials of p-hydroxyphenylglycine ("glycine") at various pH values. The selection of this material was dictated by the fact that it is used in photographic applications and is the structural analog of the well-studied metol and p-aminophenol, and, therefore, the data obtained could be used for comparison.

The measurements were carried out by oxidation titration of 0.03 M solutions of p-hydroxyphenylglycine in an atmosphere of nitrogen, carefully purified from oxygen and other impurities, and using a polished platinum electrode. A description of the method of nitrogen purification and of the control method is given in detail in [10]. The solution to be titrated was placed in the reaction cell (see Fig. 1) which was then placed in a

thermostated water bath at a temperature of 25°. The potentials were measured against a saturated calomel electrode. The p-hydroxyphenylglycine was carefully purified. Constant pH was assured by the presence in the titration mixture of salts forming buffer systems. A mixture of HCl, KCl, and potassium hydrogen phthalate was used at a pH of from 1 to 6; at a pH of from 6 to 11, a mixture of borax, HCl, and NaOH was used [11]. Measurement of the pH was carried out with a glass electrode. No pH variation was noticed during the process of titration. In an acid medium, a solution of $Ce(SO_4)_2$ was used as the oxidizing agent, while a solution of $K_3[Fe(CN)_6]$ was used in an alkaline medium.

During experiments on the titration of p-hydroxyphenylglycine in acid medium, it was observed that there were two potential surges on the titration curve; the first corresponded to two oxidation equivalents of cerium (IV) sulfate, and the second, more significant, one corresponded to four equivalents of cerium (IV) sulfate per mole of p-hydroxyphenylglycine. Only one potential surge, corresponding to four equivalents of cerium (IV) sulfate per mole of p-hydroxyphenylglycine, was observed during the back titration. This is explained by the fact that, under these conditions, the oxidation reaction proceeds in the presence of an excess of oxidizing agent. Only one potential surge, corresponding to four equivalents of $K_3[Fe(CN)_6]$ per mole of p-hydroxyphenylglycine, was observed during either the direct or the back titration in alkaline medium.

Special experiments established that, both in the first and in the second stage of oxidation, the oxidized form remains in the solution without change for some time, and the oxidation reaction proceeds reversibly. There is basis to assume that the oxidation of p-hydroxyphenylglycine in acid medium proceeds according to:

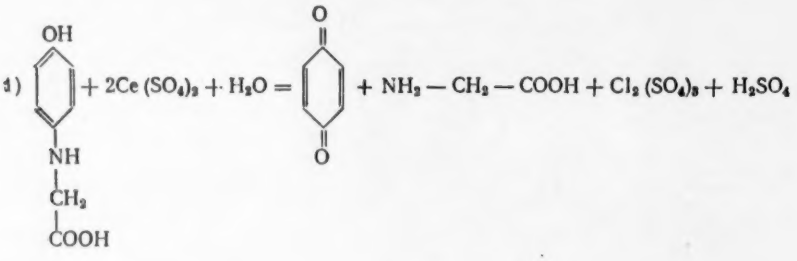

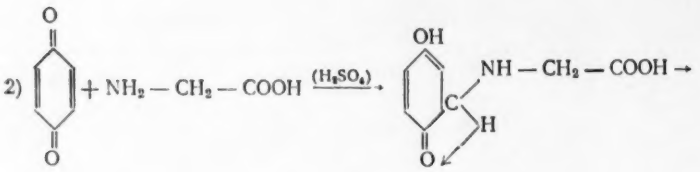

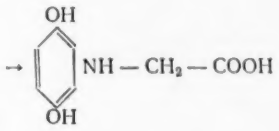

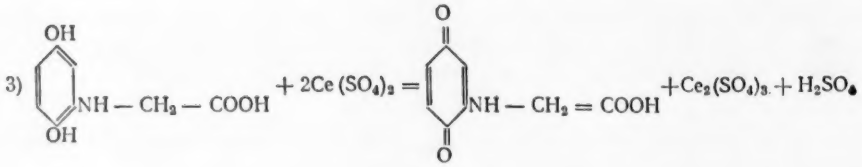

The over-all equation can be written as:

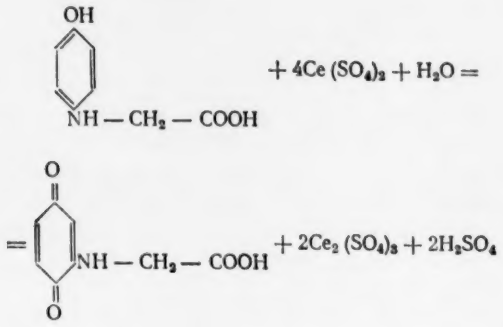

TABLE 1

pH	1.04	1.97	2.96	4.03	4.98	6.96	8.02	9.04	9.98	10.9
E_n, in mv	670.0	616.0	559.0	499.0	439.0	323.0	267.0	209.0	164.0	116.0

The values obtained for the oxidation-reduction potential of p-hydroxyphenylglycine at various pH values are presented in Table 1 and Fig. 2, where, in addition to the curve of $E_n = f(pH)$ for p-hydroxyphenylglycine, are presented curves for p-aminophenol and metol. The values presented for E_n were obtained from potentiometric titration curves for p-hydroxyphenylglycine at various pH values, and correspond to the point $\frac{[Ox]}{[Red]} = 1$ under conditions such that 1 mole of p-hydroxyphenylglycine consumes four equivalents of oxidizing agent. From Fig. 2 it is seen that the relationship $E_n = f(pH)$ for p-hydroxyphenylglycine is a straight line without breaks in the pH interval of 1.0 to 9.0. This means that the dissociation constant of p-hydroxyphenylglycine as a base is significantly less than that as an acid. The values of these constants could not be determined from the curves of $E_n = f(pH)$ in this case. Also,

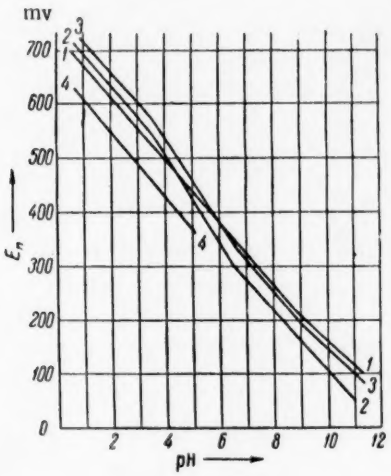

Fig. 2. Variation in E_n with pH for p-hydroxyphenylglycine during removal of 4e (1), during removal of 2e (4), metol (2), and p-aminophenol (3).

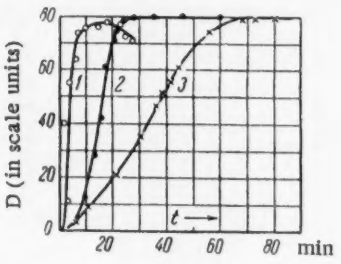

Fig. 3. Variation in rate of reduction of silver nitrate: 1) p-hydroxyphenylglycine; 2) metol; 3) p-aminophenol.

they could not be determined by the usual methods, since the oxidized form of p-hydroxyphenylglycine could not be isolated in the pure state. Therefore, we were unable to express the relationship analytically, as was done by Fieser [5] and Bogdanov [6, 7] for p-aminophenol and metol.

Comparison of the curves $E_n = f(pH)$ for p-hydroxyphenylglycine, metol, and p-aminophenol shows that E_n is more negative for p-hydroxyphenylglycine than for metol and p-aminophenol in acid medium, and that it is more positive in alkaline medium.

We observed that the reduction of $AgNO_3$ by p-hydroxyphenylglycine in acid medium proceeded more rapidly than the reduction of $AgNO_3$ by metol and p-aminophenol (Fig. 3). From photographic practice it is known that alkaline glycine developer works more slowly than p-aminophenol and metol. These facts are readily explained by the relationship, noted above, of the values of the E_n potentials of these substances at various pH values. Thus, in the experiments was observed precisely that relationship of reaction rates for the reduction of silver ions as would be expected on the basis of the electrochemical theory of development.

LITERATURE CITED

[1] G. P. Faerman, Prog. Sci. Photog. 4, 127 (1955).

[2] W. D. Bancroft, Z. Phys. Chem. 10, 387 (1892).

[3] R. Peters, Z. Phys. Chem. 26, 193 (1898).

[4] W. M. Clark, The Determination of Hydrogen Ions, Third Edition, 1928.

[5] L. F. Fieser, J. Amer. Chem. Soc. 52, 4915 (1930).

[6] S. G. Bogdanov, J. Phys. Chem. 5, 10, 1445 (1934).

[7] S. G. Bogdanov, J. Phys. Chem. 7, 5, 733 (1936).

[8] E. G. Ball and T. T. Chen, J. Biol. Chem. 102, 691 (1933).

[9] A. E. Cameron, J. Phys. Chem. 42, 1224 (1938).

[10] G. P. Faerman and Ya. M. Veprik, J. Sci. and Applied Photography and Cinematography, No. 2 (1957).

[11] Yu. Yu. Lurye, Calculating and Reference Tables for Chemists,* 1947, pp. 181-182.

Leningrad Institute of Cinema Engineers

Received October 17, 1956.

* In Russian.

INVESTIGATION, BY THE CHARGING CURVE METHOD, OF THE NATURE OF LOCAL PASSIVITY DURING ELECTROLYTIC POLISHING OF COPPER

G. S. Vozdvizhensky and A. I. Turashev

(Presented by Academician A. N. Frumkin, December 4, 1956)

A specific peculiarity of the process of electrolytic metal polishing is local passivity of the anode. Ideas on the nature of this effect remain the subject of discussions. Many of the existing theories of electrolytic metal polishing connect the mechanism of the process with the possibility of the formation of oxide films on isolated parts of the surface being treated. However, the very question of the existence of oxide films on the surface of the anode during the process of electrolytic polishing has not been decided. Some investigators consider that oxide films are formed and play an important role in the electrolytic polishing of metals [1-7]; others, having studied the condition of the electropolished surface, consider that it consists of the pure metal [8-11].

The problem of the present investigation was to investigate the formation of oxide films on a copper surface during electrolytic polishing in phosphoric acid solution, the investigation being carried out by the method of anode charging curves (anode polarization curves) using oscillographic recording. In the present case, the polarization curves had to be recorded at the high current densities at which the electrolytic polishing process is carried out. This circumstance forced us to judge the nature and properties of the layers formed on the anode surface, not by the magnitude of the corresponding potentials, but by the character of the effect of various factors on the anode polarization curve (current density, acid concentration, various additives, initial state of the surface). It is obvious that a charging curve obtained under the electrolytic polishing regime must have a specific form. A variation in factors having a known effect on the anode process must lead to a change in the character of the anode polarization curve.

EXPERIMENTAL

The anode polarization curves were recorded by means of an apparatus based on that proposed by A. Hickling [12]. In Fig. 1 is presented the polarization curve for a copper electrode, taken at a current density of 12.5 amp/dm^2 in a phosphoric acid solution of 1.55 sp. gr.

The first stage (ab), during which time the potential changed insignificantly from + 0.48 to + 0.52 volts, had the longest duration. The second stage (bc), in the potential interval + 0.52 to + 0.70 volts, was characterized by a more rapid change in potential, which changed into a jump (cd, from + 0.70 to + 0.88 volts). Owing to this jump, there was a pause in potential increase (third stage, de), after which again began a more rapid rise in potential up to the liberation of oxygen (stage fg at a potential of + 1.75 volts).

Prior to the liberation of oxygen, electrolytic polishing is possible in all stages except the first. Thus, the minimum potential at which electrolytic polishing of copper is possible lies in the region of the second stage on the charging curve.

With the aim of clarifying the nature of the first stage, experiments were carried out in which anode polarization curves were taken at various current densities and in phosphoric acid solutions of different concentrations (sp. gr. 1.55, 1.59, and 1.77).

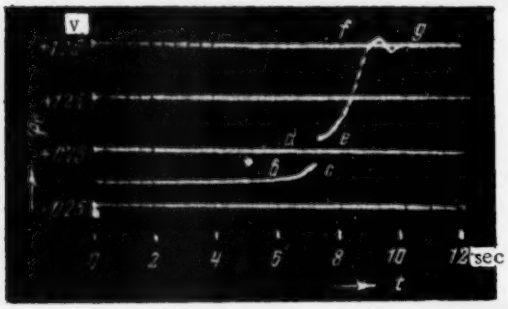

Fig. 1

It was established that, for each phosphoric acid solution investigated, the product of the current density, i, and the $^1/_2$ power of the duration of the first stage, t, is a constant. An analogous relationship was established by the investigations of Edwards [13]. Constancy of the product $it^{1/2}$ indicates that the limiting process of this stage is diffusion [14].

Furthermore, the more rapid increase in anode potential (stage bc) can be explained by electrolytic oxidation of the anode surface. The change in anode potential in the first stage was sufficient for initiation of the process of oxidation of the surface of the copper to cuprous oxide. The cuprous oxide formed led to the discontinuous change of anode potential to a value at which the formation of cupric oxide was possible, as expressed by the voltage pause on the polarization curve.

This finds confirmation in the anode polarization curves taken in the presence of various additives (glycerin, potassium hypophosphite, chromium trioxide) and on surfaces of different structures.

The addition of glycerin, which basically acts through an increase in the viscosity of the electrolyte, caused a decrease in the duration of the first stage. The addition of potassium hypophosphite, which is an energetic reducing agent, increased the duration of the second stage by a factor of two. This indicates that the potassium hypophosphite reduces the electrochemically formed cuprous oxide, acting, thereby, as a depolarizer.

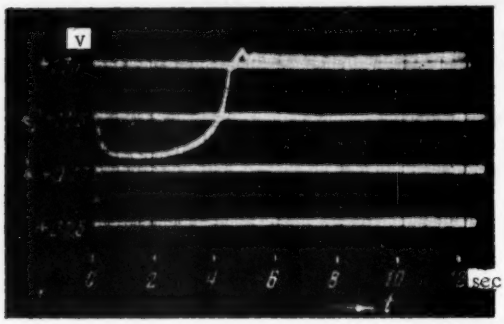

Fig. 2

In Fig. 2 is presented an anode polarization curve for a copper electrode in H_3PO_4 (d = 1.5) with the addition of 6% CrO_3. A characteristic peculiarity of polarization curves obtained in the presence of CrO_3 is a discontinuous change of potential at the beginning of anode polarization, which is caused by the formation of an oxide film on the surface of the electrode prior to superimposing the current. After the discontinuous change at the beginning of polarization, the potential falls to a value corresponding to the third stage in a solution of pure phosphoric acid. This permits us to assume that the third stage on the polarization curve obtained with a solution of pure phosphoric acid corresponds to the process of oxidation of cuprous oxide to cupric oxide.

With the addition of CrO_3 in amounts of 1, 2, 4, 6, and 8%, cuprous oxide is apparently formed on the surface of the copper electrode, since the static potential does not exceed the value of the potential in the region of the second stage. With the addition of CrO_3 in amounts of 10 and 20%, the static potential in time reaches the value of the potential of the third stage owing to the conversion of cuprous to cupric oxide.

Polarization curves obtained with surfaces which had been preliminarily electrolytically oxidized to cuprous and cupric oxides [15, 16] also confirm the idea of the formation of oxide layers during the process of electrolytic polishing of copper in phosphoric acid.

Preliminary oxidation of the surface to cuprous oxide makes the pause on the polarization curve (third stage) more definite and longer, and oxidation to cupric oxide makes the curve almost vertical.

Polarization curves during electrolytic polishing of the galvanized scrap from sulfuric acid and pyrophosphate copper plating baths indicate the different electrochemical activity of these residues as expressed by the different durations of the individual stages on the polarization curve. Apparently, oxide films of identical chemical composition have different protective actions owing to their different thicknesses. The kinetics of the growth of a film is determined by the crystalline structure of the treated surface [17].

LITERATURE CITED

[1] A. V. Fortunatov and A. V. Finkelshtein, Proc. Acad. Sci. USSR 90, 823 (1953).

[2] P. V. Shigolev and G. V. Akimov, Proc. Acad. Sci. USSR 100, 499 (1955).

[3] P. V. Shigolev and N. D. Tomashov, Proc. Acad. Sci. USSR 100, 327 (1955).

[4] A. T. Vagramyan and A. P. Popkov, Proc. Acad. Sci. USSR 102, 297 (1955).

[5] H. R. Nelson, Phys. Rev. 57, 559 (1940).

[6] T. P. Hoar and A. S. Mowat, Nature 165, 64 (1950).

[7] S. Wernick and R. Pinner, Sheet Metal Industry 30, 571 (1953).

[8] I. A. Allen, Trans. Farad. Soc. 48, 273 (1952).

[9] H. Frisby, Chem. Abstr. 43, 4960 f (1949).

[10] Finch, Proc. Third International Conference on Electrodeposition, (London, 1947), p. 43.

[11] W. Vernon, J. Inst. Met. 65, 301 (1939).

[12] A. Hickling, Trans. Farad. Soc. 41, 333 (1945).

[13] I. Edwards, J. Electrochem. Soc. 100, 189C (1953).

[14] L. Gierst and A. Juliard, J. Phys. Chem. 57, 701 (1953).

[15] B. B. Dey and A. Jogarao, et al., Chem. Abstr. 48, 11961 b (1954).

[16] A. G. Samartsev, Oxide Coatings on Metals * Izd. AN SSSR, 1944, p. 81.

[17] G. S. Vozdvizhensky, A. Sh. Valeev, and T. N. Grechukhina, J. Phys. Chem. 25, 87 (1955).

A. E. Arbuzov Chemical Institute
Kazan Branch of the Academy of Sciences, USSR.

Received December 4, 1956.

* In Russian.

ON THE RELATIONSHIP OF VISCOSITY COEFFICIENT TO THE STRUCTURE OF A SUBSTANCE IN THE LIQUID STATE

A. Z. Golik and D. N. Karlikov

(Presented by Academician G. V. Kurdyumov, November 12, 1956)

The connection between the coefficient of viscosity and other physical properties and, first and foremost, the structure of a substance in the liquid state is of great interest both in the development of the theory of the liquid state and, particularly, viscosity, and in the practice of physicochemical analysis. However, this connection has not been established up to the present time both as a consequence of the absence of the necessary information on the structure of liquids and as a consequence of insufficient study of their physical properties.

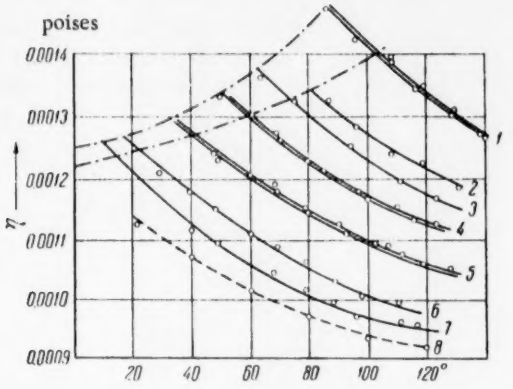

Fig. 1. Temperature dependence of the viscosity of solutions of Zn and Cd in Hg. 1) 30.8% Cd and 21% Zn; 2) 16% Zn; 3) 22% Cd; 4) 18% Cd and 12% Zn; 5) 13.9% Cd and 8.7% Zn; 6) 7.3% Cd; 7) 6.1% Cd; 8) Hg.

We attempted to surmount the difficulties arising along the road to a clarification of the connection of viscosity with the structure and physical properties of liquids by a rational selection of other structure-sensitive properties as objects of investigation and study simultaneously with viscosity. These materials for investigation were selected on the basis of similarity of their molecular structures. Density, viscosity, heat of vaporization, molecular dispersion, and critical temperature were studied in a broad temperature interval. It was shown that curves showing the dependence of viscosity and of heat of vaporization on temperature were located higher, and similar curves of compressibility were lower, the higher the critical temperature of the given substance [1].

We have also shown that the relationship of viscosity and of other structure-sensitive properties to critical temperature is a consequence of the periodic law of D. I. Mendeleev [2]. The density, viscosity, heat of vaporization, and critical temperature of molecularly mixing solutions, the components of which possess similar molecular structures, have also been studied. It was shown that viscosity-temperature curves for these solutions fall between the curves for the individual components and are higher, the higher the (pseudo) critical temperature of the given solution. With equality of critical temperatures of two or several solutions of this group, complete coincidence of the temperature-viscosity curves is observed. We have named such liquids isoviscous. We resolved to use isoviscous liquids in establishing the connection between viscosity coefficient and molecular structure.

We used, in the investigation, solutions of zinc and cadmium in mercury, the structure, viscosity, and density of which were studied by us previously [3-5]. These solutions belong to the molecularly mixing type, and their components possess similar structures; in Fig. 1 is presented the dependence of viscosity on temperature for several of these solutions.

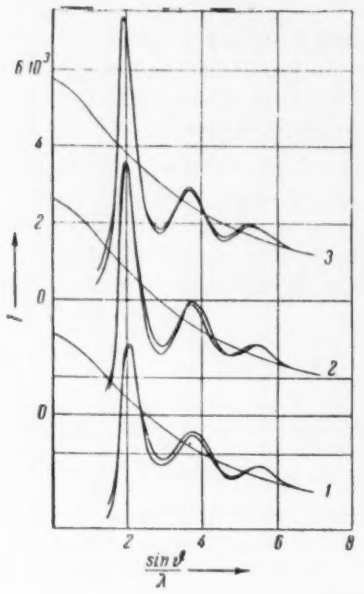

Fig. 2. Curves showing the intensity of diffracted X-rays. Isoviscous solutions in Hg: 1) 30.8% Cd and 21% Zn; 2) 18% Cd, 12% Zn; 3) 13.9% Cd and 8.7% Zn.

The following solutions are isoviscous: 13.9% cadmium in mercury and 8.7% zinc in mercury; 18% cadmium in mercury and 12% zinc in mercury; 30.8% cadmium in mercury and 21% zinc in mercury (all percents are atomic). The structure of these solutions was studied.

The source of the X-rays was a BCV-4 tube with a copper anti-cathode. Monochromatization of the X-rays was achieved by reflection of the rays from a curved quartz crystal. The distribution of the intensity of the diffracted X-rays was investigated photographically. The temperature of the metal was determined by means of a chromelalumel thermocouple. Photometric evaluation was carried out with a type MF-4 microphotometer. Not less than three photographs suitable for calculation purposes was obtained for each solution.

After elimination of polarization and absorption factors, the experimental intensity curves were reduced to electronic units. Equating of the following integral to zero served as a criterion of accurate reduction:

$$\int_0^{s_0} s^2 [i'(s) - 1]\, ds = 0,$$

where

$$i'(s) = \frac{I}{n_1 f_1^2 + n_2 f_2^2}; \quad s = 4\pi \frac{\sin \vartheta}{\lambda};$$

I is the intensity of the scattered radiation; f_1 and f_2 are atomic factors for, respectively, atoms of the first and second kinds; n_1 and n_2 are concentrations of atoms of the first and second kinds.

The experimental intensity curves in electronic units for the above-mentioned isoviscous solutions are presented in Fig. 2. As seen from the figure, curves showing the variation in intensity with $\sin \vartheta/\lambda$ for isoviscous solutions are superimposed one on the other.

In Table 1 are presented data on the positions of the maxima on these curves.

The atomic distribution functions were determined from the equation [8]

$$4\pi r^2 [c_2^1 n_1 \rho_1 (1) + c_1^2 n_2 \rho_2 (2) + 2 n_1 \rho_2 (1)] =$$
$$= 4\pi r^2 [c_2^1 n_1 \rho_1^0 + c_1^2 n_2 \rho_2^0 + 2 n_1 \rho_2^0] + \frac{2r}{\pi} \int_0^\infty i(s) \sin sr\, ds, \qquad (1)$$

where

$$c_2^1 = [f_1 / f_2]_{av}; \quad c_1^2 = [f_2 / f_1]_{av}; \quad n_1 = N_1 / N; \quad n_2 = N_2 / N; \quad N = N_1 + N_2$$

TABLE 1

Substance	Temp. °C	Major max.	2nd max.	3rd max.
[6]	20	0.190	0.360	0.525
13.9% Cd in Hg	70	0.195	0.367	0.530
18% Cd in Hg	70	0.200	0.370	0.538
30.8% Cd in Hg	110	0.202	0.373	0.540
Cd [7]	350	0.203	0.360	0.550
8.7% Zn in Hg	70	0.194	0.368	0.530
12% Zn in Hg	70	0.200	0.372	0.540
21% Zn in Hg	110	0.202	0.373	0.540
Zn [7]	460	0.228	0.380	–

$\rho_1(1) = N_1 W_1(1)/V$ is the radial density function of atoms of the first kind when an atom of this kind is found at the coordinate origin; $\rho_2(2) = N_2 W_2(2)/V$ is the radial density function of atoms of the second type when an atom of the second type is found at the coordinate origin;

$$i(s) = \frac{I/N - n_1 f_1^2 - n_2 f_2^2}{f_1 f_2} s;$$

N_1 and N_2 are the amounts of atoms of the corresponding type; V is the scattering volume; $W_1(1)$ and $W_2(2)$ are radial probability functions for atoms of the first and second kinds; ρ_1^0 and ρ_2^0 are the average densities of atoms of the first and second kinds.

The integral in Equation (1) was evaluated by the method given in [9].

In Figs. 3 and 4 are presented the atomic distribution curves, obtained by the described method, for isoviscous solutions.

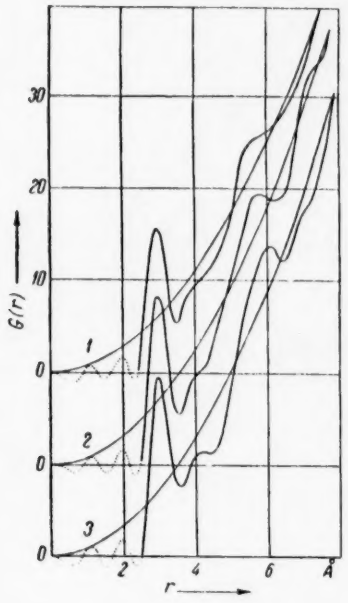

Fig. 3. Atomic distribution curves for solutions of Cd in Hg: 1) 30.8% Cd; 2) 18% Cd; 3) 13.9% Cd; $G(r) = 4\pi r^2 [c_2^1 n_1 \rho_1(1) + c_2^1 n_2 \rho_2(2) + 2n_1 \rho_2(1)]$.

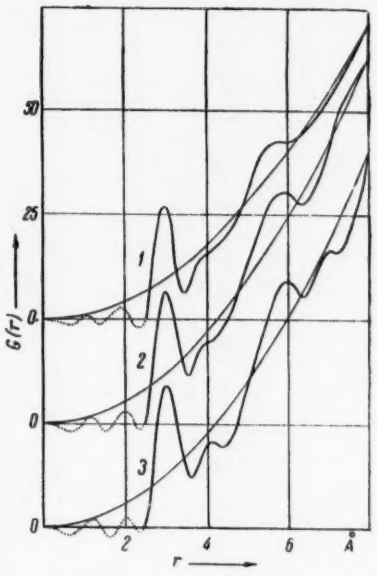

Fig. 4. Atomic distribution curves for solutions of Zn in Hg: 1) 21% Zn; 2) 12% Zn; 3) 8.7% Zn.

Analysis of the atomic distribution curves for the isoviscous solutions, just as analysis of the intensity curves, discloses their complete similarity. Consequently, liquids with the same coefficient of viscosity (isoviscous) possess, to the same close extent, the same structure.

LITERATURE CITED

[1] A. Z. Golik, S. D. Ravikovich, and A. V. Orishchenko, Ukrain. Chem. J. 17, 5, 627 (1951).

[2] A. Z. Golik, Proc. Acad. Sci. Ukrain. SSR, No. 4 (1955).

[3] A. Z. Golik, Proc. Acad. Sci. Ukrain. SSR, No. 1 (1952).

[4] A. Z. Golik and N. A. Ryndich, Ukrain. Phys. J. 1, 2, 170 (1956).

[5] A. Z. Golik and D. M. Karlikov, Proc. Acad. Sci. Ukrain. SSR, No. 3 (1957).

[6] D. N. Karlikov, A. F. Skrishevsky, and D. P. Karlikova, Sci. Records Krivoi Rog. Pedag. Inst. No. 2 (1957).

[7] C. Gamertsfelder, J. Chem. Phys. 9, 6 (1941).

[8] A. S. Lashko, Questions of the Physics of Metals and Metallurgy, 6, 66 (1955).

[9] A. S. Lashko, Proc. Acad. Sci. Ukrain. SSR, No. 3 (1953).

T. G. Shevchenko Kiev State University and the
Krivoi Rog Pedagogical Institute

Received November 6, 1956.

ON THE QUESTION OF THE EXISTENCE OF METAKAOLINITE AND THE NATURE OF THE EXOTHERMIC EFFECTS OF ALUMINA

A. M. Kalinina and E. A. Porai-Koshits

(Presented by Academician M. M. Dubinin, December 7, 1956)

As is well known [1], kaolin, in the uncalcined state, exists in the form of $Al_2O_3 \cdot 2SiO_2 \cdot 2H_2O$ crystals. On heating, dehydration occurs accompanied by an endothermic effect in the temperature range 450-600°, the kaolin being converted to the amorphous state. A number of investigators consider that the kaolin is thereby decomposed into free aluminum oxide and silica [2, 3], others [4, 5] consider that an amorphous compound (metakaolinite) is formed on dehydration. The first exothermic effect (970°) is also explained variously by crystallization of the amorphous alumina into the γ-modification [6], by the decomposition of metakaolinite into free alumina and silica with subsequent crystallization of γ-Al_2O_3 [4], by the formation of mullite $3Al_2O_3 \cdot 2SiO_2$ [7], and, finally, by the formation of sillimanite $Al_2O_3 \cdot SiO_2$ [8]. Attempts to shed light on these contradictory data by investigation of the behavior of alumina on heating to 950-1050° has also not met with success [5, 7], this apparently being explained by the dependence of this behavior on the nature of the original samples and by the experimental conditions [9]. In general, the number of detected modifications of alumina varies from four (α, β, γ, φ) [10] to ten (α, χ, η, δ, θ, κ, and 4 γ-modifications) [11, 12].

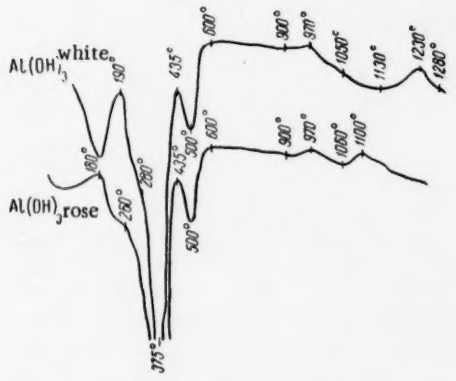

Fig. 1

The aim of the present work was to clarify, by means of thermographic and X-ray investigations, the nature of the thermal effects of alumina and to obtain additional experimental material for a solution of the problem of the existence of metakaolinite as a definite chemical compound. Aluminas obtained from aluminum nitrate, aluminum sulfate, and hydrargillite were used for this purpose. The investigation of hydrargillite, $Al(OH)_3$ (or $Al_2O_3 \cdot 3H_2O$) having the general structural elements of kaolin (layers composed of aluminum-oxygen and aluminum-hydroxyl-oxygen octahedra) [13], was of additional interest.

The X-ray investigation was carried out both in a proportional ionization chamber with a high-temperature (to 1400°) heater (CuK_α radiation, nickel filter) and with 65.1 mm diameter Debye cameras (CoK_α radiation, monochromatization by reflection from a calcite crystal).

In Fig. 1 are presented heating curves for two samples of hydrargillite, white and rose (the latter contained 0.014 % Fe_2O_3).* In addition to the previously known three endothermic effects [14], two exothermic effects

* Chemical analysis carried out in the analytical laboratory of the Institute of Silicate Chemistry of the Academy of Sciences, USSR.

were observed on the curves: in the range 940-1050° (maximum 970°) for both samples, in the range 1060 to 1150° (maximum 1100°) for the rose sample, and in the range 1180-1280° (maximum 1230°) for the white sample.

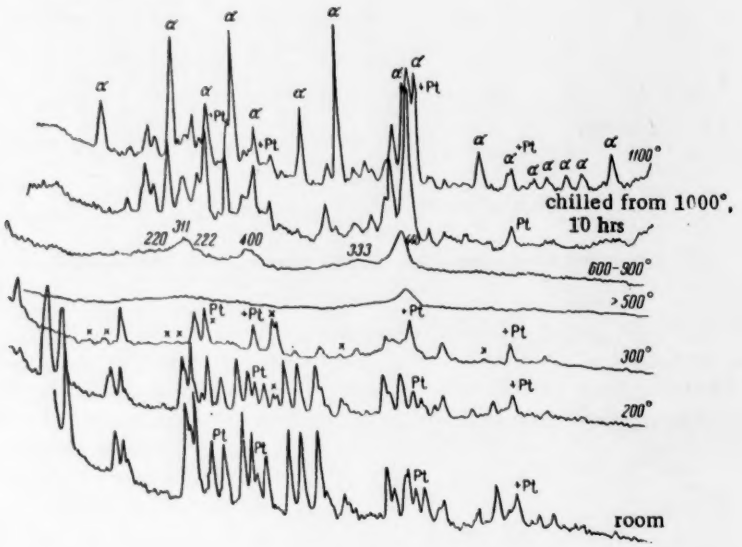

Fig. 2

In Fig. 2 are presented X-ray ionization curves obtained at the temperatures indicated at the right. At 200° (the temperature region of the first endothermic effect in which partial elimination of water occurs [14]: $Al_2O_3 \cdot 3H_2O \rightarrow Al_2O_3 \cdot 2.5\,H_2O + 0.5\,H_2O$), there was a marked appearance of the lines of a new phase (the nature of which remains unclarified and the lines of which are marked by crosses), and weakening and some dispersion of the hydrargillite lines occurred, indicating partial disintegration of its lattice. At 300° (region of the second endothermic effect where further elimination of water occurs: $Al_2O_3 \cdot 2.5H_2O \rightarrow Al_2O_3 \cdot H_2O + 1.5\,H_2O$), the hydrargillite structure completely disintegrated, and the monohydrate, $Al_2O_3 \cdot H_2O$ – boehmite, was formed, as was amorphous alumina, the insignificant amount of which is apparent from the dispersion of the maxima in the region of 31-35° angles.* The latter is confirmed by the curve obtained at 500° (third endothermic effect), where the lines of boehmite and the unknown phase completely disappeared, and the entire sample was converted to the amorphous or highly dispersed state (two very broad maxima, the position of the second of them being very close to the most intense line (440) of the low temperature modification of alumina). The formation of the finely crystalline, cubic (spinel structure, defect type) low-temperature γ-modification of alumina (γ_l) takes place at a temperature of 600°, to which the rise on the heating curve of hydrargillite corresponds (Fig. 1). The γ_l-modification of alumina is stable in the temperature range 600 to 950°. At the temperature of the first exothermic effect (maximum 1000°), the formation of the κ-modification of alumina occurred, this modification being stable over a small temperature interval; at the temperature of the second exothermic effect, the κ-modification was converted to the α-modification (corundum). The beginning of its transition to corundum depends on the presence of impurities in the samples: in the rose sample of hydrargillite, which contained 0.014% Fe_2O_3, crystallization of corundum began at 1050°, while in the white sample it began only at a temperature of 1200°.

---

* The more intense lines of platinum (the samples were held in a platinum holder during the exposure) are superimposed on certain maxima, as indicated by the sign + Pt.

The scheme of the thermal conversions of hydrargillite can be represented as follows:

$$Al(OH)_3 \text{ hydrargillite} \xrightarrow{190^\circ} \left\{ \begin{array}{c} \text{Hydrargillite,} \\ \kappa\text{-phase} \\ 200^\circ \end{array} \right\} \xrightarrow{260^\circ} \left\{ \begin{array}{c} \text{Boehmite,} \\ \kappa\text{-phase,} \\ \text{amorphous} \\ \text{alumina} \\ 375^\circ \end{array} \right\} \xrightarrow{435^\circ} \left\{ \begin{array}{c} \text{Amorphous} \\ \text{or finely} \\ \text{dispersed} \\ \text{alumina} \\ 500^\circ \end{array} \right\} \xrightarrow{600^\circ}$$

$$\xrightarrow{600^\circ} \underset{600-950^\circ}{\gamma_l\text{-}Al_2O_3} \xrightarrow{950^\circ} \underset{1000^\circ}{\kappa\text{-}Al_2O_3} \xrightarrow{1050-1200^\circ} \underset{1100-1230^\circ}{\alpha\text{-}Al_2O_3}$$

A different course of thermal conversions was observed with alumina obtained from aluminum nitrate and from aluminum sulfate (Fig. 3). On the heating curve of $Al(NO_3)_3 \cdot 9H_2O$ there were three endothermic effects (two weak with maxima at 180 and 250°, and a third, large effect with a maximum at 380°) and two exothermic effects (a clearly expressed effect with a maximum at 850° and a highly dispersed effect with a maximum at 1050°). On the heating curve of $Al_2(SO_4)_3 \cdot 18H_2O$ there were only endothermic effects with maxima at 100, 350, and 900°. No exothermic effects were observed at temperatures up to 1100°. The first two endothermic effects on the curves of both samples were due to the elimination of adsorbed water and water of crystallization.

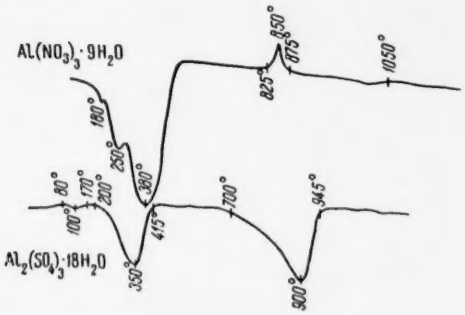

Fig. 3

At a temperature of 380° (heating curve of $Al(NO_3)_3 \cdot 9H_2O$), decomposition of the $Al(NO_3)_3$ occurred, accompanied by conversion of the material to the amorphous state [as indicated by two broad maxima on the ionization curves obtained at temperatures of 600 and 800° (Fig. 4, a)]. The maximum at a temperature of 850° (exothermic) corresponds to crystallization of the amorphous (or highly dispersed) alumina into the γ_l-modification of alumina (Fig. 4, b). This fact refutes the idea that crystallization of the γ_l-modification of alumina must be accompanied by the absorption of energy [15].

The γ_l-alumina obtained from aluminum nitrate remained stable up to the beginning of crystallization of corundum at the temperature of the second exothermic effect, 1050°.

The scheme of the thermal conversions of alumina obtained from aluminum nitrate can be represented as follows:

$$Al(NO_3)_3 \xrightarrow{380^\circ} \left\{ \begin{array}{c} \text{Amorphous or} \\ \text{highly dispersed} \\ \text{alumina} \end{array} \right\} \xrightarrow{825^\circ} \underset{850^\circ}{\gamma_l\text{-}Al_2O_3} \xrightarrow{1000^\circ} \underset{1050^\circ}{\alpha\text{-}Al_2O_3}$$

The decomposition of aluminum sulfate proceeded at temperatures lying considerably above the stable region of amorphous alumina. Therefore, crystallization of γ_l-alumina was observed simultaneously with decomposition (900°) (Fig. 4, d). The transition to α-alumina began at 1200° (Fig. 4, e), i.e., considerably above that in the case of the alumina obtained from $Al(NO_3)_3$. The scheme of the thermal conversions of the alumina obtained from aluminum sulfate has the form:

$$Al_2(SO_4)_3 \xrightarrow{900^\circ} \gamma_l\text{-}Al_2O_3 \xrightarrow{1200^\circ} \alpha\text{-}Al_2O_3$$

Thus, a clearly expressed exothermic effect at 950-1050° was obtained only with alumina obtained from hydrargillite. However, the liberation of energy in this case was dependent on crystallization of the κ-modification, while in the case of kaolin in this temperature region, there is observed the formation of γ_l-alumina [3, 6].

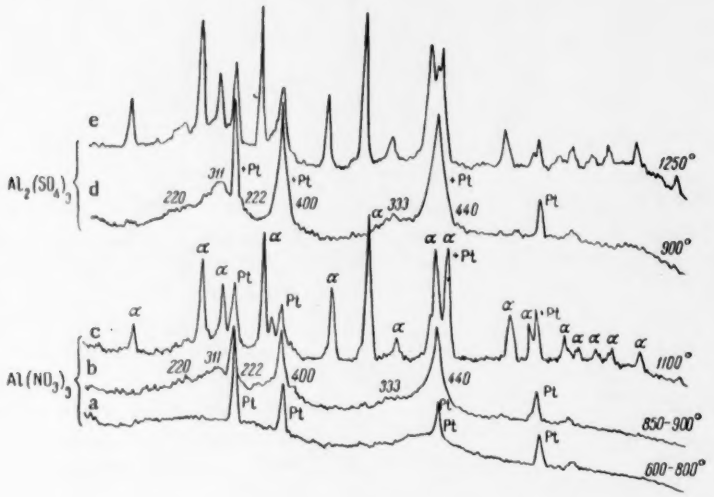

Fig. 4

As was shown above, crystallization of γ_l-alumina proceeds either after dehydration of the hydrargillite and decomposition of the nitrate, accompanied by conversion to the amorphous state, or simultaneously with decomposition, as was observed with the sulfate, but in any case at a temperature significantly below the first exothermic effect of kaolin. The absence of crystallization of alumina in the γ_l-modification from kaolin after dehydration (400-600°) indicates the presence of an intimate bond between the oxides, since free alumina would have to crystallize in the γ_l-modification at temperatures of 600-850°. X-ray pictures of Prosyansky kaolin (not purified by elutriation), obtained by us in the temperature range 600-1400°, showed that, along with the formation of mullite, the basic process, which corresponded to the first exothermic effect of kaolin (970°), is the formation of γ_l-alumina, crystallization of which proceeds only after destruction (possibly partial) of the $Al_2O_3 \cdot 2SiO_2$ complex.

LITERATURE CITED

[1] A. G. Betekhtin, Mineralogy,* 1950.

[2] E. K. Keler and A. I. Leonov, Prog. Chem. 22, 334 (1953).

[3] H. Insley and R. H. Ewell, J. Res. Nat. Bur. Stand. 14, 615 (1935).

[4] A. S. Ginzburg, Kh. S. Nikogosyan, and A. V. Chitaev, Trans. Inst. Appl. Miner. and Metallurgy, No. 22 (1926).

[5] P. Ya. Saldau, N. A. Zhirnova, and E. L. Klibinskaya, Ceram. Coll. 4, 24 (1939).

---

* In Russian.

[6] E. K. Keler and A. I. Leonov, Proc. Acad. Sci. USSR 91, 545 (1953).

[7] D. S. Belyankin and V. I. Ivanova, Coll. to Academician V. I. Vernadsky on the 50th Anniversary of His Scientific Activity, Izd. AN SSSR, 1936.

[8] V. N. Sveshnikova and V. G. Kuznetsov, Bull. Acad. Sci. USSR, Div. Chem. Sci. 1, 25 (1946).

[9] S. V. Potapenko, Miner. Raw Material, 9, 20, No. 6 (1934).

[10] D. S. Belyankin, Trans. Inst. Geol. Sci. 106, 30, 1 (1949).

[11] H. C. Stumpf, A. S. Russel, I. W. Newsome, and C. M. Tucker, Ind. and Eng. Chem. 42, 1398 (1950).

[12] E. I. W. Vervey, Zs. f. Krist. 91, 317, 3-4 (1935).

[13] X-ray Methods for the Determination of Clay Minerals,* (Foreign Lit. Press, 1955), p. 46. (Translation).

[14] K. M. Feodotyev, Coll. to Academician D. S. Belyankin on His 70th Birthday, Izd. AN SSSR, 1946.

[15] V. I. Lebedev, Proc. Acad. Sci. USSR 89, 335, 2 (1953).

Institute of Silicate Chemistry of the
Academy of Sciences, USSR.

Received December 6, 1956.

* Probably: G. W. Brindley, X-ray Identification and Crystal Structures of Clay Minerals, The Mineralogical Soc., London, 1950.

NONSTEADY STATE PROCESSES DURING ANODIC SOLUTION OF COPPER IN ORTHOPHOSPHORIC ACID

S. I. Krichmar

(Presented by Academician A. N. Frumkin, December 14, 1956)

During the study of electrochemical polishing, as well as of other electrode processes which are accompanied by significant concentration polarization, one of necessity runs afoul of phenomena whose nature is directly connected with the formation of a diffusion layer around the electrode.

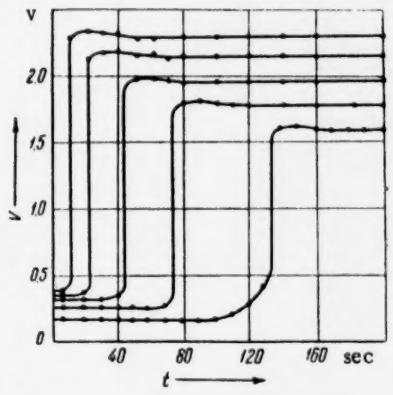

Fig. 1. Variation of V with t. H_3PO_4 concentration, 15 moles/liter.

V. I. Lainer [1] pointed out the presence of more or less sharp rises in voltage on potential-time curves obtained during electrochemical polishing of copper in orthophosphoric acid solutions. We observed analogous phenomena on current-time curves obtained while maintaining constant voltage across the bath.

During anodic solution of copper in orthophosphoric acid, maxima are observed on the voltage-amperage curves at the beginning of the limiting current plateau. The form of the curves in the limiting current region depends on the methods of obtaining the curve [2]. In the case, considered in the present work, of anodic solution of copper in phosphoric acid, nonsteady state processes during the formation of the anode layer are connected with diffusion transfer of material in the immediate vicinity of the electrode, since in highly concentrated solutions of H_3PO_4 (8-15 moles/liter) the relatively high viscosity (10-60 centipoises) probably relegates convection transfer of material during the electrolytic process to a secondary role.

The mechanism of diffusion kinetics for the case of a nonsteady state process at the cathode in an unagitated electrolyte at a fixed current strength has been described by Sand and Levich [3]. For the case considered here, the problem can be solved similarly.

The boundary and initial conditions for the molecular diffusion equation

$$\frac{\partial C}{\partial t} = D\frac{\partial^2 C}{\partial x^2} \qquad (1)$$

are the following:

$$1)\ C(0,\ y) = 0; \quad 2)\ \left(\frac{\partial C}{\partial y}\right)_{y=0} = \frac{I}{nFDS} = \text{const},$$

where C is the concentration of copper in the solution, I is the current strength, S is the electrode surface, and D is the effective diffusion coefficient.

We introduce a new variable:

$$u = C_s - C, \tag{2}$$

where C_s is saturation concentration. In terms of the new variable, the boundary problem has the form:

$$1)\ u(0,\ y) = C_s; \quad 2)\ \left(\frac{\partial u}{\partial y}\right)_{y=0} = \left(\frac{\partial C}{\partial y}\right)_{y=0} = \frac{I}{nFDS};$$

the form of basic Equation (1) is unchanged.

In this form, the boundary and initial conditions of our problem agree with conditions for the cathode; therefore, we may immediately make use of the solution proposed by Sand and Levich for the cathode:

$$u = C_s - \frac{2I}{SnF}\sqrt{\frac{t}{\pi D}}\,e^{-y^2/4\pi D} + \frac{2Iy}{SnFD\sqrt{\pi}}\int_{y/2\sqrt{Dt}}^{\infty} e^{-z^2}dz. \tag{3}$$

Substituting for $\underline{u}$ in (3) we obtain

$$C = \frac{2I}{SnF}\sqrt{\frac{t}{\pi D}}\,e^{-y^2/4\pi D} + \frac{2Iy}{SnFD\sqrt{\pi}}\int_{y/2\sqrt{Dt}} e^{-z^2}dz. \tag{4}$$

The change in the concentration of reaction products immediately at the anode is given by the equation

$$C = \frac{2I}{SnF\sqrt{\pi}}\sqrt{\frac{t}{D}}. \tag{5}$$

It was indicated above that, in the case under consideration, the concentration of material at the surface of the anode cannot increase without limit. After reaching saturation concentration, there is a jump in potential, and a new process (gas evolution) begins. Depending on the fixed current strength in the system, the potential jump begins at different time intervals: the higher the current strength, the quicker the activity at the anode disappears and the sooner the potential jump.

In Fig. 1 is presented a series of typical potential-time curves obtained during anodic solution of copper in H_3PO_4 for I(t) = const.

In Fig. 2 is shown the variation in time of initiation of the potential jump, T, with current strength in the system; the curves were constructed according to the equation

$$T_s = \left(\frac{SnFC_s}{2I}\right)^2 \pi D \tag{5a}$$

and the points are experimental data. In constructing these curves, it was assumed that the magnitude of the diffusion coefficient for the reaction products is the same as that for a molecule of acid. The diffusion coefficient

was calculated from the Stokes-Einstein equation using values for the viscosity of H_3PO_4 solutions taken from [4]. The saturation concentration was obtained by extrapolation of data [5] on the dependence of limiting current on the concentration of reaction products in the solution.*

The values of the constants in Equation (5a) are presented in Table 1 for the electrolyte concentrations investigated.

TABLE 1

H_3PO_4 conc. moles/liter	C_s moles/liter	S, cm^2	D, cm^2/sec	n
8	2.0	0.5	10^{-5}	2
10	2.2	0.4	$6.6 \cdot 10^{-6}$	2
15	2.4	0.3	$1.1 \cdot 10^{-6}$	2

From the data presented, it may be seen that the equation of Sand and Levich is completely applicable to the calculation of the time of initiation of the potential jump for high concentrations of H_3PO_4 where the natural convection transfer of material is retarded by the high viscosity of the solution. For H_3PO_4 concentrations below 6 moles/liter, this equation is not suitable, since natural convection material transfer increases considerably under these conditions.

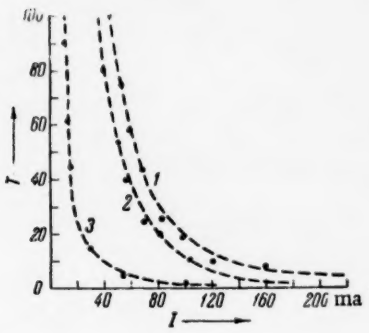

Fig. 2. Variation in T with I.
1) 8 moles/liter; 2) 10 moles/liter;
3) 15 moles/liter.

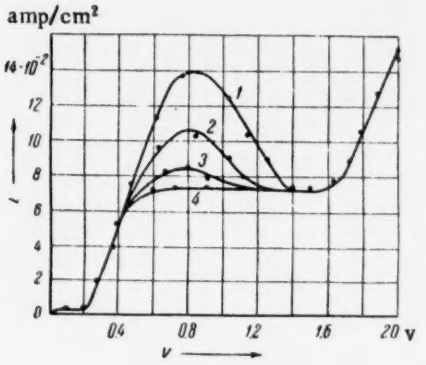

Fig. 3. Variation in I with V. Duration of polarization: 1) 10 sec; 2) 20 sec;
3) 30 sec; 4) 4 min.

On the basis of these ideas of the role of nonsteady state processes during anodic solution of metals, it is possible to give the following explanation of the maxima on the voltage-amperage curves obtained during the electrolytic polishing of copper in phosphoric acid. The usual method of taking voltage-amperage curves consists in sequentially changing the potential difference at the bath terminals and simultaneously (or subsequently)

* Since, as was shown in [5], the limiting current for the case of electrolytic polishing of copper in H_3PO_4 follows the equation: $i = nFD(C - C_0)/\delta$, where C is the concentration of products at the surface and C_0 is the concentration of products in the body of the solution, then within the limit when the concentration in the body of the solution has reached saturation we have $i = 0$ and $C = C_s$.

recording the current strength. In this method, the electrode goes from each previous measurement into a new electrochemical state in an already partially polarized condition. The intensity of the polarization is determined each time by the amount of electricity passing through the electrolytic cell, i.e., in the last analysis, by the duration of the electrolysis. Thus, if the points are taken sufficiently rapidly, the electrode goes into an electrochemical state corresponding to the limiting current but still with an unformed electrode layer; therefore, with a further increase in potential, the current strength still continues to increase for a certain time. The latter leads to a maximum on the curve in the region where limiting current begins. Thus, the size of the maximum and its form depends completely on the duration of anode polarization. This dependence is graphically illustrated by the following experiment.

In Fig. 3 is presented a series of voltage-amperage curves obtained with a 5 M solution of H_3PO_4. The points on these curves were obtained in the following manner: each time the anode was subjected to electrolysis for a strictly specified time, after which the current was interrupted, the electrode depolarized, and the subsequent measurement carried out at the new potential value. It is seen from the figure that the height of the maximum regularly decreases with an increase in polarization time, and it is completely absent at a comparatively high value of T.

LITERATURE CITED

[1] V. I. Lainer, Electrochemical Polishing and Etching of Metals, * 1949.

[2] P. M. Fedash and V. P. Galushko, Sci. Records of Dnepropetrovsk State University 37, 1817 (1951).

[3] V. G. Levich, Physicochemical Hydrodynamics,* 1952, p. 103; V. Levich, Acta Physicochim. URSS 19, 133 (1944); H. J. S. Sand, Phil. Mag. 1, 45 (1901).

[4] S. I. Sklyarenko and N. V. Smirnov, J. Phys. Chem. 25, 24 (1951).

[5] S. I. Krichmar, Proc. Acad. Sci. USSR 100, 481 (1955).

Dneprodzerzhinsk Nitrogen-Fertilizer Plant.

Received September 25, 1956.

* In Russian.

ON THE PROCESS OF COAL HALOGENATION UNDER THE INFLUENCE OF ULTRASONIC WAVES

B. I. Losev, I. E. Elpiner, and A. N. Melnikova

(Presented by Academician A. N. Frumkin, December 4, 1956)

The question of the halogenation of coal has recently became significant, since extraction of rare metals from coal is carried out primarily through halogenation of the latter. However, not only is there no accurate information on the halogenation mechanism, but the halogenation methods used are still rather ineffective. Thus, for example, the halogenation of coal proceeds extremely slowly at atmospheric pressure and room temperature. Methods providing for carrying out the halogenation process at high reaction temperatures and under pressure also result in the addition of chlorine or bromine in low percentages.

Halogenation of coal is a heterogeneous process. It takes place at the boundary separating two phases – solid coal and liquid or gaseous halogen. Naturally, more favorable hydrogenation conditions can be obtained through the use of methods for putting the solid phase in a more highly dispersed state, thereby increasing its total surface. In addition, increased activity of the reacting halogen should have an influence on the rate of the halogenation reaction. A new method used by us for the halogenation of coal – the use of ultrasonic waves – satisfies these requirements to a considerable extent. The reaction of halogens with coal is greatly accelerated by the action of ultrasonic waves, increasing considerably the yield from the reaction.

In the present communication, it will be shown that the bromination proceeds under relatively mild conditions of sonic treatment, i.e., at a comparatively low intensity of the ultrasonic waves. Moreover, the observations showed that under the influence of ultrasonic waves, not only is the reaction of liquid bromine with coal accelerated, but so is the reaction with gaseous chlorine.

We used a piezoquartz ultrasonic generator. The source of the ultrasonic waves was a circular piezoquartz plate of 50 mm diameter; the vibration frequency of the ultrasonic waves was 380 kc; the intensity was 8 watts per cm^2 of irradiated surface. The contact liquid between the emitter and the irradiated object was water. Propagation of the ultrasonic waves was accompanied by the appearance of a wave or small fountain on the surface of the water. The flask containing the reaction mixture was submerged in the "ultrasonic" fountain. The rapidly occurring (almost instantaneous) degasification of the irradiated liquid and the appearance of ripples on the surface of the liquid inside the flask indicated that the ultrasonic waves penetrated into the vessel. The distance of the reaction vessel from the emitter was 15-16 cm.

In the case of bromination, the reaction vessel contained 7 g of coal and 21 g of Br in 50 ml of distilled water. After the sonic treatment, the coal was filtered in a Buchner funnel and washed with distilled water until the wash water gave a negative reaction for bromine. The amount of bromine added to the coal was determined by the micromethod developed in the Institute of Fossil Fuels of the Academy of Sciences of the USSR: a sample of the coal weighing 6-12 mg was burned in a quartz tube in a current of oxygen; the combustion products were collected in a solution of KOH and H_2O_2, in which the bromine content was subsequently determined by titration by the Volhard method.

From the results of the investigation presented in Table 1, it is seen that 2.68 wt. % bromine (calculated on the dry coal) was added to the coal during 7 minutes bromination at room temperature, while with the same bromination time in an ultrasonic field 47.3 wt. % bromine was added. As much bromine was added to the coal during 7 minutes bromination with the indicated intensity of ultrasonic waves as was added during 20 hours at 0° without ultrasonic irradiation. In other words, the bromination process proceeded 160 times more rapidly under the influence of ultrasonic waves than under the usual conditions.

TABLE 1

Bromination of Long-Flame Coal Under the Influence of Ultrasonic Waves *

	Experimental conditions	Bromination time	Temp. °C	W^a	A^d	C^c	H^c	Br_2
Initial coal	–	–	–	3.04	12.50	81.56	6.63	–
2 g coal and 27 g Br_2 in 50 ml water	withour irrad.	20 hrs.	0	1.78	3.82	42.3	2.75	50.84
Same	" "	7 min.	20	2.91	11.68	73.7	5.79	2.68
Same	with irrad.	7 min.	20	2.87	7.01	43.41	2.85	47.3

* W^a – moisture in coal, wt. %; A^d – wt. % ash, dry basis; C^c – combustible carbon in coal, wt. %; H^c – hydrogen in the combustible matter of the coal, wt. %; Br_2 – bromine, wt. % calculated on the dry coal.

The chlorination of coal was carried out by us while slowly introducing gaseous chlorine into the reaction vessel – 2 bubbles of gas per second. Using this method of passing the gas through the reaction mixture (7 g of long-flame coal in 50 ml of distilled water), 2.98 wt. % chlorine (based on the dry coal) was introduced (the amount of chlorine was determined by the method described above). However, this percentage was considerably increased by carrying out the chlorination in a field of ultrasonic waves (Table 2).

TABLE 2

Chlorination of Long-Flame Coal Under the Influence of Ultrasonic Waves

Experimental conditions	Chlorination time, min.	Amount of chlorine, wt. % (on dry coal)
Without irrad.	20	2.98
With irrad.	10	3.48
With irrad.	20	6.91

As the table shows, the amount of chlorine reacting with the coal increased with an increase in the irradiation time. After 20 minutes in the ultrasonic field, almost 2.5 times more chlorine had reacted than during this same time without irradiation.

What mechanism was established by us for the halogenation of coal in an ultrasonic field ? It is well known that ultrasonic waves possess a dispersing action, due, most likely, to mechanical forces arising during the generation and collapse of cavitation bubbles. Considerable mechanical forces are also developed, apparently, by synchronization of the pulsation frequency of the generated gas bubbles with the frequency of the ultrasonic vibrations (resonance phenomenon). However, for the development of an appreciable dispersing effect, lengthy exposure to ultrasonic waves is required. In an analysis of the described facts, it is necessary to take into consideration the possibility of a genesis according to the cavitation electrochemical theory of ultrasonic chemical reactions – the possible appearance of activated halogen as a result of dissociation of the molecule in the cavitation voids. That the iodine molecule can dissociate with subsequent reduction in an ultrasonic field was established in 1950 [3]. It is also necessary to remember that as the result of splitting of "activated" water molecules in a cavitation void, products possessing oxidizing action appear [4, 5].

LITERATURE CITED

[1] B. I. Losev, Coll. Trans. All-Union Corres. Polytech. Inst. 1954.

[2] M. I. Shenbor, Ukrain. Chem. J. 18, 3 (1952).

[3] I. E. Elpiner and M. F. Koslesnikova, Proc. Acad. Sci. USSR 75, 6 (1950).

[4] R. O. Prudhomme and P. Grabor, J. Chim. Phys. 46, 323 (1949); M. Haissinsky and R. O. Prudhomme, J. Chim. Phys. 47, 925 (1950).

Institute of Fossil Fuels of the
Academy of Sciences, USSR.

Received October 2, 1956.

THE KINETICS OF MECHANICAL DEGRADATION OF HIGH POLYMERS

N. K. Baramboim

(Presented by Academician V. A. Kargin, December 13, 1956)

The breakdown of macromolecules of high polymers by mechanical action of various kinds appears to be a highly specific destructive process connected directly with the large dimensions of the macromolecules. The free macroradicals formed as a result of rupture by the action of mechanical forces are, in the absence of suitable acceptors, capable of undergoing the most diverse and characteristic transformations and recombinations with the formation of branched chains, cross-linked structures, copolymers, etc. In the presence of active acceptors such as atmospheric oxygen, the macroradicals may become stabilized and the process may thus have the effect of degradation of the polymer. It is this particular form of degradation which is being considered in the present communication.

In modern practice of high polymer processing one is confronted either with the intended application of the rupture of macromolecules, or with the necessity to take its occurrance into account during the mechanical treatment of the polymers. However, in spite of the enormous theoretical and practical importance of mechanical degradation,this method has only been studied in a few particular cases and for the most part within a rather narrow scope [1-3]. Recent investigations have demonstrated the possibility of widening the range of application of this phenomenon in the processing of polymers and of developing a number of original processes. However, because of the absence of systematic investigations of the dependence of mechanical degradation on the nature of the polymer, external conditions, etc., it was impossible to make any generalizations about the process even to a first degree of approximation. In view of this we have undertaken a detailed investigation of characteristic features of mechanical degradation of a wide range of hydrocarbon and hetero-chain polymers in relation to the medium, temperature and other factors with the object of discovering some general regularities governing this process.

In order to carry out the degradation in liquid as well as in gaseous media we have used different apparatus, including some of original design, in which the process could be performed under strictly controlled conditions.

In this paper we outline an experimentally founded general quantitative evaluation of the process of mechanical degradation of a number of polymers.

In Fig. 1 are plotted curves representing the variation of the molecular weight of different polymers with time during milling in a ball mill in an atmosphere of nitrogen and at a temperature of $T = -10°$. The shape of the curves indicates that the molecular weight of the products of degradation tends to a definite limit which is apparently determined by the ratio of the bond energy of the chemical bonds in the main chain to the energy of intermolecular interaction. The probability of chain rupture and the limiting molecular weights, both of which are determined by this ratio, can be calculated by the method given in [7]. However, such a calculation can only be very approximate, because at present we do not possess sufficient data for a quantitative determination of the micro and macro-heterogenities of the polymers.

Practically useful values of limiting molecular weights reached by mechanical degradation can be obtained from the experimental kinetic curves $M = f(\tau)$ by graphical extrapolation to infinite time, as shown in Fig. 2.

In the case of the polymers investigated by us the limiting molecular weights, M_∞, obtained by mechanical degradation are in the following order: polyvinylacetate – 11,000; acetyl cellulose – 10,000; polymethyl methacrylate – 9,000; polystyrene – 7,000; polyvinyl alcohol – 4,000.

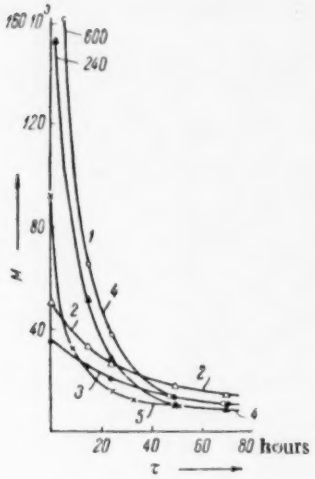

Fig. 1. Kinetic curves of mechanical degradation of different polymers: 1) polymethyl methacrylate; 2) polyvinyl acetate; 3) polyvinyl alcohol; 4) polystyrene; 5) acetyl cellulose.

Thus, while chemical or thermal degradation of a polymer leads to the monomer and its decomposition products as limiting units, it is fragments of chains which appear to be the limiting units in the case of mechanical degradation. The size of these fragments appears to be the function of the chemical nature of the polymer, other things being equal. This fragment, M_∞, is not directly related to the size of the mechanical segment of the given polymer as it depends on very definite conditions, namely, conditions under which the actual process of mechanical cracking is effected. In all probability the limiting unit in the case of each polymer depends, in general, not only on its chemical nature but also on temperature, the medium in which the process is carried out, as well as the frequency of the mechanical action. This characteristic feature of mechanical as distinct from other forms of degradation was observed in the case of all the polymers investigated so far.

From the analysis of the kinetic curves shown in Fig. 1 and using the limiting molecular weights we found – by the method of successive approximation – that the curves can be expressed with sufficient accuracy by the equation

$$M_\tau = Ae^{-k\tau} + M_\infty, \qquad (1)$$

where $A = M_0 - M_\infty$; M_τ is the molecular weight at time τ; τ is time taken for degradation; M_0 is the molecular weight before degradation; and k is the velocity constant of degradation.

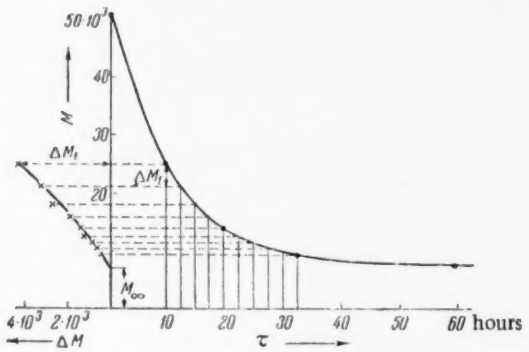

Fig. 2. Diagram for the determination of the limit, M_∞, from experimental kinetic curves. Polystyrene, t = 10°, in air.

The values of the constant k found for the polymers investigated are: polymethyl methacrylate – 0.1200; polystyrene – 0.0945; polyvinyl acetate – 0.0468; polyvinyl alcohol – 0.0237.

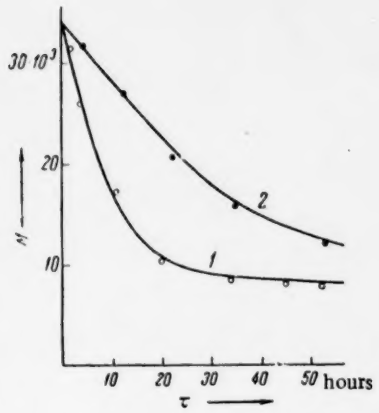

Fig. 3. Comparison of experimental (lines) and theoretical (points) values of molecular weights after mechanical degradation for different lengths of time: 1) polystyrene; 2) polyvinyl acetate.

This relation between the constants can, to a first approximation, be attributed to the difference in the rigidity of the chains and in the degree of close packing of these polymers.

Equation (1) can be obtained from theoretical considerations, if we make use of the idea of the limit of degradation. If we assume that the probability of chain rupture and hence, also, the velocity of degradation are proportional to the number of possible ruptures between the fragments whose molecular weight is equal to M_∞, then

$$\frac{-d\dfrac{M_\tau - M_\infty}{M_\infty}}{d\tau} = k\frac{M_\tau - M_\infty}{M_\infty}.$$

Separating the variables, integrating and transforming we finally obtain Equation (1). This equation is reminiscent of the kinetic equation of a first order chemical reaction, but only in form. It is valid for a given polymer and for definite experimental conditions, provided it is assumed that the fragment having the molecular weight M_∞ is the smallest kinetic unit split off by mechanical "depolymerization."

Such is the general picture of the process of mechanical degradation of amorphous glass-like polymers. The values of the constants in Equation (1) do, of course, depend on definite experimental conditions, i.e., temperature, medium and intensity of the mechanical action, etc., and can be used in evaluating the process under those conditions under which they have been determined.

In our case the experimental and theoretical values of the molecular weight after different periods of degradation are in very good agreement as will be seen from Fig. 3.

LITERATURE CITED

[1] I. Farberov and Yu. Margolina, J. Rubber Ind. No. 3, 230 (1935).

[2] P. P. Zhukov, V. A. Komarov, K. I. Gribova, and N. L. Selivanova, Synthetic Rubber, No. 4 (1936).

[3] B. Karmin and B. Betts Investigations in the Field of High Molecular Compounds, (Acad. Sci. Ussr Press, 1949), pp. 129-137.

[4] M. Pike and W. F. Watson, J. Polym. Sci. 9, 9, 3, 229 (1952).

[5] S. M. Lipatov and M. S. Schulman , Trans. All-Union Conf. Colloid Chem. (Acad. Sci. USSR Press, 1952), pp. 272-283.

[6] D. V. Zharkovsky and S. M. Lipatov, Bull. Acad. Sci. Byeloruss. SSR, 5, 115 (1953).

[7] N. V. Mikhailov and V. A. Kargin, Trans. 4th Conf. on High Molecular Compounds, (Acad. Sci. USSR Press, 1948), pp. 138-158.

Technological Institute of Light Industry,
Moscow

Received November 29, 1956.

THE C – H BOND RUPTURE ENERGY IN HYDROCARBONS

V. I. Vedeneev

(Presented by Academician N. N. Semenov, December 24, 1956)

The observed deviations from the additive nature of the heats of formation of paraffin hydrocarbons are small. This indicates that the C–H bond rupture energy, which depends to a considerable extent on the structure of the molecules, cannot be ascribed directly to the interaction between the atoms in the molecule itself. In fact, as we pass from methane to the higher members of the series the mean bond energies vary by approximately 1 kcal, whereas the corresponding bond rupture energies vary by about 8 kcal.

It is well known that in the case of diatomic molecules the energy of rupture of a single bond is exactly equal to the mean energy. When diatomic molecules undergo dissociation single atoms only are formed. The decomposition of a complex molecule gives rise to two radicals or to a radical and an atom. It is natural to assume that it is the radicals formed by the decomposition of molecules which are responsible for those variations in bond rupture energies observed experimentally. This problem has been treated in great detail by N. N. Semenov [1].

Semenov pointed out that the cause of the comparatively large variations in bond rupture energies must be sought not in the properties of the molecules RX, but in the properties of the radicals R and X formed as a result of the dissociation of the molecule, and arrived at a formula which in the case of C–H bond rupture in hydrocarbon molecules has the form

$$D(\mathrm{R}-\mathrm{H}) = D_{\mathrm{H}}^{0} - V(\mathrm{R}), \tag{1}$$

where V(R) is the energy of stabilization of the radical R and D_{H}^{0} is a constant.

The gain in energy obtained from the stabilization of the radical results from the interaction of the free valency with the remaining bonds in the radical. The extent of this effect will, of course, depend on the state of the free valency itself (π - or σ - state) as well as on the type of bond with which this free valency interacts. In addition, the extent of this interaction should, of course, vary with the distance.

Let us suppose that the energy of interaction of the free valency with the saturated bonds in the radical diminishes exponentially with distance. The energy of interaction of the free valency with one bond will be given by

$$V_n = \alpha_j e^{-\beta n}, \tag{2}$$

where α_j and β are coefficients characterizing the interaction in question, and n is the number of the carbon atom linked by the bond of the type j with which the free valency interacts. In the case of the carbon atom which carries the free valency, $n = 0$. Summating over all the bonds in the radical R we obtain

$$V(\mathrm{R}) = \sum_{j,n} j\alpha_j e^{-\beta n}, \tag{3}$$

$$D(\mathrm{R}-\mathrm{H}) = D_{\mathrm{H}}^{0} - \sum_{j,n} j\alpha_j e^{-\beta n}, \tag{4}$$

where j is the number of bonds of the j-th type attached to the n-th carbon atom. The method of expressing the distance in terms of the number of carbon atoms is, of course, a rough approximation. A comparison of the results calculated by the above formula with experimental data will show the degree of correctness of this assumption.

TABLE 1

C–H Bond Rupture Energies (in kcal)

Bond ruptured	By pyrolysis of iodine	By electron impact	By photobromination
CH_3–H	102	102	101
C_2H_5–H	97	98	98
n-C_3H_7–H	95	100	—
n-C_4H_9–H	94	101	—
sec -C_3H_7–H	89	97	—
tert -C_4H_9–H	86	89	89

It is possible to show that in calculating V(R) it is necessary to take into account the interaction of the free valency with single C–C bonds as this is automatically accounted for in the coefficients of interaction of the free valency with other bonds in the radical R.

In Table 1 are shown experimental values of the C–H bond rupture energies for paraffin hydrocarbons obtained by different methods.* The values of D(n-C_3H_7 – H) = 95 kcal and D(n-C_4H_9 – H) = = 94 kcal appear to be most reliable of all the values of D(C–H) obtained from data on the pyrolysis of iodides [3], while the values obtained for the rupture energy of the same bonds by the method of electron impact appear to be rather high [4]. If the values of D(C–H) in methyl groups of propane and butane, obtained by pyrolysis of iodides, are accepted as more accurate, then the experimental values of the bond rupture energies shown in Table 1 can be expressed satisfactorily by Formula (4), the values of the coefficients being

$$D_{\mathrm{H}}^{0} \simeq 161 \text{ kcal}$$
$$e^{-\beta} \simeq 0.4;$$
$$\alpha_j = \alpha_{\mathrm{CH}} \simeq 20 \text{ kcal}$$

The formula by which we can calculate the bond rupture energies of the C–H bonds for paraffin hydrocarbons will therefore have the form

$$D(\mathrm{C}-\mathrm{H}) \simeq 161 - 20 \sum j(0.4)^n \text{ **}. \tag{5}$$

In order to be able now to calculate D(R–H) for unsaturated hydrocarbons it is necessary to calculate first α_π, i.e., the coefficient α_j for the interaction of the free valency with a π-bond. In addition, if the free valency, existing in the "π-state," is situated in the α-position with respect to the π-bond, an amount of energy of conjugation equal to about 19-20 kcal is set free [6, 7]. Let us put $E_{\mathrm{conj}} \simeq 20$ kcal. To calculate α_π we use the value of the energy of dissociation of a hydrogen atom from the methyl group of

---

* Here the experimental values for the bond rupture energies are again taken from [2, 3].

** From Formula (5) it is easy to obtain the formula proposed by V. V. Voevodsky [5]:

$$Q_{\mathrm{CH}} = 78 + 8.0 \sum (0.40)^n i,$$

the correctness of which has been confirmed on several examples.

propylene which is equal to 77 kcal. By calculation we find $\alpha_\pi \simeq 24$ kcal. In order to calculate the bond rupture energies of C–H bonds in molecules containing conjugated π-bond systems, let us consider the benzene molecule. Let α_B denote the coefficient α_j which accounts for the interaction of the free valency with C–C bonds in benzene. Putting $D(C_6H_5 - H) \simeq 102$ kcal, we obtain $\alpha_B \simeq 11.5$ kcal.

If the benzene molecule is pictured as a system of alternating single and double bonds, the coefficient α_π for double bonds in benzene will be equal to $2\alpha_B \simeq 23$ kcal, that is, very nearly equal to the value $\alpha_\pi \simeq 24$ kcal found for the energy of interaction of the free valency with an isolated π-bond.

In view of this we may, when calculating the values of D(C–H) for molecules such as, for example, butadiene, make use of our conventional ideas of alternating single and double bonds.

TABLE 2

Bond ruptured	D(C–H) calc., kcal	D(C–H) found, kcal	Bond ruptured	D(C–H) calc., kcal	D(C–H) found, kcal
CH_3–H	101	101–102	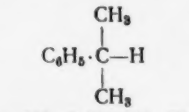	69.4	~71
C_2H_5–H	97	96–98			
n-C_3H_7–H	95.4	~95			
n-C_4H_9–H	94.7	~94			
sec-C_3H_7–H	93	89–93	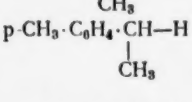	73.3	74
tert-C_4H_9–H	89	86–89			
cyclo-C_6H_{11}–H	90	~92			
$CH_2:CH\cdot CH_2$–H	77	77	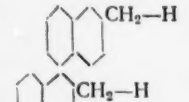	75.7	76
$CH_2:C(CH_3)\cdot CH_2$–H	75.4	~76			
$C_6H_5\cdot CH_2$–H	77.4	77.5			
o-CH_3–$C_6H_4\cdot CH_2$–H	76.7	~75	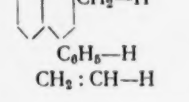	76.6	76
m-$CH_3\cdot C_6H_4\cdot CH_2$–H	77.2	~77			
p-$CH_3\cdot C_6H_4\cdot CH_2$–H	77.3	~76			
CH_3					
$C_6H_5\cdot CH$–H	73.4	~74	C_6H_5–H	102	102
			$CH_2:CH$–H	101	96–122

Having thus collected a set of coefficients α_j for the interaction of the free valency with C–H bonds, isolated π-bonds, C–C bonds such as in benzene, as well as the numerical values of D_H^0; $e^{-\beta}$ and E_{conj}, we may by means of Formula (4) calculate the C–H bond rupture energies for hydrocarbon molecules of the most diverse structure. Some results of such calculations and the corresponding experimental values are given in Table 2.

By means of Formula (4) it is possible to calculate the C–H bond rupture energies for molecules of different X-substituted hydrocarbons, where X may be a halogen atom or some other substituent. In order to do this it is necessary to calculate α_X, i.e., the coefficient α_j for the energy of interaction of the free valency with the C–X bond, from at least one experimentally determined value.

The method proposed here for the calculation of C–H bond rupture energies is, of course, very approximate, but it enables us to determine fairly rapidly and directly the C–H bond strength in hydrocarbon molecules of the most diverse structure.

LITERATURE CITED

[1] N. N. Semenov, On Some Problems of Chemical Kinetics and Reactivity, (Acad. Sci. USSR Press, 1954).

[2] T. Cottrell, The Strength of Chemical Bonds [Russian Translation] IL, 1956.

[3] M. Szwarc, Chem. Rev. 47, 75 (1950).

[4] E. W. R. Steacie, Atomic and Free Radical Reactions, New York, 1954.

[5] V. V. Voevodsky, Proc. Acad. Sci. USSR, 79, 455 (1951).

[6] J. L. Franklin and F. H. Field, J. Amer. Chem. Soc. 75, 2819 (1953).

[7] Ya. K. Syrkin and M. E. Dyatkina, Bull. Acad. Sci. USSR, Div. Chem. Sci., 1946, No. 2, 153.

Institute of Chemical Physics,
Academy of Sciences of the USSR.

Received December 21, 1956.

ON THE PROBLEM OF THE MECHANISM OF ION EXCHANGE

V. I. Gorshkov and G. M. Panchenkov

(Presented by Academician A. V. Topchiev, November 22, 1956)

Our current ideas about the mechanism of ion exchange do not allow us to form a clear picture of the influence of variations in the conditions of the exchange process, such as temperature and nature of the solvent, on the ion exchange equilibrium.

In the following we outline a mechanism of cation exchange based on results obtained in the course of investigations of ion exchange equilibria as well as on a number of other phenomena familiar from the literature (association of ions in electrolyte solutions, the dependence of the exchange capacity of weakly acid resins on the pH of the medium, slight lowering of the exchange capacity of sulfonated resins in alcohol, the possibility of ion exchange taking place between two resins, etc.).

An ion exchange resin is a high molecular weight poly-acid. When such a resin is immersed in a polar solvent, for example, water, it will undergo ionization as a result of the interaction with molecules of the solvent. However, since the anions of the resin are bound to each other they cannot distribute themselves throughout the entire volume of the solvent. As a result of the action of electrostatic forces the cations are likewise unable to diffuse throughout the volume of the solvent. As a result, an "ionic cloud" is formed near the surface of the exchange resin with a fairly high cation concentration. However, as has been shown by Sementschenko [1] and later by Bjerrum [2], in solutions of strong electrolytes at concentrations above 0.05 N association of ions can occur, i.e., a closer approach of ions of opposite sign under the action of electrostatic forces. Such association may be expected to occur with cations as well as with anions of the exchange resin. A diffuse layer of ions penetrating sufficiently far into the solvent may form on the external surface of the exchange resin, but within the resin network the thickness of this diffuse layer should, as a result of repulsion between opposite cations, be considerably less than the thickness of the external diffuse layer, and less the closer the dissociated groups are situated with respect to each other. To a first approximation the equilibrium may therefore be expressed as a two-stage process:

$$ABR \rightleftarrows A^+B^-R \rightleftarrows A^+ + B^-R, \tag{1}$$

where A^+ is the resin cation; B^-R is the anion group; ABR is the resin; A^+B^-R is the complex formed by the association of the cation and anion.

If the resin is present in a very fine state of subdivision, or if its degree of polymerization is low (so-called soluble exchange resins), the concentration of ions near its surface will not be very high and the equilibrium will be displaced to a considerable extent to the right. Under these conditions an "ionic cloud" will be formed near the surface of the resin particles. Evidence for this is provided by the fairly fast cation exchange between soluble and insoluble ion exchange resins [3].

In the case of the usual resins which do not form sols the main effect arises from the equilibrium

$$ABR \rightleftarrows A^+B^-R. \tag{2}$$

This equilibrium determines the total exchange capacity of the resin, i.e., the quantity of ions which can be exchanged under given conditions. Depending on the nature of the exchanging groups and on the conditions in which the resin is used the equilibrium may be displaced either way. Thus, in water it will, in the case of weakly acid groups such as OH and COOH, be displaced to the left and will depend strongly on the pH of the solution. In the case of sulfonic groups it will be displaced to the right.

On account of the less polar nature of alcohol the exchange equilibrium in alcoholic solutions will, even in the case of sulfonated resins, be displaced slightly to the left and the exchange capacity of the resin in anhydrous alcohol should be somewhat lower than it is in water.

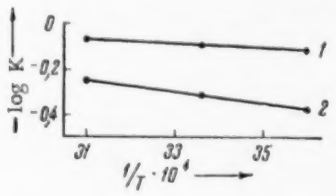

Fig. 1. Dependence of − log K on 1/T in ion exchange on H-type espatyte: 1) NaCl; 2) KCl.

A lowering of the exchange capacity has in fact been observed by us in some experiments on the exchange equilibrium of sodium chloride on sulfonated resins in 100% methanol. It was found that the higher the moisture content of the resin the nearer the exchange capacity was to its value in water. Apparently, even traces of moisture in the resin displace the equilibrium (2) to the right. As soon as the amount of water present is sufficient for all hydrogen ions to be hydrated the exchange capacity of the resin in alcohol becomes equal to its exchange capacity in water.

On adding to the solution other cations a proportion of these will displace cations of the resin and after some time an equilibrium will be established. For the sake of simplicity let us consider the exchange of monovalent ions.

In the case of the reaction $Me^+ + H^+SO_3^-R \rightleftharpoons H^+ + Me^+SO_3^-R$ we may assume that the change in free energy under standard conditions, $-\Delta F = RT \ln K$, consists of two parts: the electrostatic part, ΔF_{el}, equal to the change in free energy resulting from the substitution of a hydrogen ion in the ion pair $H^+SO_3^-R$ by a metal ion, and the nonelectrostatic part, ΔF_{nonel}, which accounts for effects resulting from the interaction of solvent molecules with ions taking part in the reaction. The first portion of this energy is equal to the work done on substitution of a hydrogen ion by a metal ion Me^+; this work is equal to the difference of the energies of electrostatic interaction of the cations H^+ and Me^+ with a resin anion.

Since the energy of interaction of a hydrogen ion with the monovalent SO_3^-R ion is given by $E_{H^+} = \epsilon^2/2Da_{H^+}$, where D is the dielectric constant, ϵ is the charge on the hydrogen ion and a_{H^+} is the distance between the ions H^+ and SO_3^-R, and since, by analogy, $E_{Me^+} = \epsilon^2/2Da_{Me^+}$, the electrostatic component of the change in free energy will be given by $\Delta F_{el} = \frac{N\epsilon^2}{2D}\left(\frac{1}{a_{H^+}} - \frac{1}{a_{Me^+}}\right)$, where N is Avogadro's number. Hence, we obtain

$$-\log K = \frac{\Delta F_{nonel}}{2.3RT} + \frac{N\varepsilon^2}{4.6DRT}\left(\frac{1}{a_{H^+}} - \frac{1}{a_{Me^+}}\right).$$

This formula helps us to explain a number of regularities discovered in the course of studies of ion exchange equilibria. Thus, using the same solvent, for example, water, we should in the case of the exchange of alkali metal ions for hydrogen obtain a linear relationship between log K and $1/a_{Me^+}$. The values substituted for a_{Me^+} were calculated for the parameter a^0 from activity coefficients by means of the Debye-Hueckel formula $\log \gamma_\pm = -A\sqrt{M}/1 + Ba^0\sqrt{M}$ [4]; in this way a linear relationship was obtained for a number of sulfonated resins studied by us. This is also in agreement with data from the literature [4, 5].

The difference in the exchange constants for one and the same metal on different resins is connected with differences in the nonelectrostatic component of the change in free energy, ΔE_{nonel}, resulting from differences in the structure of the hydrocarbon skeleton of the resins.

In the case of one and the same pair of ions exchanging in a given solvent we should expect to find a linear relationship between − log K and 1/T. Such a relationship was in fact observed in the case of the exchange of sodium and potassium ions on the H-type of several sulfonated resins (Fig. 1).

Furthermore, keeping the values of ΔF_{nonel} and $(1/a_{H^+} - 1/a_{Me^+})$ constant, a linear relationship should also be found between $-\log K$ and $1/D$.

Such assumptions may be made in the case of aqueous alcoholic solutions with low concentrations of alcohol, because in solvents of this kind the ions are preferentially hydrated (as may be inferred, for example, from measurements of ionic mobilities in aqueous alcoholic solutions [6]). Under these conditions the effect of adding alcohol is, to a first approximation, to change the dielectric constant only.

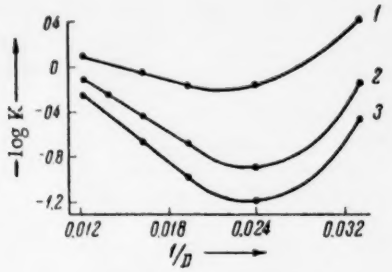

Fig. 2. Dependence of $-\log K$ on $1/D$ in ion exchange on H-type espatyte in mixtures of water and methanol: 1) LiCl; 2) NaCl; 3) KCl.

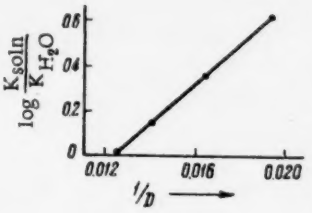

Fig. 3. Dependence of $\log \frac{K_{soln}}{K_{H_2O}}$ on $1/D$ in ion exchange with NaCl on H-type espatyte, SBS-resin and SDV-3 resin in water-methanol mixtures.

In the course of investigations of exchange equilibria of alkali metal ions on sulfonated resins in aqueous alcoholic solutions containing up to 60% alcohol we found a linear dependence of $-\log K$ on $1/D$ (Fig. 2).

It is of interest to note that differences in the structure of the hydrocarbon skeleton of the resin have no effect on the variation of the equilibrium constant with solvent composition. This is confirmed by the fact that the ratios of the equilibrium constants for the exchange between Na^+ and H^+ in aqueous alcoholic solutions to the corresponding constants in water were found to be the same for three different sulfonated resins (Fig. 3).

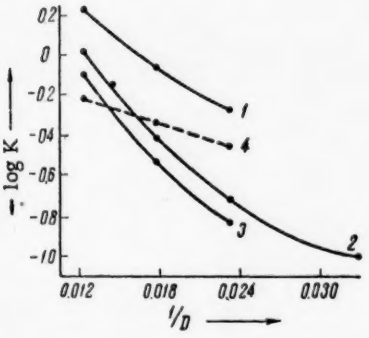

Fig. 4. Dependence of $-\log K$ on $1/D$ in ion exchange on resin SBS in aqueous acetone solutions: 1) $Li^+ - H^+$; 2) $Na^+ - H^+$; 3) $K^+ - H^+$; 4) $Na^+ - Li^+$.

In fact, in a series of investigations on the effect of additions of alcohol on the dissociation constant of acids [7, 8], on the instability constant of complexes [9], and on the normal electrode potentials [10, 11], we have likewise found a simple linear relationship between $\log K$ or the normal potentials, and $1/D$ of the solvent at comparatively low alcohol concentrations. This fact also indicates that it is possible to apply a simple electrostatic model in interpreting reactions in such solutions.

When the alcohol content is increased to 60% the linear relationship between $-\log K$ and $1/D$ is disturbed and the curve passes through a minimum (see Fig. 2). Nor do we find a linear relationship in the case of the exchange of alkali metal ions for hydrogen in aqueous-acetone solutions (Fig. 4). A linear relationship is, however, obtained for the exchange between different alkali metal ions in aqueous acetone solutions.

In order to explain these phenomena it is necessary to consider the behavior of acids in these solvents. The point is that parallel with the solvation of ions and interactions between the solvated ions which are characteristic of solutions of all electrolytes, there occurs in these solvents also a specific chemical interaction of the hydrogen ions with a single molecule of the solvent with the formation of a lyonium ion (or the hydroxonium ion, H_3O^+, in the case of water) which undergoes further solvation as a result of the orientation of the molecular dipoles of the solvent [12], just as is the case with the usual monovalent ions. This specific interaction with the first molecule of the solvent is either altogether absent in the case of all the remaining ions, or it manifests itself only to a very small degree.

In aqueous alcoholic solutions of acids hydrogen ions are preferentially hydrated [13]. The interaction of the proton with molecules of alcohol begins to be manifested only at high alcohol concentrations. This interaction will find expression in a change in the value of ΔF_{nonel} in the formula deduced above.

Acetone differs from alcohols and water as solvents in that its dipole moment (2.95 debyes) is large by comparison with the dipole moments of water (1.84 debye) and alcohols (1.69 debye for methyl alcohol, 1.70 debye for ethyl alcohol [14]). For this reason the interaction of the proton with acetone molecules becomes evident at lower concentrations than in the case of methyl alcohol.

In the course of investigations on the behavior of a number of acids in acetone-water solutions, N. A. Izmailov showed [7, 15] that the logarithm of the dissociation constants $\log K_{diss}$ of individual acids does not vary linearly with $1/D$ (as is the case in aqueous alcoholic solutions), but that the logarithm of the ratio of the dissociation constants of two acids does so. This indicates the specific character of the interaction of the proton with molecules of the solvent.

A similar relationship is found to be the case in ion exchange in aqueous acetone solutions: in the case of the exchange of alkali metals for hydrogen $\log K$ does not vary linearly with $1/D$, but the logarithm of the equilibrium constant in an exchange between two alkali metals, which constant is obtained by dividing the constants of exchange between these metals and hydrogen by each other, bears a linear relationship to $1/D$ (see Fig. 4).

This means that in ion exchange reactions in water-acetone mixtures without the participation of hydrogen ions the influence of the acetone is confined to a change in the dielectric constant of the water and a linear relationship between $\log K$ and $1/D$ is obtained. In exchange reactions in which the hydrogen ion takes active part we have, in addition, the interaction of the proton with the molecules of the mixed solvent and the linear relationship between $\log K$ and $1/D$ no longer holds.

In conclusion the authors wish to express their gratitude to M. V. Kuklanova and V. I. Slovetsky, who took part in the experimental work.

LITERATURE CITED

[1] V. Sementschenko, Z. Phys. Chem. 112, 128 (1924); J. Russ. Phys. Chem. Soc. 56, 541 (1925).

[2] N. Bjerrum, Kgl. Danske Videnskab. Selskab. 7, 9, 3 (1926).

[3] T. R. Kressman and J. A. Kitchener, Disc. Farad. Soc. 7, 90 (1949).

[4] T. R. Kressman and J. A. Kitchener, J. Chem. Soc. 1949, 1190.

[5] Boyd, Schubert and Adamson, Chromatographic Method for the Separation of Ions (Coll. Papers), [Russian Translation.] IL 1949, p. 257.

[6] T. R. Kressman and J. A. Kitchener, J. Chem. Soc. 1949, 1211.

[7] N. A. Izmailov, J. Phys. Chem. 24, 3, 321 (1950).

[8] S. Glasstone, Introduction to Electrochemistry, [Russian Translation.] IL 1951, p. 434.

[9] Ya. I. Turyan, Proc. Acad. Sci. USSR 102, 2, 295 (1955).

[10] A. E. Brodsky, Z. Phys. Chem. 121, 1 (1926); J. Russ. Phys. Chem. Soc. 61, 535 (1930).

[11] A. P. Markman and Ya. I. Turyan, J. Gen. Chem. 22, 1715 (1952).

[12] K. P. Mishchenko, J. Phys. Chem. 26, 12, 1736 (1952); K. P. Mishchenko and E. A. Podgornaya, J. Phys. Chem. 30, 2, 468 (1956).

[13] N. A. Izmailov, J. Phys. Chem. 23, 647 (1949).

[14] Chemist's Handbook, 1, (Moscow, 1951), p. 858.

[15] N. A. Izmailov and I. F. Zabara, Collected Papers on Physical Chemistry, (Acad. Sci. USSR Press, 1947), p. 310.

M. V. Lomonosov State University
Moscow.

Received November 22, 1956.

ADSORPTION OF WATER VAPOR ON SILICA GELS OF DIFFERENT DEGREES OF HYDRATION

M. M. Egorov, T. S. Egorova, V. F. Kiselev and K. G. Krasilnikov

(Presented by Academician M. M. Dubinin, December 14, 1956)

As is well known, the adsorption of water vapor on silica gels exhibits certain specific features. Thus, in papers [1-4] a detailed investigation has been made of the irreversible adsorption of water vapor resulting from the additional hydration of the surface of a silica gel in the adsorption process. In papers [2, 5] it has been established that, depending on the degree of dehydration of the surface of silica gels and of porous glasses, the adsorption isotherm of water vapor passes from a convex to a concave curve corresponding to a hydrophobic surface. Determinations of the specific surface of silica gels from adsorption isotherms of water vapor give values which are usually considerably lower than those calculated from nitrogen adsorption isotherms. The reason for this does, apparently, lie in the assumptions made in estimating the "volume of the monomolecular layer," a_m, as well as in the choice of the surface area ω_0 occupied by a water molecule in the monomolecular layer (10.6 A^2 [7], 14.8 A^2 [8]). In accordance with data given in [9] the values of ω_0 for water vary for different silica gels from 11.2 to 29.1 A^2. However, in all these investigations the authors did not carry out an analysis of the chemical composition of the surface of the silica gels and porous glasses used in the measurements. In view of this it appeared to us of interest to undertake systematic investigations of water vapor adsorption on silica gels in relation to the degree of hydration of their surfaces.

TABLE 1
Adsorption Characteristics of Silica Gels Used

Silica gel specimen	Temperature of heat treatment, °C	Specific surface, m^2/g	Main pore diameter, A	Structural water content, $\mu M/m^2$	Irreversible water adsorption after evacuation, $\mu M/m^2$	
					at 20°	at 250°
KSK-1	300	275	65	4.78	0.38	0.0
KSK-2	300	400	60	4.12	0.32	0.0
K-2	300	695	44	3.20	0.29	0.0
K-2	500	620	–	1.74	1.93	1.19
K-2	700	550	–	0.98	1.60	1.00
K-2	900	178	–	0.87	2.61	1.93

In the present investigation we have used the same silica gel specimens as those which were used in investigations [6, 10], i.e., the silica gel K-2, obtained by hydrolysis of $SiCl_4$, and carefully purified samples of the technical silica gels KSK-1 and KSK-2. In addition determinations were also carried out on samples of silica gel K-2 heated in air for 24 hours at temperatures of 500, 700, and 900°. As in the previous investigations [6, 12], the original samples were heat-treated at 300°. The specific surfaces of all the specimens investigated were determined by the BET method from nitrogen adsorption isotherms. The content of structural water in these specimens was determined previously [6]. The characteristics of these specimens are given in

Table 1. Determinations of adsorption were carried out in an adsorption apparatus including a quartz fiber spring balance. Before the actual measurements were made the samples were evacuated at a temperature of 250°.

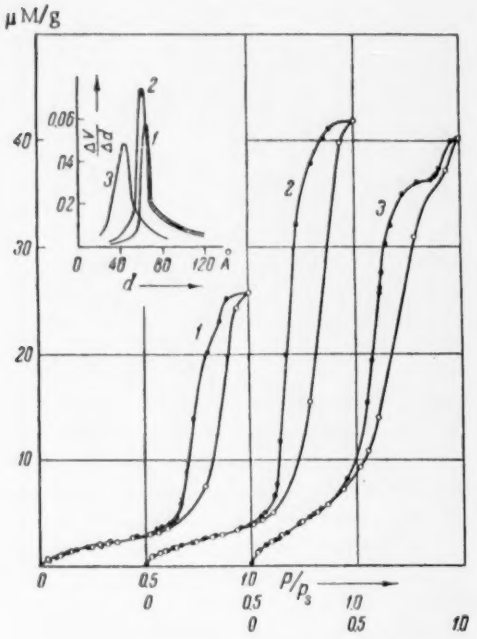

Fig. 1. Adsorption isotherms of water vapor at 15° on silica gels KSK-1 (1), KSK-2 (2) and K-2 (3). In the diagram in the inset are shown the pore volume distribution curves according to effective pore diameter which have been calculated from the desorption isotherms (black points).

In Fig. 1 are plotted adsorption isotherms of water vapor on the original silica gels and the distribution curves of the pore volumes according to their effective diameters, which were calculated from the desorption branches after having taken into account the thickness of the adsorbed film. Similar measurements on the heat-treated samples were not carried out because on such treatment only the pore volume of the silica gel changes, whereas their diameter remains practically constant [11]. In Fig. 2, A are plotted the initial portions of the curves of primary adsorption of water vapor on all the silica gels, referred to 1 m^2 of the surface. As will be seen from the diagram, in the case of three of the original samples which were heat-treated at 300° the isotherms indicate that for the same values of p/p_s the amount adsorbed diminishes with decreasing degree of hydration of the surface; this is in accordance with the observed lowering of the heat of wetting of these samples by water [6]. The states reached by water adsorption on the thermally dehydrated surfaces are not equilibrium states, because in this case hydration of the surface may take place. However, for small values of p/p_s this process of hydration will take place very slowly up to the point when monomolecular coverage is complete [5]. If, therefore, we neglect the small change in surface hydration within the period required to reach adsorption equilibrium, the isotherms shown in Fig. 2, A for silica gels K-2 heated at high temperatures may be regarded as equilibrium isotherms. On comparing these isotherms with the previous ones it will be seen that they change their shape with progressing degree of surface dehydration and become convex, and also that the adsorption capacity of the silica gel decreases.

The desorption isotherms for the initial samples (Fig. 2, B) and for the thermally dehydrated samples (Fig. 2, C) were determined after keeping the samples at $p/p_s = 1$ for 48 hours. In all cases we observed an irreversible sorption of water.* As will be seen from Table 1 the values of irreversible sorption obtained after prolonged evacuation of the samples at 20° are very small. Subsequent determinations of adsorption on such surfaces give fully reproducible results which coincide with the desorption curve; this is in accordance with results reported in [4, 5]. However, if the original samples are evacuated at a temperature of 250°, the irreversible adsorption no longer takes place and subsequent adsorption measurements give results which coincide with the corresponding isotherms shown in Fig. 2, A. Thus, the experimental data obtained by us for the original samples indicate that the degree of surface hydration is different after similar thermal treatment [6] as well as after keeping the samples in an atmosphere of saturated water vapor. The structural water content of the original silica gels given in Table 1 is approximately equal to the maximum possible for each of these specimens [6, 17].

* For convenience of comparison desorption isotherms have been reduced to zero, i.e., the values of irreversible sorption of water have been subtracted from all ordinates.

The amount of water adsorbed irreversibly by the thermally dehydrated specimens of silica gel K-2 is large and remains fairly high even after evacuation at 250°. According to the data given in Table 1 the degree of surface hydration increases after each such treatment by comparison with the original degree of hydration, but it always remains below the degree of hydration of the original specimen heat-treated at 300°. From this it follows that even for values of $p/p_s = 1$ the surface of the silica gel is not hydrated completely and that its original properties are not restored, a result which is contrary to the conclusions given in [5]. This is also confirmed by data given in [6, 16]. This very slow process of surface hydration at low relative pressures can probably be explained by the fact that up to the point when monomolecular coverage is reached the adsorbed water molecules accommodate themselves rather loosely and that there is virtually no adsorption taking place on a considerable fraction of the surface which is capable of undergoing hydration.

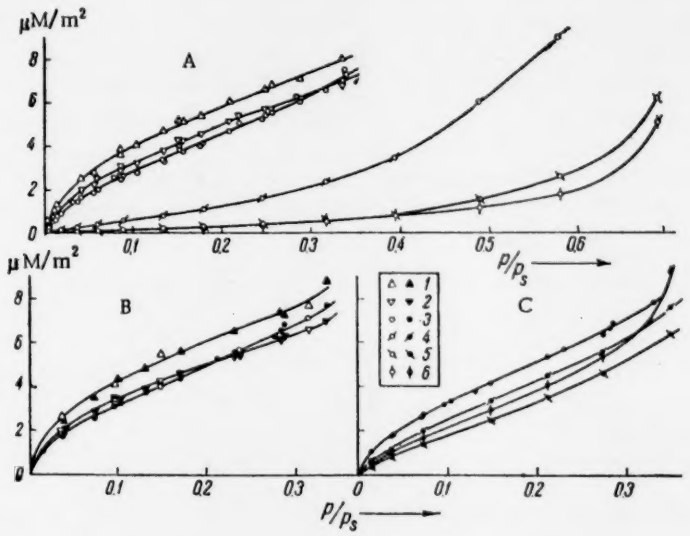

Fig. 2. Initial portions of primary adsorption isotherms (A) and of desorption isotherms (B, C) on silica gels KSK-1 (1), KSK-2 (2) and K-2 (3), heated at 300°, and on silica gel K-2 heated at 500° (4) 700° (5), and 900° (6). The black points refer to desorption.

Examination of the isotherms in Fig. 2 indicate that in the case of all the silica gels investigated the amounts adsorbed per unit area of the surface at identical relative pressures are not equal. Surfaces possessing a higher degree of hydration adsorb larger amounts, and vice versa. As a result the so-called "absolute" adsorption isotherms of water vapor on different silica gels cannot be expected to coincide with each other [12], as is the case, for example, with the nonpolar molecules of nitrogen [10]. This circumstance cannot be explained as being due to the disturbing influence of the pores [13]. In the paper [14] it was shown that in nitrogen adsorption a noticeable influence of the pores, leading to a distortion of the initial portion of the isotherms, begins only as we pass to silica gels of the very fine pore grade. The silica gels used in the present investigation were specimens of uniform large-pore size [15] for which the nitrogen adsorption isotherms, referred to unit surface area, were found to be identical [10]. Since the dimensions of water molecules are smaller than those of nitrogen, the effect of the porosity of the adsorbent will, apparently, be even less than in the case of nitrogen. We may therefore assume that differences in adsorption capacity per unit area of all the silica gels investigated are due not to structural factors of the gels, but to differences in the chemical nature of their surfaces.

Since adsorption per unit surface area decreases with increasing degree of dehydration for all values of p/p_s, the area available per one adsorbed molecule, $\omega = 1\ aN$ (where $\underline{a}$ is the amount adsorbed per unit surface area, N is Avogadro's number), increases. This indicates a looser distribution of the water molecules on the surface of the dehydrated specimens. In order to determine the surface area occupied by a molecule within the monomolecular layer it is necessary to know the "volume of the monomolecular layer," a_m. The values of ω_0 calculated for the original silica gels K-2, KSK-2 and KSK-1 from values of a_m determined from the desorption branches of the isotherms at point B, are, respectively, 55, 50 and 39 A^2, and are seen to decrease with increasing content of structural water on the surface of these gels. Values of a_m determined by means of the BET equation [9, 11] are considerably higher than those determined from the desorption curves at point B. Irrespective of the fact that on isotherms plotted in BET coordinates one can pick out an approximately linear portion, the BET equation is hardly applicable to the case of adsorption of water on silica gels because of the nonuniformity of the surface of the latter [6]. In any case, the area available per one water molecule is found to vary, even in the case of the most strongly hydrated silica gel KSK-1, between 39 and 22.5 A^2 within the p/p_s range from 0.1 to 0.3, and is thus much higher than values of ω_0 quoted in the literature (10.6 and 14.8 A^2). Values of a_m corresponding to these values of ω_0 lie already in the region of polymolecular adsorption and capillary condensation.

It must be mentioned that several assumptions made in the literature with regard to the mechanism of water adsorption and surface hydration of silica gels [2, 4, 5, 17-20] and based on adsorption measurements as well as on studies of infrared spectra of surface layers, are in direct contradiction to each other [20]. In order to elucidate these problems it is necessary to undertake further adsorption studies and at the same time to carry out spectroscopic investigations.

The authors wish to express their gratitude to B. V. Ilin for his support and discussion of the results.

LITERATURE CITED

[1] K. S. Rao, J. Phys. Chem. 45, 513 (1941).

[2] S. P. Zhdanov, Proc. Acad. Sci. USSR 621, 853 (1948).

[3] D. Papee, Compt. rend. 234, 952 (1952).

[4] N. N. Avgul, O. M. Dzhigit, A. V. Kiselev, and K. D. Shcherbakova, J. Phys. Chem. 26, 977 (1952).

[5] S. P. Zhdanov, Proc. Acad. Sci. USSR 100, 1115 (1955).

[6] M. M. Egorov, K. G. Krasilnikov, and E. A. Sysoev, Proc. Acad. Sci. USSR 108, 103 (1956).

[7] H. K. Livingston, J. Amer. Chem. Soc. 66, 569 (1944).

[8] A. V. Kiselev and N. N. Mikos, J. Phys. Chem. 21, 1223 (1947).

[9] K. S. W. Sing and J. D. Madeley, J. Appl. Chem. 4, 365 (1954).

[10] K. G. Krasilnikov, V. F. Kiselev, N. B. Kapitonova, and E. A. Sysoev, J. Phys. Chem. 31, 7 (1957).

[11] J. Bastick, Bull. Soc. Chim. France, 437 (1953).

[12] N. N. Avgul, O. M. Dzhigit, et al., Proc. Acad. Sci. USSR 77, 77 (1951).

[13] A. V. Kiselev and Yu. A. Eltekov, J. Phys. Chem. 29, 904 (1955).

[14] O. M. Dzhigit, A. V. Kiselev, and I. E. Neimark, J. Phys. Chem. 28, 1804 (1954).

[15] A. V. Kiselev, J. Phys. Chem. 23, 452 (1949).

[16] A. V. Kiselev, K. G. Krasilnikov, and V. N. Soboleva, Proc. Acad. Sci. USSR 94, 85 (1954).

[17] N. G. Yaroslavsky, J. Phys. Chem. 24, 68 (1950).

[18] A. V. Kiselev, Colloid J. 2, 17 (1936).

[19] W. A. Weyl, Res. 5, 230 (1950).

[20] V. A. Nikitin, A. N. Sidorov, and A. V. Karyakin, J. Phys. Chem. 30, 117 (1956).

M. V. Lomonosov State University, Moscow

Received December 10, 1956.

ON THE KINETICS OF ROTATIONAL ISOMERIZATION

V. A. Pozdyshev, Yu. A. Pentin, and V. M. Tatevsky

(Presented by Academician A. N. Frumkin, December 4, 1956)

The potential barrier for the interconversion of rotational isomers (trans and bent forms) of the type of 1,2-dichloroethane, $CXY_2 - CXY_2$, may be expressed in the form [1]

$$-V(\varphi) = {}^1/_6[V_0 + 2V_1 + 2V_2 - (2V_0 - 2V_1 + 2V_2)\cos\varphi - (-2V_0 + 2V_1 + 2V_2)\cos 2\varphi - (V_0 + 2V_1 - 2V_2)\cos 3\varphi]. \quad (1)$$

In Fig. 1 is shown the plot of this function (Curve I) for the transformation in the gaseous phase. In order to determine the potential function completely it is necessary to know the three parameters V_0, V_1, and V_2. A knowledge of these parameters is necessary not only in order to be able to form a picture about the nature of restricted internal rotation and of rotational isomerism of molecules, but also in order to calculate statistically their thermodynamic functions.

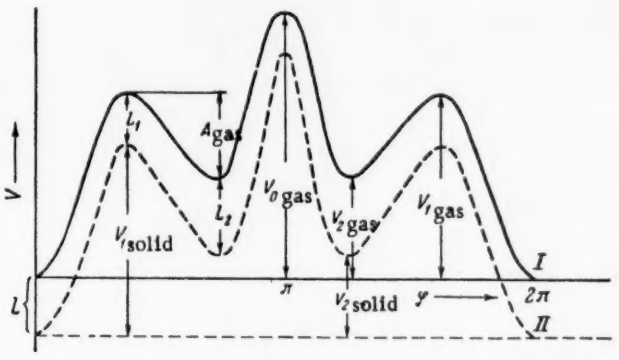

Fig. 1. Potential barrier curve for molecules of the type of 1,2-dichloroethane.

There are no direct methods for the determination of the constants V_0 and V_1 of the braking potential. In general, in the case of molecules of the type of 1,2-dichloroethane, a certain effective value of the braking potential has been determined, for example, by comparing the entropy, calculated by applying the third law of thermodynamics, with the value calculated on the assumption of unrestricted internal rotation or certain other simplified assumptions with regard to the nature of the potential barrier ($V_2 = 0$, $V_1 = V_0$). One of the

three parameters mentioned above, namely V_2, the difference in energies of the rotational isomers, can be determined accurately by experiment from the temperature dependence of the corresponding band (line) intensities of the infrared spectrum (Raman spectrum), making use of the well-known expression for the equilibrium constant of a mixture of rotational isomers.

We are now going to show that in some cases the second parameter, V_1, in the expression for the potential barrier function can be determined independently by studying experimentally the kinetics of isomerization of rotational isomers. Earlier we observed a simplification in the appearance of the infrared spectrum of crystalline propyl chloride, as compared with the spectrum of the liquid [2]. We found that the molecule of propyl chloride is present in two spectroscopically distinct rotational-isomeric forms:
C_s – trans-configuration

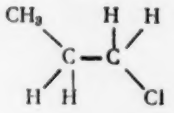

and C_1 – bent configuration

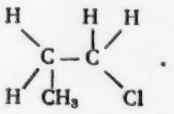

In the case of the solid phase at a certain temperature it is possible to observe a transition from the equilibrium present in a rapidly frozen vapor of the substance (both isomers present) to the equilibrium in the

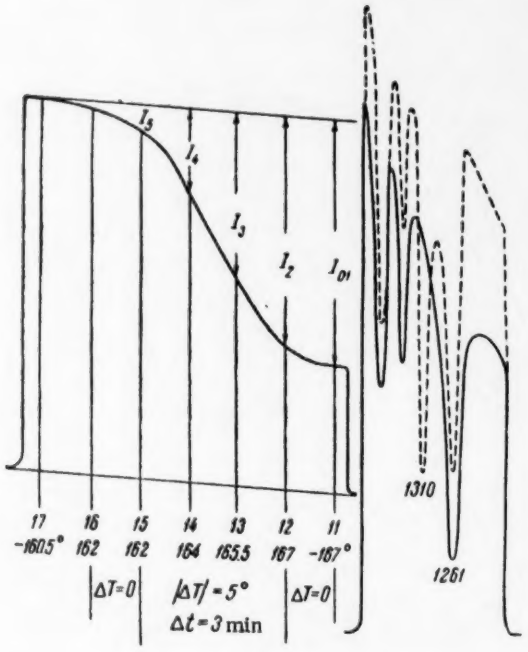

Fig. 2. Curve representing the decrease in intensity of the 1310 cm^{-1} band of propyl chloride with time and temperature.

crystalline state when practically only the trans-isomer of the substance is present [2]. In this investigation we succeeded in following the disappearance of a number of vibration frequencies in the spectrum of crystalline propyl chloride with time and within a definite temperature range.

In Fig. 2 is shown the record of the decrease in intensity of the band at 1310 cm^{-1} with time, which band we ascribe to the external distorting vibrations of the CH_2 group of the bent-isomer of propyl chloride. The process of the disappearance of several of the bands may, of course, be treated as a rotational isomerization reaction:

$$N_{bent} \rightarrow N_{trans}.$$

This reaction can be described by the kinetic equation for a unimolecular reaction, which in this case will have the form

$$N_1 = N_{01} e^{-K(t-t_0)}, \tag{2}$$

where N_0 is the number of moles of the bent isomer present at time t_0, N_1 is the number of moles of the bent isomer unchanged at the end of time t, K is the velocity constant of the reaction.

To determine the velocity constant of the reaction it is necessary to know the ratio N_1/N_{01}, which can be easily found. In fact, $I_{01} = i_{01} N_{01}$, $I_1 = i_{01} N_1$, where i_{01} is the molar intensity of the bent isomer. Hence, $N_1/N_{01} = I_1/I_{01}$. The ratio I_1/I_{01} is determined by experiment (Fig. 2).

Having thus determined the velocity constant of the reaction for different temperatures within the temperature range in which the reaction takes place (Fig. 2), we have, by means of the Arrhenius-Van't Hoff equation $\ln K = H - \frac{A_{solid}}{kT}$, calculated the activation energy A_{solid} for the isomeric transformation in the solid phase. The value of 4800 ± 500 kcal/mole thus obtained is quite reasonable, at least as regards its order of magnitude. It is possible to show that the value of V_1 gas sought can be obtained with a high degree of accuracy in the form

$$V_1\,gas = V_2\,gas + A_{solid},$$

where A_{solid} is the activation energy of the isomerization reaction in the solid phase. In Fig. 1, Curve II represents the potential barrier of internal rotation of the molecules with respect to the central C–C bond in the solid phase. As will be seen from Curves I and II (Fig. 1), it is possible to write down the following relationships between the respective quantities referred to the gas and solid phase:

$$V_1\,gas = V_2\,gas + A\,gas,\quad V_1\,solid = V_2\,solid + A\,solid,$$

$$V_1\,gas = V_1\,solid + L_1 - L,\quad V_2\,gas = V_2\,solid + L_2 - L,$$

where L_1, L_2, and L are the latent heats of vaporization at T = 0 of the pure racemic, bent, and trans forms, respectively.

From these relationships it is possible to obtain the equations

$$A\,gas = V_1\,solid - V_2\,solid + L_1 - L_2,$$

$$V_1\,gas = V_2\,gas + V_1\,solid - V_2\,solid + L_1 - L_2.$$

Since each of the quantities L_1 and L_2 are of the same order of magnitude as the expression $V_1\,solid - V_2\,solid$ (a few kcal/mole), we have

$$L_1 - L_2 \ll V_1\,solid - V_2\,solid.$$

and therefore

$$V_{1\,gas} \cong V_{2\,gas} + V_{1\,solid} - V_{2\,solid}.$$

The value of $V_{1\,gas}$ can thus be determined sufficiently accurately by studying the isomerization process in the solid phase. Having found the quantities V_1 and V_2 it is, obviously, possible to determine also the third parameter of the potential barrier curve, V_0, if we find the effective barrier by comparing the entropy determined experimentally with its value calculated statistically on the assumption of free internal rotation.

The method of investigation of the kinetics of rotational isomerization reactions outlined here for the first time opens new interesting possibilities in the study of the phenomena of restricted internal rotation and rotational isomerism.

LITERATURE CITED

[1] M. V. Volkenshtein, Proc. Acad. Sci. USSR 49, 111 (1945).

[2] Yu. A. Pentin and V. M. Tatevsky, Ibid., 108, 290 (1956).

Received August 1, 1956.

ON THE CHANGES IN THE ORDER OF SULFIDE LINKS IN IRRADIATED VULCANIZATES

A. F. Postovskaya, M. A. Salimov, and A. S. Kuzminsky

(Presented by Academician P. A. Rebinder, November 22, 1956)

In the paper [1] we showed that vulcanizates of sodium-butadiene rubber, namely, polysulfidic* and tetramethylthiuram disulfide** vulcanizates, which differ from each other in the type of cross-links, exhibit different stability toward light. The polysulfidic vulcanizate is the more stable one. When it is irradiated with ultraviolet light decomposition of the sulfur linkages takes place with the formation of free sulfur which, in contrast to elemental sulfur, does not take part in the photovulcanization process, i.e., it is "inactive." The nature of this inactive sulfur and the change in the order of sulfide links in the above-mentioned vulcanizates brought about by irradiation have not been established. It was, therefore, impossible to answer unequivocally the very important question as to why the polysulfidic vulcanizate possesses greater stability toward light than the tetramethylthiuram vulcanizate. The present paper is concerned with the investigation of this problem.

The investigation of the nature of sulfur linkages in vulcanizates is of essential importance, but the literature contains no record of satisfactory methods of determination of these linkages. Attempts to throw light on the nature of these linkages by means of chemical methods meet with considerable difficulties since it is impossible to separate sulfur structures present in the form of different sulfides, or identical sulfur structures which may be linked to the polymer chain in different ways.

Thus, for example, using sodium sulfite [2] and methyl iodide [3] it is possible to determine only the relative sulfur content in the form of polysulfides. It must be noted, however, that the results of analysis using Na_2SO_3 are affected in a complex manner by the order of the sulfide link and by the nature of the radicals R_1 and R_2 in the grouping of the type $R_1-S_n-R_2$. As the nature of this effect has not been established it is impossible to interpret the results of such an analysis with any certainty, and this may, sometimes, lead to erroneous conclusions. This may be the reason why, when using this method, no polysulfide structures could be detected in the tetramethylthiuram vulcanizate [4].

Equally, the method of exchange reactions using radioactive sulfur [5] and the thermo-mechanical method [6], based on the determination of strain relaxation in the vulcanizate at different temperatures, do not permit of a satisfactory determination of the order of sulfides in sulfur structures of vulcanizates. Spectrographic methods have not been used specifically for the solution of this problem. The paper [7] deals with infrared absorption spectra of the sulfur vulcanizate NK. The authors detected a weak absorption band at 600 cm^{-1}

---

* Composition of the polysulfidic vulcanizate: rubber 100 parts, stearic acid 2 parts, zinc oxide 5 parts, sulfur 6 parts, diphenylguanidine 1 part. Vulcanization was carried out at 143° for 20 minutes.

** Composition of the tetramethylthiuram vulcanizate: rubber 100 parts, stearic acid 2 parts, zinc oxide 5 parts, tetramethylthiuram disulfide 3 parts. Vulcanization was carried out at 143° for 90 minutes.

which they ascribed to valence vibrations of the C–S bonds; no di- or polysulfidic links have been detected. Later infrared spectra of aliphatic sulfides and polysulfides have been studied in detail [8, 9]. It has been established that the valence vibrations of the C–S and S–S bonds (maximum at 600-700 cm^{-1} [8] and 430-490 cm^{-1} [9], respectively) produce weak absorption bands in the infrared region.

In view of the fact that the concentration of sulfur linkages in soft vulcanizates is low and lies on the threshold of sensitivity of infrared spectrographic measurements, this method could not have been used in our investigations. It appears that at present it is ultraviolet spectroscopy which is the most sensitive method for differentiating between the various sulfur structures. In the paper [10] the following absorption maxima have been reported for n-hexadecyl sulfides in alcohol and hexane: n-hexadecyl sulfide 2250 A, n-hexadecyl disulfide 2480-2520 A, n-hexadecyl trisulfide 2500-2600 A, n-hexadecyl tetrasulfide 2900-3000 A, and for the hexasulfide and S_8 at 3200 A and higher. Comparing the data obtained by these authors with those reported in [11, 12] it may be concluded that absorption bands due to difference of sulfur linkages are quite intensive and characteristic of the particular type of linkage and depend little on the nature of the remaining portion of the molecule. As the order of the sulfidic linkage increases the absorption maximum is displaced toward the long-wave region of the spectrum.

In view of the above it appeared to us of interest to apply ultraviolet spectroscopy to investigate the change in the order of sulfide linkage in sulfur structures of polysulfidic and tetramethylthiuram vulcanizates after irradiation with ultraviolet light.

The investigation was carried out on vulcanizates the composition of which is given above. These vulcanizates were used in the form of films 10 μ thick, after previous removal of free sulfur, accelerators and their decomposition products by extraction with a mixture of methanol and acetone for 100 hours in an atmosphere of nitrogen. The films were irradiated with the filtered light of a mercury-quartz lamp PRK-2 of a wavelength of $\lambda > 2900$ A, from a distance of 25 cm. The absorption spectra were recorded on the universal monochromator ZMR-2 in the region 2200-7000 A. A quartz prism was used as the resolving system for the ultraviolet region, and a glass prism for the visible region.

Experimental procedure was as follows: the spectra of films of polysulfidic and tetramethylthiuram vulcanizates, purified by extraction of free additives, were recorded first. The films were then irradiated for 6 hours, followed by extraction for 100 hours after which their spectra were again recorded. In order to eliminate errors due to the experimenter himself, the same film was always used for recording the spectra. The reproducibility in parallel experiments was satisfactory – the experimental error did not exceed 1%. In order to determine the atomicity of free sulfur formed as a result of the decomposition of the sulfur linkages on irradiation of the polysulfidic vulcanizate, its spectrum in alcoholic solution was recorded and compared with the spectrum of elemental sulfur, likewise in alcoholic solution.

The results of these experiments are reproduced in Figs. 1-3.

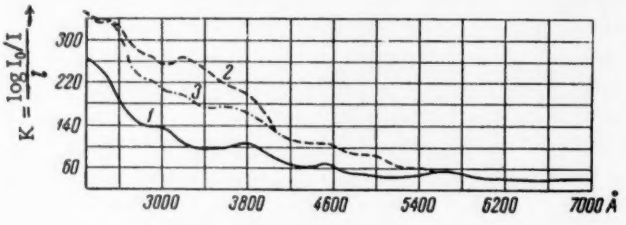

Fig. 1. Absorption spectrum of polysulfidic vulcanizate in the ultraviolet and in the visible region: 1) purified rubber; 2) extracted vulcanizate before irradiation; 3) extracted vulcanizate after 6 hours' irradiation.

As will be seen from Fig. 1, there is an increase in the intensity of absorption in the range between 2200 and 5400 A in the case of the polysulfidic vulcanizate (2) as compared with absorption by unvulcanized rubber (1). This increase is due to the presence in the vulcanizate of sulfide linkages of varying orders. The maximum in the region 2300-2500 A (Curve 2) is characteristic of mono- and disulfides. The maximum at 3250 A is due to hexasulfides. Absorption at still longer wavelengths (> 3400 A) is evidence for the presence in the vulcanizate of yet higher sulfides. Irradiation of the polysulfidic vulcanizate results in a decrease in the intensity of absorption (Fig. 1, Curve 3). This decrease is due to the breakdown of polysulfidic linkages, and in this respect sulfides of higher orders are less stable than those of lower orders.

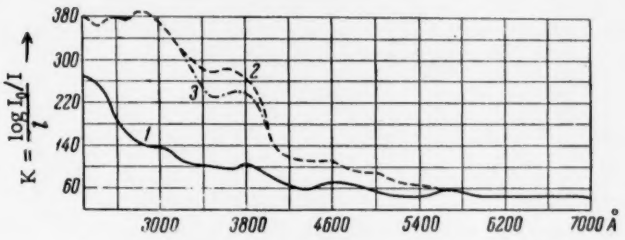

Fig. 2. Absorption spectrum of tetramethylthiuram vulcanizate in the ultraviolet and in the visible region: 1) purified rubber; 2) extracted vulcanizate before irradiation; 3) extracted vulcanizate after 6 hours' irradiation.

In the case of the tertramethylthiuram vulcanizate (Fig. 2) the absorption maximum in the region 2500-2600 A (Curve 2) corresponds to di- and trisulfides. The maximum at 2800-2900 A (Curve 2) indicates the presence of tetrasulfides. The decrease in absorption toward the longwave region indicates that the content of sulfides of higher orders is insignificant. Irradiation of this vulcanizate is accompanied by the decomposition of polysulfidic linkages, mainly of hexasulfides and sulfides of higher orders (region 3200-4000 A).

A comparison of Figs. 1 and 2 shows that both in the ultraviolet as well as in the visible region the tetramethylthiuram vulcanizate absorbs more strongly than does the polysulfidic vulcanizate, although the former contains only a quarter of the bound sulfur present in the latter. This is, apparently, due to the difference in the distribution of bound sulfur between the different types of sulfur linkages. It is known [10-12] that the intensity of the absorption bands differs with the type of sulfur linkage. Thus, the logarithms of the intensities of the absorption band maxima of different sulfides are as follows: hexasulfide (maximum at 3200 A) log ϵ 4.0, tetrasulfide (2900-3000 A) log ϵ 3.39, trisulfide (2500-2600 A) log ϵ 3.22, disulfide (2480-2520 A) log ϵ 2.63, and for the sulfide (2250 A) log ϵ 2.2. The intense band at 3250 A observed in the case of the polysulfidic vulcanizate indicates that it contains a considerable proportion of the hexasulfide, while the minimum in the region 2900-3000 A indicates an insignificant amount of tetrasulfide. The decrease in absorption at wavelengths of 2480, 2500 and 2600 A indicates that the vulcanizate contains a relatively small amount of di- and trisulfides. A different situation is observed in the case of the tetramethylthiuram vulcanizate: it contains, evidently, a considerable proportion of mono-, di-, tri- and tetrasulfides, while the content of sulfides of higher order is obviously low.

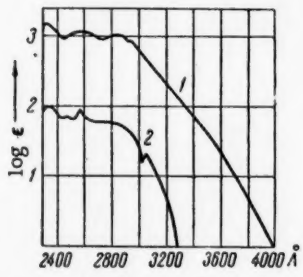

Fig. 3. Ultraviolet absorption spectrum of: 1) elemental sulfur (S_8) in alcohol; 2) inactive sulfur (formed as a result of decomposition of sulfur linkages upon irradiation of the polysulfidic vulcanizate) in alcohol.

It will be seen from Fig. 3 that the absorption region in the case of inactive sulfur lies between 2200 and 3200 A while in the case of elemental sulfur it is much wider and extends from 2200 to 4000 A. This is evidence that the atomicity of inactive sulfur is lower than that of elemental sulfur. As the vulcanizates investigated were irradiated with ultraviolet light of a wavelength > 2900 A, the inactive sulfur was activated to a limited extent in this absorption region and, as a result, did not take part in the photo-vulcanization. Elemental sulfur, on the other hand, was sufficiently activated in the region in question and, therefore, facilitated vulcanization of the rubber.

Consideration of the experimental results brings us to the conclusion that the greater degree of stability toward light of the polysulfidic vulcanizate as compared with the tetramethylthiuram vulcanizate is due to the difference in absorptions in the ultraviolet region by the corresponding sulfur linkages of these vulcanizates.

The authors wish to thank Professor V. M. Tatevsky, V. M. Gryaznov and V. D. Yagodovsky for their assistance with the experimental part of this investigation.

LITERATURE CITED

[1] A. F. Postovskaya and A. S. Kuzminsky, Proc. Acad. Sci. USSR 106, 5, 866 (1956).

[2] L. Parker, Ind. Rubber J. 108, 387 (1945).

[3] M. Selker and A. Kemp, Ind. and Eng. Chem. 36, 16 (1944).

[4] B. A. Dogadkin and Z. N. Tarasova, Colloid J. 15, 5, 347 (1953). *

[5] E. N. Guryanova, J. Phys. Chem. 28, 67 (1954).

[6] B. A. Dogadkin and Z. N. Tarasova, Proc. Acad. Sci. USSR 85, 5, 1069 (1952).

[7] N. Sheppard, and G. B. B. M. Sutherland, Trans. Farad. Soc. 41, 261 (1945).

[8] N. Sheppard, Trans. Farad. Soc. 46, 429 (1950).

[9] I. Cymerman, and J. B. Willis, J. Chem. Soc. 1951, 1332.

[10] J. E. Baer and M. Carmack, J. Amer. Chem. Soc. 71, 1215 (1949).

[11] L. I. Bellamy, The Infrared Spectra of Complex Molecules, 1955.

[12] A. E. Gillam and E. S. Stern, An Introduction to Electronic Absorption Spectroscopy in Organic Chemistry, London, 1954.

Institute of Rubber Research
M. V. Lomonosov State University, Moscow.

Received November 22, 1956.

* Original Russian pagination. See C. B. Translation.

THE ISOTOPIC EFFECT IN THE COMPRESSIBILITY AND ASSOCIATION OF DEUTERO-ALCOHOLS

I. B. Rabinovich, V. G. Golov, N. A. Efimova, and S. M. Rustamov*

(Presented by Academician A. N. Frumkin, December 4, 1956)

In the present work a study has been made of the ultrasonic velocity, a, and density, d, within a temperature range from 10° to 60-80° of the following alcohols: CH_3OH and CH_3OD, C_2H_5OH and C_2H_5OD, $(CH_3)_2CHOH$ and $(CH_3)_2CHOD$, $CH_3(CH_2)_3OH$ and $CH_3(CH_2)_3OD$, $(CH_3)_2CHCH_2OH$ and $(CH_3)_2CHCH_2OD$, $C_2H_5CHOHCH_3$ and $C_2H_5CHODCH_3$, as well as of deuterium oxide (up to 95°). The adiabatic compressibility was calculated from the formula $\beta_{ad} = 1/a^2 d$. In addition the osmotic coefficients of these alcohols were determined cryoscopically in benzene solutions in the concentration range of 0.2-1.7 mole/kg of the solvent.

The deuterated alcohols were obtained by hydrolysis of the corresponding alcoholates of aluminum and magnesium with heavy water (99.6%). All the alcohols were carefully purified and freed from moisture. With the exception of the deuterated methyl alcohol the deuterium content in the hydroxyl group of the D-alcohols was about 99%. The deutero-methanol contained 30% of its hydrogen analog. Regarding this mixture as an ideal one we referred the determined characteristics of this mixture to CH_3OD. In the acoustical measurements a stabilized generator of ultrasonic oscillations of a frequency of 3 megacycles was used. Ultrasonic velocities were determined by an optical method with an error of 1-2 m/sec. The cell was kept at a constant temperature in a thermostat operating with an accuracy of 0.05°. As will be seen from the densities in Table 2, the molar volume of the deuterated alcohols is, within the temperature interval investigated, approximately 0.2% higher than that of their hydrogen analogs.

TABLE 1
Boiling Points of Alcohols
(760 mm Hg)

Alcohol	t, °C	Alcohol	t, °C
CH_3OH	64.6	$CH_3(CH_2)_3OH$	117.8
CH_3OD	65.4	$CH_3(CH_2)_3OD$	118.2
C_2H_5OH	78.4	$(CH_3)_2CHCH_2OH$	108.0
C_2H_5OD	79.1	$(CH_3)_2CHCH_2OD$	108.2
$(CH_3)_2CHOH$	82.4	$C_2H_5CHOHCH_3$	99.5
$(CH_3)_2CHOD$	83.0	$C_2H_5CHODCH_3$	99.7

The ratio of the molecular weight determined cryoscopically to that given by the formula decreases in the order: methyl, ethyl, n-butyl alcohol, and also, in the series n-, iso-, sec-butyl alcohol. This ratio is by 2-5% larger for the deutero-alcohols than for the corresponding hydrogen analogs (Fig. 1). Since within the concentration range investigated the benzene solutions of the alcohols cannot be regarded as ideal, these ratios do not constitute accurate values of the degree of association but represent the osmotic coefficients. It is clear, however, that the increase in this coefficient with rise in concentration of the alcohols is due to an increase in their degree of association.

---

* K. G. Fedyakova assisted with the cryoscopic measurements.

TABLE 2

Density d (in g/cm³) and Ultrasonic Velocity a (in m/sec) in Alcohols.

°C	CH_3OH		CH_3OD		C_2H_5OH		C_2H_5OD		$(CH_3)_2CHOH$		$(CH_3)_2CHOD$		$CH_3(CH_2)_2OH$		$CH_3(CH_2)_2OD$		$(CH_3)_2CHCH_2OH$		$(CH_3)_2CHCH_2OD$		$C_2H_5CHOHCH_3$		$C_2H_5CHODCH_3$	
	d	a	d	a	d	a	d	a	d	a	d	a	d	a	d	a	d	a	d	a	d	a	d	a
10	0.8002	1155	0.8235	1125	0.7979	1202	0.8137	1179	—	1190	—	1183	0.8170	1295	0.8264	1281	0.8095	1238	0.8160	1222	0.8066	1253	0.8154	1256
20	0.7915	1122	0.8143	1095	0.7894	1167	0.8050	1145	0.7850	1164	0.7908	1148	0.8096	1261	0.8188	1247	0.8022	1214	0.8104	1188	0.7966	1227	0.8072	1229
30	0.7825	1089	0.8047	1064	0.7810	1133	0.7964	1111	0.7768	1129	0.7885	1113	0.8020	1227	0.8109	1213	0.7944	1174	0.8024	1155	0.7884	1192	0.7972	1185
40	0.7740	1057	0.7948	1033	0.7722	1098	0.7875	1077	0.7679	1094	0.7795	1078	0.7944	1193	0.8031	1179	0.7864	1137	0.7945	1121	0.7865	1157	0.7864	1150
50	0.7640	1024	0.7843	1001	0.7633	1064	0.7784	1043	0.7587	1059	0.7702	1043	0.7863	1159	0.7950	1145	0.7784	1104	0.7865	1088	0.7803	1122	0.7802	1115
60	0.7535	991	0.7740	970	0.7541	1030	0.7692	1008	0.7492	1024	0.7615	1008	0.7785	1125	0.7867	1112	0.7701	1071	0.7781	1055	0.7708	1087	0.7795	1080
70	—	—	—	—	0.7445	995	0.7597	974	0.7396	989	—	973	0.7701	1091	0.7782	1078	0.7615	1038	0.7698	1022	0.7610	1053	0.7709	1046
80	—	—	—	—	—	—	—	—	—	—	—	—	0.7615	1057	0.7694	1044	0.7524	1004	0.7604	989	0.7509	1019	0.7795	1012

There are, likewise, no reasons to doubt that the data plotted in Fig. 1 indicate a decrease in the degree of association through the hydrogen bond in normal alcohols with increasing number of carbon atoms in the molecule, and that the degree of association of n-butyl alcohol is greater than that of its isomers. This corresponds with a greater screening of the hydrogen bond with increasing length of the hydrocarbon radical as well as with the branching of the molecule, and is also in agreement with the difference in the boiling points and latent heats of vaporization of the butyl alcohols [5].

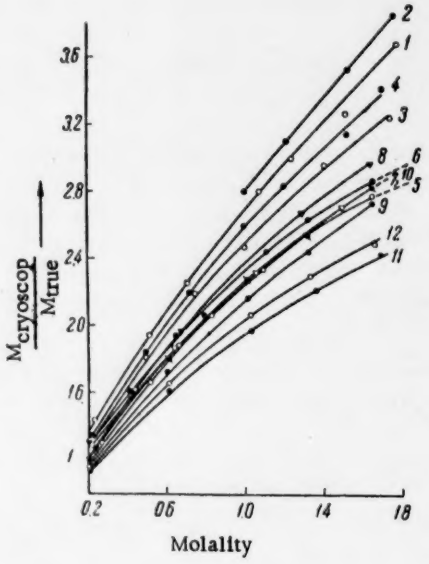

Fig. 1. Ratio of the cryoscopic molecular weight to formula molecular weight in benzene solution as a function of alcohol concentration.
1) CH_3OH, 2) CH_3OD, 3) C_2H_5OH, 4) C_2H_5OD, 5) $(CH_3)_2CHOH$, 6) $(CH_3)_2CHOD$, 7) $CH_3(CH_2)_2OH$, 8) $CH_3(CH_2)_2OD$, 9) $(CH_3)_2CHCH_2OH$, 10) $(CH_3)_2CHCH_2OD$, 11) $C_2H_5CHOHCH_3$, 12) $C_2H_5CHODCH_3$.

Thus, the results of cryoscopic measurements indicate that the deuterated alcohols are associated through the hydrogen bonds to a greater extent than are their hydrogen analogs. This conclusion is also confirmed by the fact that, as will be seen from Table 1, the deuteroalcohols investigated boil at higher temperatures than the corresponding hydrogen analogs, and that, as has been shown earlier [2], substitution of the hydrogen in the hydroxyl of the alcohol by deuterium brings about a lowering of its vapor pressure.

V. V. Tarasov suggested [6] that in the case of alcohols which exhibit chain association through hydrogen bonds, compression occurs mainly along the weaker van der Waals' bonds between the chains (associates) and not along the lines of action of the relatively strong hydrogen bonds. This is confirmed by the results of our compressibility measurements. As will be seen from Fig. 2, the compressibility of the alcohols investigated decreases in the homologous series from methyl to n-butyl alcohol by 20%, although as has already been mentioned, the degree of association through hydrogen bonds decreases in the same order (Fig. 1). This is explained by the fact that with increasing number of carbon atoms in the molecule the polarizability of the latter increases, resulting in a corresponding increase in the disperse interaction between the chains [7].

Iso- and secondary butyl alcohols possess a higher compressibility than their normal primary analog. From a comparison of our data for isopropyl alcohol with the results given by Eucken [3] for n-propyl alcohol it follows that the compressibility of the latter is lower than that of its isomer. Finally, I. G. Mikhailov [8] showed that the compressibility of n-hexyl alcohol is lower than that of its isomers. Thus, alcohols with a branched structure of molecules are characterized by a higher compressibility than are primary n-alcohols. This is explained by the fact that branching of the molecule leads to a decrease in the energy of intermolecular interaction on account of the lowering of the degree of association through the hydrogen bond as well as a weakening of the van der Waals' interaction between individual chains, an effect which is of decisive importance as regards compressibility.

In the case of all the deutero-alcohols investigated the ultrasonic velocity was lower by 10-20 m/sec than in the case of the corresponding hydrogen analogs (see Table 2). The compressibility of the deuterated alcohols is greater than that of their hydrogen analogs, the isotopic effect amounting to 1-2%, with the exception of the secondary butyl alcohols for which the difference in compressibility is of the same order of magnitude as the experimental error (0.2%). In the case of the isotopic analogs of methanol the decrease in the relative difference in compressibility with rise in temperature is very evident.

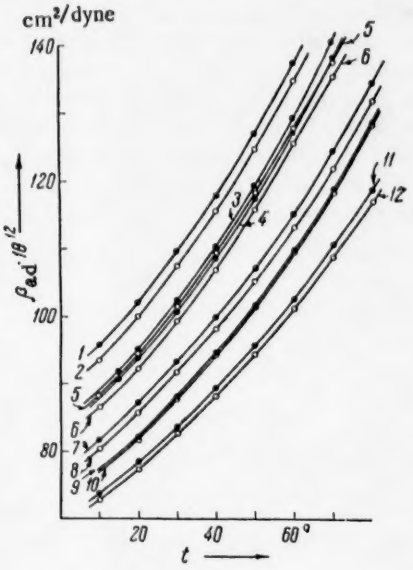

Fig. 2. Adiabatic compressibility of normal and deuterated alcohols: 1) CH_3OD; 2) CH_3OH; 3) C_2H_5OD; 4) C_2H_5OH; 5) $(CH_3)_2CHOD$; 6) $(CH_3)_2CHOH$; 7) $(CH_3)_2CHCH_2OD$, 8) $(CH_3)_2CHCH_2OH$; 9) $C_2H_5CHODCH_3$; 10) $C_2H_5CHOHCH_3$; 11) $CH_3(CH_2)_3OD$; 12) $CH_3(CH_2)_3OH$.

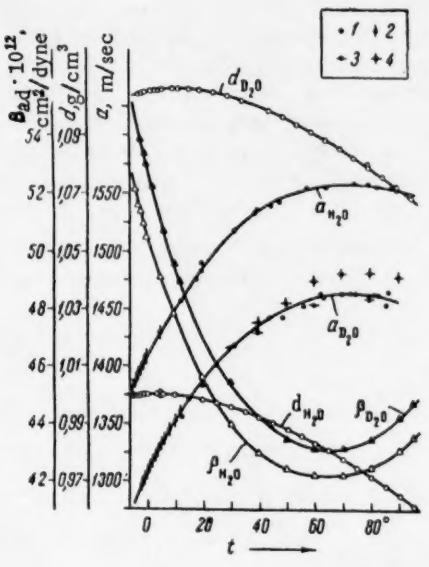

Fig. 3. Isotopic effect in the density (d), ultrasonic velocity (a) and adiabatic compressibility (β_{ad}) of heavy water. The different points on curve a_{D_2O} denote: 1) authors' data; 2) data of Lagemann and co-workers [9]; 3) Heusinger [11]; 4) Pancholy [10].

On the basis of the above considerations the isotopic effect in compressibilities observed by us means that in the case of the deuterated alcohols the interaction between individual chains (interaction between associated molecules through van der Waals' forces) is somewhat weaker than it is in the case of their hydrogen analogs.

In Fig. 3 are plotted the ultrasonic velocity, density and compressibility of water and deuterium oxide determined by ourselves as well as those reported in the literature. Up to a temperature of 40° the ultrasonic velocities reported by Lagemann and co-workers [9], as well as those reported by Pancholy [10] are in agreement with our own data within 1-2 m/sec. The data reported by Pancholy for higher temperatures are, evidently, very high and the conclusions based on these data with reference to the intersection of the $\beta - t$ curve for D_2O and H_2O at about 50° are unfounded. Our results for ultrasonic velocity in D_2O within the temperature range of 10-90° are in agreement with data reported by Heusinger [11] within about 1 m/sec (0.07%). The densities of D_2O were taken from data published recently [12].

TABLE 3

Adiabatic Compressibility, $\beta_{D_2O}\left(\frac{cm^2}{dyne} \cdot 10^{12}\right)$

t, °C	β	t, °C	β
10	49.40	65	43.05
20	47.00	70	43.10
30	45.35	80	43.45
40	44.20	90	4 4.20
50	43.50	95	44.65
60	43.15		

The existence of a minimum of the compressibility-temperature curve and of a maximum of the density curve in the case of water is explained as being the result of the superposition of two effects observed with a rise in temperature: the increase in the intensity of thermal motion (increase in compressibility) and the transition of water from a state of a high degree of association to one of a lesser degree of association, accompanied by a more dense packing of the molecules (decrease in compressibility). The fact that the compressibility of D_2O exceeds that of H_2O by 2.5-3.5% and that the minimum of the curve lies 1° above that for water (65 and 64°, respectively) means, we suggest, that in the case of heavy water the decrease in the degree of association with temperature lags behind that observed for normal water. This corresponds to an increase in the degree of association through hydrogen bonding, and, evidently, also to a decrease in the extent of van der Waals' interaction in the case of D_2O as compared with H_2O. This treatment of the problem is in agreement with the well-known isotopic effect observed in the temperature of maximum density [9], in thermal properties [3, 14], as well as in the solubility and solvent power of D_2O [4]. The decrease of ultrasonic velocity with substitution of deuterium for hydrogen in the compounds investigated is, to some extent, directly caused by the increase in molecular weight [15].

The authors wish to express their gratitude to Corresponding Member of the Academy of Sciences, U.S.S.R., A. I. Brodsky for his advice and discussion of the results.

LITERATURE CITED

[1] G. N. Lewis and R. T. Macdonald, J. Amer. Chem. Soc. 55, 3057 (1933).

[2] I. B. Rabinovich, N. A. Sokolov, and P. I. Artyukhin, Proc. Acad. Sci. USSR 105, 762 (1955).

[3] A. Eucken and M. Eigen, Z. Electrochem. 55, 343 (1951).

[4] I. B. Rabinovich and V. D. Fedorov, et al., Proc. Acad. Sci. USSR 105, 108 (1955).

[5] J. Timmermans, Physicochemical Constants of Pure Organic Compounds, 1950.

[6] V. V. Tarasov and E. G. Ponedelnikova, Proc. Acad. Sci. USSR 96, 789 (1954).

[7] Ya. K. Syrkin and M. E. Dyakina, Chemical Bond and the Structure of Molecules, 1946.

[8] I. G. Mikhailov and A. M. Nezhin, Proc. Acad. Sci. USSR 58, 1689 (1947).

[9] R. T. Lagemann, L. W. Gilley, and E. G. McLeroy, J. Chem. Phys. 21, 819 (1953); R. R. McMillan and R. T. Lagemann, J. Acoust. Soc. Amer. 19, 956 (1947).

[10] M. Pancholy, J. Acoust. Soc. Amer. 25, 1003 (1953).

[11] P. P. Heusinger, Naturwiss. 36, 279 (1949).

[12] P. Ysberg and L. Lundberg, Z. Naturforsch. 9a, 472 (1954).

[13] L. Hall, Phys. Rev. 73, 775 (1948); I. G. Mikhailov, J. Phys. Chem. 30, 466 (1956).

[14] A. I. Brodsky, The Chemistry of Isotopes, 1952; I. Kirshenbaum, Heavy Water, 1953.

[15] Tyzyo Kiyoshi, Bull. Chem. Soc. Japan 27, 300 (1954).

Institute of Chemistry
N. I. Lobachevsky State University
Gorky

Received September 1, 1956.

INVESTIGATION OF THE KINETICS OF SUPERSATURATION WITH REFERENCE TO THE FORMATION OF CRYSTALLIZATION STRUCTURES IN THE HARDENING PROCESS OF GYPSUM

E. E. Segalova, V. N. Izmailova, and Academician P. A. Rebinder

Two types of structures may be formed in disperse systems – coagulation structures and crystallization structures [1]. One of the widespread types of the latter structures is that formed in the process of hydration hardening of mineral binding materials. The strength of hardening structures results from the formation between individual crystals of hydrates, crystallized from supersaturated solutions, of strong intercrystalline contacts, that is, of points of direct junction. Such crystallization contacts are thermodynamically unstable structures [2] and their formation under the usual conditions is possible only in systems of a sufficiently high degree of supersaturation.

Mechanical destruction of crystallization structures in the course of their formation is irreversible even when the process of hydration is still far from being complete [1]. The continued hydration and the resultant crystallization of the dihydrate under these conditions do not bring about the formation of a crystallization structure. This can be explained only by the fact that in this case favorable conditions for the formation of intercrystalline contacts between individual microcrystals of the dihydrate of gypsum are absent. Evidently, this is due to the accumulation of a large quantity of the dihydrate in the suspension.

The degree of supersaturation and its variation with time in suspensions of the hemihydrate of calcium sulfate can be conveniently studied conductometrically. In our experiments we used the β-hemihydrate having an apparent specific surface of $S = 3060$ cm^2/g. In Fig. 1 is represented the variation with time of specific conductivity, being a measure of the concentration of calcium sulfate or of the degree of supersaturation in suspensions containing different amounts of the hemihydrate, at a temperature of 25°. Conductivity determinations were carried out by the usual method using alternating current.

First of all it must be noted that in all suspensions of the hemihydrate containing more than 8 g of $CaSO_4$ per liter there is the same maximum degree of supersaturation [3, 4] corresponding to a concentration of 8.0 g of $CaSO_4$ per liter in the liquid phase of the suspension, a value which is accepted as the "solubility" of the hemihydrate. This constant and high degree of supersaturation in the aqueous phase of the suspension remains unaltered as long as the rate of removal of Ca^{++} and SO_4^{--} ions from the solution due to the crystallization of the dihydrate is compensated by the rate at which these ions pass into solution. As will be seen from Fig. 1, the higher the concentration of the disperse phase the earlier does the decrease in supersaturation set in and the faster does it take place.

Figure 2 shows the variation with time of the specific conductivity of suspensions of calcium sulfate hemihydrate containing different amounts of added dihydrate. The microcrystals of the dihydrate act as ready-made crystallization nuclei thus accelerating the crystallization of gypsum. As a result, in suspensions containing the dihydrate in amounts up to 30% of the solid phase there is a decrease in the period during which the degree of supersaturation, having been attained rapidly, remains constant. Addition of more than 30% of the dihydrate to the solid phase increases the rate of crystallization of the new phase to such an extent that the maximum degree of supersaturation cannot be attained and there is a sudden sharp decrease in supersaturation

of the suspension. The amount of the dihydrate present in the system which will just prevent attainment of the maximum level of supersaturation, should increase with decreasing degree of dispersion of the dihydrate and with increasing degree of dispersion of the original hemihydrate of gypsum.

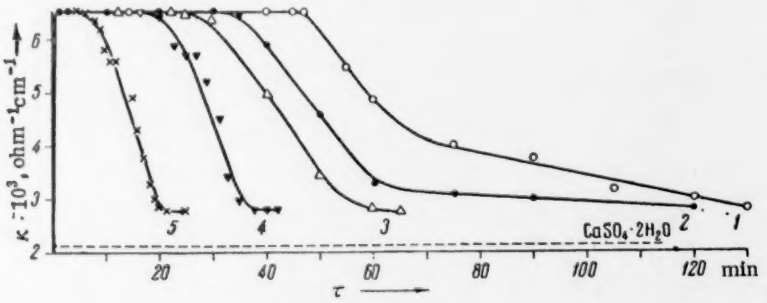

Fig. 1. Variation of specific conductivity with time in suspensions containing different amounts of $CaSO_4 \cdot 0.5\ H_2O$ per 500 ml of water: 1) 6 g; 2) 10 g; 3) 25 g; 4) 50 g; 5) 150 g.

The dependence of the degree of supersaturation on the dihydrate content of the suspension provides an explanation for the effect of additions of the ready-made new phase, the dihydrate, on the strength of the structure formed in the hardening process. Figure 3 represents the kinetics of structure formation in terms of the increase in plastic strength of pastes containing 30% of the hemihydrate of gypsum and 70% of a filler [5, 1, 2] (a mixture of ground quartz sand and the dihydrate of gypsum). Curve 1 corresponds to the original suspension without added dihydrate; Curve 2 corresponds to a suspension containing a small amount of added dihydrate. This addition of the dihydrate has the effect of shortening the induction period of structure formation [5, 1], i.e., it accelerates the hardening process, but does not affect the ultimate strength of the structure.

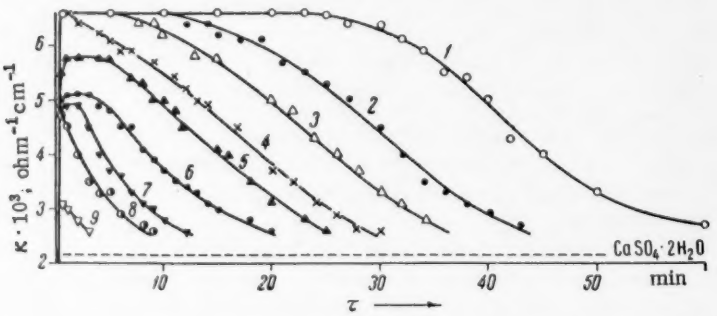

Fig. 2. Variation of specific conductivity with time in a suspension of 25 g $CaSO_4 \cdot 0.5\ H_2O$ in 500 ml of water during addition of dihydrate: 1) 0; 2) 1 g; 3) 3 g; 4) 10 g; 5) 20 g; 6) 25 g; 7) 50 g; 8) 75 g; 9) 100 g of $CaSO_4 \cdot 2H_2O$.

Subsequent curves in Fig. 3 correspond to increasing amounts of added dihydrate; the process of hardening is accelerated with each addition of the dihydrate, but the maximum strength of the structure decreases progressively.

On substituting half or all of the sand for the dihydrate (Curves 6 and 7) the strength of the crystallization structure is reduced 30-60 fold as compared with the normal strength of a corresponding mixture of mineral gypsum with sand, without the addition of the dihydrate. It must be mentioned that in these experiments hydration of the hemihydrate was always complete and hydration kinetics was always in complete agreement with the kinetics of structure formation [1].

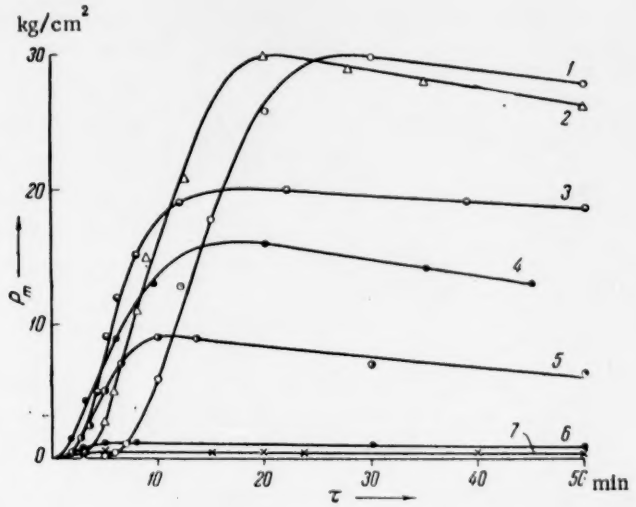

Fig. 3. Kinetics of structure formation in systems containing 30% of $CaSO_4 \cdot 0.5\ H_2O$ and 70% of filler (mixture of different amounts of sand and the dihydrate). Water/solids ratio = 0.5.

The decrease in maximum strength of the crystallization structure of gypsum observed in these experiments is due to the lowering of the maximum level of supersaturation which can be attained in the presence of added dihydrate (Fig. 2). The lowering of the degree of supersaturation (reduction of the period during which supersaturation is maintained) reduces the probability of the growing together of microcrystals, i.e., of the formation of intercrystalline contacts. In suspensions with a high dihydrate content only a low level of supersaturation is attained and is maintained for a comparatively short time. Under these conditions there is practically no formation of crystallization contacts and, consequently, no hardening structure is formed.

These are the reasons why, in suspensions in which a large quantity of the dihydrate has accumulated as the new phase continued, hydration hardening is prevented when the incompletely formed crystallization structure is broken down mechanically.

On the basis of these considerations it is now clear that in suspensions of highly disperse gypsum dihydrate which has been proposed by some authors [6] as a specific binding material, hardening through crystallization cannot take place under normal conditions: the high levels of supersaturation to which the colloidal fraction present in finely ground material can give rise, cannot be attained on account of the presence of a large quantity of the dihydrate, and recrystallization of particles of colloidal dimensions will not cause the microcrystals to grow together, but will promote their free growth individually.

In systems of this type and of sufficiently high density, as also in clays, structural strength depends on the removal of water by drying and on the resultant strengthening of coagulation contacts between the microcrystals on their extreme approach. As is well known, such structures, unlike the crystallization structures, are very unstable toward water, i.e., when moistened they completely lose their strength because of the reversibility of changes in strength of coagulation contacts with changing thickness of films of water separating the particles [7].

LITERATURE CITED

[1] V. N. Izmailova, E. E. Segalova, and P. A. Rebinder, Proc. Acad. Sci. USSR 107, 3, 425 (1956).

[2] E. E. Segalova, V. N. Izmailova, and P. A. Rebinder, Ibid., 110, 5, 808 (1956).

[3] Ya. L. Zabezhinsky, V. B. Ratinov, and T. I. Rozenberg, Ibid., 108, 6, 1137 (1956).

[4] V. B. Ratinov, Ya. L. Zabezhinsky, and T. I. Rozenberg, Ibid., 109, 5, 979 (1956).

[5] E. E. Segalova, P. A. Rebinder, and O. I. Lukyanova, Bull. Moscow State Univ., No. 2, 17 (1954).

[6] L. G. Gulinova and V. A. Ipatieva, Nonglazing Gypsum Cement and Its Uses, (Acad. Archit. Ukrain. SSR Press, 1954); I. L. Rivlin and L. P. Papkova, Trans. Kharkov Polytech. Inst. 8, No. 3, Chem. Technol. Series, 219 (1956).

[7] P. Rebinder, Disc. Farad. Soc. No. 18 (1954); P. Rebinder, and E. Segalova, Preprints Proc. 2 Internat. Congr. of Surface Activity, London, April, 1957.

Received April 2, 1957.

THE THERMAL DECOMPOSITION OF NITROCELLULOSE IN VACUUM

K. K. Andreev and B. S. Samsonov

(Presented by Academician V. N. Kondratyev November 17, 1956)

It is known that the thermal decomposition of nitrocellulose, although it is highly accelerated by failure to evacuate the gaseous decomposition products (see, for example, [1]), proceeds at a constant rate of evolution of gaseous nitrogen compounds when it is carried out in a current of inert gas [2]. This constancy of the absolute rate over a considerable portion of the disintegration indicates, however, a substantial increase in the relative rate. It might be supposed that the cause for this increase is to be found in the incomplete removal of the disintegration products during the break-down in a current of inert gas. In order to test this supposition A. D. Lebedev (1954) studied the decomposition of nitrocellulose under a continuous evacuation of the product gases at a pressure which did not exceed 5.10^{-4} mm of Hg. For determining the rate of gas evolution, the pumps were momentarily cut off; the increase in the pressure, as determined on a McLeod gauge, served as a measure of the rate of gas formation. Between the decomposition chamber and the manometer there was a liquid nitrogen trap, so that the pressure as measured was that due to the formation of those gases which, condensing with difficulty, were not retained in the trap. Contrary to expectations, the experiments of Lebedev showed that, under the indicated conditions, the absolute rate of gas formation did not decrease in the course of decomposition but increased by several fold (up to 8 times).

In connection with these results the decomposition of nitrocellulose (13.35% N) in vacuum was investigated in greater detail. In addition to determining the amount of the difficultly condensing gases there was at the same time measured the rate of formation of those gases which were caught in the trap. This was achieved by the use of two traps which were connected in parallel and alternately cut into the line. After working for a definite period, one of these traps was disconnected, the pressure of the decomposition products which arose as the result of its warming to room temperature was measured with a membrane manometer, and the volume of the gases calculated by the Clapeyron law. At the same time the loss in mass of the sample was determined with the aid of a MacBain balance. Experiments were carried out at various temperatures (160-135°).

The curves of Figure 1 show that, at 160°, the rate of formation of the gases condensed in the trap is greatest at the initial instant and continually falls, whereas the rate of production of those gases which are not caught by the trap increases in conformity with the data of Lebedev: relatively small at the beginning, it increases by 7-8 fold to a maximum and approaches the rate of formation of the condensable gases. After passing through this maximum, the rate of formation of these difficultly condensable gases diminishes. The volume of these gases amounts to from $\frac{1}{4}$ to $\frac{1}{3}$ of the total volume of the gaseous disintegration products. In conformity with the described course of the two rate curves, the net rate of gas formation remains approximately constant over a certain interval of time – up to the onset of the maximum in the curve for the formation of the difficultly condensable gases – and then sharply falls. The same picture of the decomposition process is supported by the loss in weight curves.

From the graph showing the dependence of the rates of gas formation on the temperature (Fig. 2) it is possible to calculate (Table 1) the kinetic coefficients of the Arrhenius equation. The values of E and B for the rate of decrease in mass and the rate formation of the condensable gases are practically the same. Here E is close to the energy of activation of the initial process in the decomposition of the alkyl nitrates which supposedly involves the breaking off of the NO_2 groups [3]. In turn, these quantities are very close to the values of Will [2] which were obtained from the breakdown of nitrocellulose in an inert gas current ($k = 10^{17.5} \cdot e^{-43700/RT}$). During

decomposition without evacuation of the gases, the velocity of gas formation is considerably greater and its temperature dependence is less pronounced; correspondingly B is also less.

It is to be seen from curves in Figure 1 that the dependence of the rate of gas formation on time during the decomposition of nitrocellulose in vacuum is different for the condensable and for the difficultly condensable gases. This difference is difficult to explain without having recourse to the supposition that at least two consecutive reactions are taking place during the decomposition. Judging from the character of these curves, the

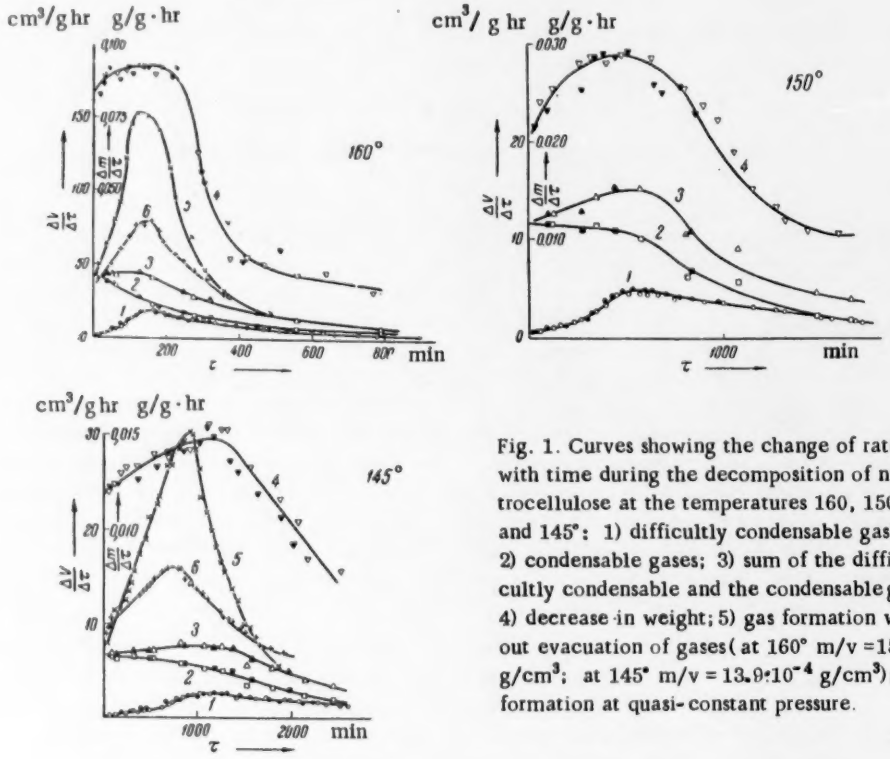

Fig. 1. Curves showing the change of rates with time during the decomposition of nitrocellulose at the temperatures 160, 150 and 145°: 1) difficultly condensable gases; 2) condensable gases; 3) sum of the difficultly condensable and the condensable gases; 4) decrease in weight; 5) gas formation without evacuation of gases (at 160° m/v = $15.8 \cdot 10^{-4}$ g/cm³; at 145° m/v = $13.9 \cdot 10^{-4}$ g/cm³); 6) gas formation at quasi-constant pressure.

formation of the condensable products should be looked on as the result of the primary processes. The formation, in addition to the condensable gases, of a nongaseous intermediate product of limited stability, the subsequent transformation of which is accompanied by the production of difficultly condensable* gases, would give that overall picture of the decomposition process which is actually observed in practice.

It is true however that even the formation of the condensable gases cannot be considered as a simple monomolecular reaction. Although at 160° there is observed a continuous decrease of rate with time according to a law which is close to that for a first order reaction, at still lower temperatures there is a considerable departure from this relationship, such as would exist if this reaction were in turn a combination of two successive (or parallel) reactions. Thus at 150 and 145° (Fig. 1) the decrease of the rate of formation of the condensable products proceeds slowly at the beginning; over a considerable period of time this rate remains constant. As a result the overall rate of gas formation markedly increases.

* It should not be thought that through this proposed reaction there can be formed only gases which are difficultly condensable; simultaneous production of condensable gases is also possible, in which case the rate of formation of these gases is the sum of the rates of the two reactions.

It follows from the facts just described, that such integral characteristics of decomposition as the overall rate of gas formation or the loss of mass are, in the case of nitrocellulose, the results of combining a series of reactions and cannot be directly employed for the calculation of the kinetic parameters of the separate reactions.

TABLE 1

The Kinetic Coefficients of the Reaction Rates for the Thermal Decomposition of Nitrocellulose in Vacuum at 135-160°

The nature of the reaction according to which the velocity constant is calculated	The initial values of the velocity constants, K, $sec^{-1} \cdot 10^5$				E, cal/ /mole	log B	The method of calculation of E
	135°	145°	150°	160°			
Loss in mass*	0.090	0.33	0.65	2.4	44600	17.8	By combination of curves showing loss in weight with time
Formation of gases	0.18	0.60	1.1	3.3	43400	17.5	According to the initial rates of gas formation
Formation of condensable gases	0.24	0.77	1.5	4.9	42100	16.9	Ditto
Formation of difficultly condensable gases	0.019	0.084	0.16	0.50	45700	17.8	By combination of the curves in the coordinates $\Delta v/\Delta\tau = f(\tau)$
Gas evolution without evacuation of the gases**	0.10	0.40	—	1.9	39200	15.0	By combination of the curves $p = f(\tau)$

* The velocity constant for the loss in weight was calculated relative to the loss in weight at τ_∞; that for the formation of gas, relative to the volume of the gases which were evolved at τ_∞.

** These experiments were carried out at 100-170°.

The experiments described above refer to the decomposition in vacuum. By carrying our pressure measurements with the membrane manometer [4] there was also studied the decomposition of nitrocellulose in a closed volume and the influence of certain additives on this decomposition. In line with earlier investigations [1], it was confirmed that the formation of gas proceeds under these conditions with a marked acceleration. At the same time the amount of gas which is formed is considerably greater than that produced in vacuum decomposition and the weight of the solid residue is less.

The acceleration of the gas formation is greater, the larger the amount of nitrocellulose per unit volume of the vessel, i.e., the greater the pressure of the decomposition products. Acceleration of the gas formation was, however, also observed in experiments at quasi-constant pressure, in which the pressure was allowed to rise to a small fixed value (20 mm of Hg), after which the gases were rapidly pumped away. Even in this case the velocity considerably increased with time (approximately twofold), from which it follows that, in conformity with the experiments in vacuum, the acceleration of gas formation during the decomposition of nitrocellulose is determined by factors other than the mere increase in the concentration of the gaseous decomposition products.

The intial rates of gas formation in vacuum and without evacuation of the gases are practically the same; the maximum velocity in the latter case ($m/v = 10\text{-}20 \cdot 10^{-4}$ g/cm^2) is only 3-4 times greater than at $5 \cdot 10^{-4}$ mm, i.e., in a pressure only one millionth as large. Otherwise expressed, the accelerating action of the gaseous decomposition products on the breakdown is so insignificant that there is scarcely a basis for considering it to be catalytic. It is also weakly dependent on the pressure in the region of small pressures. The transition from experiments at quasi-constant pressure, wherein the mean pressure amounts to 10 mm, to experiments in which

there was no evacuation of gases and $P_{max.} = 500$ mm, increases the rate of gas formation merely by twofold. For further increase of the pressure at the maximum $(\Delta v/\Delta \tau)_{max.}$ increases almost proportionally to this pressure.

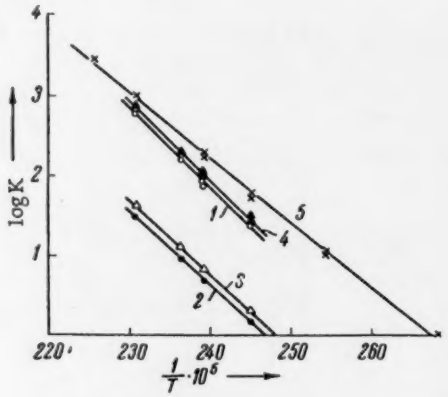

Fig. 2. The dependence of the velocity constants on the temperature: 1) formation of difficultly condensable gases; 2) formation of condensable gases; 3) total gas formation; 4) loss in weight; 5) gas formation without evacuation of gases. The constants are plotted in the graph in terms of various arbitrary units; for their absolute values see Table 1.

In light of the data which have been obtained, it is likely that the influence of the gaseous decomposition products is to be found principally in the interaction of their reactive components with one another and with the solid substance, this leading to the formation of additional quantities of gases.

Experiments on the decomposition of nitrocellulose in the presence of oxygen have shown that the latter retards gas formation at the beginning of the experiment but leads in the sequence to a sharp acceleration of the breakdown. The presence of water vapors in itself weakly accelerates the evolution of gases during decomposition; however in the presence of water and oxygen together there is an induction period, in the course of which the pressure practically remains unchanged, following which there sets in a sudden decrease in pressure and then a sharp acceleration of gas liberation. Thus the picture of the decomposition which is found in the literature (see for example [5]) and which is considered as being fixed by the action of water, is in actuality determined by the mutual action of water and atmospheric oxygen, in the presence of which these experiments are usually initiated. The difference between nitrocellulose and nitroglycerin, the decomposition of which is accelerated by water even in the absence of oxygen [6], obviously results, first of all, from the fact that in the case of nitrocellulose the nitrogen peroxide which is split off is rapidly reduced to nitric oxide, no acid is formed, and hydrolysis in their absence proceeds slowly. Oxygen, oxidizing NO, assures an adequate concentration of NO_2 and acid. It is true that according to our experiments nitric oxide also gives rise to an acceleration of the breakdown of nitrocellulose, but this action is much weaker than that of nitrogen peroxide, nitric acid, or, especially, sulfuric acid. We would like to add that the action of nitric acid has been studied both in the presence of water and in its absence. In the former case the acceleration is considerably greater. It should also be pointed out that in the decomposition of nitrocellulose in the presence of NO_2 or nitric acid, the curves showing the change of rate with time have two characteristic maxima; their magnitude and time at which they put in their appearance depend on the amount of nitric oxide or acid.

The D. I. Mendeleev Institute of Chemical Technology, Moscow

Received November 16, 1956

LITERATURE CITED

[1] A. V. Sapozhnikov, J. Russ. Phys.-Chem. Soc. 36, 836 (1904); 37, 822 (1905); 38, 1186 (1906).

[2] W. Will, Zs. f. angew. Chem., 14, 774 (1901).

[3] J. B. Levy, J. Am. Chem. Soc., 76, 3790 (1954).

[4] J. Schaeffer and J. Treub, Zs. phys. Chem., 81, 308 (1913).

[5] J. Goujon, Mem. Artill. Franc., 8, 837 (1929).

[6] K. K. Andreev and A. P. Glazkova, Proc. Acad. Sci. USSR 105, No. 2, 286 (1955).

THE EXPLOSIVE DECOMPOSITION OF HEXOGEN

A. Ya. Apin and Yu. A. Lebedev

(Presented by Academician V. N. Kondratyev December 26, 1956)

In a number of investigations [1-3] reference has been made to the dependence of the reaction of explosive decomposition on the density, the size and form of the charge, the power of the initiator and the strength of the casing. The action of these factors to a considerable degree determines the pressure change in the detonation wave front and the influence of pressure on the reversible reactions:

$$2CO \rightleftarrows CO_2 + C + 41.2 \text{ kcal}; \quad (1)$$

$$CO + H_2 \rightleftarrows C + H_2O + 31.4 \text{ kcal}; \quad (2)$$

$$H_2O + CO \rightleftarrows CO_2 + H_2 + 9.7 \text{ kcal} \quad (3)$$

The heat of explosion and the volume of the gaseous explosion products have been determined for trotyl, tetryl, picric acid and a series of other explosives which have a negative oxygen balance. However, until recently, the heat of explosion for hexogen (cyclotrimethylenetrinitramine) has been presented on the assumption that its value is independent of the explosion conditions, and of the charge density in particular.

TABLE 1

The Heat of Explosion of Hexogen at Various Initial Charge Densities (kcal/kg)

ρ, g/cm^3	for liquid water	water vapor
0.50	1.290	1190
0.65	1320	
0.70	1330	
1.00	1370	
1.15	1400	1300
1.70	1490	
1.73	1490	1400
1.74	1500	
1.78	1510	1420

In [4, 5] there is accepted for the heat of explosion of hexogen a value of 1370-1390 kcal/kg when the water is in liquid form or 1290-1370 kcal/kg when the water is in the vapor. Tonegutti [6] determined the heat of explosion for compacted hexogen as Q = 1370 kcal/kg. Medard [7] gives a still more exact value of Q = 1359.5 kcal/kg but does not indicate to what charge density of the hexogen this value of heat of explosion refers. There is, however, no point in determining the heat of explosion with high accuracy if constancy of explosion conditions is not observed.

For full explosion it is most essential to maintain constancy of charge density. As we have experimentally determined, the heat of explosion of hexogen rapidly increases with increasing charge density. These experiments were carried out in the following manner. The hexogen charge of 30-50 g weight and 20-30 mm diameter was inserted in a cylindrical copper casing with a wall thickness of 3-4 millimeters and was suspended in the center of a steel calorimeter bomb of 4.75 l volume and 250 kg weight. Prior to explosion, the air was removed from the bomb with the aid of a vacuum pump, the pressure being reduced to 0.1-1.0 mm of Hg. In these experiments carefully dried hexogen with a melting point of 202-203° was employed. High density charges were prepared by molding and charges of low density were obtained from finely precipitated hexogen.

In Table 1 there are shown values for the heat of explosion of hexogen and their dependence on the charge density. The experimental error amounted here to less than 1%.

As is to be seen from Table 1, a variation of charge density from 0.50 to 1.78 g/cm^3 alters the heat of explosion from 1290-1510 kcal/kg. This is a linear relationship (Fig. 1).

Experiment shows that the reaction of explosive transformation of the hexogen and, consequently, the heat of explosion, the volume and the composition of the explosion products strongly depend on the initial density of the explosive. The heat of explosion is not constant for the explosive. If it is agreed to refer the heat of explosion to a definite charge density of the explosive material, then for hexogen at $\rho = 1.00$ g/cm^3, Q = 1370 kcal/kg for water in the liquid form and Q = 1270 kcal/kg for water as vapor.

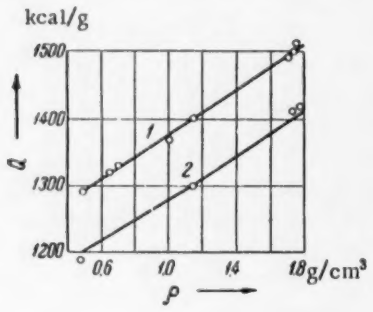

Fig. 1. The relation between the heat of explosion of hexogen and the initial charge density: 1) water in liquid form; 2) water as vapor.

By changing the charge density there is also altered the volume and the composition of the products of the explosion of hexogen; solid carbon appears in these products. In Table 2 data are presented pointing to the influence of the initial charge density on the volume and composition of the explosion products. By increasing the density from 0.50 to 1.78 g/cm^3, the content of carbon dioxide in the explosion products is increased, whereas the gas volume diminishes by more than 10%.

Under an initial hexogen density of $\rho = 1.10$ g/cm^3 the resulting explosion products have the following composition (in percent by volume): CO_2 10.47; CO 22.64; H_2O 23.97; CH_4 0.68; N_2 33.78 and H_2 8.46. On the basis of these data it is possible to set up an approximate equation for the explosive decomposition of the hexogen at $\rho = 1.10$ g/cm^3:

$$C_3H_6O_6N_6 \rightarrow 0.93\ CO_2 + 2.01\ CO + 2.13\ H_2O + 0.06\ CH_4 + 3N_2 + 0.75\ H_2. \quad (4)$$

A comparison of the heats of explosion as obtained from calorimetric measurements and from the analysis of the explosion products shows the agreement to be good. Generally speaking, if it is presumed that in the explosion of a charge of high density all of the carbon monoxide goes over into the dioxide and free carbon, the heat of explosion of the hexogen at the limit would be still higher – up to 1650 kcal/kg. For a correct evaluation of the magnitude of the heat of explosion it is of course necessary to take into account the extent of displacement of the equilibria in the explosion products under the conditions of high pressure prevailing in the detonation wave. At the present time satisfactory data as to the heat, temperature, composition and volume of the explosion products can be obtained through calculation.

TABLE 2

The Volume and the Composition of the Explosion Products from Hexogen at Various Charge Densities

ρ, g/cm^3	V, liters/kg for liquid water	V, liters/kg water vapor	CO/CO_2
0.50	730	930	4.7
1.00	690	890	2.2
1.78	630	820	1.8

The most important result which follows from this work is the fact that in the narrow zone of the detonation wave reversible processes are to be a considerable degree established in the explosion products and over the longer period of the dispersion of these products there is no essential displacement of these equilibria in the reverse direction, i.e., there is an extremely strong "quenching" of these equilibria.

Thus, the experimental determination of the heat of explosion, the composition and the volume of explosion products in the steel bomb makes it possible to obtain data which more or less indicate the true picture of

the processes occurring under the conditions prevailing in the detonation wave. A change in the "quenching" regime and a more exact determination of the heat of explosion and the composition of the explosion products for explosives in the makeup of which there are metallic and inert additives of various degrees of dispersion, would make it possible to establish a more correct conception as to the mechanism of the reactions in the detonation wave.

The determination of the heat of explosion and the composition of the explosion products for explosive charges whose diameter approaches the critical value would permit the estimation of the pressure drop in the detonation wave and the magnitude of the loss.

Received December 21, 1956

LITERATURE CITED

[1] A. Robertson and W. Garner, Proc. Roy. Soc., 103, 539 (1923).

[2] A. Haid and A. Schmidt, Zs. Ges. Schiess.-u. Sprengstoffe, 26, 8-9, 293 (1931).

[3] T. C. Sutton, Trans. Farad. Soc., 34, 992 (1938).

[4] K. K. Snitko, The Theory of Explosives,* 1936.

[5] A. Stettbacher, Explosivstoffe, 3/4, 39 (1954).

[6] M. Tonegutti, Zs. Schiess.-u. Sprengst. 32, 93 (1947).

[7] M. Medard, 27 Congr. Chim. Industr., Brussel, 1954, p. 81.

*In Russian.

THE ADSORPTION OF HYDROGEN ON NICKEL FILMS CONDENSED IN HIGH VACUUM

N. N. Kavtaradze

(Presented by Academician A. N. Frumkin, November 27, 1956)

The nature of the adsorption of hydrogen on metals is at the present time not clear. For studying this phenomenon we have made use of films which were obtained by vaporizing metals of high purity. It turned out that there were to be distinguished two groups of metals which sharply differ from one another in regard to the character of their adsorption of H_2 [1-3]. The data applying to the adsorption of H_2 on nickel permits the description of the peculiarities of the metals belonging to one of these groups. Films were prepared in a round bottom flask of 200 cm^2 inner surface area, which was sealed to a vacuum line. A vacuum of $\leq 1 - 1.5 \cdot 10^{-7}$ mm of Hg was obtained by diffusion pumps working on octoil S, and two liquid nitrogen traps. The adsorption of H_2 (and also of Kr, in the measurement of film areas) was determined at temperatures ranging from -195 to 100° and under pressures from 10^{-6} to $2\text{-}4 \cdot 10^{-2}$ mm of Hg by the admission of portions of the gas and also by the method of gas in leakage through a capillary tube [4, 5]. The pressure was measured with a Pirani manometer. The influence of the thermal effusion was taken into account by the method proposed by us in [6]. The Ni films were obtained by the electrical heating of Ni spirals (Ni 99.97%, Fe 0.018%, C 0.010%, and Si 0.010%). The electrolytic H_2 which was employed in the investigation was finally purified by diffusion through a Pd capillary.

The experimental procedure consisted of: degasing the vaporizer in a secondary vacuum line; heating the reactor with the vaporizer to 450° for 5 hours under a vacuum of $\sim 2 \cdot 10^{-7}$ mm Hg; determining calibration curves (by inleakage into the empty reactor) at 0° and at the experimental temperatures; heating the reactor to 450° in a vacuum of $\sim 1\text{-}2.5 \cdot 10^{-7}$ mm Hg; vaporizing the Ni at 0° or at $-78°$; heating the reactor with the Ni film (in case of necessity) in vacuum of $1\text{-}1.5 \cdot 10^{-7}$ mm Hg; cooling the reactor to the experimental temperature and measuring the adsorption.

At $-195°$ H_2 is very rapidly adsorbed on Ni: in the first minute after the introduction of a portion of gas there is adsorbed 91%, and in 10 minutes 98.4%, of the quantity of gas which is taken up in the experiment. Adsorption ceases 20 minutes after the beginning of the experiment and the pressure in the reactor then remains constant. Measurement of adsorption by the inleakage method (Fig. 1) shows that the pressure, which prior to experiment was $\sim 2 \cdot 10^{-7}$ mm Hg, remains $\leq 2 \cdot 10^{-6}$ mm Hg in the initial period of H_2 inleakage (from 6 to 50 minutes, depending on the film area), i.e., the hydrogen is almost instantaneously adsorbed. The pressure sharply rises only after the adsorption of $\sim 88\%$ of the total quantity of gas which is taken up in the experiment. If the inleakage of H_2 is cut off at the very beginning of this pressure increase, the value of the pressure rapidly falls to $< 10^{-7}$ mm Hg. This indicates that the adsorption in the final stage does not occur instantly. Breaking off inleakage 20-30 minutes after the beginning of the pressure increase does not lead to a change in the pressure, i.e., the adsorption is then already completed.

After the first inleakage of H_2 and evacuation of the reactor to $4 \cdot 10^{-7}$ mm Hg, a second inleakage was carried out. During the evacuation, there was removed from the film surface the less firmly bound hydrogen and a part of the Ni surface was freed. This portion is characterized by a secondary adsorption during the

second inleakage. Curves for this second inleakage do not correspond with those for the first. The second adsorption amounts to ≤ 3% of the entire amount taken up the first inleakage; its curve passes rapidly to saturation and for $P > 5 \cdot 10^{-3}$ mm Hg does not essentially change. Breaking off the inleakage of H_2 at any other stage of this adsorption makes it impossible to discover the kinetics of the latter. The curve for a third inleakage, as measured after a new evacuation of H_2, completely coincides with the preceding one. It follows from this that the adsorption of H_2 in the second and third inleakages can be looked on as completely reversible and almost instantaneous and it is accordingly permissible to consider it as a function of the pressure. The isotherm for the reversible adsorption is presented in Fig. 2; to a first degree of approximation it follows the Langmuir equation. After evacuating the reactor to $4 \cdot 10^{-7}$ mm Hg the vacuum in it remains unchanged; on elevating the temperature of the reactor to − 78° there is observed a sharp pressure increase which results from the desorption of hydrogen which was irreversibly adsorbed at − 195°. Evacuating the reactor and increasing its temperature from 0 to 200°, we found that at 150° and above the desorption of H_2 was practically complete and almost the entire film surface was free.

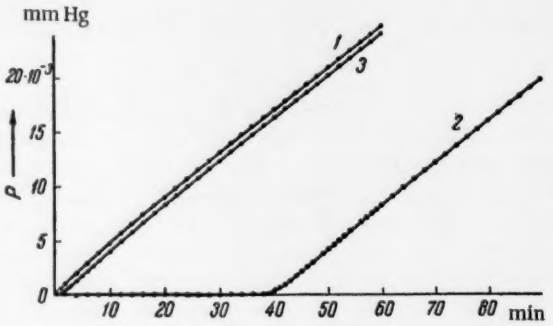

Fig. 1. The adsorption of H_2 at − 195° on a Ni film (440 A in thickness): 1) inleakage of H_2 into the empty reactor; 2) first inleakage and 3) second inleakage of H_2 into the reactor with the Ni film.

The facts just described indicate that the total adsorption of H_2, (N_Σ), even at −195° is composed of two parts: a rapid irreversible, (N_{irr}), and an instantaneous reversible, (N_{rev}), adsorption, the H_2 which is irreversibly adsorbed at − 195° being desorbed on elevating the temperature and the Ni surface proving to be practically free of it at 150°. It was established that the maximum magnitude of the reversible adsorption, ($N_{rev, max}$), at − 195°, calculated according to Langmuir equation, exceeded its magnitude at $P = 2 \cdot 10^{-2}$ mm Hg (see Fig. 2) by 1%; thus it follows that this equation is suitable for the evaluation of $N_{rev, max}$. It has also been shown that the contributions arising from the two types of adsorption of H_2 on Ni do not depend on the thickness and the area of the film.

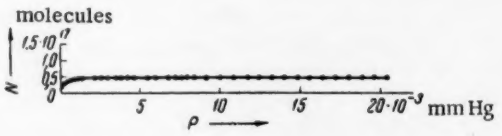

Fig. 2. The isotherm for the reversible adsorption of H_2 on a Ni film at − 195° (film thickness 440 A).

The adsorption of H_2 on Ni at -78° retains the same qualitative properties as at -195°; the difference consists entirely in an increase of the contribution of the reversible adsorption to a value of 18% of the total adsorption and in a more rapid completion of the latter. The rate of adsorption of H_2 on Ni at 0° is just as great for the admission of a portion of the gas into the reactor with a Ni film which was condensed at 0°; in the first minute there was adsorbed 95% of the total amount of gas taken up in the course of the experiment. The take-up of the remaining 5% continues, however, for 60-80 minutes. Fearing that so extended a take up of this 5% of gas was connected with the dissolving of the latter in the film and in the vaporizer (a nickel spiral of ~ 500mg weight), we measured the adsorption at 0, 50 and 100° on nickel films which had been previously

TABLE 1

The Surface Area of the Ni Film Associated with one Atom of Hydrogen Adsorbed at -195°*

Expt. No.	T_{ads} in °C	Gas	σ_G, Å^2	σ_H, Å^2	Sources
1	—195	Kr	18.5; 14.6	7.55; 5.98	Our data
2	—195	Kr	18.5; 14.6	7.78; 6.11	
3	—195	Kr	18.5; 14.6	7.53; 5.94	
4	—195	Kr	14,6	6,18	Data of Beeck [9]
5	— 78	n-C_4H_{10}	24,5	6,18	

* T_{ads} is the temperature of adsorption of the gas which has been selected for the surface measurement, σ_G is the accepted value of its contact area and σ_H is the area per atom of hydrogen.

heated to 200° in an atmosphere of H_2 ($P = 2 \cdot 10^{-2}$ mm of Hg) and then evacuated at this same temperature to $2 \cdot 10^{-7}$ mm of Hg. In this case the adsorption was rapidly completed. The data obtained (Fig. 3) show that the qualitative properties of the adsorption as determined at -195 and -78° are retained even at higher temperatures, the change in temperature resulting only in an alteration of the ratio between the reversible and the

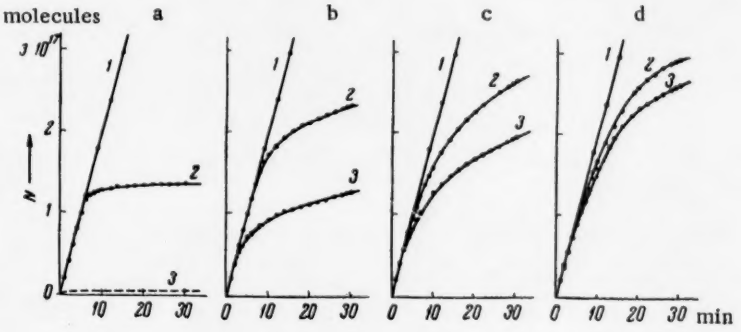

Fig. 3. The adsorption of H_2 on a Ni film (1662 A in thickness, heated to 200°) at the temperatures: a) -195°, b) 0°, c) 50°, d) 100°; 1) inleakage of H_2 into the empty reactor, number of molecules in the reactor; 2) total adsorption and 3) reversible portion of the H_2 adsorption.

irreversible parts; increasing the magnitude of adsorption simultaneously brings about an increase in the reversible part and a diminution in the magnitude of the irreversible adsorption. We also note that the initial portions of the isotherms for the reversible adsorption of H_2 on Ni at -78, 0, 50 and 100° deviate somewhat from the Langmuir equation but, as calculations have shown, are well described by the logarithmic pressure function

which has been developed by A. N. Frumkin and A. N. Shlygin [7, 8]. These qualitative characteristics of the adsorption of H_2 on Ni are also shown in the adsorption of H_2 on Fe, Cr, and Pt.

For the calculation of the coverage by the films of hydrogen adsorbed at -195°, the areas of these films were determined by the adsorption of Kr at -195°. Our data agree very well with the measurements of Beeck [9] for films which had been condensed in vacuum (see Table 1); if it is presumed that the hydrogen adsorbed at -195° is in the atomic condition, it is then possible to calculate that at this temperature and with $P = 2 \cdot 10^{-2}$ mm of Hg the surface is almost completely covered with atomic hydrogen, i.e., with a surface hydride.

A study of the influence of the sequence of temperature changes on the total adsorption has shown that in adsorption measurements beginning at the higher temperature (100°), going to the lower (-195°) and back once again to the higher temperature, the values of the adsorption are reproduced and there is no adsorption hysteresis, i.e., the adsorption curves are equilibrium curves; between 0 and -78° the adsorption passes through a maximum. On the other hand, if adsorption is measured by beginning at -195°, going to 100° and then back to -195° (Fig. 4), adsorption hysteresis puts in its appearance, but the presence of a maximum between 0 and 78° on the curve going from 0 to -195° (Curve 1') is once more confirmed. After heating the film in H_2 at 150° and evacuating the reactor to $2 \cdot 10^{-7}$ mm of Hg, the measurements were repeated in this same order (Curve 2); this confirmed the existence of hysteresis but also showed an adsorption maximum (see Curve 2'). By measuring the adsorption of H_2 on iron films the adsorption hysteresis and a maximum were confirmed even for this system but there was at the same time shown a more sharply expressed diminution of the hydrogen adsorption on lowering the temperatures from -78 to -195° or from 0 to -78 and -195°

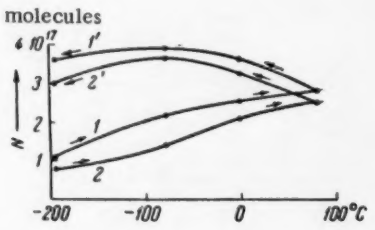

Fig. 4. The adsorption of H_2 (at a constant amount of the latter in the system) by a film of Ni (of 1674 A thickness): 1 and 1') the adsorption of H_2 on an Ni film which was heated to 150° in vacuum; 2 and 2') the adsorption of H_2 on this same film but heated in H_2 ($P \sim 2 \cdot 10^{-2}$ mm of Hg) at 150° and subsequently evacuated to $2 \cdot 10^{-7}$ mm of Hg.

The data which has been presented show that the adsorption of H_2 on Ni, as well as on Fe, Cr, and Pt, is a complex process; it is composed of a reversible and an irreversible part, the first of which strongly depends on the temperature and the pressure and the second principally on the temperature; an influence of pressure on the magnitude of adsorption is not apparent over the investigated range of pressures.

The Institute of Physical Chemistry of the Academy of Sciences of the USSR

Received November 22, 1956

LITERATURE CITED

[1] N. N. Kavtaradze, Heterogenous Catalysis in the Chemical Industry. Material from the All-Union Congress of 1953,* Moscow, 1955, p. 150.

[2] N. N. Kavtaradze, Electronic Phenomena in Catalysis and Adsorption,* Acad. Sci. USSR Press 1955, p. 235.

[3] N. N. Kavtaradze, Outlines of the Reports of the Conference on Catalytic Hydrogenation and Oxidation,* Alma-Ata, 1954, p. 24.

[4] C. Zickermann, Zs. Phys., 88, 43 (1934).

[5] S. Yu. Elovich and F. F. Kharakhorin, Problems of Kinetics and Catalysis,* 3, 225, 1937.

[6] N. N. Kavtaradze, J. Phys. Chem. 27, 1083 (1954).

[7] A. N. Frumkin and A. N. Shlygin, Proc. Acad. Sci. USSR 2, 176 (1934).

[8] A. N. Frumkin, A. N. Schlygin, Acta Physicochim., 3, 791 (1935).

[9] O. Beeck, and A. W. Ritche, Disc. Farad. Soc., No. 8, 159 (1950).

* In Russian.

THE NULL CHARGE POINTS OF CERTAIN METALS AND ALLOYS

B. S. Krasikov and V. V. Sysoeva

(Presented by Academician A. N. Frumkin January 2, 1957)

In a number of papers [1, 2] there has been pointed out the fruitfulness of the concept of the null charge point [3] as a physicochemical constant characterizing a given metal.

During investigation of the null charge potentials of metals (φ_{nc}) it was discovered that, for a given metal, the magnitude of φ_{nc} depends on a number of factors. For example, it was shown [4] that in the mercury-thallium system φ_{nc} changes in dependence on the ratio of the components in the amalgam. In [5] there has been presented an enumeration of those factors which serve to fix the values of φ_{nc} for metals; among these are the composition and the state of the metallic phase. In the present work there was undertaken the measurement of null charge potentials, the aim being to obtain new data on the relation between φ_{nc} and the metallic composition and state.

As test materials we selected monocrystalline zinc (the (0001) and (0101) faces) and alloys of iron and nickel. Zinc electrodes were prepared from chemically pure zinc which had undergone four-fold redistillation in vacuum, monocrystals being grown according to a modification of the method of Polibin and Froiman [6]. The total content of contaminants in these samples did not exceed 10^{-4}%. The iron-nickel alloys were obtained by electroprecipitation out of solutions of chlorides which had been repeatedly purified and recrystallized, use being made of previously refined iron and nickel anodes. The content of other alloying metals in these alloys did not exceed $2 \cdot 10^{-4}$%.

The electrolytes which were employed had the following compositions and properties: Σ Fe^{+2}, Ni^{+2} 100 g/l (as metal); citric acid 15 g/l; pH 4.0 ± 0.2; t = 70°, D_C = 40 a/dm^2.

Without going into details as to the method of electroprecipitation of the iron-nickel alloys, we limit ourselves here to pointing out that for the preparation of those alloys for which data are presented in Figure 3, it was necessary to prepare for each alloy separately a bath of definite concentration in the components. The measurement of the capacity of the double layer on these samples was carried out with alternating current, using a combination bridge [5] with a modification of the circuit of Dolin and Ershler [7]. All of these measurements were performed in 0.2 N Na_2SO_4 to which sulfuric acid had been added to pH 3.2. In this work all of those precautions were observed which are required in measuring double layer capacities [5, 8].

Certain results from these measurements are presented in Figures 1, 2, and 3.

In Figure 1 there are shown curves of capacity vs. the potential of the zinc electrode, from which it is to be seen that the potential of the null charge alters in dependence on the structure of the metal. For the (0001) face $\varphi_{nc} = -0.60$ v, whereas for the (0101) face $\varphi_{nc} = -0.68$ v. In the literature there is quoted a value $\varphi_{nc} = -0.63$ v, this corresponding to a polycrystalline surface which, according to the experimental data, consists of microcrystals, some with (0001) faces and some with (0101) faces.

It is clear that, depending on the density of atomic packing in the crystalline lattice of the metal, there is a variation in the energy of removal of an electron from it and consequently a variation of φ_{nc} for the metal. The smaller density of packing of nickel atoms in the (0101) face facilitates the removal of an electron (in comparison with removal from the (0001) face) and at the same time displaces φ_{nc} in the direction of negative values.

In measuring the null charge points of amalgams and alloys it must be kept in mind that an alteration in the surface concentration of one of the components, such as can result from various effects (anodic solution,

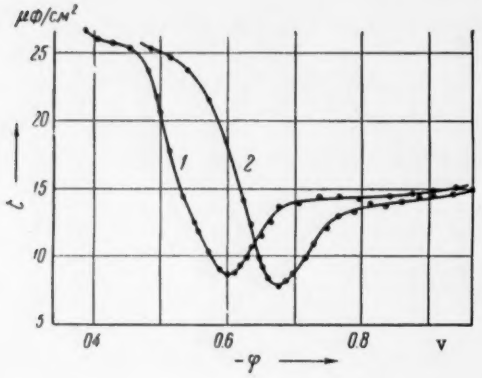

Fig. 1. The relation between the capacity of the double layer on a monocrystalline zinc electrode and the potential, in a 0.02 N Na_2SO_4 + H_2SO_4 solution (pH 3.2): 1) (0001) face; 2) (0101) face.

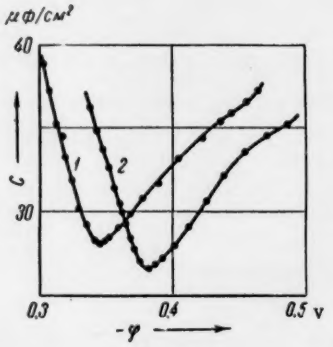

Fig. 2. The relation between the capacity of the double layer on electrodes of iron-nickel alloys and the potential, in a 0.02 N Na_2SO_4 + +H_2SO_4 solution (pH 3.2): 1) 5% Fe; 2) 25% Fe.

high exchange currents) can lead to data which are not reproducible. From this point of view the most trustworthy results are those obtained from measurements of the null charge points of alloys under small exchange currents and it was exactly for this reason that we, in investigating null charge points, hit on alloys of iron with nickel since these possess very small exchange currents.

In Figure 2 there are shown selected curves of capacity vs. potential for iron-nickel alloys in dilute solutions and, in Figure 3, the dependence of the null charge potentials of these alloys on their composition.

Measurements of φ_{nc} for pure metals, which had also been prepared by electroprecipitation, gave results which agreed well with those found in the literature [9, 10]. In view of the fact that such metals as iron and nickel are characterized by a dependence of the null charge potential on the amount of adsorbed (absorbed) hydrogen [5] (or on the pH), all of these measurements were carried out under conditions of strict constancy of pH and time of preliminary cathodic polarization at D_C = constant.

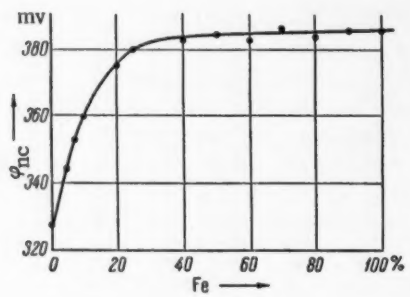

Fig. 3. The dependence of the null charge potential of iron-nickel alloys on the composition (at pH 3.2).

In the case which we have presented (Fig. 3) there is to be observed a rather sharp change in φ_{nc} with increasing content in the alloy of that metal which possesses the more negative value of φ_{nc}; even with 25% iron in the alloy φ_{nc} becomes practically equal to the null charge potential for pure iron.

The monotonic course of the curve showing the dependence of the null charge potential of an alloy on its composition is, as we see it, an indication of the fact that the iron-nickel alloys obtained by electroprecipitation are solid solutions; in the event of the formation of any compound of the type Fe_xNi_y there would be observed a sharp change in the energy of electron removal and the monotonic course of the φ_{nc} vs. alloy composition relation would be disturbed.

Thus it can be supposed that, in the absence of factors capable of disturbing this monotonic dependence of the null charge potential on alloy composition, the null charge potential of an alloy, even at relatively small

concentrations of iron, should be determined by the energy of electron removal from the latter, since this is the metal which has the more negative value of φ_{nc}.

The data presented in this work clearly illustrate the necessity of taking into account the composition and the state of metallic phase in measurements of the null charge potentials.

The A. A. Zhdanov State University in Leningrad and the Scientific Research Institute for Telephone Communication

Received December 11, 1956

LITERATURE CITED

[1] B. V. Ershler, Reports of the Conference on Electrochemistry,* Acad. Sci. USSR Press, 1953, p. 357.

[2] L. I. Antropov, Reports of the Conference on Electrochemistry,* Acad. Sci. USSR Press, 1953, p. 380.

[3] A. N. Frumkin, Reports of the Conference on Electrochemistry,* Acad. Sci. USSR Press, 1953, p. 21.

[4] A. Frumkin and A. Gorodetzkaja, Zs. phys. Chem., 136, .3-4, 215; . 6, 451 (1928).

[5] V. L. Kheifets and B. S. Krasikov, Proc. Acad. Sci. USSR 109, 586 (1956).

[6] P. A. Polibin and A. I. Froiman, J. Exp. Theo. Phys. 3, 162 (1933).

[7] P. I. Dolin and B. V. Ershler, J. Phys. Chem. 14, 886 (1940).

[8] T. I. Borisova, B. V. Ershler and A. N. Frumkin, J. Phys. Chem. 22, 925 (1948).

[9] V. L. Kheifets and L. S. Reishakhrit, Annals of the Leningrad State University, Div. Chem. Sci. No. 169, 173 (1953).

[10] E. O. Ayazyan, Proc. Acad. Sci. USSR 100, 473 (1955).

* In Russian.

THE TRANSFER OF ENERGY DURING RADIOLYSIS OF BENZOYL PEROXIDE SOLUTIONS

V. A. Krongauz and Kh. S. Bagdasaryan

(Presented by Academician V. A. Kargin, December 30, 1956)

In the action of ionizing radiation on organic solutions the initially absorbed energy can be transferred from one component to another, and there will thus be a breakdown of the "law of neutralization" [1-5]. In order to elucidate the influence of the solvent on this energy transfer, we have studied the radiolysis of solutions of benzoyl peroxide in benzene, cyclohexane and ethyl acetate. Radiolysis was carried out in the absence of air and under the action of the γ-rays from Co^{60}. The differential dosage was $1.74 \cdot 10^{15}$ ev/ml·sec. The initial rate of peroxide decomposition was determined iodometrically, the amount of decomposed peroxide not exceeding 10-20% of the intial concentration.

In Figure 1 there is shown the dependence of the initial rate of radiolysis of benzoyl peroxide in benzene on the initial concentration. Of the total energy which is taken up by the solution, the benzoyl peroxide absorbs a portion which is proportional to the electron fraction of the peroxide in solution. A calculation for the number of peroxide molecules which would decompose as a result of the absorption of 100 ev of energy by the peroxide itself at a concentration of 0.01 moles/l, leads to a value of 1760. This quantity is 20 times greater than the number of peroxide molecules which would decompose if it were supposed that the entire 100 ev which was absorbed by the peroxide went into rupturing the $-O-O-$ bonds.

In order to explain the high radiational yield in the decomposition of benzoyl peroxide, we set up experiments with diphenylpicrylhydrazyl (DPPH) in which there was determined the yield of free radicals, both from pure benzene and from solutions of benzoyl peroxide in benzene. The variation of the concentration of the DPPH was determined spectrophotometrically. The critical concentration of DPPH, i.e., the concentration required for the capture of all of those radicals which are formed in the radiolysis, had been measured earlier [6]. This quantity proved equal to $1 \cdot 10^{-4}$ moles/l. The yield of free radicals resulting from the radiolysis of pure benzene was determined by us to be 0.75 per 100 ev, which agrees well with the data of other authors [5, 7].

The point B on the axis of ordinates in Figure 1 corresponds to the rate of formation of free radicals in pure benzene. Since this rate is considerably lower than that of the decomposition of the peroxide the high radiational yield in the peroxide breakdown cannot be explained by the interaction of the peroxide with such radicals.

In Figure 2 there is shown the relation between the rate of formation of the initial free radicals in the irradiation of peroxide solutions in benzene and the peroxide concentration, as determined with DPPH (Curve I). For comparison there is also shown Curve II which corresponds to the initial section, OA, of the curve of Figure 1, but is constructed by supposing that each decomposing peroxide molecule gives two radicals. These two curves practically coincide. From this it follows that the radiolysis of the peroxide in benzene does not proceed according to a chain mechanism. In a chain decomposition, the rate of decoloration of the DPPH would be less than the rate of breakdown of the peroxide under the same conditions since the DPPH would "intercept" the free radicals which are carrying on the chain. The absence of a chain decomposition is also indicated by the fact that the rate of radiolysis of the peroxide in the presence of methyl methacrylate, a strong inhibitor of the chain breakdown of peroxides [8], proves to be equal to the rate of radiolysis without it (Fig. 1).

It can be presumed that the high radiational yield from the decomposition of the peroxide is a result of the transfer of energy from the initially excited benzene molecules to the peroxide molecules. To support this supposition the radiolysis of peroxide solutions in benzene was investigated in the presence of the condensed aromatic hydrocarbons, anthracene and phenanthrene. It is known that diluted solutions of these compounds fluoresce under the action of ionizing radiation. This phenomenon is related to the transfer of energy

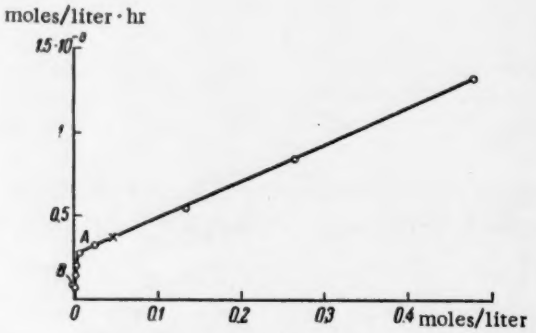

Fig. 1. The dependence of the rate of radiolysis of benzoyl peroxide on the initial peroxide concentration in benzene. The crosses denote the rate of peroxide radiolysis in the presence of 0.02 moles/*l* of methyl methacrylate.

from the solvent to the dissolved substance [9, 10]. It could be expected that the introduction of these fluorescing materials into the peroxide solution would lead to a diminution of the rate of peroxide radiolysis, since a part of the excited benzene molecules would transfer their energy to the molecules of these substances.

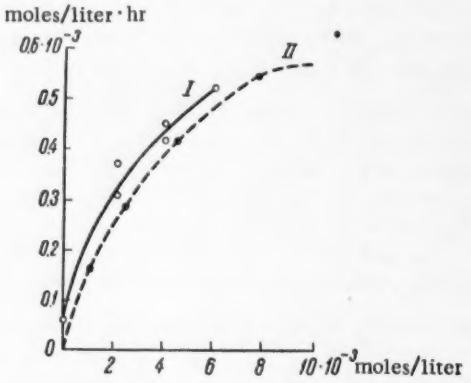

Fig. 2. The dependence of the rate of formation of free radicals on the peroxide concentration in benzene: 1) the rate of consumption of DPPH; 2) the doubled rate of peroxide decomposition.

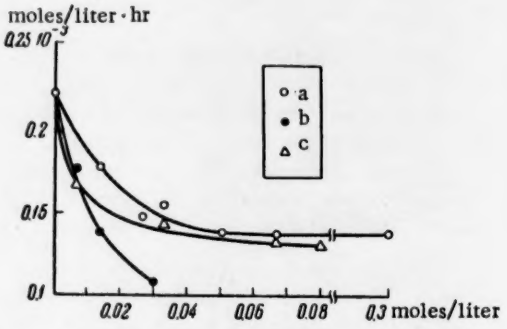

Fig. 3. The dependence of the rate of radiolysis of the peroxide on the concentration of added phenanthrene (a), anthracene (b) and benzoic anhydride (c). Concentration of benzoyl peroxide = $= 4.5 \cdot 10^{-3}$ moles/*l*.

From Figure 3 it is to be seen that anthracene and phenanthrene show a protective action in respect to the peroxide. The anhydride of benzoic acid also protects the peroxide from decomposition. However, as is to be seen from the figure, the rate of peroxide radiolysis reaches a limiting value and does not further diminish with an increase in the concentration of the protecting additive. This can be explained by the fact that the molecules of the fluorescing material, having obtained energy from the excited benzene molecules, are deactivated

not only by the emission of fluorescent light but also by the transfer of energy to the peroxide molecules. It is not difficult to show that this leads to the attainment of a limiting rate of peroxide decomposition under a sufficiently high concentration of the fluorescing material.

In Figure 4, I shows the dependence of the rate of peroxide radiolysis in cyclohexane, and in ethyl acetate, on the initial concentration. Since the solubility of the peroxide in cyclohexane at room temperature does not exceed 0.03 moles/l, it was not possible (in cyclohexane) to follow the change in the rate of radiolysis of the peroxide above this concentration. It is, however, to be seen from the figure that in these two solvents the rates of radiolysis of the peroxide coincide.

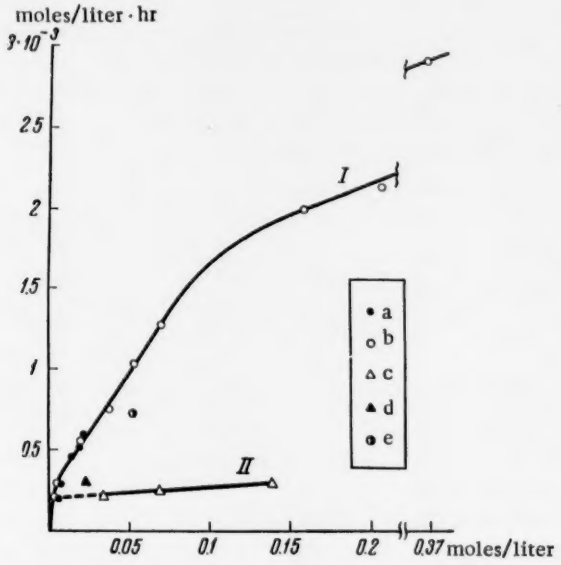

Fig. 4. The dependence of the rate of peroxide radiolysis on the initial concentration in solutions of cyclohexane (a), ethyl acetate (b), ethyl acetate with methyl methacrylate at 0.02 moles/l (c), with phenanthrene at 0.1 moles/l (d) and with benzene at 0.4 moles/l (e).

The introduction into a solution of the peroxide in cyclohexane, or in ethyl acetate, of 0.02 moles/l of methyl methacrylate sharply diminishes the rate of decomposition of the peroxide (Fig. 4, II), which indicates a chain decomposition of the peroxide during radiolysis in these solvents. The determination of the yield of free radicals from the pure solvents and from solutions of the peroxide in these solvents, using DPPH (critical concentration, 10^{-3} moles/l), shows that in the presence of the peroxide the rate of formation of free radicals is practically equal to the rate of their formation in the pure solvents. Consequently transfer of energy from these solvents to the peroxide does not take place, since in the contrary case, in addition to the radicals which would be formed from the solvent, radicals would also be formed because of decomposition of the peroxide resulting from the energy transfer (as is observed in the benzene solutions).

It is clear that chain decomposition of the peroxide is initiated by those radicals which are formed in radiative decomposition of the solvent. Making use of the stationary state principle, it is possible to obtain the following expression for the rate, V, of the chain decomposition of the peroxide:

$$V = k_p (v_i / k_r)^{1/2} [BP] + v_i,$$

where k_p and k_r the constants for chain propagation and rupture, and k_i is the rate of initiation. The value of k_i can be determined by extrapolating the linear portion of Curve I (Fig. 4) down to intersection with the axis of ordinates. Departure from a linear relationship for the rate of decomposition at peroxide concentration exceeding 0.1 moles/l is connected with the inhibiting action of the aromatic products of the peroxide decomposition [11]. As is to be seen from Figure 4, the rate of peroxide decomposition is considerably diminished by the presence of small quantities of benzene and phenanthrene. From the slope of the straight line II (in the presence of methyl methacrylate chain decomposition does not take place) it is possible to calculate the radiational yield for that breakdown of the peroxide which results from energy absorption by the peroxide itself. This quantity amounts to 40 molecules per 100 ev.

From a comparison of the data on the radiolysis of benzoyl peroxide in various solvents it is to be seen that the transfer of energy from the solvent to the dissolved material depends essentially on the nature of solvent.

We consider the following processes as occurring during the radiolysis of solutions of the peroxide in benzene: 1) formation of excited benzene molecules as a result of the absorption of radiational energy; 2) spontaneous deactivation of the excited benzene molecules; 3) transfer of energy from the excited benzene molecules to the peroxide and the decomposition of the latter; 4) decomposition of the peroxide as a result of the absorption of energy of the γ-radiation by the peroxide itself.

On the basis of this proposed scheme, and utilizing the steady state principle, it is possible to obtain the following expression for the rate of radiolysis of benzoyl peroxide in benzene:

$$V = \frac{I_{abs}\, k_1 k_3 [BP]}{k_2 + k_3 [BP]} + k_4 I_{abs} [BP], \qquad (1)$$

where I_{abs} is the energy absorbed by the solution and k_1, k_2, k_3 and k_4 are the velocity constants for the reactions 1, 2, 3 and 4.

At low concentrations of the peroxide the energy absorption of the peroxide itself is small and the second term in Equation (1) can be neglected (Section OA, Fig. 1). In this case $1/V$ depends linearly on $1/[BP]$, which permits the graphic determination of k_2/k_3 ($4 \cdot 10^{-6}$ moles/l). Knowing this quantity it is then posssible to determine the mean lifetime of the excited benzene molecules, making use of the familiar theory of the quenching of fluorescence [12]. Supposing that deactivation of excited benzene molecules occurs at each collision with peroxide molecules, there is obtained for the lifetime of the excited molecules a value of $\sim 10^{-7}$ seconds.

It is possible to suppose that by increasing the concentration of the peroxide above the value of 0.01 moles/l (the linear segment of the curve of Figure 1), all of the excited molecules of benzene which are capable of transferring energy to the peroxide will deactivate only according to reaction 3 and that further increase of the rate with concentration will be brought about by the absorption of energy in the peroxide itself. However, a more detailed analysis of the course of the curve at higher concentration necessitates the admission that there exist excited benzene molecules with shorter life times in the excited condition and that these molecules begin to play an essential role under increased concentration of the peroxide.

The L. Ya. Karpov Physicochemical Institute of Scientific Research

Received December 27, 1957

LITERATURE CITED

[1] J. Manion and M. Burton, J. Phys. Chem., 56, 560 (1952).

[2] M. Burton and W. Patrick, J. Phys. Chem., 58, 421 (1954).

[3] W. Patrick and M. Burton, J. Phys. Chem., 58, 424 (1954).

[4] T. S. Nikitina and Kh. S. Bagdasaryan, Collected Papers on Radiation Chemistry,* Moscow, 1955.

[5] L. Bouby and A. Chapiro, J. Chim. Phys. 52, 645 (1955).

*In Russian.

[6] A. Chapiro, J. Chim. Phys. 51, 165 (1954).

[7] E. Weber, P. Forsyth and R. Schuler, Rad. Res., 3, 68 (1955).

[8] Kh. S. Bagdasaryan and R. I. Milyutinskaya, J. Phys. Chem. 27, 427 (1953).

[9] H. Kallmann and M. Furst, Phys. Rev., 79, 857 (1950).

[10] H. Kallmann and M. Furst, Phys. Rev., 94, 503 (1954).

[11] K. Nozaki and P. Bartlett, J. Am. Chem. Soc., 68, 1686 (1946).

[12] S. I. Wawilow, I. M. Frank, Zs. Phys., 69, 100 (1931).

AN INVESTIGATION BY THE FILTRATION METHOD OF THE MECHANICAL PROPERTIES OF THIN LIQUID FILMS IN CONCENTRATED EMULSIONS

S. V. Nerpin and N. F. Bondarenko

(Presented by Academician A. N. Frumkin January 24, 1957)

Earlier investigations have established that the normal viscosity is maintained down to the solid surface in nonpolar liquids of low volatility and down to the solvate layer boundary in polar liquids of this type [1].

For the study of the mechanical properties of volatile liquids (aqueous electrolytic solutions) we employed a filtration viscosimeter, a highly concentrated benzene-water emulsion, stabilized with saponin, being used as a finely porous filter. In addition, observation of the influence of filtration on the stability of this system made it possible to obtain direct information as to the role of the mechanical properties of thin films in stabilizing emulsions. The structure of the emulsion is to be seen in the microphotograph (Fig. 1). The good resolution of this system in the micrsocope and the fact that the aqueous films formed parallel* boundary surfaces for neighboring droplets, simplified filtration calculations and permitted the evaluation of the viscosity and the magnitude of the limiting shear stress in the investigated liquid.

In decreasing the temperature to 0°, the b nzene droplets solidify at + 5.5°C; the films,however, remain in the liquid form.

The thickness of the films was determined by dividing the volume of the aqueous medium contained in unit volume of the system by one-half of the specific surface. The latter was found from the microphotograph of the emulsion [4], using the formula:

$$\Omega = \frac{4}{\bar{\lambda}},$$

where λ is the mean length of segment intercepted on an arbitrary line by the droplet walls.

The calculations which were carried out for emulsions of limiting concentration, prepared in 10% aqueous saponin solutions, showed that the mean thickness of the aqueous films was of the order of 10^{-5} cm. This small film thickness assured a low value of the viscous strains in the liquid during filtration under easily measurable pressure differentials, which in turn permitted the observation of very minute plastic shear stresses in liquids which did not strictly follow Newton's equation and which were subject to the well known Shvedov-Bingham law.

At the same time, at relatively high values of the pressure differential there could be determined the true viscosity of the liquid in the thin film.

The experimental emulsions of maximum concentration (97.3-97.6% benzene and 2.4-2.7% aqueous stabilizer solution) were introduced into the measuring cylinder with the aid of a spiral [5]. The attempt to increase the benzene concentration led in every case to a separation of the excess of benzene on the surface of

*The parallelness of the boundary surfaces of the free films was experimentally established in [2] and also follows from the theory of their equilibria [3].

the system. The emulsion was placed in a special receptacle with a chamber diameter of 5.5 cm and a depth of 0.6 cm, to which, from the one side, water was fed under pressure; to the other side there was attached a thin measuring tube, held in a horizontal position.

For determining the magnitude of the true viscosity, filtration was carried out under pressure differentials of the order of 100 cm. The limiting shear stresses were measured by lowering the pressure to a value which corresponded to the initial filtration gradient under which the movement of the liquid practically ceased. The liquid shear strength in these films was also determined from the departure of the filtration from Darcy's law at decreasing pressure differentials.

The estimation of the order of magnitude of the viscosity and the shear stress at the boundary surface was carried out with the following approximation expressions, which are based on the well known equations for the movement of liquid between parallel plates:

$$\eta = \frac{\rho g \chi H^3 I}{R 12 q_{sp}}; \qquad \tau_0 = \frac{\rho g P}{\Omega} I_0. \tag{1}$$

Here q_{sp} is the specific discharge rate per unit cross section of specimen; R is a coefficient which takes into account the convolutions of the filtration paths; I is the pressure gradient; I_0 is the initial gradient; P is the porosity and χ is the specific perimeter of the films in the cross section of the filter, determined from the relation $2\chi = \Omega$. In the case of streamlining of the emulsion drops, it is possible to set R = 2.

For determining the quantity τ_0 from the departure of the filtration from the Darcy law, it was possible, by making use of the well known solutions for viscous-plastic flow [6], to obtain the following equation which established a relation between the initial filtration gradient, I_0, and the ratio between the actual discharge rate, q, at a gradient I, and the discharge rate, q_D, which should be observed with this filter at this gradient, if the filtration strictly followed the Darcy law:

$$\left(\frac{I_0}{I}\right)^3 - 3\left(\frac{I_0}{I}\right) - 2\left(\frac{q}{q_D} - 1\right) = 0.$$

The principle conclusion which followed from these experiments was that the liquid contained in the thin films separating individual droplets possesses the normal viscosity which is characteristic of the liquid in bulk; at the same time there was disclosed in this liquid traces of plasticity in the form of a limiting shear stress, τ_0, of the order of $5 \cdot 10^{-3}$ dyne . cm^{-2}, which is overcome during the movement of the liquid.

These conclusions apply to the films separating liquid droplets as well as to those which separate the solidified particles of benzene.

We give an example of the determination of η and τ_0 for an emulsion of 97.5% concentration. By the method earlier described the following values were obtained for the specific surface and wetted perimeter: $\Omega = 5200\ cm^{-1}$ and $\chi = 2600\ cm^{-1}$. By dividing the specific volume of the aqueous medium by one half of the specific surface there was found a mean film thickness of $0.96 \cdot 10^{-5}$ cm. With a pressure of 100 cm and a specimen depth of 0.5 cm, the flow through the filter had a characteristic specific discharge rate of $q_{sp} = 2.55 \cdot 10^{-6}$ cm/sec. Setting these values into the equation for the viscosity η, we found the latter to have the value of $0.734 \cdot 10^{-2}$, which agrees in order of magnitude with the usual value for the viscosity of water at room temperature.*

*The discrepancy here is easily explained by the fact that we did not take into account the Gibbs swelling at the points of contact of the boundary surfaces. As a result of the increased dispersion of the system during emulsification, the films which separate the newly formed surfaces must, for the most part, be produced at the expense of the volume of liquid which is contained in these triangles. In the investigated emulsions of limiting concentration these swellings, at first clearly visible, finally disappear from the field of vision and consequently their dimensions did not exceed 0.2-0.3 μ. Knowing this dimension it was easy to calculate the part of the flow which took place along such paths.

(Footnote continued on following page).

For the determination of the quantity τ_0 in the case under consideration, there were combined the results of experiments on filtration through a single specimen at pressure differentials of 1 m and 1.5 cm; from the value of the ratio q/q_D the initial filtration gradient, $I_0 = 0.6$, was obtained and from Equation (1) it was then found that τ_0 was of the order of $3 \cdot 10^{-3}$ dyne $\cdot$ cm^{-2}.

With a view to investigating the influence of the electrolyte content of aqueous solutions on the film thickness and the course of filtration, there was carried out a series of experiments with emulsions which had been prepared in aqueous solutions of varying electrolyte (NaCl) content, namely: 10^{-4} N, 10^{-3} N, 10^{-2} N and 10^{-1} N.

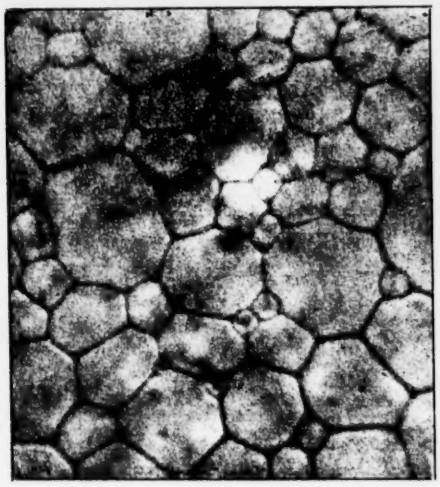

Fig. 1. The structure of an emulsion of high concentration (not saturated).

Through the emulsion there was filtered that same aqueous solution which had gone into its preparation.

These experiments showed that increasing the electrolyte concentration diminished the filtration current (Figs. 2 and 3). From the microphotographs it was clear that with increasing concentration of the electrolyte, there was an increase in the dispersion of the system, this corresponding to a diminution of the mean depth of the aqueous films

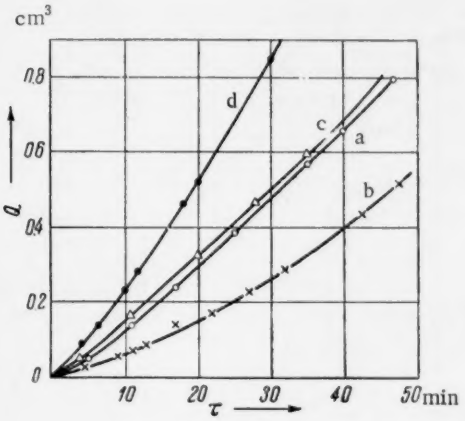

Fig. 2. The course of filtration of aqueous solutions through a specimen of emulsion: a) 10^{-1} N, b) 10^{-2} N, c) 10^{-3} N, d) 10^{-4} N.

A decrease in the permeability of the emulsion was observed only up to a definite value of electrolyte concentration which was of the order of 10^{-2} N. Raising the concentration above 10^{-2} N, the filtration current once more increased (Fig. 3). This fact can be given the following explanation.

According to a theory which has been confirmed by direct experimentation [3], an increase of electrolyte concentration brings about not only a diminution of the depth of the aqueous films but also a decrease in the maximum value of the cleavage forces generated by them. Both of these factors impair the breakdown of droplets; the mobility of the liquid in these films diminishes in proportion to their thinning and there is thus a smaller

---

• Footnote continued from preceding page.

Making use of the equation for flow through capillaries of triangular form, there results

$$q = \frac{\sqrt{3}a^4 \rho g I}{R320\ \eta}$$

where a is the length of the side of the triangle and R is the coefficient of path convolution, which must here be set as $R = \pi/2$. Supposing normal viscosity and determining the number of swellings per 1 cm^2 from the microphotograph $4.25 \cdot 10^{-6}$, we found that in our case the current passing along these paths amounted to $2.3 \cdot 10^{-7}$ cm sec^{-1}, i.e., to about 10% of the entire flow.

likelihood of the rapid formation of new films which could separate the drops, and a decrease of that force barrier which hinders drop coagulation limits the degree of dispersion, since an increase of the latter would entail a rise of that capillary pressure on the layer from the direction of the drops, which is due to their dome-shaped form on the filter boundary.

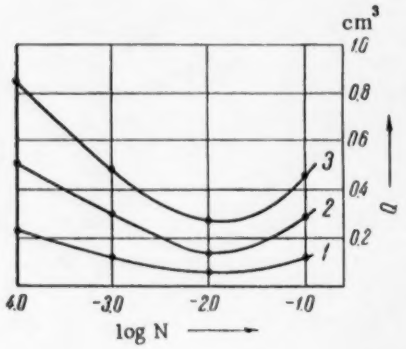

Fig. 3. The volumes of electrolytic solutions of various concentrations which were filtered through the viscosimeter during fixed periods of time: 1) in 10 minutes, 2) in 20 minutes, 3) in 30 minutes.

A deterioration in the condition for emulsificiation must lead to a retention of the aqueous solution in the Gibbs swellings and to an increase of the degree to which these participate in the filtration, which in turn determines the increase in the permeability of the system.

The maintenance of emulsion stability during filtration through the films, once the limiting shear resistance has been overcome, and the alteration in the filtration and the dispersion with varying electrolyte content in a single medium, point to the thermodynamic character of the film equilibrium, which in the case under consideration results from the basic ionic-electrostatic component of the cleaving pressure.

It is also interesting to note that here the forces of molecular and ionic-electrostatic interaction are basic to the process of gelatinization in the system. Actually, the components of this system possess practically normal fluidity whereas the system as a whole is a gel, possessing a considerable modulus of shear elasticity. The nature of this elasticity has already been considered in earlier works [7, 8]

The authors present their sincere thanks to B. V. Deryagin for discussion of the results of this work and for valuable advice during its performance and to L. Ya. Kremnev for his cooperation in carrying out the experiments.

The Leningrad Institute of Water Transport Engineers

Received January 22, 1957

LITERATURE CITED

[1] V. V. Karasev and B. V. Deryagin, Colloid J. 15, No. 5 (1953).*

[2] B. V. Deryagin and A. S. Titiyevskaya, Colloid J. 15, No. 6 (1953).*

[3] B. V. Deryagin and S. V. Nerpin, Proc. Acad. Sci. USSR, 99, No. 6 (1954).

[4] B. V. Deryagin, Proc. Acad. Sci. USSR, 53, No. 7, (1946).

[5] M. Ya. Kremnev and V. S. Kuprik, Proc. Acad. Sci. USSR, 80, No. 4 (1951).

[6] M. P. Volarovich and A. M. Gutkin, J. Tech. Phys. 16, No 3 (1946).

[7] B. Deryagin and E. Obukhov, J. Phys Chem. 7 (1936).

[8] I. F. Efremov and S. V. Nerpin, Proc. Acad. Sci. USSR, 113, No. 4 (1957).*

* [See S. B. translation.]

A GENERALIZED FORMULATION OF THE GIBBS INEQUALITY

L. S. Palatnik and A. I. Landau

(Presented by Academician N. V. Belov December 26, 1956)

Symbolism: V, S, P, and T are respectively the volume, entropy, pressure and temperature of the entire heterogeneous system; M_i and $\mathfrak{M}_i$ are respectively the mass and the chemical potential of the i-th component over the entire system; v_j, s_j and m_j are respectively the specific volume, the specific entropy and the mass of the j-th phase of the system; x_{ij} and μ_{ij} are respectively the concentration and the chemical potential of the i-th component in the j-th phase, and $\underline{n}$ and $\underline{r}$ are respectively the number of components and the number of phases in the system.

Any multicomponent heterogeneous system, including those in which one, or several, of the components are missing in various phases (i.e., in which the solubility of certain components can be neglected in certain phases), may be represented by a concentration matrix $\| x_{ji} \|$ ($i = 1, 2, \ldots n$; $j = 1, 2, \ldots, r$). In the analytical discussion of thermodynamic systems it is usually implicitly assumed that this matrix is of maximum rank, i.e., that its defect $\sigma = 0$. Thus the phase rule and the inequality $r \leq n + 2$ as derived by Gibbs [1] apply only to those thermodynamic systems for which $\sigma = 0$.

It is possible, however, to present actual thermodynamic systems for which $\sigma > 0$. As examples there might serve those systems for which $\sigma = 1$ and $r \leq n$; these have been referred to in Gibbs' work ([1], pp. 147-148) and have been considered in greater detail by A. V. Storonkin [2].

As will be seen subsequently, the case of a system with $\sigma = 1$ and $r \leq n$ is an exceptional one and the number of possible thermodynamic systems for which $\sigma > 0$ is considerably greater. Among the latter are certain thermodynamic systems with maximum or minimum pressures and temperatures, ones in which the various phases are of identical composition (for example phases in points of different concentrations, allotropic phases), certain systems in the separate phases of which not all of the components participate, etc. It is the aim of the present work to clarify the rules which apply to thermodynamic systems with $\sigma > 0$.

It is, first of all, not difficult to show for any thermodynamic system at equilibrium, that, regardless of the value of σ there must exist equality of the pressures, temperatures and chemical potentials of the respective components in the various phases and that the Gibbs-Duhem equation is valid when written for each separate phase of the heterogeneous system. The number of intensive thermodynamic degrees of freedom [3] for the open system can be determined either from the Gibbs-Duhem equations [1, 2] or from the equalities involving the chemical potentials [4-7].

If any additional conditions or restraints are imposed on a thermodynamic system, these must clearly be appended to the Gibbs-Duhem equations or to the equalities among the chemical potentials before a calculation of the number of thermodynamic degrees of freedom of the system is undertaken. In the case under consideration such supplementary conditions are ones which are involved in setting the concentration matrix defect equal to σ, where $\sigma \geq 0$. The equalities among the chemical potentials, together with the imposed conditions, can be written in the following form:

$$\mu_{i1}(P, T; x_{11}, \ldots, x_{n1}) = \ldots = \mu_{ir}(P, T; x_{1r}, \ldots, x_{nr}), \quad i = 1, 2, \ldots, n; \tag{1}$$

$$x_{1j} + x_{2j} + \ldots + x_{nj} = 1, \quad j = 1, 2, \ldots, r; \tag{2}$$

$$\begin{vmatrix} x_{11} & \ldots & x_{1,\,r-\varkappa-\sigma} & x_{1j} \\ \ldots & \ldots & \ldots & \ldots \\ x_{r-\varkappa-\sigma,\,1} & \ldots & x_{r-\varkappa-\sigma,\,r-\varkappa-\sigma} & x_{r-\varkappa-\sigma,\,j} \\ x_{i1} & \ldots & x_{i,\,r-\varkappa-\sigma} & x_{ij} \end{vmatrix} = 0, \quad \begin{matrix} i = r-\varkappa-\sigma+1, \ldots, n, \\ j = r-\varkappa-\sigma+1, \ldots, r, \end{matrix} \tag{3}$$

where $\varkappa$ is the larger of the numbers r-n and 0, and $\det \| x_{lm} \| \neq 0$ (l, m = 1,2, ..., r-$\varkappa$-σ). If $x_{uv} = 0$, the corresponding function $\mu_{uv}(P, T; x_{1v}, x_{2v}, \ldots, x_{nv})$, falls out of Equation (1).

In a similar fashion the Gibbs-Duhem equations, together with the conditions for the concentration matrix to be of less than maximum rank, can be written in the following form:

$$-v_j dP + s_j dT + x_{1j} d\mathfrak{M}_1 + x_{2j} d\mathfrak{M}_2 + \ldots + x_{nj} d\mathfrak{M}_n = 0, \quad j = 1, 2, \ldots, r; \tag{4}$$

$$\begin{vmatrix} x_{11} & \ldots & x_{1,\,r-\varkappa-\sigma} & x_{1j} \\ \ldots & \ldots & \ldots & \ldots \\ x_{r-\varkappa-\sigma,\,1} & \ldots & x_{r-\varkappa-\sigma,\,r-\varkappa-\sigma} & x_{r-\varkappa-\sigma,\,j} \\ x_{i1} & \ldots & x_{i,\,r-\varkappa-\sigma} & x_{ij} \end{vmatrix} = 0, \quad \begin{matrix} i = r-\varkappa-\sigma+1, \ldots, n, \\ j = r-\varkappa-\sigma+1, \ldots, r. \end{matrix} \tag{5}$$

In the relations (1)–(3) the variables are the quantities P, T and the entire set of the x_{ij}, and the chemical potentials, μ_{ij}, are functions of these variables. On the other hand, in relations (4)–(5), the variables are the quantities P, T and the entire set of the $\mathfrak{M}_l$, and the v_j, s_j and all of the x_{ij} are functions of these variables. In this respect relations (3) and (5) differ in their content although they are identical in form.

It is, however, easy to see that both relation (3) and relation (5) impose the same number of restraints on the thermodynamic system. This last is true even in the case when some part of the indicated relation is an identity.

Thus we have written two systems of equations, the system (1)–(3) and the system (4)–(5), each one of which will impose the same number of conditions (restraints) on an open thermodynamic system with $\sigma \geq 0$. It is easy to show that for $\sigma \leq 2 - \kappa$ both of these systems of equations actually give, under the appropriate treatment, the same number of intensive thermodynamic degrees of freedom. However, with $\sigma > 2-\kappa$ the rank of the following matrix, composed of the coefficients of all the differentials in Equation (4), becomes less than maximum:

$$\begin{pmatrix} -v_1 & s_1 & x_{11} & x_{21} & \ldots & x_{n1} \\ -v_2 & s_2 & x_{12} & x_{22} & \ldots & x_{n2} \\ \ldots & \ldots & \ldots & \ldots & \ldots & \ldots \\ -v_r & s_r & x_{1r} & x_{2r} & \ldots & x_{nr} \end{pmatrix}. \tag{6}$$

Thus in the system (4)–(5) additional degrees of freedom appear which are not met in the system of Equations (1)–(3). This lack of agreement between the values obtained for the number of degrees of freedom points up the impossibility of the existence of thermodynamic equilibrium in a system for which $\sigma > 2-\kappa$. Thus it is always true that $\sigma \leq 2-\kappa$. Since σ is obviously a positive quantity, the inequality which we have obtained can be once more rewritten as:

$$0 \leq \sigma + \kappa \leq 2. \tag{7}$$

Equation (7) is a generalization of the Gibbs inequality, $r \leq n+2$, or $\kappa \leq 2$, to the case of a thermodynamic system for which $\sigma \geq 0$. We will designate this as the matrix condition for phase equilibrium since into it there enters the magnitude of the defect, σ, of the concentration matrix $\| x_{ij} \|$. The method which has been followed in deducing relation (7) represents a new proof of the Gibbs' inequality and differs from those proofs which have been developed earlier [1, 2, 4-7].

We will now fix the value of P, or of T, in the equations (1)–(3) and (4)–(5). Then the terms in dP or in dT fall out of Equation (4) and matrix (6) takes on one or the other of the two following possible forms;

$$\begin{pmatrix} -v_1 & x_{11} \cdots x_{n1} \\ -v_2 & x_{12} \cdots x_{n2} \\ \cdots & \cdots \\ -v_r & x_{1r} \cdots x_{nr} \end{pmatrix} \quad \text{or} \quad \begin{pmatrix} s_1 & x_{11} \cdots x_{n1} \\ s_2 & x_{12} \cdots x_{n2} \\ \cdots & \cdots \\ s_r & x_{1r} \cdots x_{nr} \end{pmatrix}. \tag{8}$$

It is easily seen that with $\sigma \leq 1-\kappa$ the matrices (8) retain maximum rank and the systems of equations (1)–(3) and (4)–(5) thus yield the same number of thermodynamic degrees of freedom for an open system. With $\sigma > 1-\kappa$ the matrices (8) will in every case be of less than maximum rank. In such a situation the systems of equations (1)–(3) and (4)–(5) will yield different values for the number of degrees of freedom, this indicating the impossibility of the existence of equilibrium in a thermodynamic system for which $\sigma > 1-\kappa$ at P = const (or T = const). On the other hand with $P \neq$ const and $T \neq$ const the case arises of a thermodynamic system with $\sigma + \kappa = 2$. From a comparison of these two cases it follows that in a thermodynamic system with $\sigma + \kappa = 2$ there must exist an invariant equilibrium which on fixing P or T will be redundantly defined. In a similar fashion (fixing the values of P and of T in the equations (1)–(3) and (4)–(5) and then comparing this with the case in which either P = const or T = const) it is easily shown that with $P \neq$ const and $T \neq$ const and $\sigma + \kappa = 1$ a monovariant equilibrium will exist in the thermodyanic system which, on fixing either P or T, becomes an invariant equilibrium and, on fixing both P and T, is redundantly defined. We note that the monovariant properties in this particular instance of a thermodynamic system with $\sigma = 1$ and $\kappa = 0$ (i. e., one for which $r \leq n$) were first pointed out by A. V. Storonkin [2].

In light of the above results the significance of condition (7) becomes clear. From this condition it clearly follows that with $\sigma + \kappa > 2$. redundancy of definition arises in a thermodynamic system (or in any fundamental equations describing this system) even if P and T are not fixed beforehand for it. By direct test it is easy to show that such redundancy of definition actually arises in the system of equations (1)–(3) when $\sigma + \kappa > 2$. In particular, as is known, such redundancy appears in the system (1)–(3) when $\sigma = 0$ and $\kappa > 2$.

The redundancy of definition in the system of equations (1)–(3) can be tied up with a definite group of the relations from this system rather than the entire system. In the same way the invariant determinateness of the variables when $\sigma + \kappa = 2$ or their monovariant determinateness when $\sigma + \kappa = 1$ (in both cases with $P \neq$ const and $T \neq$ const) can in the general case be inherent in a definite group of relations in this system and not in the entire system of equations (1)–(3).

With the aid of the generalized "center of gravity" rule [8] it is not difficult to show that $\sigma + \kappa = z$, where z is the number of the phase masses, m_j, which can be arbitrarily altered under fixed values of the quantities P, T and M_i ($i = 1, 2, \ldots, n$). From this there arise the following criteria for invariance and monovariance in a thermodynamic system: for $z = 1$ the system is monovariant and for $z = 2$ it is invariant. For $z = 3, 4 \ldots$ we should, in analogy with two preceding cases, expect thermodynamic systems possessing negative degrees of variance respectively equal to $-1, -2, \ldots$. In actuality even for $z > 2$ a thermodynamic system cannot exist in equilibrium and " a negative variance" in the mathematical sense corresponds to a redundancy of definition in the system of equations (1)–(3). From this point of view we can interpret anew the physical meaning of the matrix condition (7) for phase equilibrium (i. e., the condition $z \leq 2$). Actually, when $\sigma + \kappa = z > 2$, even the assignment of a basic set [3] of external parameters, V, S and all of the M_i, does not open the possibility of uniquely determining each of the masses m_j of the thermodynamic system, i.e., of determining all of the latter's internal parameters (among which the masses m_j are included). On the other hand, it follows from the fundamental equations of the thermodynamic system [1, 9] that the maximum number of independent external parameters of a system is n + 2 and the quantities V, S and the set of the M_i exhaust this number. Thus for $\sigma + \kappa > 2$

the thermodynamic system either is not uniquely determinant in principle, which cannot be admitted, or the fundamental equations in such a case incompletely described the thermodynamic system, i. e., these relations lose their claim to being fundamental equations. As we see, the matrix condition (7) for phase equilibrium solves all of the difficulties which can arise since it forbids the existence of equilibrium systems with $\sigma+\kappa>2$.

The A. M. Gorky State University in Kharkov

Received February 17, 1956

LITERATURE CITED

[1] J. W. Gibbs, Thermodynamic Works,* 1950.

[2] A. V. Storonkin, The Conditions for Thermodynamic Equilibrium in Multicomponent Systems,** 1948.

[3] L. S. Palatnik and A. I. Landau, Proc. Acad. Sci. USSR, 102, 125 (1955).

[4] M. Plank, Introduction to Theoretical Physics,* (Part 5), The Theory of Heat, 1935.

[5] N. S. Kyrnakov, Introduction to Physicochemical Analysis,** 1936.

[6] L. D. Landau and E. M. Lifshits, Statistical Physics,** 1951.

[7] M. A. Leontovich, Introduction to Thermodynamics,** 1951.

[8] L. S. Palatnik, Proc. Acad. Sci. USSR, 95, 1227 (1954).

[9] D. S. Korzhinsky, Proc. Acad. Sci. USSR, 64, 361 (1949).

* Russian translation.

** In Russian.

A METHOD FOR TESTING THE EQUATION OF STATE OF GASES AT HIGH TEMPERATURES

S. S. Semenov

(Presented by Academician V. N. Kondratyev December 11, 1956)

The shock tube* has recently come into use for investigating the properties of gases at high temperatures. In the present work there is considered a method for testing the equation of state and determining the energies of dissociation and ionization of the gases** in the shock tube. In [2] the results obtained from measuring the velocity of stationary detonation in a 50% mixture of oxygen and dicyan were compared with calculations made on the basis of the Zeldovich theory [3], supposing thermodynamic equilibrium to exist directly behind the detonation front. It was established that the most trustworthy values are: $D_{N_2} = 9.76$ ev and $D_{CO} = 11.1$ ev. However there are fundamental defects in [2] and this procedure cannot be considered as a general one [4].

Other methods of investigation involve the measurement of the velocity of the shock wave, which completely fixes the equilibrium condition of the gas behind the front, and the determination of one other parameter; such results, taken together, make it possible to check the doubtful constants in the equation of state (for example, the energy of dissociation or of ionization). Thus, in addition to the velocity of the shock wave, in [4] there was also measured the speed of the piston which generated this wave, and in [5], the velocity of the shock wave which was reflected from the closed end of the tube. In [6] the second measured parameter was the number M***.

In the note [7] it was proposed to determine the change in the velocity of the shock wave through the change in the concentration of the test gas in a mixture of the latter with some monatomic gas (for diminishing the influence of the variation in the diaphragm rupture, the pressures of the propelling gas and the investigated gaseous mixture were to be held constant). All of these methods suffer from a number of objections.

It is known that directly behind the fronts of the incident and the reflected shock waves there exist extensive relaxation zones in which thermodynamic equilibrium is not established. This is explained by the fact that at relatively low temperatures there is a slow excitation of the vibrational degrees of freedom behind the shock wave whereas at high temperatures there are large deviations of the internal energy from the equilibrium values, so that the energy of dissociation is, as it were, increased. In addition, in the reflection of the shock wave there takes place a considerable (5-10 fold) contraction in the region of uniform parameters which renders investigation difficult.

Finally, the presence of the boundary layer which develops on the walls of the shock tube influences the gas velocity behind the incident wave; an interaction of the shock wave with this boundary layer results and errors are thereby introduced into the measurements. It is also known that the front of the shock wave does not of necessity coincide with the origin of luminescence [8].

---

*See the bibliography to [1].

**The spectral data on a number of fundamental diatomic molecules (for example, N_2, CO and others) cannot be unambiguously interpreted [13] for the determination of their dissociation energies. Verification can be obtained, but not always in an exhaustive fashion, by the method of explosions [11] or through mass spectra [12].

***We note that over the range of pressures investigated in [6] the dependence of the number M on the shock wave velocity is not well defined, as authors of that work have supposed it to be.

Thus inaccuracies in the measurement of the velocity of the shock wave and the particles behind it can lead to large errors in the value of the relative density. There is another method which can be successfully

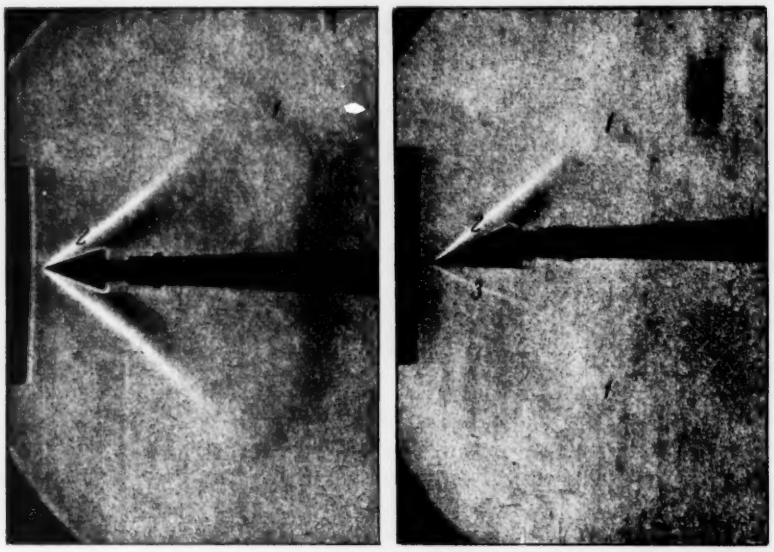

A B

Fig. 1. A) the associated compression jump on a wedge behind the shock wave in air: 1) the shock wave, 2) the compression jump, 3) rarefraction; B) the associated compression jump and the Mach wave on a semiwedge behind the shock wave in air: 1) the shock wave, 2) the compression jump, 3) rarefraction, 4) the Mach wave.

applied in the shock tube for testing the equation of state; here, in addition to the shock wave velocity, there is also measured the angle of the associated oblique jump as observed on wedge-shaped models of varying angular opening. The density ratio in the oblique compression jump is equal to:

$$\frac{\bar{\rho}}{\rho_0} = \frac{\tan \vartheta}{\tan(\vartheta - \varphi)},$$

where $\rho_0, \bar{\rho}$ are respectively the gas density before and after the jump and ϑ is the angle of the associated oblique compression jump for a rotation of the flow through an angle φ.

A comparison of the experimental data with theoretical calculations makes it possible to determine the true equation of state.

The factors which assure high accuracy for this method are as follows:

1. The density ratio for the oblique compression jump is very sensitive to the energies of dissociation and ionization.

2. For shock tube flow of sufficient duration (longer than the time required for establishing equilibrium in the gas behind the shock wave and for forming the oblique compression jump) the absence of equilibrium does not exert a noticeable influence on the magnitude of the angle of the associated oblique jump since the leading flow of gas has a high temperature and the perturbation of the parameters in the oblique jump is relatively small.

3. The fundamental experimental quantities are angular magnitudes which can be measured with reasonable ease and with the requisite degree of precision. Corrections which are connected with the presence of a boundary layer on the model are not great and can be easily taken into account.

4. There is a considerable diminution in the influence of the boundary layer which forms on the tube walls.

5. The magnitude of the angle of the associated jump depends rather weakly on the velocity of the leading shock wave and, also, on the pressure in the quiescent gas in front of it.

6. The method is a universal one, and can be employed for testing the equation of state for any gas over wide ranges of temperatures and pressures.

Typical experimental results are shown in Figure 1, in which there are presented shadow photographs of the flow behind the shock wave in air. There are visible the weak perturbations (from which the number M can be determined), the shock wave and the associated compression jump. In Figure 2, the theoretical results

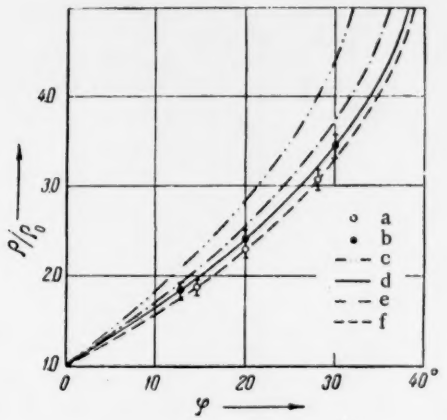

Fig. 2. The test of the equation of state. a, b) experiments in the shock tube (a) nitrogen, b) air); c-f) theoretical calculations. Air: c) according to the thermodynamic function of [10], $D_{N_2} = 7.38$ ev; d) according to the function of the Energetics Institute of the Academy of Sciences of the USSR, $D_{N_2} = 9.76$ ev. Nitrogen: e) according to the data of [9], $D_{N_2} = 7.38$ ev; f) according to the data of [9] and the Energetics Institute of the Academy of Sciences of the USSR, $D_{N_2} = 9.76$ ev.

are compared with the experimental data. For the calculation of the oblique compression jump in nitrogen there have been employed the data of the Energetics Institute of the Academy of Sciences of the USSR and of [9], and, for air, the thermodynamic functions of Bethe ($D_{N_2} = 7.38$ ev) [10] and the Energetics Institute of the Academy of Sciences of the USSR ($D_{N_2} = 9.76$ ev).

On the basis of the results which have been obtained the conclusion can be drawn that the energy of dissociation of nitrogen is $D_{N_2} = 9.76$ ev and that the thermodynamic functions of air based on this value of the energy of dissociation are very close to the true ones.

Received November 27, 1956

LITERATURE CITED

[1] S. S. Glass and G. N. Patterson, J. Aeronaut. Sci., Reprint No. 564, 1 (1955).

[2] G. B. Kistiakowsky, H. T. Knight and M. E. Malin, J. Chem. Phys., 20, No. 5, 876 (1952).

[3] Ya. B. Zeldovich, J. Expt.-Theor. Phys. 10, No. 5, 542 (1940).

[4] R. H. Christian, F. L. Jarger and R. E. Duff, J. Chem. Phys., 23, No. 11, 2042(1955).

[5] S. P. Toenies and E. F. Greene, J. Chem. Phys., 23, No. 7, 1366(1955).

[6] A. Hertzberg, Jet Propulsion, 26, No. 7(1) 549(1956).

[7] K. Wray and D. F. Horning, J. Chem. Phys., 24, No. 6, 1271(1956).

[8] R. Shreffler and R. H. Christian, J. Appl. Phys., 25, No. 3, 324(1954).

[9] W. Fickett and R. D. Cowan, J. Chem. Phys., 23, No. 7, 1349(1955).

[10] L. Moore, J. Aeronaut. Sci., 19, No. 8(1952).

[11] A. M. Gurvich and Yu. Kh. Shaulov, Thermodynamic Investigations by the Explosion Method and Calculations for Combustion Processes,* Moscow, 1955.

[12] S. M. Hendric, J. Chem. Phys., 22, 1503(1954).

[13] A. Geidon, The Energy of Dissociation and Spectra of Diatomic Molecules,** Foreign Lit. Press, 1954.

*In Russian.
**Russian translation.

THE INFLUENCE OF THE ADDITION OF SURFACE ACTIVE SUBSTANCES ON THE INTENSITY OF THE VIBRATIONAL PULVERIZATION OF CEMENT

L. I. Edelman and D. S. Sominsky

(Presented by Academician P. A. Rebinder December 30, 1956)

The phenomenon of decreasing hardness (or strength) through adsorption was discovered by P. A. Rebinder and his collaborators and has been studied by them in works on various types of solid bodies [1]. This effect is to be observed, for example, in the wet pulverization of refractory materials [2], dyestuffs [3] and ores [4]. In particular, the effect has been demonstrated and studied in cement clinkers during wet and dry dispersion in the ball mill [5, 6]. It has been shown that the introduction of certain surface active substances permits a considerable increase in the degree of dispersion of cement. At times, however, the increased rate of pulverization has been ascribed not only to the effect of adsorbitive diminution of the hardness but also to the disintegrating action of the surface active additives [6].

We have investigated the influence of the addition of surface active substances on the rate of pulverization during the grinding of portland cement (from the Gigant mill; nominal initial specific surface area 3300 cm^2/g; chemical composition: SiO_2 – 32.8%, Fe_2O_3 – 3.85%, Al_2O_3 – 4.25%, CaO – 52.6%, MgO – 3.30% and SO_3 – 1.44%) in a laboratory vibration mill of 10 liter capacity. The volume of the crushing bodies (steel spheres of 10 mm diameter) amounted to 80%, and that of the pulverized material to 32%, of the volume of the mill chamber.

The hydrophobic additives, mylonaphth, acidol-mylonaphth and oleic acid and the hydrophillic additive sulfonated alcoholic waste – calcium lignosulfonate (SAW) were studied at concentrations ranging from 0.1 to 1% of the cement weight. These additives were introduced into the cement prior to grinding and were carefully mixed with it: the mylonaphth, acidol-mylonaphth and oleic acid, in the pure form, and the sulfonated alcoholic waste as a 50% aqueous solution.

The degree of dispersion of the cement was determined from the magnitude of the nominal specific surface area, S_1, of a layer of compressed powder, following the Kozen-Karman method of air penetration and using an apparatus which had been developed in our laboratory [7]. The true value, S_2, of the surface area, as determined by us in individual cases through the method of low temperature nitrogen adsorption (the BET method, [8]), was approximately 6 times greater than the nominal. Thus, for example, the true specific surface area of the initial cement, determined by the BET method, amounted to 2.17 m^2/g whereas the nominal value as determined by the method of air penetration was 0.33 m^2/g.

The experimental data on the kinetics of dry grinding of the cement at a frequency n = 3000 vib/min and an amplitude A = 2.5 mm show that the introduction of surface active substances exerts an intensifying action on the cement dispersion (Fig. 1). This is expressed in a greater increase of the specific surface area of the material, as compared with that observed during grinding without additives. Quantitatively this increase of the surface area varies from 10 to 30% depending on the nature of the additive, its concentration and the duration of grinding. Hydrophobic additives are more active in this respect than is the sulfonated alcoholic waste.

The introduction of surface active additives thus permits a reduction in the time of grinding of the cement. So, for example, with the indicated operating parameters for the vibro-mill, the time required for grinding the cement down to $S_1 = 5000$ cm^2/g is reduced by 20-40% and that required for grinding to $S_1 = 6000$ cm^2/g by 50%, on the average.

A sedimentation analysis of the granular composition of the cement showed that the increase of the specific surface which is caused by the introduction of additives results from an increase in the fractions of fine particles (with radii up to 5 μ); the content of the coarse fraction (10-20 μ) is at the same time diminished while

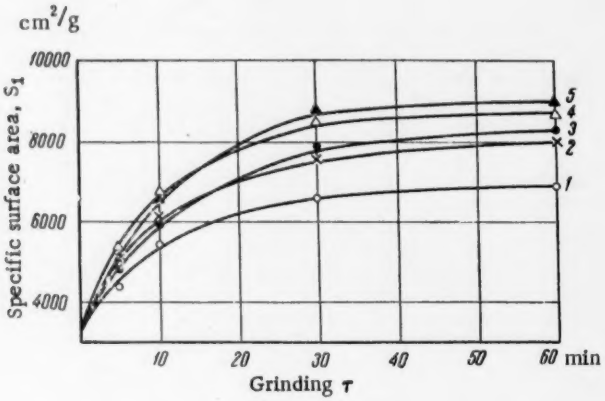

Fig. 1. The influence of the addition of surface active substances on the kinetics of cement grinding: 1) without addition, 2) sulfonated alcoholic waste, 0.2%, 3) mylonaphth, 0.3%, 4) acidol-mylonaphth, 0.3%, 5) oleic acid, 0.2%.

that of the particles of intermediate diameters (5-10 μ) remains practically unaltered (Table 1).

Over the interval from 0.1 to 0.5% the influence of a surface active substance, and of oleic acid in particular, on the grinding, increases in proportion to its relative content in the cement (Fig. 2). A further increase in the acid content does not enhance its effectiveness in short time grinding (up to 20 min), but brings about a further augmentation of the specific surface during grindings of about 1 hour duration.

TABLE 1

The Granular Composition of Cements Which Have Been Ground in the Presence of Surface Active Substances; n = 3000 vib/min, A = 2.5 mm, τ = 30 min.

Surface active additives	Limiting radii for the fractions, μ			
	< 2	2-5	5-10	10-20
	Content of fraction, %			
Without additive	35	31	17	17
Mylonaphth, 0.3%	39	35	18	8
SAW, 0.2%	34	38	19	9
Mylonaphth, 0.3%, in a 10% Na_2CO_3 solution	49	28	16	7

Thus in the initial stages of grinding the optimal oleic acid concentration is 0.5% whereas for obtaining the maximum increase in the specific surface at the end of the grinding at least 1% of the acid is required. From this it follows that, depending on the desired dispersion of the granulated product, there exists an optimal concentration of the surface active substance which leads to the maximum increase of the specific surface. Thus for a 30 minute grinding of the cement, the optimum oleic acid concentration amounts to 0.5% and with this the increase of the specific surface area is at least 50% greater than that obtained by grinding without the use of a surface active additive.

The effectiveness of the action of surface active additives on the kinetics of cement grinding and its dependence on the frequency and amplitude of vibration of the mill were investigated. Grinding the cement at n = 1500 vib/min and at amplitudes ranging from 1.9 to 6.5 mm (the power expended on the grinding was W = 0.85 – 8.0 kilowatts) showed that the introduction of surface active additives brings about practically no dispersing action under these conditions. By grinding the cement at n = 3000 vib/min (W = 1.4–4.5 kilowatts) it was established that with small amplitudes, of the order of 1.0 mm, surface active substances exert almost no influence on the pulverization; the effectiveness of the additive action appears at A > 2 mm; and reaches a maximum at A ~ 2.5 mm. Thus in the region of the

optimal parameters for vibrational grinding the influence of the surface active additives becomes clearly expressed at sufficiently high frequencies and amplitudes.

This leads to the conclusion that the observed intensification of vibrational grinding of the cement under the influence of surface active additives is brought about, not by the prevention of aggregation of the particles of the finely dispersed material, (i.e., not by the stabilization of the latter), but by the initial effect of adsorptive diminution of hardness, since the stabilizing (deaggregating) action of the surface active additives is clearly not related to the mechanism of grinding.

The adsorptive character of the process of intensification of cement pulverization is confirmed by its dependence on the additive concentration. Calculations which were carried out on the basis of the true specific

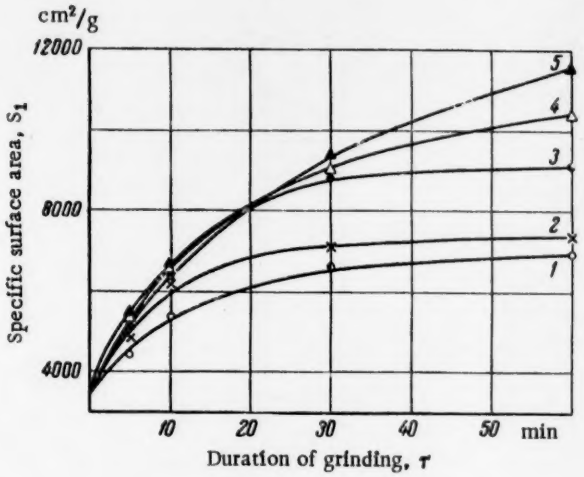

Fig. 2. The influence of the concentration of oleic acid on the kinetics of cement grinding: 1) 0%, 2) 0.1%, 3) 0.2%, 4) 0.5%, 5) 1%.

surface area of the cement, as determined by the BET method [8], showed that for the formation of a saturated monolayer of oleic acid on the cement there is required for the initial material, 0.4%, and for the end product, 0.8%, of the surface active additive per mass of cement, which agrees very well with the experimental data (Fig. 2).

The experimental results make it possible to consider that the basic factor which conditions the intensification of the pulverization of cement through the adsorptive diminution of the hardness is a sufficiently high frequency of vibration. The power which is expended on the pulverization, regardless of the frequency of vibration, obviously plays a secondary role. Thus for n = 1500 vib/min and A = 6.5 mm the power required amounted to 8.0 kilowatts and with n = 3000 vib/min and A = 2.5 mm it was 3.6 kilowatts and, nevertheless, the influence of surface active additives was to be seen only in the second case.

These results are in conformity with the ideas of P. A. Rebinder and his collaborators [1], as to the role of hardness reducing substances in periodic disintegrating actions on solid bodies.

The All-Union Scientific Research Institute for New Problems in the Production of Construction Materials which are Based on Fine Pulverization

Received December 30, 1956

LITERATURE CITED

[1] P. Rebinder, Zs. f. Phys., 72, 91 (1931); P. A. Rebinder and N. A. Kalinovskaya, J. Tech. Phys., 2, No. 7-8, (1932); J. Phys. Chem., 5, No. 2-3, (1934); P. A. Rebinder and E. K. Venstrem, Izv. OMEN, Acad. Sci.,

USSR, phys. ser., No. 4-5(1937); P. A. Rebinder, L. A. Shreiner and K. F. Zhigach, Hardness Reducing Solutions in Boring,* Moscow-Leningrad(1944); V. I. Likhtman, P. A. Rebinder and G. V. Karpenko, The Influence of Surface Active Media on the Deformation of Metals,* Moscow(1954); P. A. Rebinder et al., Investigations in the Field of Surface Phenomena,* Moscow-Leningrad(1936), P. A. Rebinder, Jubilee Annual Dedicated to the 30th Anniversary of the Great October Socialistic Revolution, 1, Acad. Sci., USSR Press(1947).

[2] G. V. Kukolev and L. G. Melnichenko, Refractories, 13, 447(1948).

[3] V. I. Byalkovsky and I. A. Kudinov, Ceramics Annals, No. 10(1940).

[4] L. M. Chernyi, Trans. Ins. of Mined Chemical Raw Stuffs, No. 1(1950).

[5] S. V. Shestoperov et al,, Concrete Cement with Plasticizing Additives,* Moscow(1952).

[6] M. I. Khigerovich, Trans. Ins. of Cement, No. 3(1950); Doctoral Dissertation, Moscow(1955).

[7] D. S. Sominsky and G. S. Khodakov, Communication No. 21 VNIITISM(1956).

[8] D. S. Sominsky and G. S. Khodakov, Chemical Science and Industry, No. 2(1956).

*In Russian.

THE KINETICS OF THE FORMATION OF ALCOHOL AND ALKYL ACID IN THE REACTION OF PROPYLENE AND AQUEOUS SULFURIC ACID

S. G. Entelis, V. E. Petrakovich, G. V. Korovina and N. M. Chirkov

(Presented by Academician V. N. Kondratyev January 19, 1957)

There has been a great deal of work devoted to the study of the kinetics of the absorption of the olefins by sulfuric acid [1-6]. In most of this work there is a common fundamental defect, namely that the experiments were carried out under such conditions that the rate of absorption was limited by diffusional processes.

An exception is the work of Kh. R. Rustamov [5], in which there is a detailed study of the true kinetics of the overall absorption of propylene and n-butylene by thin films of sulfuric and phosphoric acids under conditions which excluded the possibility of diffusional difficulties.

We have studied the kinetics of the absorption of propylene by 67% H_2SO_4 at 42, 50, 70, 75, 80 and 90° and under an initial pressure, $P^0C_3H_6$, of ~300 mm of Hg. In the individual experiments the amount of the acid was varied from 2.5 to 11 g. The experiments were carried out in a closed glass system (Fig. 1) which was equipped with a glass circulating pump, 1. With the aid of this pump, propylene containing the necessary amount of water vapor was pumped through the reactor, which, in turn, was filled with sulfuric acid. This reactor was in the form of a glass vessel of 60 cm^3 volume, inside of which there was fused a plate of porous glass (Schott 2), 20 mm in diameter. The propylene passed through the acid converting the entire mass of the latter into a compact foam. Reaction took place between the gas, the major portion of which was in the form of bubbles, and the acid film. Under these conditions it was possible to observe the true kinetics of the absorption of the propylene without diffusional interference.

The course of the reaction was followed both by the decrease of pressure in the closed system with a gas volume of 2 *l* and by analysis of the reaction mixture for its content of alkyl acid and alcohol. Analysis for the alkyl acid was carried out acidometrically [6, 7]. The alcohol was determined by the method of oxidation titration. For separating the alcohol from the alkyl acid which interferes with its determination, the solution containing water, H_2SO_4, the alkyl acid and alcohol was neutralized with a concentrated KOH solution and the water, together with the alcohol, was distilled off in vacuum (at approximately 30 mm) at 35-40°. The first receiver was cooled with a salt-ice mixture; the second with liquid air.

The velocity constant for the overall absorption was calculated from the mean rate along the initial segment of the kinetic curve (Fig. 2) at 3-4% conversion, it being supposed that the rate of the reverse reaction is at first negligibly small. The values of the constant which were determined in this way are close to those obtained from the data of Kh. R. Rustamov [5] who designedly so worked as to avoid diffusional effects. In Table 1 values are given for the velocity constant of over all propylene absorption by 67% H_2SO_4, these values having been reduced to the basis of 1 g of acid and 1 *l* of volume for the space above the acid.

The observed proportionality between the rate of overall absorption and the amount of acid (Fig. 3) served as confirmation of the fact that we were actually working in the kinetic region. This proportionality indicated that the entire mass of acid contained in the vessel simultaneously took part in the reaction.

TABLE 1

Temperature in °C		42	50	70	75
$K \cdot 10^{-4} \cdot min^{-1}$	Our data	3.32	5.71	9.6	11.0
	According to Rustamov	4.46	5.75	11.7	13.8

The experiments which were carried out at 70° were interrupted from time to time and the reaction mixture was analyzed for its content of alkyl acid and alcohol. The data thus obtained are presented in Table 2. As is to be seen from this table, the initial rate of alcohol formation exceeded that of alkylation almost by a factor of 4.

TABLE 2

The Kinetics of the Formation of Isopropyl Alcohol and Alkyl Acid at 70° (the amount of 67% H_2SO_4 was 7.7 g; the volume of the gaseous phase, 2 liters)

$P^0_{C_3H_6}$, mm Hg	Time in min	Absorption of C_3H_6, mmoles	Formation of i-$C_3H_7SO_4H$, mmoles	Formation of i-C_3H_7OH, mmoles
314.5	60	6.4	1.8	4.6
308.5	101	7.1	0.8	6.3
303.0	139	10.1	2.0	8.4
306.0	180	12.3	2.9	9.4
305.0	225	13.6	3.0	10.6
306.0	249	12.5	3.5	9.0
310.0	360	12.7	3.2	9.5
312.5	456	14.9	3.8	11.1

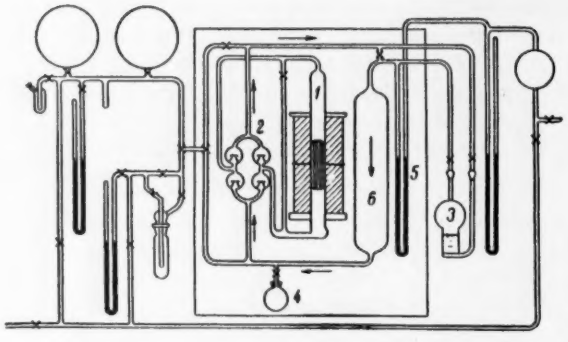

Fig. 1. Sketch of the apparatus: 1) glass circulating pump; 2) pump valves; 3) reaction vessel; 4) bulb with water; 5) manometer for following the progress of the reaction; 6) ballast volume.

Without going into the details of the complex acid catalyzed processes which occur during the dissolving of propylene in the acid, it is possible to represent these processes in the form of three reversible reactions:

I. The formation of the alkyl acid

$$C_3H_6 + H_2SO_4 \underset{k_2}{\overset{k_1}{\rightleftarrows}} i\text{-}C_3H_7SO_4H.$$

II. The direct formation of the alcohol

$$C_3H_6 + H_2O \underset{k_4}{\overset{k_3}{\rightleftarrows}} i\text{-}C_3H_7OH.$$

III. The hydrolysis of the alkyl acid

$$i\text{-}C_3H_7SO_4H + H_2O \underset{k_4}{\overset{k_5}{\rightleftarrows}} i\text{-}C_3H_7OH + H_2SO_4.$$

Whether the principle alcohol production is through II or III has not been established in the literature up to the present time. However, the very fact of the production of alcohol in parallel with the alkyl acid (see the kinetic curves in Fig. 2) excludes the possibility of its entire formation by the hydrolysis of the acid according to reaction III. We will now compare the experimental curves for the formation of the products with theoretical curves obtained from the scheme presented above, making various suppositions as to the relationships between the velocity constants for the separate steps.

We introduce the dimensionless concentrations, $\alpha = x/a_0$ and $\beta = y\beta a_0$; a_0, $\underline{x}$ and $\underline{y}$ being concentrations of the various substances in the liquid phase: a_0 is the initial concentration of the C_3H_6, $\underline{x}$ is the instantaneous concentration of the i-$C_3H_7SO_4H$ and $\underline{y}$ the instantaneous concentration of the i-C_3H_7OH. Supposing that the concentrations of H_2SO_4 and H_2O remain unaltered in the course of the reaction, we write:

$$\frac{d\alpha}{dt} = k_1'(1-\alpha-\beta) - k_2\alpha - k_3'\alpha + k_6'\beta; \quad (1)$$

$$\frac{d\beta}{dt} = k_1'(1-\alpha-\beta) - k_4\beta - k_5'\alpha - k_6'\beta. \quad (2)$$

Here $k_1' = k_1[H_2SO_4]_0$; $k_5' = k_5[H_2SO_4]_0$ and $k_6' = k_6[H_2O]_0$.

By solving this system of linear equations, we obtain the law covering the variation of the concentrations of i-$C_3H_7SO_4H$ and i-C_3H_7OH with time:

$$\alpha = P_1 e^{r_1 t} + Q_1 e^{r_2 t} + \frac{\gamma_1}{\rho}; \quad (3)$$

$$\beta = P_2 e^{r_1 t} + Q_2 e^{r_2 t} + \frac{\gamma_2}{\rho}, \quad (4)$$

where

$$P_1 = -\frac{k_1' + r_2\gamma_1/\rho}{r_2 - r_1}, \quad P_2 = -\frac{k_3' + r_2\gamma_2/\rho}{r_2 - r_1},$$

$$Q_1 = \frac{k_1' + r_1\gamma_1/\rho}{r_2 - r_1}, \quad Q_2 = \frac{k_3' + r_1\gamma_2/\rho}{r_2 - r_1}.$$

$$r_{1,2} = \frac{(k_3' + k_4 + k_6' + k_1' + k_2 + k_5) \pm \sqrt{(k_3' + k_4 + k_6' + k_1' + k_2 + k_5)^2 - 4\rho}}{2},$$

$$\rho = (k_1' + k_2 + k_5)(k_3' + k_4 + k_6) - (k_6' - k_1')(k_5' - k_3'),$$

$$\gamma_1 = k_3'k_6 + k_1'(k_4 + k_6'), \quad \gamma_2 = k_1'k_5' + k_3'(k_2 + k_5).$$

We will now find the time dependence of α and of β for various relations between the velocity constants of the separate steps. For the carrying out of calculations according to the derived equations it is necessary to evaluate the velocity constants for the separate steps. Supposing, as a first approximation, that the formation of i-$C_3H_7SO_4H$ and i-C_3H_7OH is entirely by reactions I and II respectively, we find the constants k_1 and k_3 from the mean rates along the initial segments of the kinetic curves for the alcohol and the alkyl acid We neglect the reverse reactions at small degrees of conversion. Since the absolute amount of dissolved propylene is unknown, the velocity constants are found as quotients of the rate and the partial pressure of the propylene. Thus the Henry Law coefficient enters into the velocity constant

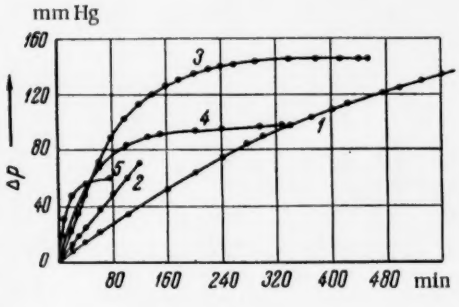

Fig. 2. The kinetic curves for the over all absorption of propylene in 67% H_2SO_4. Volume of the gas phase, 2 *l*; amount of acid, 7.7 g; $P^0_{C_3H_6}$ = 310 mm of Hg; 1) 42°; 2) 50°; 3) 70°; 4) 80°; 5) 90°.

Case 1. The reaction of alkyl acid hydrolysis is lacking, i e., $k_5' = k_6' = 0$. Starting from the kinetics, supposing equilibrium and setting $k_1' = 1$, we obtain: $k_2 = 4$, $k_3 = 4$, $k_4 = 6.5$. After substituting the values of these constants into Equations (3) and (4), there results:

$$\alpha = 13.45 \cdot 10^{-2} - 6.1 \cdot 10^{-2} e^{-11.15\tau} - 7.35 \cdot 10^{-2} e^{-7.35\tau},$$

$$\beta = 33.0 \cdot 10^{-2} - 37.8 \cdot 10^{-2} e^{-11.15\tau} + 4.8 \cdot 10^{-2} e^{-7.35\tau}.$$

By taking $k_1' = 7.7\ 10^{-4}$. min^{-1} as a unit, we introduce a new measure of time, $\tau = k_1' t$, where t is the time in minutes.

Case 2. The alcohol is formed simultaneously with the i-$C_3H_7SO_4H$, as well as through the hydrolysis of the latter. The true concentration of the physically dissolved propylene is clearly much less than the measured concentrations of i-C_3H_7OH and i-$C_3H_7SO_4H$. Thus in order that the hydrolysis rate be equal to or less than the rate of addition of C_3H_6 to H_2O and to H_2SO_4 according to reactions II and I, the constants k_5 and k_6 must be

less than k_1 and k_3. We again suppose that $k_1' = 1$, $k_2 = 4$, $k_3 = 4$, $k_4 = 7$ and $k_5 = k_6 = 0.5$ ($k_5 = k_6$ is assumed for simplicity):

$$\alpha = 12{,}3 \cdot 10^{-2} - 5{,}3 \cdot 10^{-2} e^{-11{,}15\tau} - 7{,}0 \cdot 10^{-2} e^{-5{,}86\tau},$$
$$\beta = 28 \cdot 10^{-2} - 45 \cdot 10^{-2} e^{-11{,}15\tau} + 17 \cdot 10^{-2} e^{-5{,}86\tau}.$$

Finding, from the values of α and β, the corresponding amounts of i-$C_3H_7SO_4H$ and i-C_3H_7OH, it is possible to construct theoretical curves for the formation of the latter substances and to compare these with the experimental curves (Fig. 4). As is to be seen from the figure the experimental points lie closer to the curve which

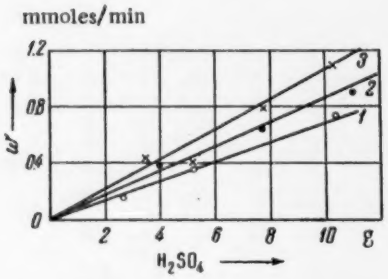

Fig. 3. The dependence of the initial rate of reaction for the over all absorption of C_3H_6 in 67% H_2SO_4 on the amount of the acid. The volume of the gaseous phase 2 l, $P^0_{C_3H_6}$ = 310 mm of Hg; 1) 42°; 2) 50°; 3) 70°.

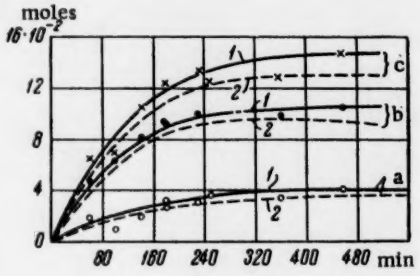

Fig. 4. A comparison of the experimental data (points) with calculated values (crosses): 1) Case 1; 2) Case 2; a and b are the kinetic curves for the formation of i-$C_3H_7SO_4H$, (a), and i-C_3H_7OH, (b); c is the amount of absorbed propylene.

corresponds to Case 1. The calculated values for the reaction of hydrolysis of the alkyl acid show a pronounced deviation from the experimental results.

From the brief analysis which has been presented it is possible to draw the conclusion that the principal part of the alcohol, if not the entire mass of it, is formed, not as a result of the hydrolysis of the i-$C_3H_7SO_4H$, but simultaneously with the latter through the reaction of C_3H_6 with water.

The Institute of Chemical Physics of the Academy of Sciences of the USSR

Received January 16, 1957

LITERATURE CITED

[1] H. S. Davis and R. Schuler, J. Am. Chem. Soc., 52, 721 (1930).

[2] V. V. Pigulevsky and N. V. Rudakova, Material on Cracking and the Chemical Treatment of its Products,* No. 1, 1933, p. 67.

[3] V. G. Moor, Material on Cracking and the Chemical Treatment of its Products,* No. 3, 1936, p. 108.

[4] M. A. Kerdivarenko, P. K. Migal and M. Kh. Kishinevsky, J. Appl. Chem. 28, 459 (1955).**

[5] Kh. R. Rustamov, Doctoral disser., Inst. Chem. Phys. Acad. Sci. USSR 1954.

[6] R. Robey, Ind. and Eng. Chem., 33, 1077 (1941).

[7] R. W. Schrage and E. H. Amick, Ind. and Eng. Chem., 42, 2550 (1950).

[8] A. V. Rakovsky, Chemical Kinetics and Catalysis,* Moscow-Leningrad, 1932, p. 26.

* In Russian.

** See C. B. Translation.

ABSORPTION SPECTRA OF SOME DYES IN MIXED SOLVENTS

Kh. L. Arvan and N. V. Ivanova

(Presented by Academician A. N. Terenin, January 2, 1957)

As was reported earlier [1] for some dyes in mixed solvents (water-organic solvent) a displacement of the absorption band toward longer wavelength had been observed relative to its position in each of the pure solvents. We were unable to relate this displacement to a change in the physicochemical properties of the solvent (viscosity, refractive index, dipole moment, volume, etc.) on changing its composition.

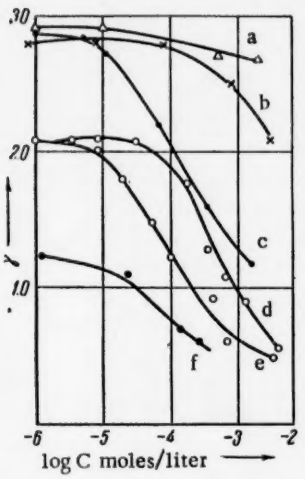

Fig. 1. The relation of the ratio of the absorption maxima of some dyes to the concentration of the dye in aqueous solutions: a) Rose Begal; b) eosin; c) rhodamine B; d) pyronine G; e) methylene blue; f) toluidine blue.

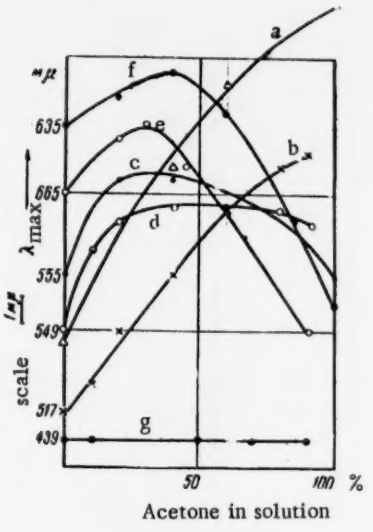

Fig. 2. The relation of the position of the absorption band maxima of some dyes to the composition of the solvent (water-acetone). The numbers at the left show the value of the absorption band maxima in aqueous solutions. g) tartrazine; the other curve symbols are the same as in Fig. 1.

As a result of this, a hypothesis was put forward on the mixed solvation of dyes in such solutions.

The magnitude of the relative displacement of the band is determined both by the composition of the solvent and by the properties of the dissolved dye. In particular, the capacity of the dye for association in aqueous solutions turned out to be considerable. This capacity, as was pointed out, can be characterized, in

the first approximation, by the value γ – the relation of the long wave and the short wave maxima of the absorption bands ascribed to monomers and dimers. The relation of the value of this ratio to the dye concentration in an aqueous solution determines the greater or lesser tendency of the dye to associate. Furthermore, the steepness of the slope of the γ-curve as well as the dye concentration at which a deviation of the curve from the horizontal commences should be examined.

The relation of the value of γ to concentration in aqueous solutions for some of the dyes investigated is shown in Fig. 1, and the relation of the position of the absorption band maximum to composition of the mixture (water-acetone) for these dyes is shown in Fig. 2. It follows from a comparison of the figures that the greatest dependence of the form of the absorption band on concentration, characterized by the change in value of γ, is observed for those dyes which have the greatest displacement of the absorption band in mixtures, relative to their position in the pure solvents (methylene blue, rhodamine B, toluidine blue). Rhoduline orange, Night blue, Nile blue and Capri blue behave analogously. The dependence of the value of γ on dye concentration in aqueous solutions is much weaker for those dyes whose absorption band in mixtures occupies a position between those it would occupy in the pure solvents (for example, eosin and Rose Bengal).

Furthermore, a monotonic displacement of the absorption band with change in dye composition is observed for tartrazine, Congo red and some other dyes, whose absoption spectra hardly change with changing dye concentration.

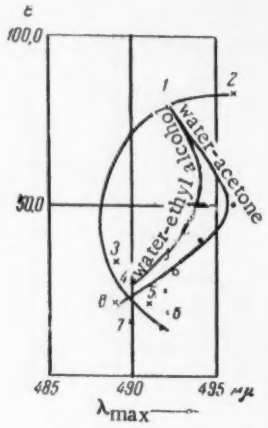

Fig. 3. The relation of the position of the absorption band maximum of rhoduline orange NO to the dielectric constant of the solvent (for pure solvents and mixtures): 1) water; 2) formamide; 3) methyl alcohol; 4) ethyl alcohol; 5) propyl alcohol; 6) butyl alcohol; 7) amyl alcohol; 8) acetone.

A nonmonotonic displacement of the absorption bands with change in the composition of the mixed solution (water-dioxane) analogous to that described above, was observed by Klochkov [2] for nonassociating compounds, namely phthalimides. The author explained this by the dependence of the position of the absorption band on the dielectric constant of the solvent. Actually, in this case, the position of the absorption band for pure solvents, as well as their mixtures is determined by the dielectric constant of the solvent.

As can be seen in Fig. 3, the positions of the absorption bands of the associating dyes investigated by us in mixtures, do not coincide with their positions in pure solvents with corresponding dielectric constants. Furthermore, the displacement of the spectrum by changing the composition of the mixed solvent is opposite to that observed in an analogous change of the dielectric constant by substituting one pure solvent for another. Due to this, the relative displacement of the spectra in mixed solvation is somewhat increased by considering the effect of the dielectric constant of the solvent.

It follows from all this data that the formation of mixed solvates, characterized by the displacement of the absorption bands, is mainly observed in associating dyes. The question arises as to whether the presence of associates in solution are essential for mixed solvation. However, a specific investigation showed that the relative displacement of the absorption band did not depend on the dye concentration, i.e., on its dispersion.

In this relation, only the tendency of a given dye toward association, i.e., its structure, is essential. In connection with the parallelism of association and mixed solvation processes, it may be supposed that they are due to the presence of the same groups in the dye molecules and the same intramolecular forces. The mobile equilibrium in the solution is determined by the domination of one process by the other. Presumably, this should explain the stopping of dye association when mixed solvates arise [1].

In conclusion, we would like to thank Professor M. V. Savostyanova for constant interest in the work.

LITERATURE CITED

[1] Kh. L. Arvan, Bull. Acad. Sci. USSR, Phys. Series, 20, 443 (1956).

[2] V. P. Klochkov, Optics and Spectroscopy 1, 4, 546 (1956).

Received December 21, 1956.

A STUDY OF THE $Zn \rightleftharpoons Zn^{++}$ EXCHANGE PROCESS ON THE FACES OF A ZINC MONOCRYSTAL USING RADIOACTIVE INDICATORS

B. N. Bushmanov and G. S. Vozdvizhensky

(Presented by Academician A. N. Frumkin, January 2, 1957)

In recent times, it has been made progressively more apparent that electrochemical processes and among them those which determine the sign and magnitude of the electrode potential, depend on the crystallographic orientation of the sample [1, 2]. Previously, only contradictory data existed on the potentials of monocrystals of zinc, aluminum, copper, iron, etc. Now, we may take it as firmly established that the various faces of these monocrystals have different potentials in the absence of a current as well as with polarization [3-7]. The potential difference between different faces may attain several tenths of millivolts and considerably increase in the case of polarization, with an increase in the density of the current.

Thus, it is apparent that the atom $\rightleftharpoons$ ion exchange processes on the different faces of metal monocrystals differ considerably in their nature and kinetics. The use of radioactive indicators is one of the methods for quantitative study of exchange currents [8, 9]. Sufficiently reliable data were obtained by this method in the case of exchanges at an amalgam-solution boundary [10, 11]. More complicated relations exist at solid metal surfaces. Haissinsky, et al. ([12] and others cited by [14]), carried out a series of investigations aimed at studying the connection between the exchange rates and the electrode potentials of metals. The authors arrived at the conclusion that the atom $\rightleftharpoons$ ion exchange reactions proceeded very rapidly, that they were reversible and did not depend on the metal surface. Other investigators [13] found that the state of the surface affected the exchange rate. The changes in exchange rate were ascribed to differences in crystal structure [14]. At the same time, some considered that the exchange between a metal and its radioactive ions is not a result of a simple transfer due to the electrode potential [14], but that in the given case, it is complicated by adsorption and other processes, occurring on the metal surface.

EXPERIMENTAL

We chose zinc monocrystals as the subject of our investigation. This choice was dictated by the fact that the greatest difference in the properties of the various crystal faces could be expected with zinc [15]. Besides that, other electrochemical properties of zinc monocrystals have been studied in our laboratories [3, 4]. Finally, zinc has a radioactive isotope Zn^{65} which has a convenient half-life for radiochemical measurements.

We obtained the zinc monocrystals using a variation of Bridgman's method [16, 17] developed by us. The faces of the base were exposed by breaking the samples, cooled in liquid oxygen, and the prism faces were exposed by sawing. The samples were then finished with emery paper Nos. 00,000 and 0000 and electrolytically polished in Faust's electrolyte [18].

All the surface of the samples, except the surface of the face investigated, was sealed with bakelite lacquer. After the surface being investigated was electropolished, the samples were kept for a certain time in a 0.03 M solution of zinc sulfate labelled with the radioactive isotope Zn^{65} and washed with distilled water. 7-10 samples of each crystallographic orientation were simultaneously tested in each series of experiments.

We give the results of one group of experiments to illustrate the suitability of the measurement procedure used (see Table 1 ; 8 pairs of samples with an area of 1 cm^2 were investigated in each series).

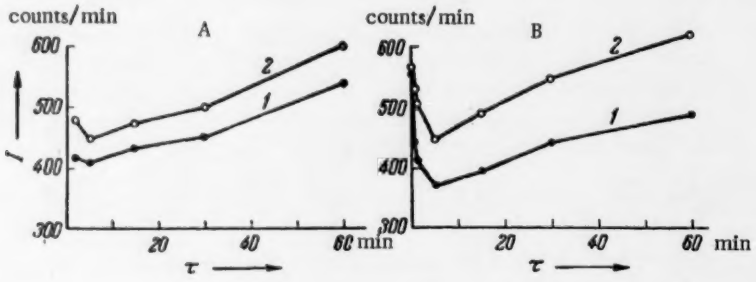

Fig. 1. A) The relation of the activity of zinc monocrystal faces to time;
B) the same for samples connected in couples; 1) base, 2) prism.

These results are shown graphically in Fig. 1, A, starting with a 1 minute exchange time. Exchange times of 5 and 30 seconds produced a wide scattering of points so that the results of these measurements cannot be considered sufficiently reliable.

TABLE 1

Exchange time	Base		Prism	
	$I \pm \Delta I$		$I \pm \Delta I$	
	counts/min	%	counts/min	%
5 sec	821±41	100±5	674±107	79±13
30 »	597±55	100±9	596± 71	100±12
1 min	421±15	100±4	485± 16	118± 4
5 »	411±14	100±3	446± 20	108± 3
15 »	439±19	100±4	483± 24	110± 3
30 »	464±11	100±2	493± 18	106± 4
60 »	545±21	100±4	602± 30	110± 6

Note: I – Average activities, acquired by samples in the exchange process, ΔI – mean square error of activity measurements [19].

It can be seen from Table 1 and Fig. 1, A, that the activity acquired by the prism face is approximately 10% greater than that acquired by the base. By itself, this result may not appear convincing enough as the limits of the region of error for the base and the prism almost touch. We note, however, that as a result of 52 series of measurements, the activity of 736 samples was measured and the average ratio I_{pr}/I_{base} obtained was equal to 108%.

According to us, the surface of polycrystalline zinc (after removal of the deformed metal layer) consists of a mosaic of surfaces of two crystallographic faces – base and prism, shortcircuited through the body of the sample itself. It is known that the galvanocouple, base-prism, possesses an electromotive force [3, 4], which probably has a specific effect on the course of the processes determining the activity of the samples.

To check this hypothesis we studied the process using samples of base-prism connected in a galvanocouple (see Table 2; 9 pairs of samples with an area of 1 cm^2 were investigated in each series). These data are shown graphically in Fig. 1, B (starting with 1 minute). In this case the anisotropic effect is expressed more strongly than in the preceding case and is approximately 25%.

TABLE 2

Exchange time	Base $I \pm \Delta I$		Prism $I \pm \Delta I$	
	Counts/min	%	Counts/min	%
5 sec	565±64	100±11	575±93	102±16
30 »	444±18	100± 4	539±34	121± 8
1 min	412± 9	100± 2	511±11	124± 3
5 »	369±17	100± 5	450±10	122± 3
15 »	393±13	100± 3	495±13	126± 3
30 »	442±13	100± 3	554±17	125± 4
60 »	489±15	100± 3	629±14	129± 3

It follows from the above that the course of the atom $\rightleftharpoons$ ion exchange process on the faces of a zinc monocrystal depend on the crystallographic orientation. The exchange proceeds more intensively on the less densely packed face of the prism which has a more negative potential.

The exchange equilibrium on a prism face is displaced toward the formation of ions and on a base face toward the formation of atoms when base and prism samples are connected in shortcircuited couples, which always occurs on the surface of a polycrystalline metal. The effect of crystallographic orientation on the activity acquired by the samples in this case appears more marked.

LITERATURE CITED

[1] S. M. Kochergin, Prog. Chem. 24, 6, 779 (1955).

[2] N. S. Akhmetov, Trans. Kazan Chem.-Tech. Inst. 19-20, 261 (1954-1955).

[3] N. S. Alhmetov and G. S. Vozdvizhensky, J. Appl. Chem. 29, 1196 (1956).*

[4] N. S. Akhmetov and G. S. Vozdvizhensky, Trans. Kazan Chem.-Tech. Inst. 21, 65 (1956).

[5] G. S. Vozdvizhensky, V. A. Dmitriev, and E. V. Rezhevsky, J. Phys. Chem. 29, 280 (1955).

[6] H. I. Engell, Naturwiss., 5, 124 (1955).

[7] Kamiya, Kagaku, 1, 42 (1954). [Cited from Russian J. Chem. No. 4, No. 11653 (1956)].

[8] O. Khan, Applied Radiochemistry, (Leningrad-Moscow, 1947), p. 179.

[9] O. Maiers and R. Prestwood, Coll. The Use of Radioactivity in Chemical Investigations** (Foreign Lit. Press, 1954), p. 11.

[10] V. A. Pleskov and N. B. Miller, Trans. Conf. on Electrochemistry, (Moscow, 1953), p. 165.

[11] V. V. Losev, Proc. Acad. Sci. 100, 1, 111 (1955).

[12] M. Haissinsky, Nature, 136, 141 (1935).

[13] M. Quintin, P. Sue, and M. Bizouard, Compt. rend. 226, 1723 (1948).

* [See C. B. translation].

** [Russian translation].

[14] M. T. Simnad, Coll. The Properties of Metal Surfaces, (Moscow, 1954), p. 7.

[15] G. V. Akimov, Trans. Conf. on Electrochemistry, (Moscow, 1953), p. 105.

[16] B. N. Bushmanov, J. Phys. Chem. 30, 7, 1668 (1956).

[17] B. N. Bushmanov, Trans. Kazan Chem.-Tech. Inst. 21, 79 (1956).

[18] O. Zmeskal, Metall. Progress 47, 4, 729 (1945).

[19] V. I. Spitsyn, P. N. Kodochigov, et al., Working Procedures Using Radioactive Indicators, (Moscow, 1955), p. 113.

Kazan Aviation Institute

Received January 2, 1957.

THE APPLICATION OF LABELLED ATOMS TO THE STUDY OF THE MECHANISM OF ANODE EVOLUTION OF OXYGEN

M. A. Gerovich, R. I. Kaganovich, V. M. Vergelesov, and L. N. Gorokhov

(Presented by Academician A. N. Frumkin, December 22, 1956)

On the basis of results obtained from the investigation of the mechanism of oxygen evolution at a platinum electrode in concentrated solutions of sulfuric and perchloric acids with large anode polarizations, a hypothesis was put forward on the participation of the acid anion in this process [1]. We considered that the use of acid labelled with the heavy oxygen isotope O^{18} would be effective in checking such an idea.

It was to be expected that the oxygen, evolved by the electrolysis of labelled acid at low overvoltage values (up to 0.9 v), would not contain the heavy oxygen isotope, while the oxygen evolved at higher overvoltage values, following the sharp climb of the polarization curve (Fig. 1), caused by the adsorption of the acid anion, would be enriched in O^{18}.

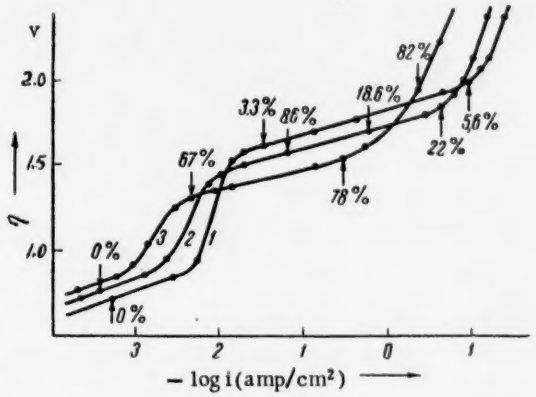

Fig. 1. Anode polarization curves of a platinum electrode in perchloric acid: 1) 5.8 N; 2) 7.6 N; 3) 10 N.

This report gives an account of the results of experiments in which perchloric acid labelled with O^{18} was used as electrolyte. We chose this system as according to [2], perchloric acid does not undergo isotopic exchange of oxygen with water, while such an exchange does occur in sulfuric acid, especially at a high temperature [3].

The labelled perchloric acid was prepared in the following way: potassium perchlorate $KClO_4$ was prepared by anodic oxidation of potassium chloride in heavy oxygen labelled water (1.34% O^{18}) to potassium

chlorate $KClO_3$, with subsequent oxidation of the latter, also in labelled water; the washed out and recrystallized labelled potassium perchlorate was distilled with strong sulfuric acid (98%) under vacuum; anhydrous perchloric acid vapor was condensed in a cooled receiver, then purified by two distillations and diluted with normal doubly distilled water to the required concentration. *

The electrolysis of perchloric acid was carried out in an electrolytic cell in the form of a U-tube with anode and cathode spaces separated by a glass filter. A bridge for controlling the anode potential during the electrolysis process and an outlet for the oxygen evolved were sealed into the anode space. The oxygen was collected in a bell under water after which it was transferred to an evacuated ampule; first the oxygen was passed through a trap with a cooling mixture which froze out moisture. In all cases before proceeding with an experiment an electrolysis was carried out for 2 hours at the given potential to fill the small air space in the anode limb of the electrolyzer with evolved oxygen. The experiments were carried out at a temperature of +20° and in 10N perchloric acid, also at a temperature of −30°.

The results of the isotopic analysis of oxygen evolved during the electrolysis of solutions of four concentrations with different overvoltage values are given in Table 1.

TABLE 1

Electrolyte	Overvoltage in v	Anode current density, amp/cm²	Amount of O^{18}, in %	Enrichment in O^{18}, in %	Proportion of acid anion participation in %
Normal water	—	—	0 198	0	—
Perchloric acid, 20°					
1 *N**	2.57	$6.0 \cdot 10^{-2}$	0.213	0.015	2.7
1 *N*	2.95	$1.5 \cdot 10^{-1}$	0.216	0.018	3.3
5.8 *N*	0.71	$5.2 \cdot 10^{-4}$	0.198	0	0
5.8 *N*	1.62	$3.0 \cdot 10^{-2}$	0.216	0 018	3.3
5.8 *N*	1.98	9.6	0.229	0.031	5.6
7.6 *N*	0.74	$3.6 \cdot 10^{-4}$	0 198	0	0
7.6 *N*	1.54	$4.0 \cdot 10^{-2}$	0.253	0.055	8.6
7.6 *N*	1.70	$5.2 \cdot 10^{-1}$	0.317	0.119	18.6
7.6 *N*	1.80	4.0	0.339	0.141	22.0
10 *N*	1.30	$4.3 \cdot 10^{-3}$	0.627	0.431	67.0
10 *N*	1.55	$2.7 \cdot 10^{-1}$	0.697	0.499	78.0
10 *N*	1.96	2.4	0.722	0.524	82.1
10 *N*	4.25	5.3	0.723	0.525	82 3
Perchloric acid, −30°					
10 *N*	2.75	2.1	0 738	0.541	84.5
10 *N*	4.25	4.25	0.743	0.546	85.3

* For the amount of heavy oxygen isotope in the original solutions of perchloric acid before electrolysis, see footnote at bottom of page.

* According to the data from mass-spectrometric analysis, the perchlorate obtained contained 1.34 % of the heavy oxygen isotope, the 5.8 N perchloric acid contained only 0.75% and the 7.6 and 10 N perchloric acid had 0.836%.

To explain the reason for the decrease in O^{18} content of the perchloric acid as compared with that of the labelled perchlorate used, the sulfuric acid distilled from the mixture with perchloric acid remaining after the preparation of anhydrous perchloric acid, was electrolyzed. The oxygen evolved turned out to be enriched in the heavy isotope O^{18} by 0.074%. It was thus established that isotopic exchange of oxygen occurred between the anions ClO_4^- and SO_4^{2-} when dry potassium perchlorate was heated with 97-98% sulfuric acid.

An examination of the data given in Table 1 shows that oxygen evolved with an overvoltage of up to 0.8 v does not contain an excess of O^{18}. This confirms the hypothesis put forward earlier that at low anode polarizations the evolution of oxygen proceeds without the participation of the acid anion by the decomposition of surface oxides and water discharge. At higher overvoltages, corresponding to the upper section of the polarization curve, the oxygen proved to be enriched in the heavy isotope O^{18}. Moreover, the amount of O^{18} increased with an increase in the concentration of acid anion and a higher overvoltage.

If the proportion of acid anion participation in the process of anode formation of oxygen is expressed as the ratio of excess O^{18} content in the oxygen evolved during electrolysis to that in the original acid, then it is equal to zero at low overvoltage values and for high overvoltages, for example 1.55-1.6 v, it is equal to 3.3% for 5.8 N perchloric acid, 18.5% for 7.6 N and 78% for 10 N. This is illustrated graphically in Fig. 1, where the values of the proportion of acid anion participation are shown in percentages depending on the overvoltage value at which the electrolysis is carried out.

Thus, from the data obtained, it follows that at high overvoltage values corresponding to the upper section of the polarization curve, a change in the mechanism of oxygen evolution occurs, caused by the participation of acid anions adsorbed in the electrode.

In analyzing analogous polarization curves which they obtained in perchloric acid (from 0.5 to 9 M), Beck and Molton [4] considered that the transition to the upper or, as they call it, Tafel, straight line was due to to the discharge of ClO_4^--ions with formation of the ClO_4 radical. Thus, they considered that in the upper section there are two distinct regions of overvoltage with different mechanisms of oxygen evolution: the first region, directly following the bend in the curve in which no decomposition of the ClO_4 radical was observed and the oxygen is evolved by the reaction of the radical with water according to the scheme $2ClO_4 + H_2O \rightarrow$ $\rightarrow 2HClO + 2HClO_3 + {}^3/_2\, O_2$, and the second region, starting at currents which are approximately 10 times greater than those corresponding to the beginning of the bend in the curve in which chlorine dioxide is found, formed by the decomposition of the ClO_4 radical as indicated in papers [5, 6].

In the light of results obtained by us such a hypothesis on the mechanism of oxygen evolution does not seem completely correct. Actually, an analysis of the anolyte after electrolysis of 10 N perchloric acid carried out at a current density which corresponded to the beginning of the upper section of the polarization curve, did not show the presence of chlorine dioxide nor of ClO_3^- - ion, while the proportion of participation of ClO_4^- - ion in the process of oxygen evolution according to mass-spectrometric data reached 67%. We detected the appearance of chlorine dioxide in the anolyte and observed, simultaneously, an increase in the proportion of acid anion participation in oxygen evolution to 78% only at higher current densities ($3 \cdot 10^{-1}$ amp/cm^2).

The quantitative determination of chlorine dioxide in the anolyte was carried out iodometrically [5], while that of chlorate-ion by a colorimetric method (photoelectrocolorimeter of the type FEK-52) using the reaction with phenylanthranilic acid in a strong sulfuric acid medium, thus allowing the determination of a ClO_3 -ion content of less than 0.005 mg/ml [7]. In the case of the electrolysis of more dilute solutions of perchloric acid, an analogous picture was observed with the only difference that at current densities corresponding to the beginning of the upper section of the curve, traces of ClO_3^- -ion were detected amounting to 0.2% of the proportion of acid anion participation, while the presence of chlorine dioxide was detected in the anolyte at current densities higher than that used for the electrolysis of 10 N acid.

On the basis of these data, we may suppose that for polarization during which chlorine dioxide would be detected, regardless of the observed enrichment of the oxygen in O^{18} isotope, the oxygen is not evolved as a result of ClO_4^- -ion discharge. The sharp increase in the electrode potential apparently causes a strong deformation of the adsorbed anions. This creates the conditions for the oxygen exchange reaction between adsorbed anion and the surface oxide of the platinum and for the enrichment of the evolved oxygen in O^{18} isotope. Only at high current densities (from 10^{-1} amp/cm^2 and higher), at which an increase in the slope of the polarization curves is again observed, does the partial discharge of acid anion start, accompanied by the formation of ClO_3^- ions in the anolyte and by the evolution of ClO_2.

It should be noted that the aqueous oxygen, distilled from the acid after electrolysis, had the usual isotopic composition, which indicates that there was no isotope exchange between the electrolysis products or semiproducts, found on the electrode surface, and water and confirms the irreversibility of the electrochemical stage of the formation of surface oxide.

In conclusion, we would like to express our thanks to Academician A. N. Frumkin for valuable advice during discussion of the results of this work.

LITERATURE CITED

[1] R. I. Kaganovich, M. A. Gerovich, and E. Kh. Enikeev, Proc. Acad. Sci. 108, 107 (1956).

[2] A. I. Brodsky and N. A. Vysotskaya, Proc. Acad. Sci. 101, 869 (1955).

[3] J. L. Hyde, J. Amer. Chem. Soc. 63, 873 (1941).

[4] T. R. Beck and R. W. Molton, J. Electrochem. Soc. 103, 4, 247 (1956).

[5] G. Grube and K. H. Mayer, Z. Elektrochem. 43, 11, 860 (1937).

[6] K. Sugino and S. Aoyagi, J. Electrochem. Soc. 103, 3, 166 (1956).

[7] N. A. Bilyk, Trans. Odessa State Univ. Coll. Chem. Fac. 3, 127 (1953).

M. V. Lomonosov State University of Moscow

Received December 7, 1956.

ELASTIC-RESILIENCY AND VISCOUS-PLASTIC PROPERTIES OF THERMOSETTING PLASTICS

I. F. Kanavets and L. G. Batalova

(Presented by Academician P. A. Rebinder, November 20, 1956)

Changes in the mechanical properties of thermosetting plastics under the effect of temperature and the prolonged action of loads have not been studied thoroughly. A closer link between the structure of the material and its mechanical properties based on contemporary ideas on high polymers and the work of P. A. Rebinder results from measuring the kinetics of the development of pure shearing after the application of a given constant pressure and the kinetics of recovery from deformation after unloading [1].

The investigations were carried out using the most important types of plastics, based on phenol-formaldehyde and aniline-formaldehyde resins of the bakelite and lacquer types. Samples for the tests were prepared by hot molding using processes that gave the degree of hardening of the resins required for technical products. The measurements of the elastic-resiliency and viscous-flow properties of the hardened plastics were carried out on specially constructed apparatus, which allowed the measurement of the shearing strain, developed by a constant force in the regions of elastic-resiliency and plastic flow, as angle of turn in degrees with an accuracy of up to 0.2°.

The measurements were carried out on cylindrical samples of 10 mm diameter and 100 mm length in the effective section, at stresses of 50 to 425 kg/cm^2, temperatures from 20 to 180° and times from 1 to 500 hours.

The magnitude of the torque, which was constant with respect to time, was set by a load suspended on a pulley with a 100 mm radius. The relaxation stress in the materials and the ultimate shear stress P_K were measured with a pendulum dynamometer by the decrease in the angle of oscillation of the pendulum with time. The modulus of elasticity, coefficient of viscosity and relaxation time were calculated by the method explained in P. A. Rebinder's paper [1].

As a result of the measurements carried out it has been established that:

1. Thermosetting plastics at normal temperature and under the effect of a constant, continuously acting load at stresses above the yield point P_K, besides resilient and elastic deformation, also sustain residual deformation. Irreversible deformation is observed also after tempering the sample at a temperature of 90° for 15 hours.

2. Loading causes resilient deformation in various types of materials at normal temperature that is 2 to 3 times greater than the elastic deformation (Fig. 1). In unloading the sample, the resilient recovery is also 2 to 3 times greater than the elastic recovery. Resilient and elastic deformation are greater on loading than unloading, the modulus of elasticity is 2 to 3 times greater than that of resiliency.

The moduli of resiliency and elasticity are greater during the unloading and subsequent reloading than at the primary loading (Tables 1 and 2).

The magnitude of the resilient deformation grows with increase in stress, in proportion to the applied stress up to 300 to 350 kg/cm^2, while the elastic deformation also increases with an increase in time of action of the force.

The moduli G_1 and G_2 remain practically unchanged under a load of up to 325 kg/cm² and at normal temperature. Depending on the grade of the material, the value of the modulus of resiliency under shearing action lies within the limits of 16,000 to 22,000 kg/cm², while the modulus of elasticity is within the limits of 50,000 to 79,000 kg/cm². A certain decrease in the moduli when the stress is increased from 325 kg/cm² to 425 kg/cm² and then an increase with repeated loading (see Tables 1 and 2) are explained not by the development of new chemical bonds on loading, but by the destruction of infrequent links between the different molecular aggregates and with repeated loadings more frequently cross linked polymer chains begin to play a part.

TABLE 1

Changes in Elastic-Resiliency and Viscous-Plastic Properties of Press-Material K-18-2 in Relation to Temperature.

	Temperature, °C							
	20	60	80	100	120	140	160	180
G, kg/cm²	22140	14300	10000	7000	4900	3850	1920	1635
$\eta_1 \cdot 10^{-13}$, poise	6400	450	160	60	25	10	5 88	8.62
$\tau_1 \cdot 10^{-10}$, sec	289	31.4	16	8.58	5.1	2 59	3.03	5.28
G_2, kg/cm²	59700	25000	17200	10550	5000	2000	792	400
$\eta_2 \cdot 10^{-11}$, poise	2400	180	75	25	6.86	1.3	2.79	4.71
$\tau_2 \cdot 10^{-7}$, sec	402	72	43.7	23.7	13.7	6.5	35	118

3. The duration of the action of the force decreases the value of the resilient deformation recovery in the following way: after 30 seconds (material of K-18-2 grade) the resilient deformation is greater on loading than on unloading by 10%; after 20 hours – by 25% and after 500 hours – by 50%. This also indicates the partial breakdown of bonds (infrequently "knitted" separate chains). Elastic deformation, however, on loading with increased time of loading action, surpasses by approximately 45-60% the deformation on unloading. The end of the development of elastic deformation and emergence of a straight line (the tangent whose slope is used to determine viscosity) at normal temperatures and stresses above yield point are observed during the time from 100 to 300 hours and more, depending on the grade of the material.

TABLE 2

Changes in Moduli of Resiliency and Elasticity of Press-Material K-18-2 in Relation to Temperature (Under Load).

	Temperature, °C							
	20	60	80	100	120	140	160	180
G_1, kg/cm²	87000	85000	23000	15000	9230	9250	6100	7310
G_2, kg/cm²	180000	62000	43000	29200	22000	16000	11480	9800

To obtain invariable values for viscosity and relaxation periods, the duration of the experiment must be greater than the time indicated for the development of elastic deformation and emergence of a straight line. By increasing the stress above yield point to the breakdown of the material in a shorter testing time, a certain increase (within the two-fold limit) of viscosity and relaxation periods is observed. Therefore, machine testing, carried out with small, practically possible loading rates, do not give invariable indices of viscosity and relaxation periods. The relaxation periods τ_1 and τ_2 of thermosetting plastics are measured in tens of years (see Table 1 and Fig. 3).

4. Resilient and elastic deformations increase with increase in experimental temperature (Fig. 1). Besides that, elastic deformation remains less than the resilient at a temperature lower than that of thermostability (T_s) while it increases sharply in comparison with the resilient at temperatures above T_s. This indicates that there is no frequent "knitting" of polymer molecules within the whole volume of the material.

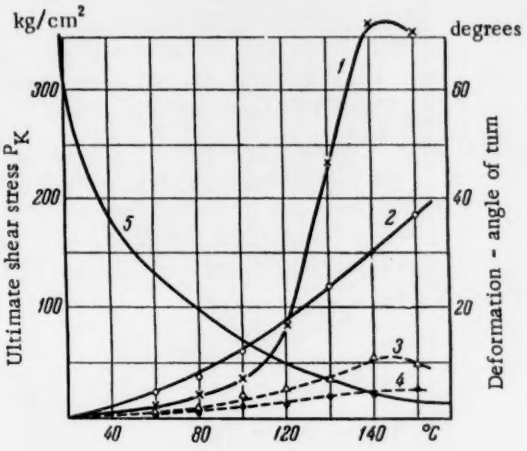

Fig. 1. The increase in the resilient (1) and elastic (2) deformation on loading in relation to temperature, as well as after removal of load – resilient (3) and elastic recovery (4); 5 – decrease in the ultimate shear stress with increase in temperature. In repeated experiments P_K was higher than 250 kg/cm².

5. The stress applied decreases with the passage of time not to zero but to a certain limit of P_K of the order of 200-250 kg/cm², which determines the ultimate shear stress and appears as a measure of the branching of the polymer chains and structural lattice in phenol-aldehyde plastic. In a repetition of the experiments the value of P_K increased from 250 to 350 kg/cm² (Fig. 1). The limit of shear stress decreased with an increase in temperature by the same law: $P_K = Ae^{-u/kT}$ (A is constant, U is the bond energy), by which the coefficient of viscosity decreases with increase in temperature.

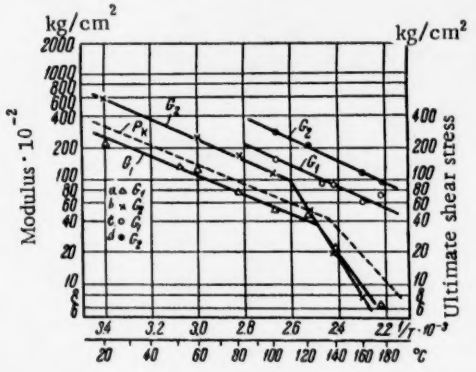

Fig. 2. Changes in the modulus of resiliency under shearing action G_1 and in the modulus of elasticity G_2 of grade K-18-2 material and ultimate stress under shear P_K in relation to the reciprocal absolute temperature: a, b) G_1 and G_2 under load; c, d) G_1 and G_2 on unloading.

6. The ultimate shear stress P_K, the moduli of resiliency and elasticity plotted against the reciprocal absolute temperature in semi-logarithmic coordinates are expressed by two intersecting lines (Fig. 2). The break point falls in the temperature region of thermostability (approximately 137°). The bond energy, determined by the tangent of the slope of the lines at the section below the temperature of 130°, lies within the limits of 3300 to 3830 cal/mole of the units. This indicates the predominance of hydrogen type intramolecular bonds. Above 130°, the slope

of the lines to the absicissa is greater (Fig. 2). The activation energy, determined by the slope of the lines, changes from 8900 to 17,650 cal/mole of units. Such a value for the activation energy is observed in the hardening processes of phenolformaldehyde resins in press-powders [2].

Consequently, under the effect of shearing deformations in technical materials prepared on the basis of phenol-cresol- and aniline-formaldehyde resins, a further chemical hardening process occurs only at temperatures above 130°. These experiments confirm the fact that the time of seasoning, established by the outer appearance of the phenol-aldehyde plastics, does not ensure the completion of the reaction. Furthermore, after the completion of the reaction, the shearing deformations (in repeated experiments) overcome the resistance only of the hydrogen bonds. This is indicated by the parallel course of the two upper lines (Fig. 2), for which the bond energy lies within the limits of 3300-3800 cal/mole of units.

7. The fact that at normal temperature, resilient deformation is greater than elastic, while the modulus of resiliency is less than that of elasticity, indicates a friable plastic structure which is sparsely "knitted" by hydrogen bonds. Under the effect of loading, the sparse lattice is broken and therefore on reloading and on increasing the deformation the more frequent interlocking of the branched polymer chains is overcome and this explains the absence of full reversibility under repeated loading as not only due to the great viscosity of the elastic flow.

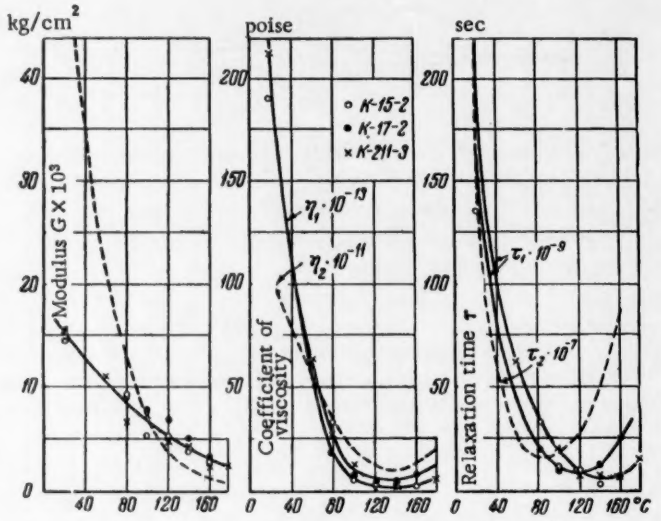

Fig. 3. Changes in the modulus of resiliency G_1 and elasticity G_2, coefficient of viscosity η_1 and relaxation time τ_1 of viscous flow and coefficient of viscosity η_2 and relaxation time τ_2 in the region of elastic flow in relation to temperature.

Some authors appraise this effect as the consolidation of the material on repeated loading [3]. The "knitting" of the polymer chains in the aggregare in the phenol-formaldehyde press-materials does not spread through the whole thickness of the material, and due to this it is possible that the development of elastic deformation to a high value in comparison with the resilient one is actually observed at temperatures higher than T_s and at stresses higher than the elastic limit (Fig. 1).

8. A decrease in moduli of resiliency G_1 and elasticity G_2 and viscosities of plastic η_1 and elastic η_2 flow (relaxation periods τ_1 and τ_2) with increase in temperature is observed only up to the temperature of thermostability. At temperatures higher than T_s, there is an increase in η_1 (and τ_1), while η_2 (and τ_2) increase much more than η_1 and τ_1 (Fig. 3). This is explained by the chemical reaction which occurs in thermosetting press-materials under the effect of temperatures higher than 130° and of shearing deformation.

The shearing deformations partially destroy the friable resin structure and thus eliminate steric hindrances to the entry into reaction of unreacted products. As a result of such a reaction the "knitting" of polymer links in the chains prevails and, to a lesser degree, the "knitting" of separate aggregates with each other takes place and this explains the greater increase of the relaxation period of elastic flow τ_2 as compared with the period of plastic flow τ_1, at temperatures higher than 130° (Fig. 3).

Due to these reasons, objects of thermosetting plastics are made stronger when a greater degree of the friable resin structure is destroyed in flow during the formation of the objects than when the objects are formed with almost complete absence of material flow.

LITERATURE CITED

[1] P. A. Rebinder, Trans. Inst. Phys. Chem. No. 1, (Acad. Sci. USSR Press, 1950).

[2] I. F. Kanavets, Proc. Acad. Sci. 95, 6 (1954).

[3] G. L. Slonimsky, V. A. Kargin, and L. I. Golubenkova, Proc. Acad. Sci. 93, 2 (1953).

Scientific Research and Design Institute of Plastics

Received November 16, 1956.

THE MECHANISM AND ISOTOPE EFFECT OF THE PRIMARY ACT OF THERMAL DECOMPOSITION OF CHLOROFORM

A. E. Shilov and R. D. Sabirova

(Presented by Academician N. N. Semenov, January 3, 1957)

In recent papers on thermal decomposition of organic halogen derivatives, one of two mechanisms have usually been assumed for the elementary act of molecular decomposition of these compounds: the radical mechanism with breaking of the C–Hal ($R-X \rightarrow R\bullet + X\bullet$) bond or the molecular mechanism of directly splitting off H–Hal through a four membered transition complex (for example,

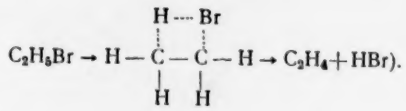

$C_2H_5Br \rightarrow H-C-C-H \rightarrow C_2H_4+HBr$).

In principle, a third mechanism of molecular decomposition could be visualized; the splitting out of H–Hal from one of the carbon atoms with the primary formation of the divalent C derivative:

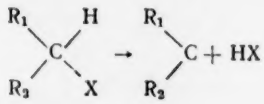

$\rightarrow C + HX$

We shall call this mechanism biradical.* The biradical decomposition mechanism has been assumed at different times for some compounds but has not been sufficiently substantiated in any of the cases.

While studying the thermal decomposition of methane chloro derivatives, we came to the conclusion that such a mechanism, the direct splitting out of the hydrogen halide, does occur in the case of chloroform and methylene chloride.

Data on chloroform and also deuterochloroform $CDCl_3$ decomposition are presented in this paper.

The reaction was investigated in a vacuum flow system, similar to the one used for the investigation of C_2H_5Cl decomposition [1]. The chloroform was passed at low pressures through the heated reaction vessel in excess toluene vapor or without a carrier gas. The reaction products together with the undecomposed chloroform entered a trap system where they were analyzed. As is known [2], HCl and C_2Cl_4 as well as a small amount of C_2Cl_6, C_2HCl_5, etc. are the products of thermal decomposition of chloroform. HCl and C_2Cl_6 were

---

* This name is to a great extent conditional as the particle formed may not perhaps be a biradical in the strict sense of this word (for example CO).

quantitatively determined in our experiments. Hydrogen chloride was determined by titration with alkali and a micro Volhard titration. In experiments with $CDCl_3$, for the determination of DCl in hydrogen chloride, the latter was treated with CH_3MgI to give methane which was analyzed on a mass-spectrometer for CH_3D content.* Special experiments with a previously prepared mixture of HCl and DCl showed that the isotopic composition of the methane coincided with the composition of the hydrogen chloride used with an accuracy of 1%. By this method it was possible to analyze for less than $1 \cdot 10^{-4}$ mole of DCl. C_2Cl_6 was frozen out in a U-tube, which was cooled to between −40° and −50°, and determined by weighing.

TABLE 1

Sample no.	P_{CHCl_3}, mm	$P_{C_2H_4CH_3}$, mm	τ_k, sec	k, sec^{-1}
1	35.9	—	0.324	0.294
2	29.3	—	0.354	0.279
3	29.0	—	0.354	0.266
4	23.1	—	—	0.300
5	19.0	—	0.456	0.249
6	17.3	—	0.426	0.281
7	10.6	—	0.78	0.182
8	9.6	—	1.01	0.203
9	7.66	10.1	0.288	0 266
10	6.40	—	1.24	0.143
11	2.03	11	0.294	0.250
12	1.84	13.8	0.416	0.272
13	1.18	15.2	0.366	0.282

Deuterochloroform was synthesized from chloral by treating it with a solution of K_2CO_3 in heavy water (b. p. 61°, n_D^{20} = 1.4452).

In experiments on the investigation of the isotope effect, normal chloroform was synthesized by the same method. Toluene was prepared by the hydrolysis of pure paratoluenesulfonic acid by distillation on a column (b. p. 110.5°, n_D^{20} = = 1.4968).

Chloroform decomposition was investigated in the range 485-660°. The results of experiments at 584° are given in Table 1. It can be seen that chloroform decomposition follows the monomolecular law.

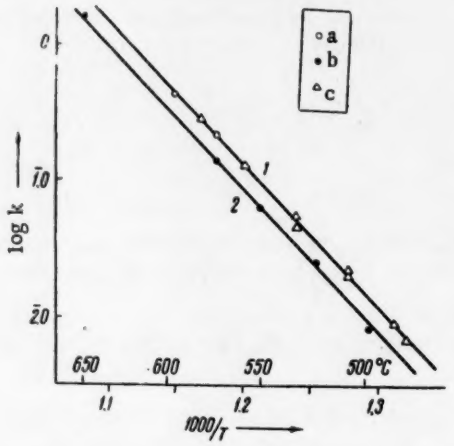

Fig. 1. The relation of the reaction rate constant k to temperature: a) $CHCl_3$ in a toluene stream; b) $CDCl_3$ in a toluene stream; c) $CHCl_3$ with no carrier gas.

* Mass-spectrometric analysis of the HCl and DCl mixture itself turned out to be extremely difficult.

In experiments without a carrier gas, a rate constant of the first order (the constants were calculated on HCl) was maintained at 16-36 mm pressure but fell at lower pressures. No fall in the rate constant was observed in a toluene stream at low pressures of $CHCl_3$; furthermore, the reaction rate in toluene and with no carrier gas was the same. This, on the one hand, shows that the fall in constants at low pressures is due to energetic, and not chemical, factors and, on the other, proves the absence of an inhibiting effect of toluene in the decomposition reaction. It is important to note that in experiments using a toluene stream, there was almost no dibenzyl in the reaction products (less than 2-3% of the HCl). The amount of hexachloroethane in the reaction products without a carrier gas was approximately 10% of the HCl.

Packing the reaction vessel with glass wool or quartz glass did not cause any noticeable change in the reaction rate. The relation of the rate constants to temperature in the coordinates $\log k$, $\frac{1}{T}$ (Fig. 1, Line 1) is expressed by the formula:

$$k = 2.63 \cdot 10^{11} e^{-\frac{47000}{RT}} \ \text{sec}^{-1}$$

These data are in sharp contradiction to the radical mechanism of $CHCl_3$ decomposition, put forward in the recent paper by Sameluk and Bernstein [2]:

$$CHCl_3 \rightarrow Cl\cdot + \cdot CHCl_2$$
$$Cl + CHCl_3 \rightarrow HCl + \cdot CCl_3$$
$$\cdot CHCl_2 + CHCl_3 \rightarrow CH_2Cl_2 + \cdot CCl_3.$$

Actually, the decomposition rate constant is too great (the activation energy too small) for homogeneous radical decomposition at the C–Cl bond, which should proceed with an activation energy, equal to D(C–Cl) in $CHCl_3$ ($\sim$ 70 kcal). The radical mechanism, in carrying out the reaction in toluene, would have lead to the formation of dibenzyl in an amount comparable with that of HCl (compare with the decomposition of methane bromo derivatives [3, 4]), since of the two particles formed ($Cl\cdot$ and $\cdot CHCl_2$) at least the chlorine atom would have reacted with toluene with the formation of a benzyl radical. Neither can we accept some chain system of $CHCl_3$ decomposition, as the absence of inhibition of the reaction by toluene indicates the absence of chains.

TABLE 2

Decomposition of $CHCl_3$ and $CDCl_3$ in Toluene (t = 57°).

Sample no.	p_{CHCl_3}, mm	p_{CDCl_3}, mm	p_{total}, mm	τ_k, sec	k_{CHCl_3}	k_{CDCl_3}
1	0.758	—	19.4	0.681	0.222	—
2	0.856	—	19.1	0.656	0.233	—
3		1.295	17.4	0.700		0.135
4	—	2.51	17.0	0.706	—	0.145
5	—	2.69	19.6	0.672	—	0.143
6	—	2.85	19.1	0.709	—	0.138
7	3.89	—	23.5	0.687	0.258	—
8	4.16	—	22.3	0.720	0.209	—
9	4.17	—	22 7	0.687	0.234	
			Average	. . .	0.231±0.008	0.140±0.003

It is interesting to compare the data on chloroform and deuterochloroform decomposition. It is obvious from Table 2 that the decomposition occurs with an obvious isotope effect. The ratio of the decomposition rates of light and heavy chloroform at 574° is equal to 1.65. The relation of the decomposition rate of $CDCl_3$ to temperature is shown in Fig. 1 (Line 2). The slope of the line, similar to that of $CHCl_3$, gives a value of of 47 ± 2 kcal for the activation energy. The accuracy of the experiment, however, was not sufficient for determining the separate contribution of the isotope effect to the value of the activation energy and the pre-exponential factor.

Table 3 gives data on some experiments on the determination of the isotopic composition of hydrogen chloride in $CDCl_3$ reaction products. As can be seen from the table, about 35% of DCl is contained in the hydrogen chloride, formed by $CDCl_3$ decomposition in excess toluene. It is remarkable that this relative amount of DCl does not depend on the ratio of $CDCl_3$ and toluene, on temperature or on time of contact. The isotope effect in chloroform decomposition indicates that the H atom participated in the rate determining step. The formation of considerable amounts of DCl in $CDCl_3$ decomposition in toluene and the fact that the reaction was first order indicates that this rate determining step is the biradical decomposition:

$$CHCl_3 \rightarrow HCl + CCl_2 \qquad (1)$$

Actually, in the case of the primary formation of atomic chlorine it should react with toluene (which is always present in excess) with the formation of light HCl alone. To prove this, experiments were carried out in which molecular chlorine was added to the stream of $CDCl_3$ in toluene (under conditions of slight $CDCl_3$ decomposition). The hydrogen chloride formed turned out to be light. Furthermore, if the isotopic composition of the hydrogen chloride formed had been the result of the competing reactions of the Cl atom with light toluene and heavy chloroform, then the amount of DCl in the products would have depended on the ratio of chloroform to toluene in the stream. Actually, this was not observed. The large amount of light HCl in the hydrogen chloride in the reaction products of $CDCl_3$ in toluene indicates, however, that part of the hydrogen chloride (approximately half, as shown by experiments without toluene) was formed not by Reaction (1) but by some reaction with toluene. Special experiments carried out at temperatures up to 700° and a contact time up to 0.4 seconds, showed that DCl does not exchange readily with toluene under these conditions. Furthermore, if there was exchange of the DCl first formed with toluene then the isotopic composition of the hydrogen chloride would have depended on the time of contact.

TABLE 3

Sample No.	t, °C	P_{CDCl_3}, mm	$P_{C_6H_5CH_3}$, mm	τ_k, sec	DCl, %
1	587	7.01	—	1.48	84
2	582	3.36	15.9	0.490	36
3	622	0.764	14.0	0.216	33.4
4	652	0.286	16.8	0.178	39
5	652	1.88	16.9	0.362	35
6	652	0.507	18.9	0.107	30
7	652	0.570	15.9	0.338	38

Taking into consideration the equality of the reaction rates in toluene and with no carrier gas, we presume that a secondary reaction with HCl formation takes place in both cases. The following reactions are possible.

Without a carrier gas: $CCl_2 + CHCl_3 \rightarrow HCl + C_2Cl_4$; in toluene: $CCl_2 + C_6H_5CH_3 \rightarrow HCl + C_6H_5CH =$ $= CHCl$.

The formation of C_2Cl_6 is, apparently, the result of dimerization of CCl_3 radicals, possibly formed by the reaction $2CCl_2 \rightarrow CCl + CCl_3$. Of course, such a mechanism of secondary reactions is purely hypothetical. However, regardless of this, the primary decomposition of chloroform by the biradical mechanism seems to us proved.

We consider it our duty to express our thanks to V. L. Talroz, V. I. Gorshkov, and V. E. Skurat for carrying out the mass-spectroscopic analyses.

LITERATURE CITED

[1] A. E. Shilov, Proc. Acad. Sci. 48, 601 (1954).

[2] G. P. Sameluk and R. B. Bernstein, J. Amer. Chem. Soc. 76, 3793 (1954).

[3] A. H. Sehon and M. Szwarc, Proc. Roy. Soc. A 209, 110 (1951).

[4] M. Szwarc and A. H. Sehon, J. Chem. Phys. 19, 66 (1951).

Institute of Chemical Physics of the
Academy of Sciences, USSR.

Received December 30, 1956.

CALCULATION OF THE HEAT AND ENTROPY OF ADSORPTION FROM A SINGLE ADSORPTION ISOTHERM

B. P. Bering and V. V. Serpinsky

(Presented by Academician M. M. Dubinin, January 10, 1957)

Determinations of the heat and entropy of sorption in relation to the amount of substance sorbed are usually carried out either by direct calorimetric measurements or by thermodynamic calculations based on an experimental determination of the temperature coefficient of sorption. The fundamental principles underlying each of these methods are well understood and do not raise any doubts. However, both these methods, particularly the first one, are very laborious and entail a high standard of experimentation. Below we are going to show under what conditions these important thermodynamic characteristics of sorption can be calculated from a single adsorption isotherm.

The extensive experimental work which has accumulated over several decades shows that in the great majority of cases the fundamental postulate of the potential theory of adsorption, put forward by Polanyi already 40 years ago, has been excellently supported by the facts. According to this postulate the so-called adsorption potential $\epsilon = -RT \ln h$ (where h is the relative pressure) is independent of the temperature when the fully occupied adsorption space $\varphi = aV$ (a = adsorption, V = molar volume of the adsorbate) remains constant, i.e.,

$$(\partial \varepsilon/\partial T)_{\varphi} = -R\,(\partial T \ln h/\partial T)_{aV} = 0. \tag{1}$$

It is easily seen that the shape of the curve $\varphi = f(\epsilon)$, the so-called characteristic curve, is determined uniquely by a single adsorption isotherm, and in accordance with Equation (1) the characteristic curve, in turn, determines uniquely the adsorption isotherm at some other temperature close to that of the first isotherm, i.e., it determines the temperature coefficient of adsorption. Thus, if Condition (1) is fulfilled, it should be possible to calculate the heat and entropy of sorption from a single adsorption isotherm.

In fact, if we choose the quantities aV, T and $\ln h$ as our variables, we can express the thermal equation of adsorption in the form $F(aV, T, \ln h) = 0$. Hence we obtain:

$$-\left(\frac{\partial aV}{\partial T}\right)_{\ln h} = \left(\frac{\partial aV}{\partial \ln h}\right)_T \left(\frac{\partial \ln h}{\partial T}\right)_{aV} = V\left(\frac{\partial a}{\partial \ln h}\right)_T \left(\frac{\partial \ln h}{\partial T}\right)_{aV}. \tag{2}$$

From Condition (1) it follows that

$$(\partial \ln h/\partial T)_{aV} = -\ln h/T. \tag{3}$$

In addition, we have the relation:

$$\left(\frac{\partial aV}{\partial T}\right)_{\ln h} = a\left(\frac{\partial V}{\partial T}\right)_{\ln h} + V\left(\frac{\partial a}{\partial T}\right)_{\ln h} = \alpha aV + V\left(\frac{\partial a}{\partial T}\right)_{\ln h}, \tag{4}$$

where α is the thermal coefficient of bulk expansion of the adsorbate.

Combining Equations (2), (3) and (4) we obtain

$$(\partial a/\partial T)_{\ln h} = (\partial a/\partial \ln h)_T \ln h/T - \alpha a. \tag{5}$$

If a different set of variables is chosen, the thermal equation of adsorption can also be expressed in the form Ψ (a, T, ln h) = 0, whence it follows that

$$(\partial a/\partial T)_{\ln h} = -(\partial a/\partial \ln h)_T (\partial \ln h/\partial T)_a. \tag{6}$$

Equating (5) and (6) and bearing in mind that in accordance with the Clapeyron-Clausius equation $(\partial \ln h/\partial T)_a = q/RT^2$, where q is the true heat of adsorption, we finally obtain

$$q = Q - \lambda = \alpha RT^2 (\partial \ln h/\partial \ln a)_T - RT \ln h. \tag{7}$$

In this equation Q represents the differential heat of adsorption and λ the heat of condensation of the adsorbate.*

If, as is usual, we now consider the standard state of the adsorbate as that of the liquid at the same temperature as the adsorbate and at the pressure of its own saturated vapor, and if we equate Expression (7) with the Gibbs-Helmholtz equation,

$$q = \varepsilon - T (\partial \varepsilon/\partial T)_a = RT (\partial \ln h/\partial T)_a - RT \ln h, \tag{8}$$

we at once obtain an expression for the differential entropy of adsorption:

$$\Delta S = (\partial \varepsilon/\partial T)_a = -\alpha RT (\partial \ln a/\partial \ln h)_T. \tag{9}$$

We have now collected considerable amount of experimental data which show that heats of adsorption calculated from a single adsorption isotherm by means of Equation (7) are in very good agreement with direct calorimetric measurements and with the results of reliable calculations based on adsorption isosteres. The scope of this communication makes it necessary for us to limit ourselves to a few examples illustrating this agreement.

In Fig. 1, Curve 1 represents the differential heat of adsorption Q of ammonia on active charcoal as a function of the amount adsorbed, calculated using Equation (7) and the adsorption isotherm at 0° taken from the data of Titov [1]. The points represent values of Q calculated from calorimetric measurements carried out by Titov. In the same figure, Curve 2 represents values of Q calculated in a similar manner using Equation (7) and the adsorption isotherm of n-hexane on active charcoal at 20° as determined by N. N. Avgul, A. V. Kiselev et al. [2]. The black points correspond to the calorimetric determinations of the same authors.

In Fig. 2 is represented a similar comparison of values calculated from Equation (7) (line) with those obtained directly by calorimetric determinations by Beebe, Kington, Polley and Smith [3] (points) in the case of the adsorption of n-butane on graphitized carbon black Spheron-6 at 0°. In view of the absence of tabulated data in the paper by these authors the initial portion of the curve could not be calculated with a reliable degree of accuracy and is, therefore, traced as a broken curve. Finally, Curve 3 in Fig. 1 represents a comparison of results calculated from Equation (7) (continuous curve) with results calculated from isosteric heats of adsorption

* It can be shown that, in general, if $\xi \equiv (1/aV)(\partial\, aV/\partial T)_{\ln h} \neq 0$, which is equivalent to the nonfulfillment of Condition (1) postulated by Polanyi, Equation (7) can be replaced by

$$q = (\alpha - \xi) RT^2 (\partial \ln h/\partial \ln a)_T - RT \ln h. \tag{7a}$$

It must be noted that Equations (7a) and (7) may be obtained directly from the Gibbs-Helmholtz equation.

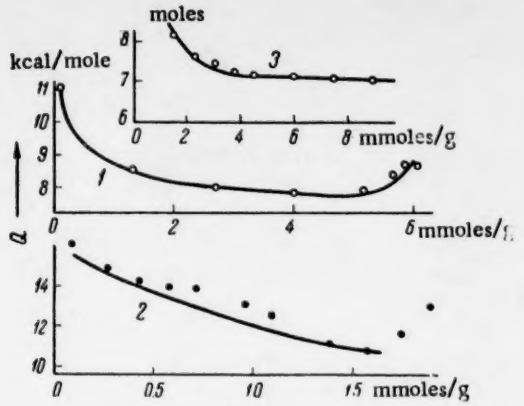

Fig. 1

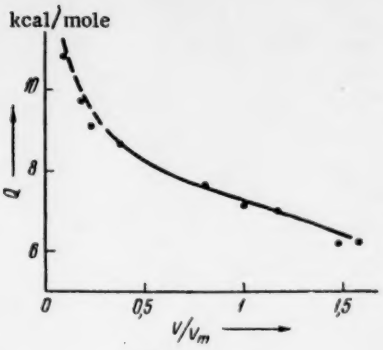

Fig. 2

by means of the Clapeyron-Clausius equation. These data refer to the adsorption of furane on silica gel at 25° [4]. The circles represent values of Q given in communication [4].

From the sequence of considerations leading to Equation (7) it is evident that this equation holds only if Condition (1) is fulfilled. Nevertheless, Equation (7) may be expected in many cases to furnish good agreement with experiment even when Condition (1) is not fulfilled. In fact, we have

$$Q = -T\Delta S + \varepsilon + \lambda, \tag{10}$$

while from Equation (7a) it follows that any deviation from Condition (1) affects only the term $T\Delta S$. Therefore, in cases where the contribution of this term in Equation (10) is small even considerable values of ξ will introduce only a small error in the value of Q. The magnitude of the term $T\Delta S$ can be judged directly from the shape of the adsorption isotherm since it is directly proportional to the derivative $(\partial \ln h/\partial \ln a)_T$. It may be expected (and this is borne out by calculation) that, for example, in the region of capillary condensation or in the region where adsorption isotherms of water vapor on carbon black adsorbents exhibit a steep rise, the differential heats of adsorption calculated from Equation (7) will always be close to values determined experimentally.

It must, however, be stressed that on theoretical grounds it is entirely inadmissible to neglect the term $T\Delta S$. The equating of $\underline{q}$ to ϵ, as has been done by Halasz, Schay and Szonyi [4] is, obviously, equivalent to confusing the change in internal energy with the change in free energy. In many cases in calculations of Q the term $T\Delta S$ has a decisive significance.

In conclusion it may be mentioned that if the analytical expression of the equation of the adsorption isotherm is known, it is possible, by combining the latter with Equation (7), to obtain the corresponding analytical form of the dependence of the differential heat of adsorption on $\underline{a}$ or $\underline{h}$. There are reasons to believe that the method of analysis of adsorption problems ensuing from this may prove to be very promising.

The authors wish to express their sincere gratitude to M.M. Dubinin for his interesting and valuable criticisms.

Institute of Physical Chemistry
Academy of Sciences of the USSR

Received January 7, 1957

LITERATURE CITED

[1] A. Titoff, Zs. phys. Chem. 74, 641 (1910).

[2] N. N. Avgul, G. I. Berezin et al., J. Phys. Chem. 31, No. 3 (1957).

[3] R. A. Beebe, G. L. Kington, M. H. Polley and W. R. Smith, J. Am. Chem. Soc. 72, 40 (1950).

[4] I. Halasz, G. Schay and S. Szönyi, Acta chim. Acad. Sci. Hung. 8, 43 (1955).

ADSORPTION OF ALIPHATIC ALCOHOLS FROM SOLUTIONS ON SILICA GEL AND "WHITE SOOT"

A. K. Bonetzkaya and K. G. Krasilnikov

(Presented by Academician M. M. Dubinin, January 8, 1957)

The adsorption of alcohols and acids of a homologous series from nonpolar solvents on porous hydrophilic adsorbents – silica gels and alumino-silicates – has been studied in papers [1, 2, 11]. These investigations have established that the limiting adsorbed amounts of the substances decreases with increasing length of the hydrocarbon radical, while the limiting adsorbed volume in the case of the comparatively large-pore adsorbents studied remains constant [3, 11] (the law of the constancy of the limiting adsorbed volume [4]). The decrease in the adsorption of members of increasing molecular weight in a homologous series has been related to bulk interactions in solutions (change in solubility of the members of a homologous series [1]), or has been attributed to the influence of the porous structure of the adsorbent in the sense that instead of the formation of regularly oriented layers there takes place complete filling up of the pores with molecules of the adsorbate [3, 5].

As has been indicated in papers [2-4], in the case of nonporous hydrophilic adsorbents it may be expected that the limiting adsorbed amount of alcohols and acids of a homologous series remains constant. This is in accordance with the assumption that the adsorbed molecules are oriented in such a way that they interact with the surface through their polar groups while the hydrocarbon radical chains are turned towards the solution, that is, the molecules form a layer which is structurally similar to condensed films of aliphatic compounds on a water surface. In this case the number of molecules per unit area of the surface will not depend on the length of the hydrocarbon radical. In the case of nonporous hydrophobic adsorbents measurements of adsorption of infinitely soluble alcohols and acids from their aqueous solutions [6, 7] have shown that the limiting adsorbed amounts increase with increasing number of carbon atoms in the molecule. The investigation of adsorption from solutions on porous and nonporous adsorbents with surfaces of identical nature is of considerable interest because it permits of an assessment of the influence of the porous structure of the adsorbents and is also useful for the purpose of deciding the orientation of the adsorbed molecules in the surface layer. In the case of hydrophobic adsorbents a comparison of the adsorption isotherms of some organic substances from aqueous solutions on carbon and nonporous soot has been described in [8]. As far as is known to us corresponding data for hydrophilic adsorbents are not available.

In the present work we have carried out measurements of the adsorption of normal aliphatic alcohols from solutions in CCl_4 on two specimens of silica of different structure. The porous sample was the silica gel KSK-2 [9] having a prevalent pore diameter of 60 A and a specific surface area of 400 m^2/g. The specimen used as the nonporous adsorbent was the so-called "white soot" obtained in the form of a very loose powder (loose specific gravity 0.025 g/cm^3) by burning the vapor of the ethyl ester of orthosilicic acid. Its specific surface area was determined by the B.E.T. method from the adsorption isotherms of nitrogen as well as by statistical evaluation of electron microphotographs and was found to be equal to 240 m^2/g and 220 m^2/g, respectively.* The closeness of these values indicates that white soot is practically a nonporous adsorbent. The same conclusion may be derived from the data given in paper [10] which describes a study of the adsorption of Freon vapor (CCl_2F_2) on a similar silica preparation. The content of structural water in the prepared samples was 4.2 $\mu M/m^2$ in the

* The first type of measurements have been carried out by E. A. Sysoev, the second by E. A. Leontyev to both of whom the authors express their thanks.

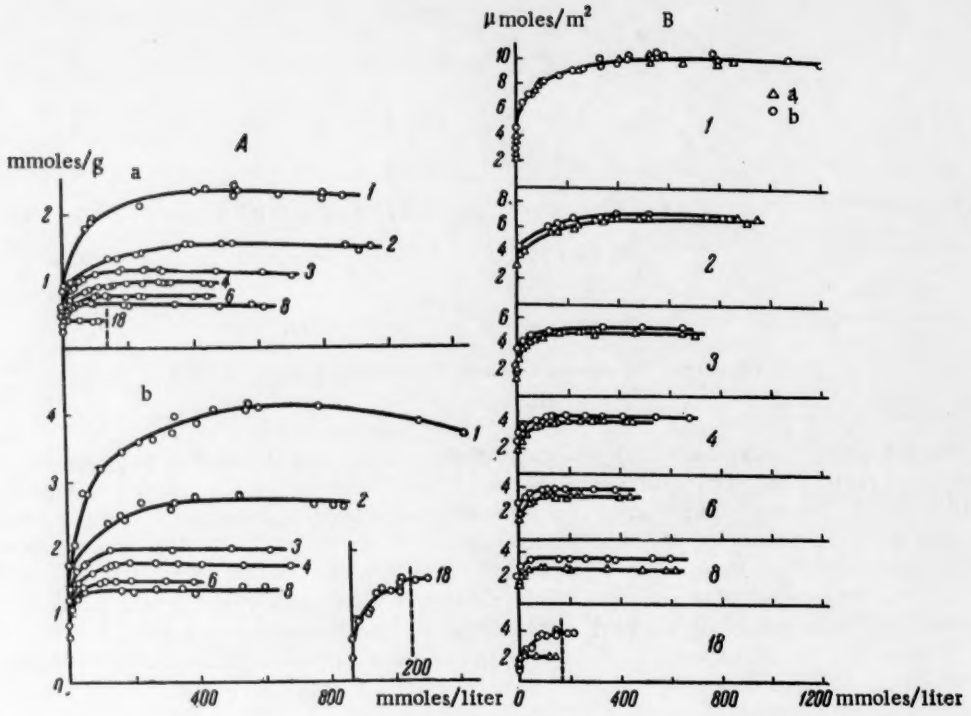

Fig. 1. Adsorption isotherms of n-alcohols from CCl_4 on "white soot" (a) and on silica gel (b) referred to 1 g of the adsorbent (A) and to 1 m^2 of its surface area (B); the numbers on the curves denote the number of carbon atoms in the molecule of a given alcohol.

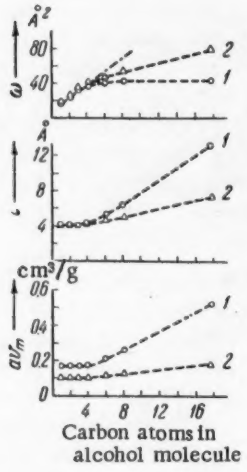

Fig. 2. Areas occupied by one molecule in the surface layer, ω; thickness of the adsorbed layer, τ; and the limiting adsorbed volumes, av_m, of n-alcohols on silica gel (1) and "white soot" (2).

case of the silica powder, and 4.1 $\mu M/m^2$ in the case of the silica gel. Thus, the two adsorbents differed greatly in their structure, but both possessed practically the same degree of surface hydration. On account of the large volume taken up by the silica powder and the resultant lowering of the relative amount of adsorbate extracted from the solution, it was difficult to carry out adsorption measurements at high concentrations. We therefore limited ourselves to the determination of those portions of the isotherms corresponding to constant adsorption which in the case of all the alcohols investigated was attained at concentrations of about 5% on the pure solvent [11].

As will be seen from Fig. 1A, the results obtained for silica powder and for silica gel do not differ from each other. In both cases the limiting adsorbed amount decreases with increasing length of the hydrocarbon radical and is displaced towards the region of lower equilibrium concentrations [12]. Similar results were obtained on the same silica gel with n-heptane as solvent, with the exception of methyl alcohol which is only partially soluble in heptane and in which case the adsorption isotherm was S-shaped [13].

TABLE 1

Limiting Adsorbed Amounts and Limiting Adsorbed Volumes of a Number of n-Alcohols on "White Soot" and on Silica Gel

Alcohol	White soot			Silica gel		
	x_∞, mmoles/g	a_∞, mmoles/g	$a_v v_m$, cm³/g	x_∞, mmoles/g	a_∞, mmoles/g	$a_v v_m$, cm³/g
Methyl	2.40	2.49	0.10	4.10	4.25	0.17
Ethyl	1.60	1.69	0.10	2.75	2.90	0.17
Propyl	1.18	1.26	0.10	2.10	2.23	0.17
Butyl	1.00	1.05	0.10	1.80	1.90	0.17
Hexyl	0.80	0.85	0.11	1.54	1.65	0.21
Octyl	0.67	0.73	0.12	1.45	1.58	0.25
Octadecyl	0.51	0.51	0.17	1.56	1.56	0.52

If it is assumed that the observed decrease of the limiting adsorbed amount in the order of a homologous series may be due to the competition of the solvent for the adsorbent surface, then adsorption of the solvent will, evidently, increase as that of the alcohol decreases, i.e., as we pass from lower to higher alcohols. We have made attempts to determine the extent of adsorption of the solvent in these systems. For this purpose the adsorption isotherm of octyl alcohol on silica gel was extended into the region of high concentrations. On extrapolating the curved portion of this isotherm to the point of its intersection with the axis of abscissae we obtained values close to the concentration of the pure alcohol. Since extrapolation effected in this manner cannot yield sufficiently accurate results, we have carried out supplementary determinations of the adsorption of CCl_4 from its solutions in octyl alcohol over the concentration range in question. However, within the limits of experimental error no observable adsorption could be detected. From the isotherms obtained we have calculated the full amounts, a, of the adsorbed substances in the surface layer (Table 1).

Thus, the decrease in the adsorption of alcohols with increasing length of their hydrocarbon radicals is not affected by the porosity of the adsorbent nor can it, apparently, be attributed to the competition of the solvent. This phenomenon can be explained if it is assumed that the alcohol molecules are oriented in the dense adsorbed layer in such a way that most of the hydrocarbon radical chains actually "lie" on the surface. Similar conclusions with regard to the orientation of molecules in the surface layer have been drawn in paper [14] on the basis of results of adsorption studies of benzene on silica gel from solutions in heptane as well as from the adsorption of fatty acids on carbon from aqueous solutions [15]. Under these circumstances the area occupied by a molecule in the surface layer will, of course, depend on the length of the hydrocarbon radical. However, as will be seen from Fig. 2, which illustrates this relationship, the two quantities are not directly proportional to each other. Whereas in the case of the first members of the series the area per one CH_2-group is equal to about 8 A^2 it decreases markedly with decreasing length of the hydrocarbon radical. At the same time the thickness of the adsorbed layer increases from 4.2 A* for the lower alcohols to 7.1 A on silica powder and to 13.0 A on silica gel in the case of octadecyl alcohol. This would lead us to conclude that the manner of orientation of the adsorbed alcohol molecules on partially dehydrated surface of silica [16] varies as we pass from the lower to the higher alcohols. The molecules of the latter apparently accommodate themselves at an angle to the surface. It must, however, be borne in mind that in the case of silica gel the possibility of changes in the orientation of the adsorbed molecules inside fine pores may be limited by their geometrical dimensions. For this reason the areas per molecule and the thickness of the adsorbed layer in the case of the higher alcohols may be treated as average values relating to a given specimen of silica gel.

In order to elucidate the effect of porosity on the magnitude of limiting adsorption the data obtained were referred to 1 m^2 of the surface. The comparison of isotherms of this type on silica powder and silica gel for each of the alcohols investigated is illustrated in Fig. 1B. As will be seen, the adsorption isotherms of methyl alcohol

* According to the data given in [15] the cross section of the hydrocarbon chain may be pictured in the form of a rectangle having sides of 4.12 and 4.49 A.

are identical in the case of both adsorbents. Furthermore, with increasing number of carbon atoms in the alcohol molecule adsorption on the porous specimen – the silica gel – reaches relatively higher values than the corresponding values on the nonporous silica powder. The increase in limiting adsorbed amounts in the transition from large-pore to fine-pore silica gel has been observed by the authors in paper [14] and has been attributed to increased intensity of the adsorption potential in fine pores. A similar explanation may be put forward in this case; however, in contrast with the findings of the authors of [14] in which case this effect was observed with decreasing pore size of the adsorbent, in our experiments it manifested itself with increasing dimensions of the adsorbed molecules, the pore dimensions remaining constant.

As will be seen from Table 1 and Fig. 2, the limiting adsorbed volume of all the alcohols investigated on the nonporous silica powder varies little. Even if we consider only the first members of the series, including butyl alcohol it will be evident that the constancy of the adsorbed volume is in this case not due to the influence of the porous structure of the adsorbent, but is the result of the orientation of molecules in the surface layer mentioned above. As we pass to higher alcohols the limiting adsorbed volume on the silica gel investigated increases markedly. On the other hand it is well known that in the case of adsorbents of fine porosity the limiting adsorbed volume may decrease as a result of the ultra-porosity effect [11]. In cases where pore dimensions of the adsorbent and the nature of their distribution are such that the opposing effects due to each of these factors are mutually compensating, the limiting adsorbed volume of members of a homologous series will remain constant.

The authors wish to express their sincere gratitude to Academician M. M. Dubinin and to B. V. Ilyin for their interest in this work and discussion of the results.

M. V. Lomonosov State University
Moscow

Received December 29, 1956

LITERATURE CITED

[1] F. E. Bartell and G. H. Scheffler, J. Am. Chem. Soc. 53, 2507 (1931).

[2] A. V. Kiselev, I. A. Vorms , et al., J. Phys. Chem. 19, 83 (1946).

[3] A. V. Kiselev, J. Phys. Chem. 23, 452 (1949).

[4] K. D. Shcherbakova and A. V. Kiselev, Collected Papers on Physical Chemistry, Acad. Sci. USSR Press, 1947, p. 225.

[5] R. D. Hansen and R. S. Hansen, J. Coll. Sci. 9, 1 (1954).

[6] R. S. Hansen and R. P. Craig, J. Phys. Chem. 58, 211 (1954).

[7] A. V. Kiselev and I. V. Shikalova, J. Phys. Chem. 30, 94 (1956).

[8] A. V. Kiselev, Yu. S. Nikitin and Yu. A. Eltekov, J. Phys. Chem. 30, 334 (1956).

[9] M. M. Egorov, T. S. Egorova, V. F. Kiselev and K. G. Krasilnikov, Proc. Acad. Sci. USSR, 114, No. 3 (1957). *

[10] P. C. Carman and F. A. Raal, Proc. Roy. Soc. A 209, 59 (1951).

[11] A. V. Kiselev, Investigations in Chromatography, Acad. Sci. USSR Press, 1952, p. 71.

[12] V. K. Semenchenko, Colloid J., 9, 125 (1947).

[13] O. M. Dzhigit, A. V. Kiselev and K. G. Krasilnikov, Proc. Acad. Sci. USSR, 58, 413 (1947).

[14] A. V. Kiselev and Yu. A. Eltekov, Proc. Acad. Sci. USSR, 100, 107 (1955).

[15] A. Blackburn and J. J. Kipling, J. Chem. Soc. 1955, 1493.

[16] G. I. Aleksandrova, V. F. Kiselev, et al., Proc. Acad. Sci. USSR, 108, 283 (1956).

* [See C. B. translation].

THE EQUATION OF NONSTEADY DIFFUSION TOWARDS A STATIONARY ELECTRODE

A. V. Gorodysky and Academician (Ukr. Acad. Sci.) Yu. K. Delimarsky

It is currently accepted [1-3] that diffusion of the reacting substance towards a stationary electrode is determined by the following two conditions formulated by Cottrell [4] and McGillavry and Rideal [5]: (1) the concentration c_0 of the reacting substance is the same throughout the mass of the electrolyte up to the moment when the current is switched on, and (2) at any time t after the current has been started the ion concentration of the electrode surface is equal to zero. In other words, in the case of linear diffusion we have

$$c(x, 0) = c_0; \tag{1}$$

$$c(t, 0) = 0; \tag{2}$$

while in the case of spherical diffusion the conditions

$$c(r, 0) = c_0 \tag{3}$$

$$c(r_0, t) = 0 \tag{4}$$

hold (x and r are the coordinates, and r_0 is the radius of the spherical electrode).

In accordance with these conditions the solution of the general equation of diffusion

$$\frac{\partial c}{\partial t} = a\Delta c \tag{5}$$

gives in the case of linear diffusion

$$\left(\frac{\partial c}{\partial x}\right)_{x=0} = \frac{c_0}{\sqrt{\pi a t}}; \tag{6}$$

and in the case of spherical diffusion

$$\left(\frac{\partial c}{\partial r}\right)_{r=r_0} = \frac{c_0}{\sqrt{\pi a t}} + \frac{c_0}{r_0}, \tag{7}$$

where a is the coefficient of diffusion.

Conditions (1), (2) and (3), (4) do not account for the convection of the electrolyte and determine the diffusion process only when all mixing has ceased. For this reason experimental data are expressed exactly by Equations (6) and (7) only in the case of immobilized (gelled) solutions [2] and only for short time intervals after the start of the current when convection effects are small [2, 3, 6]. However, under the usual conditions

of electrolysis the electrode current decreases with time from the moment it is started, until it reaches a certain constant value which does not change further [2, 3, 6, 7], an effect which is contrary to that predicted by Equations (6) and (7).

From these facts it follows that the process of diffusion of the reacting substance towards the electrode reaches a certain steady value after a time when the concentration gradient of the diffusing substance on the electrode surface remains constant. Under these conditions, i.e., when the steady state of diffusion has been reached, the thickness of the diffusion layer attains a constant value, a practically constant concentration c_0 being maintained at its external boundary. This conclusion is in agreement with the theory of convection diffusion due to Levich [8, 9] according to which under conditions of the steady state the significant variations in concentration of the diffusing substance within a given diffusion layer are linear in nature. Hence follows an additional boundary condition of diffusion of the reacting substance towards a fixed electrode: at a certain definite distance l, or $\rho - r_0$, from the electrode the concentration of the reacting substance is maintained at a constant level c_0. In other words, in the case of linear diffusion we have

$$c(l, t) = c_0; \tag{8}$$

and in the case of spherical diffusion

$$c(\rho, t) = c_0. \tag{9}$$

From Conditions (8) and (9) it does not follow, however, that under conditions of nonsteady diffusion the thickness of the diffusion layer remains constant. What merely happens is that at a certain distance from the electrode the concentration of the diffusing substance does not fall below its initial value, which is, evidently, due to the natural convection of the diffusing substance.

Taking into account Conditions (1), (2) and (8) and (3), (4) and (9), solution of Equation (5) with the aid of the Laplace integral gives, in the case of linear diffusion,

$$\left(\frac{\partial c}{\partial x}\right)_{x=0} = \frac{c_0}{l}\left[1 + 2\sum_{k=1}^{\infty}\exp\left(-\pi^2 k^2 \frac{at}{l^2}\right)\right], \tag{10}$$

and in the case of spherical diffusion

$$\left(\frac{\partial c}{\partial r}\right)_{r=r_0} = \frac{c_0}{r_0} + \frac{c_0}{\rho - r_0}\left[1 + 2\sum_{k=1}^{\infty}\exp\left(-\pi^2 k^2 \frac{at}{(\rho - r_0)^2}\right)\right]. \tag{11}$$

The relationships deduced above have been checked experimentally by recording current-time curves during the deposition of mercury on a fixed spherical mercury cathode and of silver on a fixed plane silver cathode, as well as by means of data obtained by other authors [2, 3, 7]. In these experiments the electrolyte was not mixed artificially, because we were interested, in the first place, in the case of natural convection and diffusion of the reactant. In analyzing the experimental data we made use of the following approximate equations of the diffusion current deduced from Equations (10) and (11) after neglecting all the terms of the series $\sum \exp\left[-\pi^2 k^2 \frac{at}{l^2}\right]$, with the exception of the first one:

$$j = j_\infty + nFa\frac{C_0}{l}2\exp\left(-\frac{\pi^2 at}{l^2}\right) \tag{12}$$

for linear diffusion, and

$$i = i_\infty + nFa\frac{c_0}{\rho - r_0}2\exp\left(-\frac{\pi^2 at}{(\rho - r_0)^2}\right) \tag{13}$$

for spherical diffusion. In these equations i_∞ denotes the current density at time t = ∞, i.e., the density of the stabilized current, and i denotes the density of the diffusion current. In the first case we have

$$i_\infty \text{ (linear)} = nFa\frac{c_0}{l}\ . \tag{14}$$

and in the second case

$$i_\infty \text{(spherical)} = nFa\left(\frac{c_0}{r_0} + \frac{c_0}{\rho - r_0}\right). \tag{15}$$

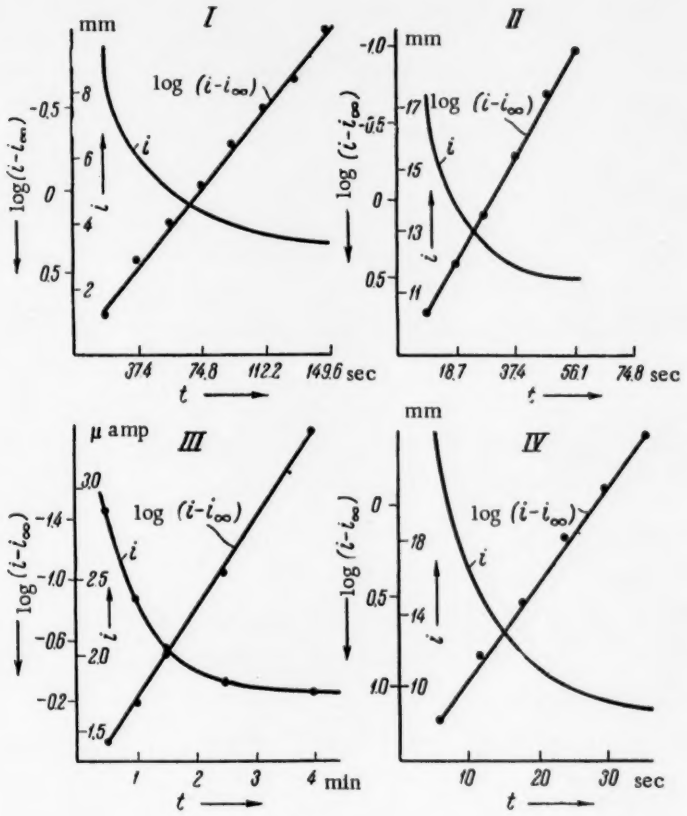

Fig. 1. Current-time curves: I) deposition of mercury on a mercury cathode, U = 12.5 millivolts; II) deposition of silver on a silver cathode, U = 175 millivolts; III) oxidation of $Fe(CN)_6^{4-}$ ions on a platinum anode [2], electrode F; IV) deposition of zinc on a platinum cathode [2], U = 1.20 volt.

Equations (12) and (13) reduce to the form

$$t = A - B\ln(i - i_\infty), \tag{16}$$

where

$$A = \frac{l^2}{\pi^2 a} \ln\left(2nF \frac{c_0}{l}\right), \quad B = \frac{l^2}{\pi^2 a}; \tag{17}$$

for linear diffusion, and

$$A = \frac{(\rho - r_0)^2}{\pi^2} \ln\left(2nF \frac{c_0}{(\rho - r_0)}\right), \quad B = \frac{(\rho - r_0)}{\pi^2 a}. \tag{18}$$

for spherical diffusion.

The current-time curves were recorded automatically on the photo-drum of the polarograph at constant electrode potentials. On closing the circuit the reflected light spot of the mirror galvanometer was deflected sharply from its zero position and then moved slowly in the opposite direction describing the current-time curve. Equations (12), (13) and (16) approach Equations (10) and (11) closer the greater the value of $\underline{t}$ is. For t = 0 Equations (10) and (11) have, in general, no physical meaning. In practice, however, good agreement between Equation (16) and Equations (10) and (11) is obtained for values of $\underline{t}$ of the order of 1 second, i.e., the duration of the initial deflection of the galvanometer.

The curves i = f(t) obtained by us as well as those obtained by other authors have been plotted in the coordinates $\underline{t}$ and log $(i - i_\infty)$; some of these curves are shown in Fig. 1. The values of i_∞ were determined from the plots. In all cases investigated we observed a linear dependence of $\underline{t}$ on log $(i - i_\infty)$, which confirms the correctness of Equation (16) and the assumptions made. Also, the quantities A and B were in all cases independent of the potential applied to the electrodes.

In conclusion we wish to express our thanks to Academician A. N. Frumkin for his valuable advice during the discussion of this work.

Institute of General and Inorganic Chemistry
Academy of Sciences of the USSR

Received September 17, 1956

LITERATURE CITED

[1] I. M. Kolthoff and J. J. Lingein, Polarography, Moscow-Leningrad, 1948, p. 31.

[2] H. A. Laitinen and I. M. Kolthoff, J. Am. Chem. Soc. 61, 3344 (1939).

[3] E. M. Skobets and N. S. Kavetsky, J. Phys. Chem. 24, 1486 (1950).

[4] F. G. Cottrell, Zs. phys. Chem. 42, 385 (1903).

[5] D. McGillavry and E. K. Rideal, Rec. Trav. Chem. Pays Bas, 56, 1013 (1937).

[6] Yu. K. Delimarsky, B. F. Markov and L. S. Berenblyum, J. Phys. Chem. 27, 1848 (1953).

[7] E. M. Skobets, P. P. Turov and V. D. Ryabokon, Factory Labs. 14, 772 (1948).

[8] V. G. Levich, J. Phys. Chem. 22, 575 (1948).

[9] A. N. Frumkin, V. S. Bogatsky, Z. A. Iofa and B. N. Kabanov, The Kinetics of Electrode Processes, Moscow, 1952, p. 79.

ANODIC PASSIVATION OF CHROMIUM IN ACID SOLUTIONS

V. M. Knyazheva and Ya. M. Kolotyrkin

(Presented by Academician A. N. Frumkin, February 6, 1957)

In the paper [1] we have discussed some data concerning the electrochemical behavior of chromium and nickel in solutions of K_2SO_4, obtained by the potentiostatic method of polarization measurements. It has been shown that the curve obtained by this method which expresses the relation between the constant rate of dissolution and the potential, may be used to determine the polarization limits of the region of passivation as well as the extent of corrosion losses within this region and does, therefore, constitute an important characteristic of the metal with regard to its corrosion behavior.

In the present investigation we have studied by means of the potentiostatic method the electrochemical behavior of pure chromium metal on its passivation as the anode in solutions of sulfuric acid at different concentrations (1.0; 0.10; 0.01 N). The constant rate of dissolution of the metal was determined not only from the final value of the anode current necessary to polarize the electrode in order to maintain a given value of the potential, but, also, by analyzing the solution quantitatively for chromium ions. Within the range of potentials more negative than the potential of the reversible hydrogen electrode, as referred to identical solutions in which dissolution of the chromium was effected spontaneously, the analytical method of the determination of the rate of dissolution was unique. By means of the colorimetric method using diphenyl carbazide it was possible to determine Cr^{+3} and Cr^{+6} ions in solutions at concentrations up to $2 \cdot 10^{-8}$ g/cm^3. The content of Cr^{+2} ions was determined iodometrically; the sensitivity of this method was two orders lower than the sensitivity of the diphenyl carbazide method. All determinations were carried out in an atmosphere of purified nitrogen. The methods of preparation and preliminary purification of the electrodes and solutions were those described in communication [1]. Each experiment was conducted at a constant temperature maintained with an accuracy of $\pm$ 0.1°C. The electrodes used were first activated by cathodic polarization. The cathode current was then switched off and the rate of dissolution and the value of the steady potential of activated chromium in the solution under investigation was determined. Within the range of anodic currents the current density was allowed to reach a constant value at a given constant potential; the electrode was then polarized for a determined time in a fresh portion of the solution and the latter was subsequently analyzed for dissolved products.

The dependence of the constant rate of dissolution on the potential.* In the case of the 1.0 N solution of H_2SO_4 this dependence is illustrated by the Curve ABCDE (Fig. 1). This curve resembles in its general shape the corresponding curves obtained previously for nickel in a solution of K_2SO_4 [1] and for stainless steel No. 18-8 in a solution of H_2SO_4 [2]. At potentials more negative than -0.350 volt an increase in the potentials was accompanied by an increase in the rate of dissolution according to the general Tafel straight line having a slope of 0.07.

Within the range of potentials from -0.350 to 0.00 volt (portion BC) the constant rate of dissolution decreases with the potential, although this relationship again follows the Tafel straight line but with a slope of opposite sign. When the solutions from experiments within this range of polarization potentials were analyzed for dissolved products both Cr^{+2} and Cr^{+3} ions were found in proportions approximately equal to equilibrium concentrations.

* All potentials are referred to that of the normal hydrogen electrode.

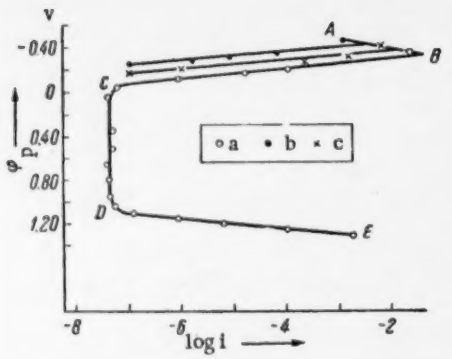

Fig. 1. The dependence of the logarithm of the constant rate of dissolution on the potential in solutions of H_2SO_4 at different concentrations: a) 1.0 N H_2SO_4, B) 0.1 N H_2SO_4, c) 0.01 N H_2SO_4.

TABLE 1

Concentration of Cr ions, in g-equivs/liter $\cdot 10^4$		Potential, referred to normal hydrogen electrode		
$[Cr_2O_7^{2-}]$	$[Cr^{3+}]$	Exp.	Calc.	$\Delta\varphi$
7.54	1.01	1.252	1.255	+0.003
8.64	0.986	1.252	1.256	+0.004
9.50	1.08	1.252	1.255	+0.003

Over a considerable range of potentials between 0.0 and +1.10 volt (portion CD) the steady rate of dissolution was found to be constant and equivalent to a current density of $5 \cdot 10^{-8}$ amp/cm^2. A similar absence of variation of the rate of dissolution with potential was observed by B. V. Ershler [3] in the case of a platinum electrode in HCl solutions and by Bonhoeffer and co-workers [4] in the case of an iron electrode in H_2SO_4 solutions.

As has been observed previously [1], the rapid rise of the potential to higher positive values within this region is again accompanied by an increase in the rate of dissolution analogous to that observed on the activated surface of the metal, and only after prolonged polarization of the electrode at a different potential does the rate of dissolution attain the minimum steady value corresponding to that given by the curve in question.

As results of analyses have shown, within the given region of polarization potentials the chromium passes into solution principally in the form of the trivalent ions.

At potentials above +1.10 volt (portion DE) superpassivation of the chromium takes place. As will be seen from Fig. 1, a further increase in the potential is accompanied by an increase in the rate of dissolution in accordance with the Tafel straight line having a slope of 0.04 volt. In Table 1 are given results of the analysis of the solution for chromium ions dissolved from the electrode at a potential of 1.252 volt, that is, within the range of polarization potentials in question. In the same table are shown the calculated values of the potential corresponding to the oxidation-reduction equilibrium between the tri- and hexavalent ions in the concentration ratio found. As will be seen from Table 1, the calculated values of the potential are practically identical with those determined experimentally. This result is evidence either that within the range of superpassivation chromium dissolves with the simultaneous formation of Cr^{3+} and $Cr_2O_7^{2-}$ ions in ratios corresponding to equilibrium conditions, or, as is more probable, that equilibrium between these ions is established rapidly.

The influence of the pH of the solution. Data characterizing the rates of spontaneous dissolution and the steady potentials of activated chromium in solutions of H_2SO_4 at different concentrations are plotted in Fig. 1 as individual points. These points lie practically on the same linear segment AB which may be regarded as the continuation of the polarization curve obtained in 1.0 N H_2SO_4 on the activated surface of chromium. This shows that the dependence of the rate of dissolution of activated chromium on the potential in solutions of sulfuric acid at different concentrations is expressed by one and the same kinetic curve. In this respect the behavior of chromium is similar to that of nickel which has been investigated by Ya. M. Kolotyrkin and A. N. Frumkin [5].

A change in the pH of the solution brings about a marked change in the electrochemical behavior of chromium within the region of passivation. As will be seen from Fig. 1, a decrease in the concentration of the acid is accompanied by a displacement of the upper limit of the range of passivation potentials in the direction of negative values. On the basis of the data obtained the relationship between the potential, corresponding to incipient passivation, and the concentration of the acid satisfies the equation:

$$\varphi_n = -0.350 + 0.050 \log C$$

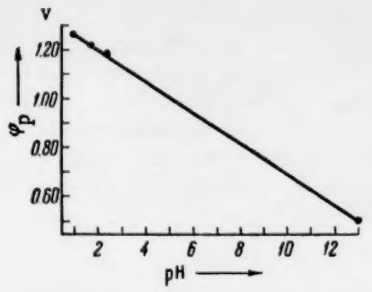

Fig. 2. Dependence of the polarization potential on the pH of the solution within the region of superpassivation at constant anodic polarization current ($i = 1 \times 10^{-4}$ amp/cm^2).

A decrease in the concentration of the acid also displaces the portion of the polarization curve, lying within the region of superpassivation, in the direction of negative potentials. As will be seen from Fig. 2, the dependence of the potential corresponding to the same rate of dissolution of chromium in this region on the concentration of H_2SO_4 is expressed by a straight line having the slope $\left(\frac{\partial \varphi}{\partial pH}\right)_i$, approximately equal to 0.063. The same relationship is found to be valid for data obtained in 0.1 N NaOH.

If we take into consideration the dependence of the rate of dissolution of chromium, within the region of superpassivation, on the potential and the pH of the solution, it can be shown that the limiting stage of the reaction as a result of which dissolution of the chromium takes place within the range of polarization potentials in question, involves two OH^- ions and three electrons. This conclusion is in agreement with results obtained recently by Heumann and Rösener [6].

The influence of the temperature. In Fig. 3 are shown results obtained in 0.1 N solution of H_2SO_4 at three different temperatures, namely, 25, 50 and 75°C. A rise in temperature brings about, first of all, a marked increase in the rate of dissolution of chromium within the region of passivation.

On the basis of these results we have determined the activation energy of the process for that region of polarization potentials over which the constant rate of dissolution does not depend on the potential. The value obtained was close to 5,000 cal.

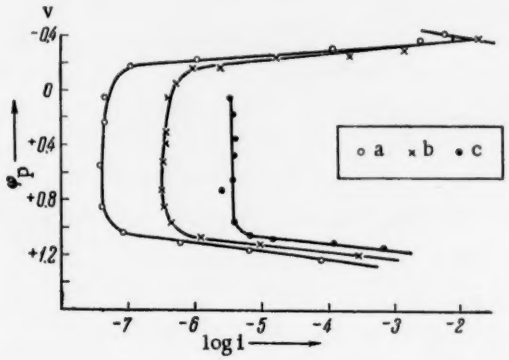

Fig. 3. Dependence of the logarithm of the steady rate of dissolution of chromium on the potential in a solution of 0.1 N H_2SO_4 at different temperatures: a) 25°, b) 50°, c) 75°C.

In the previous communication we have suggested that anodic passivation of chromium is not due to the formation of a phase film on the surface of the metal, but to the retardation of the anodic reaction resulting from the variation in the composition of the metallic surface with time and potential brought about by its adsorption-chemical interaction with the oxygen present in the water. This conclusion is supported by the results of polarization measurements obtained in the present investigation. In Fig. 4 are plotted values corresponding to the initial current densities at corresponding potentials, together with the curve of steady polarization potentials. As will be seen from this figure, when the points corresponding to the final constant

current density at each given potential (circles) are joined to the points corresponding to the initial current density at the next higher positive potential (dots), there are obtained straight lines having a slope very close to that of the upper linear segment of the curve representing the dependence of the rate of dissolution of activated chromium on the potential. Thus, if we ignore or reduce to a minimum various time effects, we are led to the conclusion that the polarizability of chromium and, consequently, the dependence of the rate of dissolution on the potential remains within the passivation region the same as it is in the activated state of the metal. In our opinion this is contrary to the concept of the existence on the surface of the passivated metal of a film of an oxidized phase; the presence of such a film should, in fact, bring about an increase in the polarizability of the electrode.

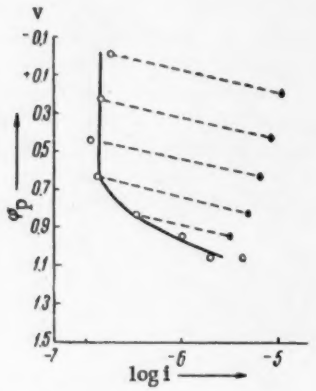

Fig. 4. Dependence of the logarithm of the rate of dissolution of chromium on the potential and time in a solution of 0.1 N H_2SO_4 at t = 50°.

In accordance with the concepts outlined the observed position of the upper limit of the range of passivation on the pH of the solution finds a comparatively simple explanation. If it is assumed that the adsorbed ions are OH^- ions, it is easily shown that the extent to which the surface is covered by these ions and, consequently, the extent of its passivation, should vary not only with the potential, but also with the pH of the solution. It is also obvious that the higher the concentration of OH^- ions the more negative will be the potential at which these ions will begin to penetrate the surface layer, that is, the potential at which passivation by adsorption can begin. On the basis of the adsorption mechanism of passivation the observed dependence of the steady rate of dissolution of the metal on the potential can, likewise, be explained simply if it is taken into account, as has been done previously [1, 2], that the composition of the metallic surface which determines the overvoltage of the anode reaction, varies exponentially with the potential.

L. Ya. Karpov Institute
of Physical Chemistry

Received December 12, 1956

LITERATURE CITED

[1] Ya. M. Kolotyrkin and V. M. Knyazheva, J. Phys. Chem. 30, 1990 (1956).

[2] N. Ya. Bune and Ya. M. Kolotyrkin, Proc. Acad. Sci. USSR, 111, 1050 (1956).

[3] B. V. Ershler, Proc. Third Conference on Corrosion of Metals, 2, Acad. Sci. USSR Press, 1943, p. 52.

[4] K. F. Bonhoeffer, Zs. Elektrochem. 59, 594 (1955); U. F. Frank and K. Weil, Zs. Elektrochem. 56, 814 (1952); K. U. Weil, and K. F. Bonhoeffer, Zs. Phys. Chem. 4, 175 (1955).

[5] Ya. M. Kolotyrkin and A. N. Frumkin, Proc. Acad. Sci. USSR, 33, 446 (1941).

[6] Ih. Heumann, and W. Rösener, Zs. Elektrochem. 59, 722 (1955).

INVESTIGATION OF THE KINETICS AND MECHANISM OF THE THERMAL DECOMPOSITION OF ISOBUTYLENE

Yu. I. Lyadova, V. I. Vedeneev and V. V. Voevodsky

(Presented by Academician N. N. Semenov, January 14, 1957)

One of us [1, 2] has proposed the chain thermal decomposition of olefins, based on the premise that a H atom is redistributed between a radical of the allyl type and the olefin molecule with the formation of the alkyl radical and diene:

$$R_1CHCH\dot{C}HCH\,(R_2)\,R_3 + R_1CHCHCH_2CH\,(R_2)\,R_3 \rightarrow R_1CHCHCHC\,(R_2)\,R_3 + \\ + R_1CH_2\dot{C}HCH_2CH\,(R_2)\,R_3$$

or

$$R_1\dot{C}HCH_2CH_2CH\,(R_2)\,R_3.$$

With this theory it was possible to satisfactorily explain the composition of the products obtained in the thermal decomposition of structurally different olefins.

This theory could not be directly extended to the cracking of such simple olefins as C_3H_6 and iso-C_4H_8, due to the absence of H atoms capable of entering into the redistribution reaction, in the allyl radicals formed from them.

It was postulated [2] that in the case of C_3H_6 and iso-C_4H_8 the addition of the allylic radical to the double bond of the olefin always precedes the formation of the reaction products.

It seemed of interest to us to make a detailed study of the thermal decomposition of isobutylene, paying special attention to obtaining additional data on the chain character of this decomposition and to verify the hypothesis that it is possible for a H atom to transfer from various radicals to the double bond of an olefin.

An ordinary static vacuum apparatus was used to study the cracking of isobutylene in the temperature interval from 542 to 620° and pressure interval from 100 to 500 mm Hg. To answer the question of whether it is possible for a H atom to transfer from a radical to an olefin molecule, we ran some experiments with mixtures of iso-C_4H_8 and C_2H_4 in the temperature interval from 542 to 600° and pressure interval from 200 to 600 mm Hg.

A preliminary study of the reaction kinetics for the thermal decomposition of isobutylene was made on the basis of the change in the total pressure, which was measured using a membrane manometer. The maximum rates of $\frac{dp}{dt}$, found from the Δp - time curves, are proportional to the initial iso-C_4H_8 pressure in the pressure interval from 30 to 500 mm Hg. This indicates that the reaction is of the first order. The energy of activation of the reaction based on the change in the maximum velocities with temperature proved to be $E = 49.5 \pm 3$ kcal./mole. Earlier found values are 53.7 kcal./mole in the interval 580-630° [3], and 67 kcal. per mole in the interval 780-810° [4].

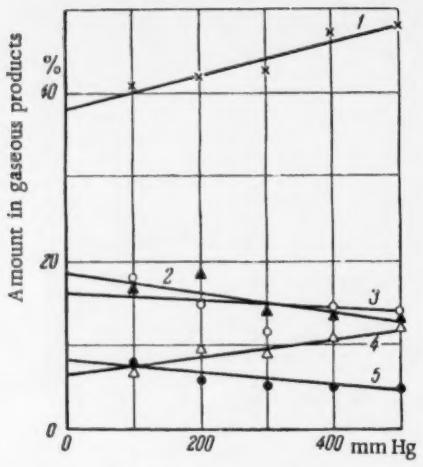

Fig. 1. Composition of the gaseous products as a function of the pressure in the cracking of iso-C_4H_8; T = 542°, $\Delta p/p_0 = 0.1$, 1) CH_4, 2) C_3H_6, 3) H_2, 4) C_4H_{10}, 5) C_2H_4.

The thermochromatographic method of gas analysis was used to study the kinetics of the process for the consumption of isobutylene and accumulation of the products. It revealed that the main gaseous products of isobutylene cracking are C_3H_6, CH_4, iso-C_4H_{10}, C_2H_4 and H_2, together with small amounts of C_2H_6 and C_3H_8.

The change in the composition of the gaseous products with change in the pressure and percent conversion for T = 542° is shown in Figs. 1 and 2. Similar relationships are also plotted for T = 600, 568 and 555°.

Extrapolation of the curves, describing the relationship between the composition of the gaseous products and the percent conversion, to zero percent conversion permits establishing the primary products of the reaction and their ratios.

In view of the difficulties associated with making a detailed analysis of the obtained liquids, we estimated their amount and the carbon-hydrogen ratio in them on the basis of the balance between the consumed isobutylene and the obtained gaseous products. Calculation revealed that about a third of the consumed isobutylene (on the basis of carbon) is converted to a liquid. On increasing the percent conversion the amount of liquids is increased somewhat (up to half of the consumed isobutylene). When the temperature is raised the fraction of liquids with respect to the consumed isobutylene is reduced somewhat. The carbon-hydrogen ratio in the liquid was ≈1.

Experiments on the cracking of iso-C_4H_8 revealed that up to 10% of isobutane is formed as one of the

TABLE 1

	p_0, mm Hg	$\frac{\Delta p}{p_0} \cdot 10^2$	t, min	Final C_2H_4, mm Hg	C_2H_4 consumed, mm Hg	Final iso-C_4H_8, mm Hg	iso-C_4H_8, consumed, mm Hg	C_2H_4 consumed, %	iso-C_4H_8 decomposed, %	H_2	CH_4	C_2H_6	C_3H_8	i-C_4H_{10}
										mm Hg				
C_2H_4 / i-C_4H_8	200	0	2.5	193	7	—	—	3.5	—	—	—	3.5	—	—
$C_4H_8 : C_2H_4 = 1:1$	200	12.5	2.5	7.2	—	137	63	—	31.5	16.8	38.5	1.9	17.3	4.0
	400	5	2.5	142	58	118	82	29	41	33.6	61.5	34	27.4	3.4

primary products. The amount of isobutane increases with increase in the pressure and reduction in the temperature. This shows that the addition of a H atom to the double bond of isobutylene is accomplished under our conditions.

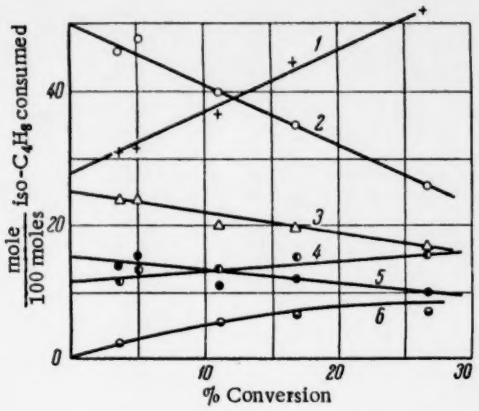

Fig. 2. Composition of the gaseous products as a function of the percent conversion in the cracking of iso-C_4H_8; T = 542°, p = 300 mm Hg pressure, 1) CH_4, 2) C_3H_6, 3) iso-C_4H_{10}, 4) H_2, 5) C_2H_4, 6) C_2H_6.

To obtain additional data on the transfer of a H atom to the double bond of an olefin we studied the cracking of mixtures of iso-C_4H_8 and C_2H_4.

In Table 1 the results of one of these experiments with T = 600° and p = 400 mm Hg pressure for a 1 : 1 mixture of iso-C_4H_8 and C_2H_4 are compared with the results of cracking pure iso-C_4H_8 and C_2H_4.

The data given in Table 1 permit making a number of conclusions. First of all, they support the theory of a chain mechanism for the reaction; an increase in the consumption rate of iso-C_4H_8 in the presence of C_2H_4 cannot be explained within the framework of the theories that postulate a purely radical or molecular mechanism for the process. The same conclusion can be reached from an analysis of the data showing the formation of a large amount of ethane (34 mm). On the other hand, the formation of ethane in such large quantities is still another proof that it is possible for a H atom to transfer to the double bond of an olefin.

We believe that our experiments support the theory that in the cracking of isobutylene the reaction exists:

$$\dot{R} + i\text{-}C_4H_8 \rightarrow M + \dot{C}_4H_9,$$

and that in a mixture of isobutylene and ethylene the reaction exists:

$$\dot{R} + C_2H_4 \rightarrow M + \dot{C}_2H_5.$$

A comparison of the data on the analysis of the primary gaseous products and on the composition of the liquids leads to the conclusion that the earlier proposed scheme of V. V. Voevodsky for the cracking of C_3H_6 and iso-C_4H_8 is inadequate. It would be necessary to introduce new methods of transforming the iso-$\dot{C}_4H_7$ radical into the scheme. The decomposition of iso-$\dot{C}_4H_7$ into $\dot{C}H_3$ and allene can be postulated as being such a method, and also the reaction for the transfer of a methyl radical from iso-$\dot{C}_4H_7$ to the isobutylene molecule.

$$CH_2C(CH_3)\dot{C}H_2 + i\text{-}C_4H_8 \rightarrow CH_2CCH_2 + \begin{matrix} CH_3CH_2C(CH_3)_2 \\ \text{or} \\ \dot{C}H_2C(CH_3)_3 \end{matrix}$$

The formation of allene in the cracking of isobutylene, which was observed by Rice [5] and by Szwarc [4], can serve as some support to the theory that such reactions can exist. Allene is unstable under our conditions. Special experiments made with the addition of allene revealed that in the time, commensurate with the time of running the experiments, the allene disappears completely from the gas phase.

Institute of Chemical Physics
Academy of Sciences of the USSR

Received January 12, 1957

LITERATURE CITED

[1] V. V. Voevodsky, Proc. Acad. Sci. USSR, 94, 909 (1954).

[2] V. V. Voevodsky, Problems of Chemical Kinetics, Catalysis and Reactivity, p. 150 (1955).

[3] M. J. Molera, F. J. Stubbs, J. Chem. Soc., 1952, 381.

[4] M. Szwarc, J. Chem. Phys. 17, 292 (1949).

[5] F. O. Rice, L. Wall, J. Am. Chem. Soc., 72, 3967 (1950).

THE NATURE OF CATALYTIC CURRENTS OF HYDROGEN IN POLAROGRAPHY

S. G. Mairanovsky

(Presented by Academician A. N. Frumkin, January 7, 1957)

The origin of catalytic waves of hydrogen [1-5] is usually explained as being due to a reduction in the energy of activation of hydrogen ion discharge under the influence of catalysts. In accord with this catalytic waves should have an irreversible character and their halfwave potentials should change with the pH of the solution. However, this does not agree with experiment, at least not in the catalysis of organic compounds. Thus, Kirkpatrick [3] found that the potentials of the waves, produced by alkaloids, are almost independent of the pH; the same was observed by Kuta and Drabek [4] for the waves catalyzed by pyridine.

It is logical to assume that the discharge of the pyridinium ion, determining the catalytic wave, proceeds by the same mechanism as the discharge of N-substituted quaternary pyridinium salts [6], i. e. that it represents a reversible electrochemical process with subsequent rapid dimerization of the electrode products, leading, however, in contrast to the N-substituted salts, not to the dimer [6], but instead to the evolution of H_2 and the regeneration of pyridine. The validity of this postulation is shown in the present paper, and here we have also estimated for one of the cases the values of the velocity constants for the reactions, determining the catalytic wave.

The general scheme for the catalytic process can be depicted as follows [5, 7]:

$$B + DH^+ \underset{k_3}{\overset{k_1}{\rightleftarrows}} BH^+ + D, \quad (a) \qquad BH^+ + e^- \overset{E}{\rightleftarrows} BH, \quad (b) \qquad 2BH \xrightarrow{k_3} 2B + H_2. \quad (c)$$

The catalyst (capable of existing in both acidic (BH^+) and basic (B) forms) in the acidic, cationic form BH^+ discharges reversibly at the cathode, giving BH radicals. The radicals then quickly dimerize, regenerating the catalyst in the basic form B and giving a molecule of hydrogen. Then the basic form, reacting with the proton-donor DH^+, found at the electrode, migrates into the acidic form, and the whole cycle is repeated. Applying the calculation method of Brdicka and Wiesner [8-10] to this scheme, we obtain for a substance balance [5]:

$$i = \varkappa([BH^+]_o - [BH^+]_s) + sF\mu_1(k_1[DH^+]_s[B]_s - k_2[BH^+]_s[D]_s), \tag{1}$$

$$i = \varkappa([B]_o - [B]_s) - sF\mu_1(k_1[DH^+]_s[B]_s - k_2[BH^+]_s[D]_s). \tag{2}$$

$$sF\mu_3 k_3[BH]_s^2 + \varkappa[BH]_s = i. \tag{3}$$

Here $\varkappa$ is the constant of the Ilkovich equation (it is taken the same for all forms of the catalyst), s is the average surface area of the dropping electrode, μ is the thickness of the reaction layer [8, 9, 11], index s relates to the surface concentrations of the substances, and o relates to the volume concentrations.

From these equations it follows that

$$i = \frac{\varkappa([BH^+]_o - [BH^+]_s) + P\varkappa[B]_o - R\,[BH^+]_s}{1-P}, \tag{4}$$

$$P = \frac{k_1 sF\mu_1 [DH^+]_s}{\varkappa + k_1 sF\mu_1 [DH^+]_s}, \tag{5}$$

$$R = k_2 sF\mu_1 [D]_s (1-P). \tag{6}$$

In well buffered solutions with a constant height of the mercury column P = const, R = const, $[DH^+]_s = [DH^+]_o$ and $[D]_s = [D]_o$.

For the limiting current ($[BH^+]_s \rightarrow 0$) we obtain from (4):

$$i_{lim} = \frac{\varkappa([BH^+]_o + P[B]_o)}{1-P} = \frac{\varkappa[B]_o}{1-P}\left(\frac{[BH^+]_o}{[B]_o} + P\right) \tag{7}$$

Comparing (4) and (7) we find that $[BH^+]_s = (i_{lim} - i)(1-P)/(\varkappa + R)$. We find $[BH]_s$ in the following manner. The second term on the left side of equation (3) is usually several orders smaller than the first; consequently, neglectin the small value $\varkappa [BH]_s$ and assuming [9, 11] that $\mu_3 = (D/k_3[BH]_s)^{1/2}$, we obtain from (3): $[BH]_s = (i/sFk_3^{1/2}D^{1/2})^{2/3}$, where D is the diffusion coefficient. Substituting the values $[BH^+]_s$ and $[BH]_s$ in the Nernst equation, we obtain the general equation for a catalytic wave:

$$E = E_0 + \frac{RT}{F}\ln\frac{i_{lim} - i}{i^{1/3}} + \frac{RT}{F}\ln\frac{(1-P)(sF)^{1/3}(k_3 D)^{1/3}}{\varkappa + R} \tag{8}$$

or

$$E = \varepsilon_0 + \frac{RT}{F}\ln\frac{i_{lim} - i}{i^{1/3}}, \tag{9}$$

where ϵ_0 is a constant, equal to the potential at $i^{2/3} = i_{lim} - i$; E_0 is the normal potential of the redox system. We will examine the particular cases of catalytic currents of hydrogen in well buffered solutions. With a very small velocity k_1 for the catalytic process (a) and a high $[BH^+]_o$, i. e. when $p << 1$ and $\kappa >> R$, the current in accord with (4) and (7) is determined by the diffusion of BH^+ and, the same as the diffusion current, is proportional to $(h)^{1/2}$ or $t^{-1/2}$ (h is the height of the mercury column over the electrode, and t is the dropping time). In this case Equation (8) becomes identical with the expression for the diffusion wave of a reversible process with rapid dimerization of the electrode products [9, 12], studied on the example of the reduction of N-alkylpyridinium salts [6]. The halfwave potential $E_{\frac{1}{2}}$ in this case becomes more negative by ~19 mv with a ten-fold increase in either t or C (C = $[BH^+]_o$ + $[B]_o$ – the analytical concentration of the catalyst in the solution).

With sufficiently high velocities for the catalytic process and low $[BH^+]_o$ ($[BH^+]_o << [B]_o$) the current is determined mainly by the velocity of the catalytic process (a) [5]. Here two cases can be encountered.

I. If the velocity of the reverse reaction (k_2) is also quite high, then $R >> \kappa$ and $\mu_1 = (D/k_2[D]_s)^{1/2}$; here, if $p << 1$, then κP and R, and consequently also the catalytic current, are independent of either h or t [5]. The value ϵ_0 in this case is independent of C and t and is a characteristic electrochemical constant of catalyst BH^+ at a given pH for the solution. The value $E_{\frac{1}{2}}$, as can be seen from (5), (7) and (8), is determined by the equation:

$$E_{1/2} = E_0 + \frac{RT}{F}\ln\frac{(k_3 C)^{1/3}(\varkappa P)^{1/3}}{(k_2[D]_o)^{1/3}[sF(1-P)]^{1/3}D^{1/3}}, \tag{10}$$

i. e. $E_{1/2}$ becomes more positive by ~19 mv with a ten-fold increase in C and is independent of $\underline{t}$.

II. If the velocity of the reverse reaction (a) is small, then μ_1 can expand to the dimensions of the diffusion layer and become equal to $0.233\sqrt{Dt}$ [13]. In this case R, and with $P \ll 1$ also i_{lim}, increase with decrease in $\underline{h}$; here i_{lim} is proportional to either $h^{-1/2}$ or $t^{1/2}$. Actually, an increase in the catalytic current with decrease in h was observed by a number of investigators [4, 14]; in accord with (8) ϵ_0 in this case is independent of C, but with change in $\underline{t}$ as a function of the ratio between the values κ and R it can shift toward either positive or negative potentials. The $E_{1/2}$ of these waves is determined by the equation

$$E_{1/2} = E_0 + \frac{RT}{F} \ln \frac{(1-P)^{2/3} sF (k_1 k_3)^{1/3} C^{2/3} D^{1/3} (0,233\, t^{1/3})^{1/3}}{\kappa + R}, \qquad (11)$$

i. e. $E_{1/2}$ with a ten-fold increase in C becomes more positive by ~19 mv, while with an increase in $\underline{t}$ it becomes either more positive, by a maximum of ~ 38 mv (with $\kappa \gg R$), or more negative – in the limiting case ((with $\kappa \ll R$) by ~ 19 mv (since κ is proportional to $t^{-1/2}$, while R in the given case ~ $t^{1/2}$).

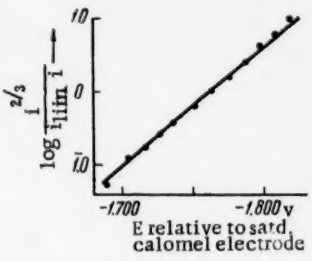

Fig. 1. Relationship between log $i^{2/3} / (i_{lim} - i)$ and E for catalytic waves, produced by pyridine in 0.1 M borax solution.

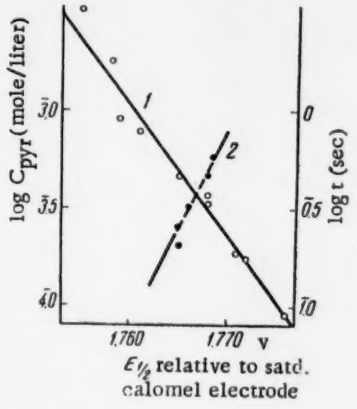

Fig. 2. $E_{1/2}$ as a function of the C of pyridine (1) and of the dropping time (2) in 0.1 M borax solution.

To verify the derived relationships we studied the catalytic hydrogen waves, produced by pyridine in 0.1 M borax solution and borate buffer solutions. The work was done at 25°. The capillary of the dropping electrode was fitted with a little paddle for the required removal of the drops [15]; its $\underline{m}$ and $\underline{t}$ at h = 50 cm were respectively 3.82 mg/sec. and 0.26 sec. The potentials of the electrode were measured potentiometrically with the saturated calomel electrode as reference. These values were corrected for the iR_{ohm} in the cell. $E_{1/2}$ was found by interpolation on linear (in the middle portion) graphs ($\log[i/(i_{lim}-i)]$, E). The current rate was corrected for residual current. The solutions were blown with nitrogen to remove oxygen.

The experimentally found relationship between $\log[i^{2/3} / (i_{lim} - i)]$ and E is shown in Fig. 1; its linear character and the value of the slope are in exact agreement with equation (8). The value ϵ_0, in accord with (8), is independent of C and at h = 50 cm in 0.1 M borax solution is equal to –1.759 v. The value of the wave i_{lim} in 0.1 M borax solution increases with decrease in $\underline{h}$ almost proportionally to $h^{-1/2}$, which corresponds to a slow reverse reaction (a). In good quantitative agreement with theory for this case ($[BH^+]_0 \ll [B]_0$, $\kappa \ll R$) $E_{1/2}$ becomes more positive with increase in C and more negative with increase in $\underline{t}$ (Fig. 2).

Since in alkaline solutions the proton-donor DH^+ is water [4, 5] and D corresponds to OH^- ions, then an increase in the pH of the solution should increase the velocity of the reverse catalytic reaction and in that way reduce μ_1. At a sufficiently high pH (for pyridine at pH $\geq$ 10) μ_1 ceases to depend on t; a reduction in μ_1 in turn leads to a decrease in P, and consequently, also in i_{lim}. At $P \ll 1$ it follows from (5) and (7) that $i_{lim} = k_1 sF [H_2O] (D/k_2 [OH^-]s)^{1/2}$, i. e. i_{lim} at sufficiently high values of the pH is independent of t and changes proportionally to $[OH]^{-1/2}$. Experiment supports this conclusion. The values $E_{1/2}$ and ϵ_0, in accord with (8), become more negative with increase in the pH (due to increase in R).

The intersection of the catalytic waves with the so-called Fournier waves (Fig. 3), obtained by applying to the electrode, besides a constant voltage, also a small sinusoidal voltage [16-18, 6], can serve as additional evidence of the reversible nature of the electrode process in the catalytic liberation of hydrogen. It is interesting to mention that, due to the influence of the preceding reaction, the potential at the point of intersection E• is located considerably closer to $E_{1/2}$ in the case of the catalytic waves than for the reverse process with subsequent dimerization [6].

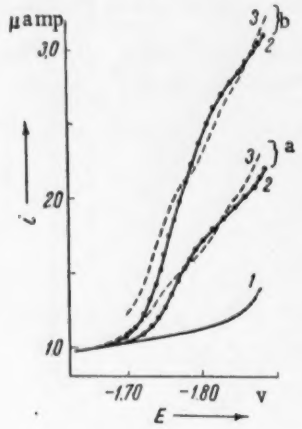

Fig. 3. Ordinary polarograms (2) and Fournier waves (3) with $E_{\sim}$ = 50 mv, 100 htz.; ground 0.1 M borax solution (1). Pyridine concentration: a) $3.9 \cdot 10^{-4}$ M, b) $7.9 \cdot 10^{-4}$ M.

An estimate of the velocity constant of the reaction was made, proceeding from the relationships for the catalytic current in 0.1 M borax solution at 25°. For the calculation we used the following data: κ = 4.05 μamp · liter/mmole (taken equal to the κ of the N-methylpyridinium radical [6]), $s = 8.5 \cdot 10^{-3}$ cm², $\mu_1 = 5.7 \cdot 10^{-4}$ cm according to (13) (at t = 0.26 sec), $[OH^-] = 1.7 \cdot 10^{-5}$ mole/liter (pH = 9.24). Since under these conditions $[BH^+]_0 / [B]_0 \ll P$ and $C \approx [B]_0$, then from the experimental value i_{lim}/C = 1.98 μamp · liter/mmole = const (at t = 0.26) it is found from (7) that P = 0.329 and from (5) it is found that $k_1 \cdot [H_2O] = 4.3$ sec^{-1} ($k_1 = 7.8 \cdot 10^{-2}$ liter/mole · sec). From the value $K = k_1 [H_2O]/k_2 = 1.7 \cdot 10^{-9}$ the value $k_2 = 2.5 \cdot 10^9$ liter/mole · sec was obtained. It is assumed that $E_0 \approx E^\bullet = -1.778$ v [6, 16-18], then from the experimental value $\epsilon_0 = -1.759$ v and $R = 13.3 \cdot 10^3$ μamp · liter/mmole [from (6)] the value 10^{14} liter/mole · sec. is obtained from (8) for k_3. This value is considerably higher than the velocity constant for the dimerization of N-methylpyridinium radicals [6].

The reversible nature of the electrode process is retained in unbuffered solutions; however, due to pH change in the pre-electrode area, the i-E curves of the catalytic waves stretch along the E axis. It can be postulated that a similar mechanism for the catalytic process also exists in catalysis involving other catalysts with an onium structure [7]; in any case, catalytic waves are not associated with a reduction in the energy of activation of hydrogen ion discharge, and their potentials are determined only by the electrochemical properties of the catalysts.

In conclusion the author considers it his pleasant duty to thank Academician A. N. Frumkin for discussing the problem.

The N. D. Zelinsky
Institute of Organic Chemistry
Academy of Sciences of the USSR

Received January 5, 1957

LITERATURE CITED

[1] Ya. Geirovsky, The Polarographic Method, p. 94. Leningrad. 1937.

[2] E. Knobloch, Coll., 12, 407 (1947).

[3] H. F. W. Kirkpatrick, Quart. J. Pharm. Pharmacol., 20, 87 (1947).

[4] Ya. Kuta and I. Drabek, Coll. Czechoslovak. Chem. Studies, 20, 902 (1955).

[5] S. G. Mairanovsky, Bull. Acad. Sci. USSR, Div. Chem. Sci., 1953, 615, 815.*

[6] S. G. Mairanovsky, Proc. Acad. Sci. USSR 110, 593 (1956).*

[7] S. G. Mairanovsky and M. B. Neiman, Proc. Acad. Sci. USSR, 87, 805 (1952).

[8] R. Brdička, K. Wiesner, Coll., 12, 138 (1947).

[9] V. Hanuš, Chem. Zvesti, 8, 702 (1954).

[10] S. G. Mairanovsky and M. B. Neiman, Proc. Acad. Sci. USSR, 82, 93 (1952).

[11] D. Kern, J. Am. Chem. Soc., 75, 2473 (1953).

[12] J. Koutecký, V. Hanuš, Coll., 20, 124 (1955).

[13] J. Koutecký, R. Brdička, V. Hanuš, Coll., 18, 622 (1953).

[14] V. Vojir, Coll., 18, 629 (1953).

[15] E. M. Skobets and N. S. Kavetsky, Factory Labs., 15, 1299 (1949).

[16] M. Fournier, C. R., 232, 1673 (1951).

[17] G. Buchanan, R. Werner, Austral. J. Chem., 7, 239 (1954).

[18] J. Tachi, Bull. Chem. Soc. Japan, 28, 25 (1955).

* Original Russian pagination. See C. B. Translation.

IONIC EXCHANGE ON ALUMINOSILICATE CATALYSTS IN A STREAM OF ALKALI WITH SMALL CONTACT TIMES

G. M. Panchenkov, Z. V. Gryaznova and I. M. Kuvshinnikov

(Presented by Academician A. V. Topchiev, January 19, 1957)

Aluminosilicate catalysts, possessing great industrial importance, have been the subject of a number of studies [1-9]. Many of the studies have been devoted to elucidating the nature of the acidic and exchange capacity of aluminosilicates [2-7]. However, here complete clarity has not yet been achieved. The present paper is devoted to a further study of the mechanism for the ionic exchange of aluminosilicate catalysts. For this purpose we studied the kinetics of ionic exchange under dynamic conditions in both alkaline and neutral media.

In our study we used a commercial catalyst analyzing 14% Al_2O_3 and 86% SiO_2, and a catalyst analyzing 37% Al_2O_3 and 63% SiO_2, prepared by mixing the corresponding hydrogels with subsequent drying at 100°. Several portions of the catalyst were ignited at 500, 750, 1100 and 1300°C. The catalyst had the shape of small cylinders with a height of 4 mm and a diameter of 3 mm. We also used a ground catalyst, sifted through a screen with a mesh size of 200 to 350. The experiments were run under dynamic conditions with various rates of flow for the NaOH, LiOH and KOH solutions. To run the experiments under dynamic conditions a catalyst layer one tablet thick was placed in a crucible with a No. 1 glass filter. The alkali solution flowed through the crucible at a constant rate. After passing through the catalyst layer the solution was collected in small flasks, which were changed at periodic intervals. The alkali concentration in the test specimen was determined by titration with phenolphthalein. The results of the experiments on ionic exchange in alkaline medium are plotted in Figs. 1 and 2. Along the ordinate in these figures is plotted the value $\underline{a}$ – the amount of H^+ in milligram equivalents exchanged by 100 g of the catalyst with a given volume of the solution, while along the abscissa is plotted the volume of solution passed through the catalyst layer at a definite rate.

TABLE 1

The Rate of Ionic Exchange (With Respect to the Concentration) as a Function of the Heat Treatment of the Catalyst Analyzing 14% Al_2O_3 and 86% SiO_2

Expt. Nos.	Ignition temperature, in °C	Ignition time, hours	V/C
1	100	10	45
2	500	8	40
3	500	16	30
4	750	16	30
5	1100	4	24
6	1300	2	4

As can be seen from Fig. 1, the ordinary saturation curve is obtained for ionic exchange under dynamic conditions. The initial portion of this curve is well approximated by two straight lines. The slope tangents of the straight line sections characterize the velocity of the ionic exchange. The magnitude of the slope tangent of the second section (V) depends on the flow rate and is proportional to the concentration of the solution. The velocity of the ionic exchange also depends on the degree of previous heat treatment of the catalyst. The ignition was run in a stream of dry air. Since the rate of process V is proportional to the concentration of the solution, in Table 1 the function V/C was used, which is independent of the concentration.

On the basis of the experiments made by us to study the kinetics involved in the transformation of hydrocarbons on aluminosilicate catalysts and the data given in Table 2

it can be concluded that to obtain a catalyst with a constant activity it is necessary to subject it to heat treatment for not less than 16 hours at 500-700°C.

The kinetics curves showing the ionic exchange of aluminosilicate catalysts, deactivated by ignition at 1100 and 1300°, are characterized by linear initial portions of the curve without a break. A 10% reduction in the volume (shrinkage) of the catalyst is observed when it is ignited at temperatures up to 1100°, but here the catalyst still retains considerable acidity. The shrinkage reaches 60% when the ignition is up to 1300°, while the acidity drops to nearly zero.

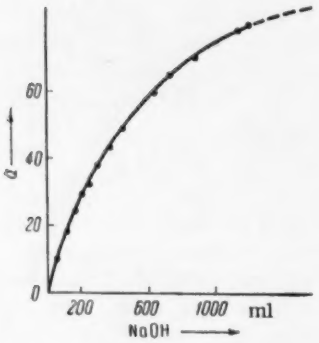

Fig. 1. Kinetics of the ionic exchange under dynamic conditions on unignited industrial catalyst. C_{NaOH} = 0.007 N, v_n = 0.2 ml/min.

For the unignited catalyst the kinetics curves at times do not start from zero. As was shown by additional studies, this was due to adsorption of ammonia by the catalyst. This, and also the variable moisture, explain some of the differences in the velocity of the ionic exchange under similar conditions. If the catalysts had been previously ignited, then a good reproducibility of the results was steadily observed. Curve III in Fig. 2 describes the results of three experiments, run under similar conditions with a catalyst that had been ignited at 500° for 16 hours. As can be seen from the graph, all of the points of the three experiments lie well on one curve. The experiments with the powdered catalyst are described by a continuous curve without a break in the initial portion, in which connection the velocity of the exchange shows a 20-fold increase (Fig. 2, IV).

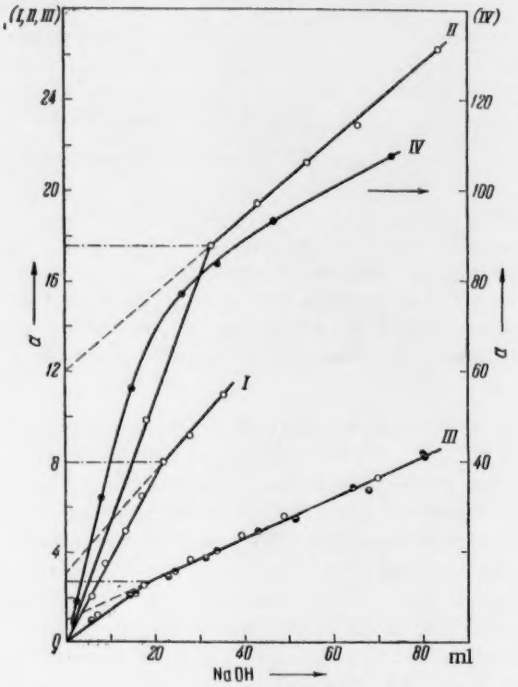

Fig. 2. Ionic exchange under dynamic conditions: I) unignited industrial catalyst; C_{KOH} = 0.010 N, v_n = = 2.8 ml/min.; II) unignited catalyst with composition 37% Al_2O_3 and 63% SiO_2; C_{NaOH} = 0.055 N, v_n = 3.6 ml/min.; III) industrial catalyst, ignited at 500° for 16 hours; C_{NaOH} = 0.010 N, v_n = 3.5; 3.1; 2.9 ml/ /min.; IV) powdered industrial catalyst, ignited at 500° for 16 hours; C_{NaOH} = 0.010 N, v_n = 2.96 ml/min.

The most probable reason for a break in the kinetics curves is a difference in the availability of the surface and interior (found inside the pores and between the pockets) exchange-capable catalyst centers. In this case the break is explained by a completion of neutralizing the surface centers. The amount of the latter can be determined graphically. If the surface and interior ionic exchange processes are consecutive in nature, then the amount of surface acidic centers is determined by the ordinate of the break a_0; if the processes are of a parallel nature, then this value is determined by the point of intersection of the continuation of the second section of the kinetics straight line with the ordinate a'. The values of ordinates a_0 and a' are given in Table 2. The study was made with NaOH solution and only in individual cases, indicated in Table 2, with LiOH and KOH solutions.

At sufficiently small alkali concentrations (up to 0.015N) the base is almost completely neutralized by the surface hydrogen ions. In this case the consecutive process for the neutralization of the surface and interior hydrogen ions is observed, and consequently the value a_0 determines the number of surface hydrogen ions. An increase in the alkali concentration proves sufficient to effect simultaneous neutralization of both the surface and interior ions. In this case the number of surface ions is determined by the value a_0'. From Table 2 it can be seen that for the unignited industrial catalyst the amount of hydrogen ions on the surface of the catalyst is approximately equal to 7 mequiv. per 100 g of catalyst, and for the ignited catalysts it is equal to 3 mequiv. per 100 g of catalyst. For the unignited catalyst with composition 37% Al_2O_3 and 63% SiO_2 a_0' = 12, which is natural, since it is known that the catalyst analyzing 30% Al_2O_3 and 70% SiO_2 shows a maximum acidity. It has the greatest number of exchange centers in general and surface centers in particular.

TABLE 2

Magnitude of the Values a_0 and a_0'. Layer One Tablet Thick. Catalyst Analyzing 14% Al_2O_3 and 86% SiO_2

Normality of starting alkali C_{orig}	Flow rate, v_n, ml/min	a_0, mequiv. H^+ / 100 g	a_0', mequiv H^+ / 100 g
Unignited catalyst			
0.006	2.4	7.0	2.0
	4.0	6.8	4.0
0.010	2.5(LiOH)	8.7	3.3
	2.8(KOH)	8.0	3.1
	2.5	8.5	3.3
	2.7	4.8	1.3
	3.0	8.0	3.0
0.015	2.5(LiOH)	5.5	2.3
Average		7.2	
0.055	3.1	30	6.5
	4.8	20	6.5
	3.6*	17.6*	12.0*
Layer thickness 4 cm			
0.007	3.5	8.5	2.0
0.011	0.5	8.0	2.8
Average		8.2	
0.098	1.8	46	20
Layer one tablet thick. Catalyst ignited at 550-750°			
0.010	2.9	3.2	1.3
	3.1	3.2	1.0
	3.5	3.0	1.0
	3.8	3.1	1.6
Average		3.1	

* The experiment was run with the catalyst analyzing 37% Al_2O_3 and 63% SiO_2.

A visible increase in the values a_0 and a_0' is observed for an alkali concentration of about 0.1 N. This can be explained by the fact that at such concentrations a part of the alkali is consumed in dissolving the catalyst [10]. Studies made with LiOH, NaOH and KOH solutions revealed that the nature of the alkali ion does not affect the value of a_0'.

On the basis of the obtained data it is obvious that the slowest stage of the whole process is the diffusion into the depths of the pores. At the break point, after completing the process of surface neutralization, the exchange rate is determined only by the diffusion into the depth of the pores. As a result, the reason for not obtaining smooth curves, but instead curves with a break, is the sharp change in the rate of the process. This theory as the reason for the break is supported by the data obtained for the ionic exchange of an aluminosilicate catalyst under dynamic conditions in a solution of neutral salts. In this case the break on the kinetics curve is absent, for the reason that here the ionic exchange process proceeds at a rate that is 10^3 times slower than in alkali solution. The absence of a break on the kinetics curve for the ionic exchange of an aluminosilicate catalyst that had been ignited at 1100 and at 1300° can be explained in this manner. At 900-1000° the aluminosilicate suffers decomposition into γ-Al_2O_3 and mullite [11], which are weaker acidic agents than the aluminosilicic acids. Here the rate of the neutralization process is quite small, and a break is not observed. The absence of a break point on the kinetics curves in the neutralization of the ground catalyst with alkali solution (Fig. 2, IV) is another indication of the validity of the above discussed ionic exchange mechanism. The latter does not permit explaining a break in the kinetics curves on the premise that acids of different strength are present.

The studies of Danforth [12] show that the catalytic activity as a function of the degree of catalyst poisoning by alkali solutions is decribed by a broken line with two breaks. The author pays attention only to the second

break. At the same time, in all cases still another break is observed on the curve at the point where the catalyst absorbed 2 mequiv. per 100 g of catalyst. This is in good agreement with the results obtained by us for catalysts that had been subjected to heat treatment.

As a result, it is possible to arrive at the following conclusion: the concentration of the external active centers on an aluminosilicate catalyst can be easily and quickly determined by the method of neutralizing it with alkali solution. It should be indicated that this method cannot be general for all acidic and oxide catalysts, and is suitable only in the cases where the ionic exchange rates on the surface and in the interior of the pores are strongly different.

The M. V. Lomonosov
State University (Moscow)

Received January 9, 1957

LITERATURE CITED

[1] V. I. Vernadsky, Outlines of Geochemistry, 1934; V. I. Vernadsky and S. I. Kurbatov, Earth Silicates, Aluminosilicates and Their Analogs, Moscow, 1937.

[2] Yu. A. Bitepazh, J. Gen. Chem., 17, 199 (1947).

[3] A. P. Ballod and K. V. Topchieva, Prog. Chem., 20, 161 (1951).

[4] Ch. Thomas, Ind. and Eng. Chem., 41, 2564 (1949).

[5] G. M. Panchenkov, Bull. Moscow State Univ., No.6, 105 (1948).

[6] A. Oblad, T. Milliken and G. Mills, Coll. "Catalysis in Organic Chemistry"*, pp. 185-240, IL, 1953.

[7] K. G. Miesserov, Prog. Chem., 22, 3, 279 (1953).

[8] Y. Trambouze, L. de Mourgues, and M. Perrin, J. Chim. Phys., 51, 723 (1954).

[9] J. E. Mapes and R. P. Eischens, J. Phys. Chem., 58, 1059 (1954).

[10] A. P. Ballod, Candidate's Dissertation, Moscow State Univ., 1950.

[11] V. T. Barret, M. G. Zaucher and I. G. Smit, Paper at the International Conference on Catalysis, Philadelphia, 1956.

[12] J. Danforth, J. Phys. Chem., 58, 1030 (1954).

* [Russian translation.]

THE INFLUENCE OF THE CONCENTRATION OF THE ELECTROLYTE (COPPER SULFATE) SOLUTION ON THE EXCHANGE SORPTION OF FATTY ACID CRYSTALS

A. A. Trapeznikov

(Presented by Academician P. A. Rebinder, January 26, 1957)

It was shown [1] that crystals of fatty acids are capable of sorbing cations from aqueous solutions of salts, with conversion into the corresponding metallic soaps. The rate of the exchange reaction depends to a strong degree on the temperature, which in part is associated with the polymorphous transformations of the acid crystals and the influence of hydration on them. It was established that especially intense penetration of metal cations into the lattice occurs at temperatures lying close to the melting point of the acid.

In this paper we studied the liberation of hydrogen ions by crystals of lauric, myristic, palmitic and stearic acids in aqueous $CuSO_4$ solutions of variable concentration, which was estimated by the change in pH using a glass electrode and an LP-3 lamp potentiometer. The $CuSO_4$ solutions with contained acid crystals were kept in closed vessels at room temperature ($t \approx 20°$). To accelerate the process the crystals of the acids (Kahlbaum) were ground in a mortar. The concentration of the $CuSO_4$ solutions was varied from 0.0004 to 0.5 N; here the natural values of the pH, arising as the result of hydrolysis, lay in the range 6.0-3.8.

The curves for G' – the amount of liberated H^+ ions, calculated in equivalents on the total weight of taken acid, as a function of the original pH values of the solutions (Table 1) for the C_{16}, C_{14} and C_{12} acids at different periods of time, up to 200 days, are shown in Fig. 1. The curves for all of the acids pass through a maximum, lying at pH = 4.75, and corresponding to C = 0.05 N and a 10-fold amount of salt with respect to the taken weight of acid. For the three indicated acids the position of the maximum is practically independent of the chain length of the homologous acid and is determined by the nature of the electrolyte ($AgNO_3$, $Th(NO_3)_4$, $Ce(NO_3)_3$).

The height of the curve, i. e. the intensity of H^+ ion liberation is increased when the chain length of the homologous acid is made shorter. This is explained by the fact that transition to a lower homolog is equivalent to raising the temperature for the higher homolog, which is in accord with earlier data [1].

Of especial interest are the reasons for the appearance of a maximum on the curve expressing the relationship between H^+ ion liberation and the concentration C of the solution. With increase in C_{CuSO_4} the reaction, proceeding by the scheme

$$2RCOOH + CuSO_4 = (RCOO)_2 Cu + H_2SO_4,$$

should be shifted to the right, although excess accumulations of H^+ ions as the result of hydrolytic decomposition of the $CuSO_4$ in concentrated solutions and as the result of exchange sorptions could hinder the exchange.

Consequently, the first hypothesis reduces to the premise that in more concentrated solutions the reaction is retarded due to the reverse reaction of decomposition of the formed copper soap. However, this is refuted by the fact that the absolute values of the pH, obtained as the result of exchange sorption in solutions of medium concentration, are lower than those obtained in solutions of higher concentration (Table 1)•. Consequently, it is necessary to explain the anomaly of the exchange-sorption liberation of H^+ ions in a different manner.

• The LP-3 potentiometer is labeled to give an accuracy of ± 0.1 pH. Here the values are expressed in hundredths of a pH. They cannot be considered accurate in all cases; however, in many series of experiments with stable operation of the potentiometer they, apparently, correctly reflect the course of the pH change with concentration.

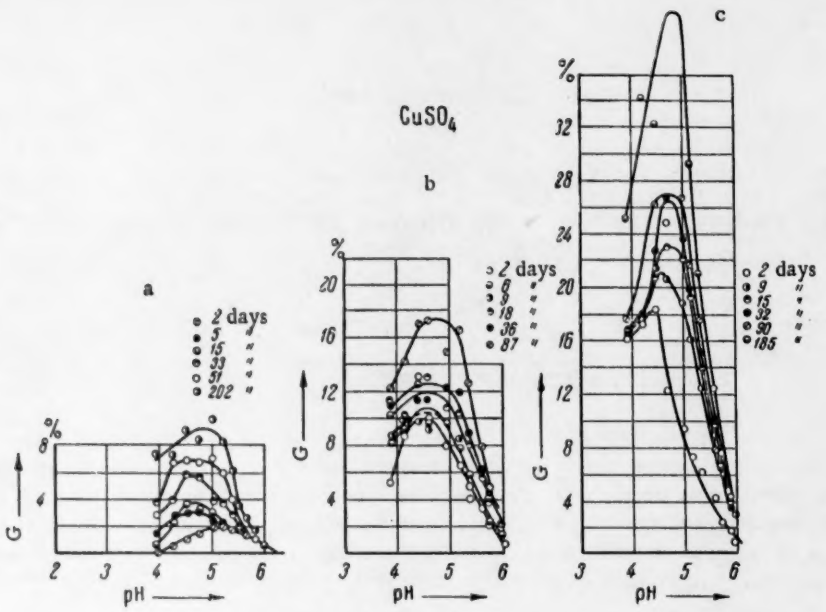

Fig. 1. G' as a function of the pH for crystals of palmitic (a), myristic (b) and lauric (c) acids in $CuSO_4$ solutions.

TABLE 1

Values of the pH in the Original $CuSO_4$ Solutions and in the Same Solutions After Adding a Known Weight of Fatty Acid Crystals

	Lauric acid, weight m = 0.025 g					Palmitic acid, weight m = 0.032 g				
C	orig.	2 days	15 days	90 days	185 days	orig.	2 days	5 days	51 days	202 days
0.5	3.90	3.03	3.02	3.00	2.86	3.94	3.93	3.85	3.53	3.3
0.2	4.22	3.04	3.02	2.95	2.75	4.27	4.10	3.80	3.41	3.3
0.1	4.47	3.02	2.95	2.87	2.78	4.53	4.06	3.68	3.43	3.32
0.05	4.68	3.20	2.93	2.90	2.70	4.75	4.10	3.78	3.45	3.36
0.02	5.00	3.32	2.95	2.87	2.70	5.01	3.98	3.70	3.45	3.30
0.01	5.13	3.43	3.01	2.96	2.83	5.20	4.02	3.98	3.55	3.38
0.005	5.32	3.50	3.15	3.05	2.97	5.39	4.12	4.08	3.70	3.52
0 002	5.59	3.68	3.29	3.40	3.20	5.65	4.22	4.19	4.02	3.76
0.001	5.72	3.92	3.47	3.53	3.42	5.82	4.31	4.28	4.19	3.89
0 0004	5.88	4.04	3.70	3.72	3.65	6.00	4.69	4.52	4.47	4.09
0.0002						6.00	4.65	4.59	4.62	3.89

When the exchange sorption on palmitic acid in $AgNO_3$ solutions was studied by the conductometric method we found that the conductivity of the $AgNO_3$ solution is lowered at first, passes throught a minimum, and then rises, exceeding the original value (Fig. 2). This indicates that at first the total concentration of the electrolyte diminishes, evidently due to the molecular sorption of $AgNO_3$, and only after this, when as the result of exchange the amount of H^+ ions becomes sufficiently great, does the conductivity attain higher values. From this it follows that when discussing the processes for exchange sorption on fatty acid crystals it is necessary to consider molecular sorption. This also followed from our earlier data with $Th(NO_3)_4$.

Molecular sorption should increase with increase in electrolyte concentration, for which reason a reduction in the rate of H^+ ion liberation with increase in the $CuSO_4$ concentration may be associated with the influence of molecular sorption. It should be mentioned that retardation of the reaction at higher C_{CuSO_4} values cannot be blamed on a reduction in the activity of the solution. Apparently, the kinetics of the process, depending on the arising of some sort of potential barriers, plays the chief role here.

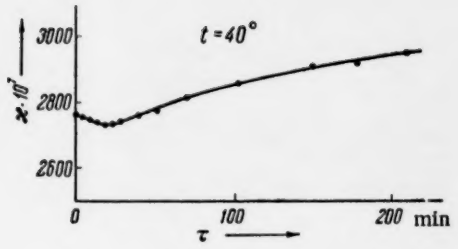

Fig. 2.

Retardation of the process for the liberation of H^+ ions is more weakly expressed for the shorter homologous acids, and consequently an increase in the activity of the acid and of the mobility of its molecules in the crystal, i. e. an increase in the "porosity" of the lattice, corresponding to elevation of the temperature for the higher homologous acids, reduces the hindering action of the barriers. This hypothesis is supported by some additional experiments, made with increased amounts of acid (stearic) in solutions of higher concentration than that corresponding to the maximum on the curve $\Delta[H^+] = f(C)$.

In the experiments, relating to the curves shown in Fig. 1, we took small weights of acid, corresponding to 0.000125 g.-equiv. When the weight of acid was increased the rate of H^+ ion liberation, and together with it the shape of the curve $\Delta[H^+] = f(C)$, changed sharply and the anomalous curve with a maximum was converted into the normal curve of constant increase in $\Delta[H^+]$ with C. Here the pH dropped to values that were much lower than the lowest values obtained with the small weights (Table 2). This can be seen from Fig. 3 for stearic acid (in this case the maximum $\Delta[H^+]$ with a small weight lies at a lower concentration than for the C_{12}, C_{14} and C_{16} acids).

TABLE 2

Values of the pH for Crystals of Stearic Acid in $CuSO_4$ Solutions

Weight of stearic acid, g	$C=0.2N$		$C=0.01N$		$C=0.002N$	
	orig.	after 262 hrs.	orig.	after 168 hrs.	orig.	after 116 hrs.
0 0355	4.16	4.01	5.20	3.94	5.53	4.01
0.1775	4.18	3.54	5.20	3.69	5.51	3.85
0.8875	4.18	3.17	5.17	3.55	5.48	3.81

An increase in the weight of acid means that a smaller amount of adsorbed substance is available per unit of sorbent surface, and consequently the hindering process, i. e. the specific influence of the passivator is reduced. Due to the large surface area of the sorbent the reaction succeeds for a short time in progressing only in the surface layers, without penetrating into the interior of the crystal. Consequently, the "barricading" action of the adsorbed anions is hardly exerted.

• The time shown here relates to obtaining some practical limit in the pH changes.

Penetration of the electrolyte into the lattice of the acid begins, apparently, at the more damaged portions of the crystals, at their corners and edges, where the packing of the acid molecules is more imperfect and the polar groups are more available to the electrolyte molecules. Apparently, hydration of the polar groups of the acid molecules and adsorption of the electrolyte on them weaken the reactivity between oppositely directed acid molecules in the crystal. This is especially facilitated by either elevation of the temperature or shortening of the homolog chain. The exchange process consists of a number stages: hydration of the polar groups of the acid molecules, weakening or rupture of the bonds between oppositely placed acid molecules and dissociation of the carboxyl group with H^+ ion liberation, replacement of the latter by a metal cation and formation of a molecule of metallic soap, and the creation of a seed crystal of the soap and its growth. In this connection the ratio of the lattice parameters of the acid and soap, and also the radius of the cation, probably bear great importance.

Molecular sorption can proceed on undissociated molecules and is more intense at low temperatures. When crystals undergo polymorphous transformations it is probable that the acid molecules in them can change from "dimers" to "monomers" in a short time. At the moment of rupture or weakening of the hydrogen or dipole bond between two acid molecules they acquire a great tendency to dissociate and exchange. Consequently, polymorphic transformation accelerates exchange reactions (besides simple increase in the internal surface of the crystal due to its reconstruction).

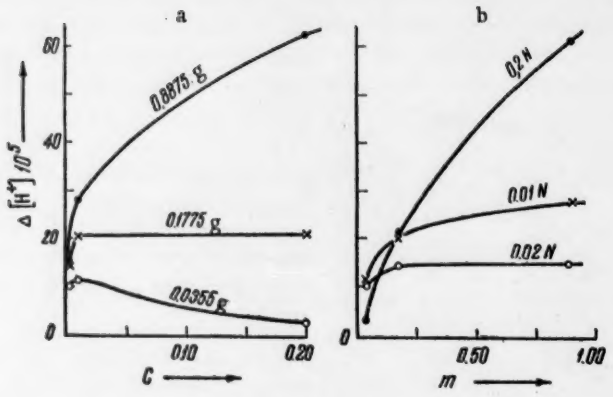

Fig. 3. Dependence of $\Delta[H^+]$ on C (a) and on m(b) for crystals of stearic acid in $CuSO_4$ solutions

A transition in the sorption from exchange to molecular when the electrolyte concentration was increased was observed for the case of gelatin [2]; however, here it was not indicated that molecular sorption can hinder exchange sorption.

The author wishes to thank L. K. Serebryanikova and V. V. Constantinova for making the measurements.

Institute of Physical Chemistry
Academy of Sciences of the USSR

Received January 24, 1957

LITERATURE CITED

[1] A. A. Trapeznikov, Proc. Acad. Sci. USSR, 47, 277, 349 (1945); A. A. Trapeznikov and M. E. Lipets, J. Phys. Chem. (USSR), 21, 109 (1947); M. E. Lipets and A. A. Trapeznikov, J. Phys. Chem. (USSR), 23, 981 (1949).

[2] A. G. Pasynsky and Z. Zolotareva, J. Phys. Chem. (USSR), 16, 27 (1942).

PROCEEDINGS OF THE ACADEMY OF SCIENCES OF THE USSR

Section: PHYSICAL CHEMISTRY

Volume 114, Issues 1-6

May-June, 1957

TABLE OF CONTENTS

	Page	Russian Issue No.	Russian Page
1. Investigation of Adsorption at High pressures. B. N. Vasilyev, B. P. Bering, M. M. Dubinin and V. V. Serpinsky	265	1	131
2. Kinetic Relationships During Ignition by a Hot Surface in Conditions of the Internal Combustion Engine. A. N. Voinov	269	1	135
3. Investigation of the Structure of Humic Acids in Bituminous Coals. V. I. Kasatochkin and N. K. Larina	273	1	139
4. Concerning the Change of the Electrochemical Activity of Zirconium under the Action of Radiation. I. L. Rozenfeld and E. K. Oshe	277	1	143
5. The Properties of Plastic Masses Filled with Graphite and the Effect of High Filling. B. L. Tsetlin, L. P. Yanova, G. K. Sibirskaya and P. A. Rebinder	281	1	146
6. Determination of the Oxidation-Reduction Potentials of p-Hydroxyphenylglycine. Ya. M. Veprik and G. P. Faerman	285	2	354
7. Investigation, by the Charging Curve Method, of the Nature of Local Passivity During Electrolytic Polishing of Copper. G. S. Vozdvizhensky and A. I. Turashev	289	2	358
8. On the Relationship of Viscosity Coefficient to the Structure of a Substance in the Liquid State. A. Z. Golik and D. N. Karlikov	293	2	361
9. On the Question of the Existence of Metakaolinite and the Nature of the Exothermic Effects of Alumina. A. M. Kalinina and E. A. Porai-Koshits	297	2	365
10. Non-Steady State Processes During Anodic Solution of Copper in Orthophosphoric Acid. S. I. Krichmar	303	2	369
11. On the Process of Coal Halogenation Under the Influence of Ultrasonic Waves. B. I. Losev, I. E. Elpiner and A. N. Melnikova	307	2	372
12. The Kinetics of Mechanical Degradation of High Polymers. N. K. Baramboim	311	3	568
13. The C–H Bond Rupture Energy in Hydrocarbons. V. I. Vedeneev	315	3	571
14. On The Problem of the Mechanism of Ion Exchange. V. I. Gorshkov and G. M. Panchenkov	319	3	575
15. Adsorption of Water Vapor on Silica Gels of Different Degrees of Hydration. M. M. Egorov, T. S. Egorova, V. F. Kiselev and K. G. Krasilnikov	325	3	579

(continued)

TABLE OF CONTENTS (Continued)

	Page	Russian Issue No.	Russian Page
16. On the Kinetics of Rotational Isomerization. V. A. Pozdyshev, Yu. A. Pentin and V. M. Tatevsky	331	3	583
17. On the Changes in the Order of Sulfide Links in Irradiated Vulcanizates. A. F. Postovskaya, M. A. Salimov and A. S. Kuzminsky	335	3	586
18. The Isotopic Effect in the Compressibility and Association of Deutero-Alcohols. I. B. Rabinovich, V. G. Golov, N. A. Efimova and S. M. Rustamov	339	3	590
19. Investigation of the Kinetics of Supersaturation with Reference to the Formation of Crystallization Structures in the Hardening Process of Gypsum. E. E. Segalova, V. N. Izmailova and P. A. Rebinder	345	3	594
20. The Thermal Decomposition of Nitrocellulose in Vacuum. K. K. Andreev and B. S. Samsonov	349	4	815
21. The Explosive Decomposition of Hexogen. A. Ya. Apin and Yu. A. Lebedev	355	4	819
22. The Adsorption of Hydrogen on Nickel Films Condensed in High Vacuum. N. N. Kavtaradze	359	4	822
23. The Null Charge Point of Certain Metals and Alloys. B. S. Krasikov and V. V. Sysoeva	363	4	826
24. The Transfer of Energy During Radiolysis of Benzoyl Peroxide Solutions. V. A. Krongauz and Kh. S. Bagdasaryan	367	4	829
25. An Investigation by the Filtration Method of the Mechnical Properties of Thin Liquid Films in Concentrated Emulsions. S. V. Nerpin and N. F. Bondarenko	373	4	833
26. A Generalized Formulation of the Gibbs Inequality. L. S. Palatnik and A. I. Landau	377	4	837
27. A Method for Testing the Equation of State of Gases at High Temperatures. S. S. Semenov	381	4	841
28. The Influence of the Addition of Surface Active Substances on the Intensity of the Vibrational Pulverization of Cement. L. I. Edelman and D. S. Sominsky	385	4	844
29. The Kinetics of the Formation of Alcohol and Alkyl Acid in the Reaction of Propylene and Aqueous Sulfuric Acid. S. G. Entelis, V. E. Petrakovich, G. V. Korovina and N. M. Chirkov	389	4	848
30. Absorption Spectra of Some Dyes in Mixed Solvents. Kh. L. Arvan and N. V. Ivanova	393	5	1043
31. A Study of the $Zn \rightleftharpoons Zn^{++}$ Exchange Process on the Faces of a Zinc Monocrystal Using Radioactive Indicators. B. N. Bushmanov and G. S. Vozdvizhensky	397	5	1046
32. The Application of Labelled Atoms to the Study of the Mechanism of Anode Evolution of Oxygen. M. A. Gerovich, R. I. Kaganovich, V. M. Vergelesov and L. N. Gorokhov	401	5	1049

(continued)

TABLE OF CONTENTS (Continued)

	Page	Russian Issue No.	Russian Page
33. Elastic-Resiliency and Viscous-Plastic Properties of Thermosetting Plastics. I. F. Kanavets and L. G. Batalova	405	5	1053
34. The Mechanism and Isotope Effect of the Primary Act of Thermal Decomposition of Chloroform. A. E. Shilov and R. D. Sabirova	411	5	1058
35. Calculation of the Heat and Entropy of Adsorption from a Single Adsorption Isotherm. B. P. Bering and V. V. Serpinsky	417	6	1254
36. Adsorption of Aliphatic Alcohols from Solutions on Silica Gel and "White Soot." A. K. Bonetzkaya and K. G. Krasilnikov	421	6	1257
37. The Equation of Nonsteady Diffusion Towards a Stationary Electrode. A. V. Gorodysky and Yu. K. Delimarsky	425	6	1261
38. Anodic Passivation of Chromium in Acid Solutions. V. M. Knyazheva and Ya. M. Kolotyrkin.	429	6	1265
39. Investigation of the Kinetics and Mechanism of the Thermal Decomposition of Isobutylene. Yu. I. Lyadova, V. I. Vedeneev and V. V. Voevodsky	433	6	1269
40. The Nature of Catalytic Currents of Hydrogen in Polarography. S. G. Maironovsky	437	6	1272
41. Ionic Exchange on Aluminosilicate Catalysts in a Stream of Alkali with Small Contact Times. G. M. Panchenkov, Z. V. Gryaznova and I. M. Kuvshinnikov.	443	6	1276
42. The Influence of the Concentration of the Electrolyte (Copper Sulfate) Solution on the Exchange Sorption of Fatty Acid Crystals. A. A. Trapeznikov	447	6	1280